

Thermal power generation

2010.08.19

Written by

Olav Bolland



Department of Energy and Process Engineering - NTNU

2010

Content

Symboler	4
1 Gas turbines	7
1.1 What is a gas turbine	7
1.2 Classification of gas turbines	10
1.3 Recuperated gas turbines.....	16
1.4 Forbrenning	18
1.5 Brennverdi.....	20
1.6 Virkemåte for aksiel kompressor og turbin.....	21
1.7 Air intake system.....	24
1.8 Compressor cleaning	25
1.9 Relation between isentropic and polytropic efficiencies	25
1.10 Gassturbinens innløpstemperatur	30
1.11 Turbine cooling	33
1.12 Gas turbine combustors.....	45
1.13 Gas turbine performance model	51
1.14 Off-design calculation of a single-shaft gas turbine	55
1.15 Part-load performance of a gas turbine in a combined cycle	61
1.16 Air filter and exhaust duct pressure drop	66
1.17 Gas turbine instrumentation and control system.....	67
1.18 Dampinjerte gassturbiner/Steam-injected gas turbines	74
1.19 Gas turbine database	77
2 Gas turbine fuels	86
2.1 Introduction	86
2.2 Why fuel specifications for gas turbines	86
2.3 ISO-specifications for gas turbine fuels.....	87
2.4 Significance of specifications for gas turbine fuels	87
2.5 Non-fuel contaminants	93
2.6 Fuel treatment technology.....	94
2.7 Natural gas composition - example.....	96
3 HRSG design	97
3.1 Introduction	97
3.2 Properties of water/steam.....	98
3.3 Tubes and tube arrangement	98
3.4 Tube material and selection	102
3.5 Feedwater tank/deaerator	103
3.6 Dew point of exhaust gas – possible corrosion	107
3.7 Drum	108
3.8 TQ-diagram of a HS _R G	111
3.9 Computational procedure for a pressure level in a HRSG	114
4 Steam turbines	117
4.1 Principles of impulse and reaction stages	117
4.2 Turbine types.....	119
4.3 Steam turbine expansion path	123
5 Combined Cycle	130
5.1 What is a Combined Cycle.....	130

5.2 Virkningsgrad for kombinerte prosesser	131
5.3 Alternatives to the steam cycle	133
5.4 Cycle configurations	133
5.5 Miljøutslipp fra en kombinert prosess.....	137
6 Coal power plants	139
6.1 Coal fired power plants	139
6.2 Internal combustion engines	154
6.3 Flue gas cleaning technologies in power plants.....	154
7 Steam cycle cooling systems.....	158
8 Efficiency calculation.....	165
8.1 Mechanical efficiency	165
8.2 Generator efficiency	165
8.3 Auxiliary power	165
8.4 Efficiency calculation.....	165
8.5 Fans and blowers.....	166
9 Simulering av dampprosess	167
9.1 Design vs. simulering.....	167
9.2 Simulering av motstrøms varmeveksler.....	168
9.3 Beregning av varmeovergangstall.....	169
9.4 Simulering av dampturbiner.....	171
9.5 Simuleringseksempel	171
10 Typical computational assumption for steam cycles	172
10.1 Coal & natural gas fired boilers	172
10.2 HRSG 172	
10.3 Condenser.....	173
10.4 Steam turbines.....	173
10.5 Pumps 173	
10.6 Feedwater preheating	173
10.7 Fans and blowers.....	174

Symboles

A	strømningsareal	m^2
\vec{C}	absolutt hastighet	m/s
c_p	spesifikk varmekapasitet ved konstant trykk	$\text{kJ}/(\text{kg}\cdot\text{K})$
c_{pc}	varm væske spesifikk varmekapasitet ved konstant trykk	$\text{kJ}/(\text{kg}\cdot\text{K})$
c_{ph}	kald væske spesifikk varmekapasitet ved konstant trykk	$\text{kJ}/(\text{kg}\cdot\text{K})$
c_{pk}	kompressor spesifikk varmekapasitet ved konstant trykk	$\text{kJ}/(\text{kg}\cdot\text{K})$
c_{pt}	turbin spesifikk varmekapasitet ved konstant trykk	$\text{kJ}/(\text{kg}\cdot\text{K})$
d_i	rørs indrediameter	m
d_y	rørs ytrediameter	m
h	entalpi	kJ/kg
\bar{h}	dannelsesentalpi	kJ/kg
h_d	varmeovergangstallet på dampsiden	$\text{W}/\text{m}^2\text{K}$
$h_{d,0}$	varmeovergangstallet på dampsiden for et bestemt designpunkt	$\text{W}/\text{m}^2\text{K}$
h_g	ytre varmeovergangstallet	$\text{W}/\text{m}^2\text{K}$
$h_{g,0}$	ytre varmeovergangstallet for et bestemt designpunkt	$\text{W}/\text{m}^2\text{K}$
Δh	entalpi endring	kJ/Kg
ΔH_{net}	entalpiøkning i et arbeidsmedium	kJ/Kg
HHV	Øvre brennverdi (Higher Heating Value)	kJ/kg
κ	isentropopeksponent	
LHV	Nedre brennverdi (Lower Heating Value)	kJ/kg
\dot{m}	massestrøm	kg/s
\dot{m}_c	kaldvæske massestrøm, varmeveksler	kg/s
\dot{m}_{fuel}	brenselforbruk	kg/s
\dot{m}_g	gass massestrøm	kg/s
$\dot{m}_{g,0}$	gassmassestrøm for et bestemt designpunkt	kg/s
\dot{m}_h	varmvæske massestrøm, varmeveksler	kg/s
MW	molvekt	kg/kmol
N	turtall	
Nu	Nusselts tall	
P	trykk	N/m^2
ΔP_{af}	trykktap i luftfilter	N/m^2
ΔP_c	trykktap i brennkammer	N/m^2
Pr	Prandtls tall	
R	gasskonstant	$\text{kJ}/(\text{kg}\cdot\text{K})$
Re	Reynolds tall	
Q	varmemengde	kJ/kg
Q_H	tilført varmemengde	kJ/kg
Q_{net}	netto levert varmemengde	kJ/kg
Q_{ut}	levert varmemengde ved en høyere temperatur	kJ/kg
ΔQ	varmemengde økning	kJ/kg
T	temperatur	K
$T_{i,\text{Exh}}$	Exhaust gas temperature at position i	$^\circ\text{C}/\text{K}$
T_n	Steam/water temperature in HRSG at position n	$^\circ\text{C}/\text{K}$

T_c	kaldvæske temperatur, varmeveksler	K
$T_{c,ut}$	kaldvæske utløpstemperatur, varmeveksler	K
T_h	varmvæske temperatur, varmeveksler	K
T_h	høyere temperatur i en termodynamisk prosess	K
$T_{h,ut}$	varmvæske utløpstemperatur, varmeveksler	K
T_l	lavere temperatur i en termodynamisk prosess	K
ΔT	temperatur økning	K
ΔT_{pinch}	temperature difference in HRSG pinch point	K
$\Delta T_{SUP,hot end}$	Temperature difference between steam and exhaust gas the superheater hot end	K
U	varmeovergangstall	$\text{W}/\text{m}^2\text{K}$
U_0	varmeovergangstall for et bestemt designpunkt	$\text{W}/\text{m}^2\text{K}$
\vec{U}	periferihastighet	m/s
v	hastighet	m/s
\vec{V}	relativhastighet	m/s
W	teknisk arbeid	kJ/kg
W_{compr}	teknisk arbeid for en kompressor	kJ/kg
W_{turb}	teknisk arbeid for en turbin	kJ/kg
W_{GT}	teknisk arbeid for en gassturbin	kJ/Kg
W_{net}	netto levert arbeid	kJ/Kg
α	vinkel	
β	strømvinkel	
$\Delta \varepsilon$	eksergi endring	kJ/Kg
γ	effektfaktor	
η_{Carnot}	Carnot-virkningsgraden	
η_{en}	energivirkningsgrad	
η_{GT}	gassturbinens virkningsgrad	
η_{is}	isentropisk virkningsgrad	
η_p	polytropisk virkningsgrad	
λ	luftoverskuddstall, virkelig luftmengde/støkiometrisk luftmengde	
μ	viskositet	$\text{N}\cdot\text{s}/\text{m}^2$
μ_g	gassviskositet	$\text{N}\cdot\text{s}/\text{m}^2$
ρ	tetthet	kg/m^3
φ	brenselfaktortall, støkiometrisk luftmengde/virkelig luftmengde ($1/\lambda$)	

Indekser

P	produkter
r	reaktanter
r	referanseverdi
0	innløp luftfilter (gas turbine)
1	innløp kompressor (gas turbine)
2	innløp brennekammer (gas turbine)
3	innløp turbin (gas turbine)
4	utløp turbin (gas turbine)
1	Superheater hot end (HRSG)
2	Between superheater and evaporator (HRSG)
3	Between evaporator and economiser (HRSG)

4 Economiser cold end (HRSG)
Exh Exhaust or Exhaust gas

Abbreviations

ECO = Economiser
EVA = Evaporator
SUP = Superheater

1 Gas turbines

1.1 What is a gas turbine

A gas turbine is an open Brayton cycle, see Figure 1 (Saravanamuttoo, Rogers et al., 2001), (Boyce, 2002). It consists basically of a compressor, combustion chamber and turbine. The compressor draws air from the ambient and compresses it to a pressure in the range 10-35 bar, depending upon type of gas turbine. The pressurised and hot air is then used as combustion air in the combustion chamber, in which a fuel is injected and combusted continuously. The most common fuel in gas turbines is natural gas (for about 80% of all gas turbines), but also other fuel gases and distillate oil are used in gas turbines. The temperature at the exit of the combustion chamber may be up to about 1500 °C. The hot pressurised gases, or combustion products/exhaust gas/flue gas, are then expanded to slightly above atmospheric pressure in a turbine. In both the compressor and turbine, the conversion between the energy contained in the working fluid and the power transferred by the shaft, is carried out by compressor and turbine stages. A stage is two rows of blades, where one of the row blades is attached to the shaft (rotating blades, rotors) and the other to the casing (stators). A turbine stage is depicted in Figure 2. The gas turbine cycle is shown in a temperature-entropy diagram in Figure 3.

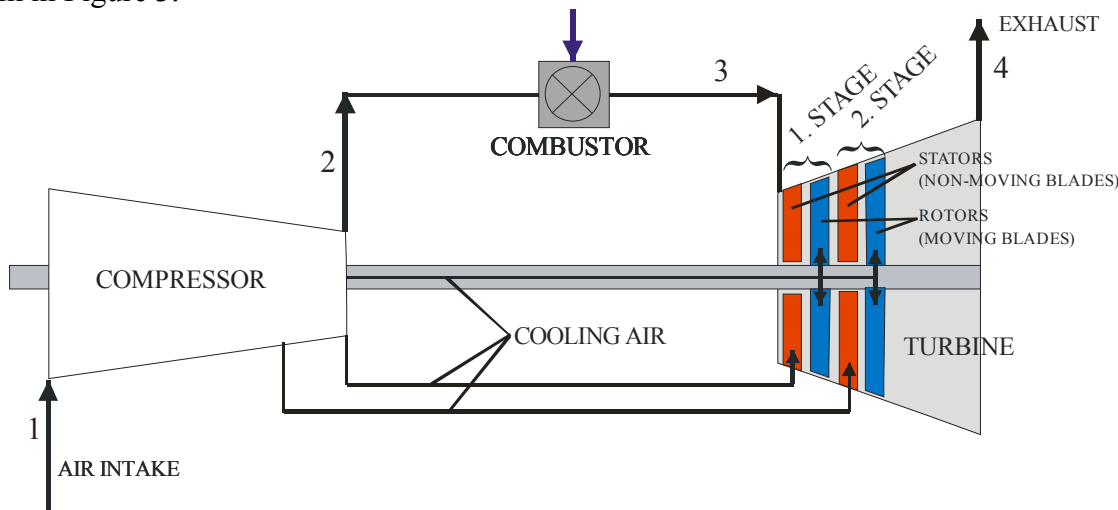


Figure 1 A gas turbine, consisting of a compressor, combustion chamber and turbine. Two stages of the turbine are shown, as well as principal cooling air flows.

The temperature at the exit of the combustor chamber, “turbine inlet temperature” or TIT, is preferably as high as possible with respect to cycle efficiency and specific power¹, but is limited by the materials and the cooling system of the gas turbine. In order to limit the TIT, the combustion takes place with a rather high excess air ratio, 2.5-3.0.

¹ Specific power is normally defined as the gas turbine net power output divided by the air flow rate – $\text{kJ}_{\text{power}}/\text{kg}_{\text{air}}$

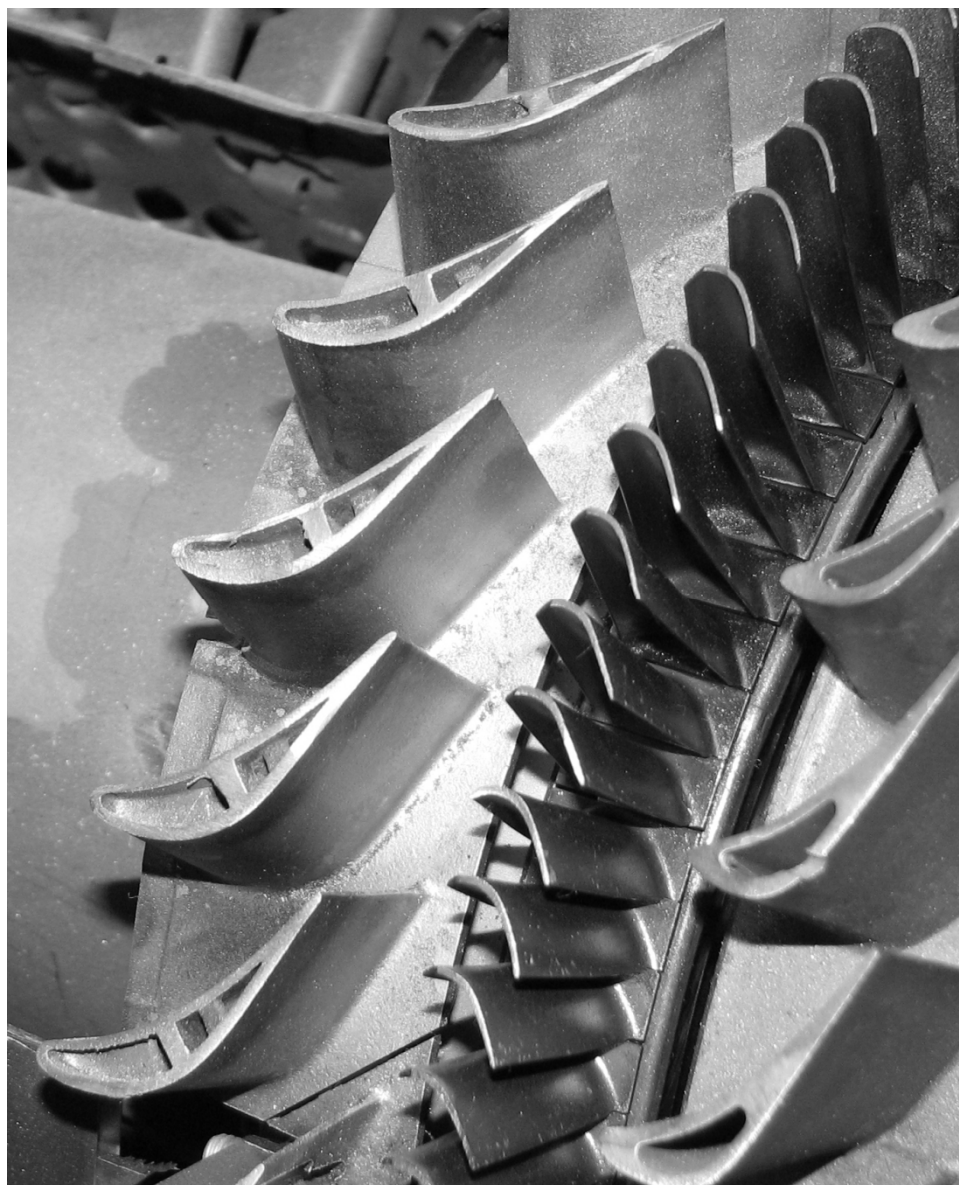


Figure 2 Turbine stage with stators to the left which main function is to act as nozzles to increase the velocity of the gas primarily in the tangential direction, by converting pressure energy to kinetic energy. To the right of the stators are the rotors, which function is to convert the kinetic energy to power by causing a rotation of the shaft.

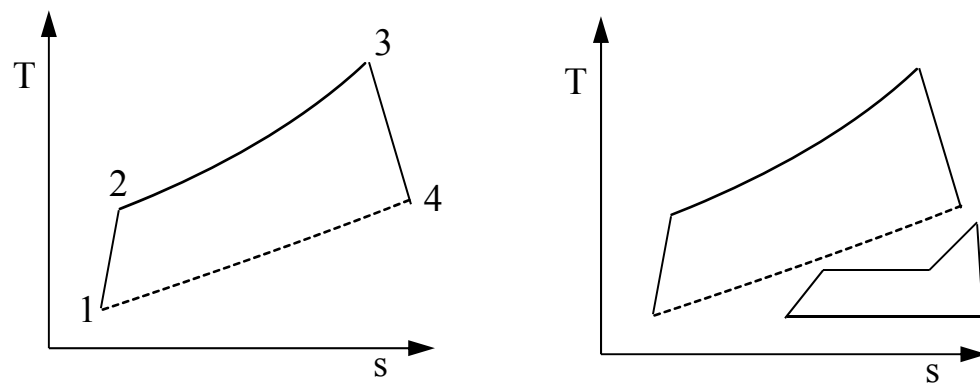


Figure 3 Temperature-entropy diagram of a gas turbine cycle (left) and combined gas turbine and steam turbine cycle (right).

The three process steps compression, combustion and expansion are also taking place in an internal combustion piston engine. The main difference between that and a gas turbine, is that the three process steps in a gas turbine are continuous and that they take place in different units.

When compressing the air, power is required. When expanding the hot gas through the turbine, power is generated. The turbine typically generates twice the power consumed by the compressor. The difference is the net power of the gas turbine, which can through the shaft drive an electric generator in a power plant, drive a natural gas compressor or a big pump.

The conversion of the fuel energy (lower heating value) to power – the efficiency – is in the range 35-40% for large gas turbines used in power plants, 37-42% for medium-sized (10-50 MW) gas turbines based on aero engine design, 25-32% for gas turbines mainly made for propulsion purposes (1-10 MW), and 20-30% for so-called micro turbines (50-300 kW).

Figure 4 depicts the temperature and pressure throughout a gas turbine. The exhaust (or flue gas) from the gas turbine has a temperature in the range 450-650 °C, depending upon type of gas turbine. The energy contained in the exhaust gas represents the almost all of the fuel heating value that is not converted to work.

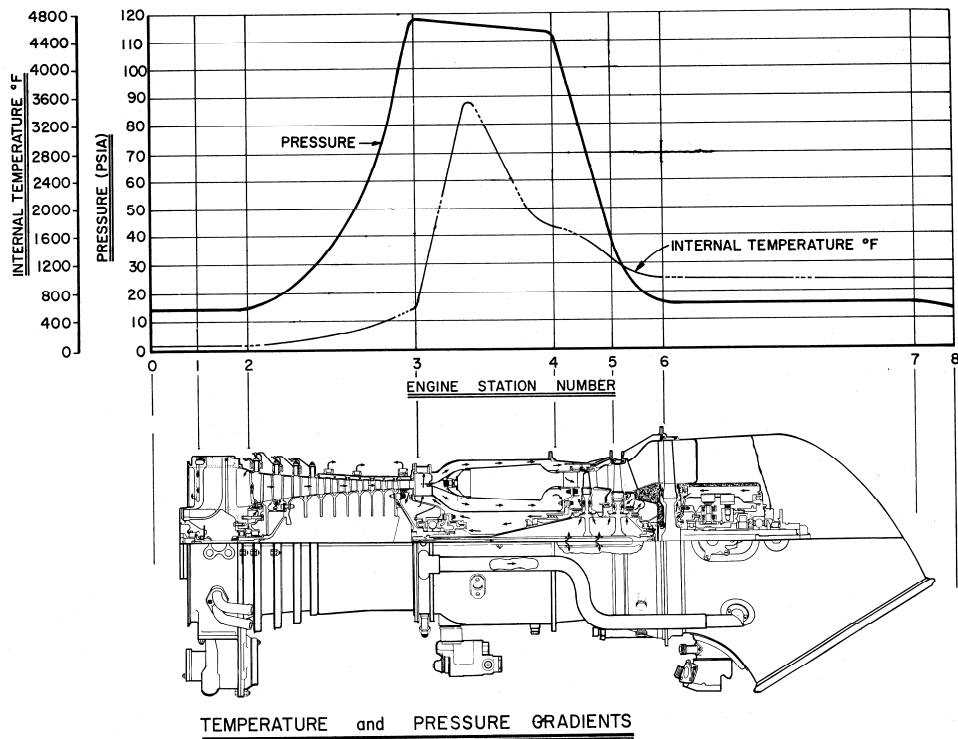


Figure 4 Temperature and pressure thorugput a gas tuirbine. $^{\circ}\text{C}=(\text{F}-32)*5/9$, bar=psia/14.7

1.2 Classification of gas turbines

Classification of gas turbines can be done by number of shafts, aeroderivate/industrial design philosophies and whether it is axial or radial type compressor and turbine.

When classifying gas turbines it is common to distinguish between aeroderivate gas turbines and industrial gas turbines, see Figure 5. The former type of gas turbines were originally designed as jet engines, but was later redesigned to become gas turbines. Basically, the redesign is to replace the engine nozzle by a power turbine. Typical characteristics of aeroderivate gas turbines compared to industrial gas turbines are high power-to-weight ratio, compact by volume and high pressure ratio. Historically the technology development of gas turbines was driven by the significant effort that was made to improve military jet engines. The most advanced technology was first implemented in jet engines, and then later in gas turbines. Aeroderivate gas turbines used to be regarded as more advanced in term of materials, efficiency and maintainability. This has changed during the 1990s, as the economical importance of large industrial gas turbines has increased as more and more natural gas fired power plants have been taken into use. Today, very much the same design philosophy and technology are used both for aeroderivate and industrial gas turbines.

The compressor(s) and turbine(s) of a gas turbine are connected by one or more shafts. One of the shafts is coupled to the external consumer of the shaft power, and transfers the net power produced by the gas turbine, see Figure 6. The external consumer of the shaft power is a generator, gas compressor, or propeller. In case of power generation, the generator and the connected shaft is running at constant speed; either 3000 rpm (50 Hz) or 3600 rpm (60 Hz). For some small and medium-sized gas turbines, the operating speed is higher and the coupling to the generator is geared. Aeroderivate gas turbines are made with multiple shafts, running at different speed.

Industrial gas turbines are mainly made as single-shaft engines, but there are also some dual-shaft industrial gas turbines. In general, the multi-shaft gas turbines operate with better part-load efficiency than the single-shaft gas turbines. One can also argue that a multi-shaft gas turbine is easier to redesign. All gas turbines above 100 MW, as of 2008, are of the single-shaft design. There are also many gas turbines smaller than 100MW with the single-shaft design.

Aeroderivate GT

- Based on jet engine design
- High power/weight-ratio
- Compact by volume
- High pressure ratio (up to 35)

10-20 years ago:

Industrial type GT or Heavy Duty GT

- Not designed to fly
- Low power/weight-ratio
- Medium compact to bulky
- Moderate pressure ratio (10-18)

Aeroderivate GTs: advanced technology, high maintenance requirements

Industrial type GTs: conventional technology, low maintenance requirements

Now

Same technology applied in both types of GTs

Figure 5 Classification of gas turbines by aeroderivate or industrial type of design. Since about 1990 the differences between the two has decreased a lot.

The compression and expansion in most gas turbines above 10 MW is accomplished by axial-type compressor and turbine. For smaller gas turbines, many use of radial-flow compressor and turbines. In general, radial-type is suited for small-to-medium volumetric flow rates and high pressure ratio, while the axial-type is best suited for large volumetric flow rates and low-to-medium pressure ratio. The largest gas turbines (in 2008; 330 MW) operates with a compressor inlet air flow of about 600 m³/s and a pressure ratio of about 20, for which the axial-type compressor and turbine is the only choice.

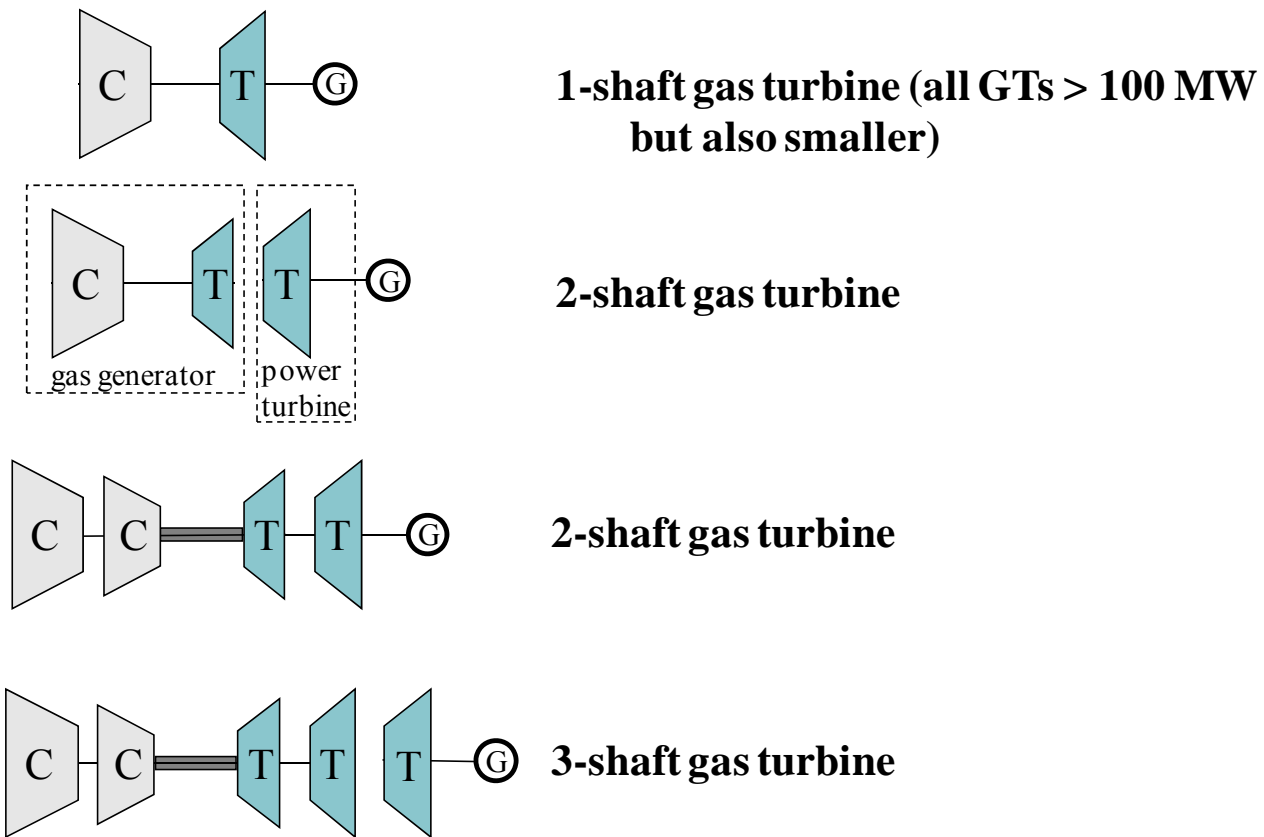
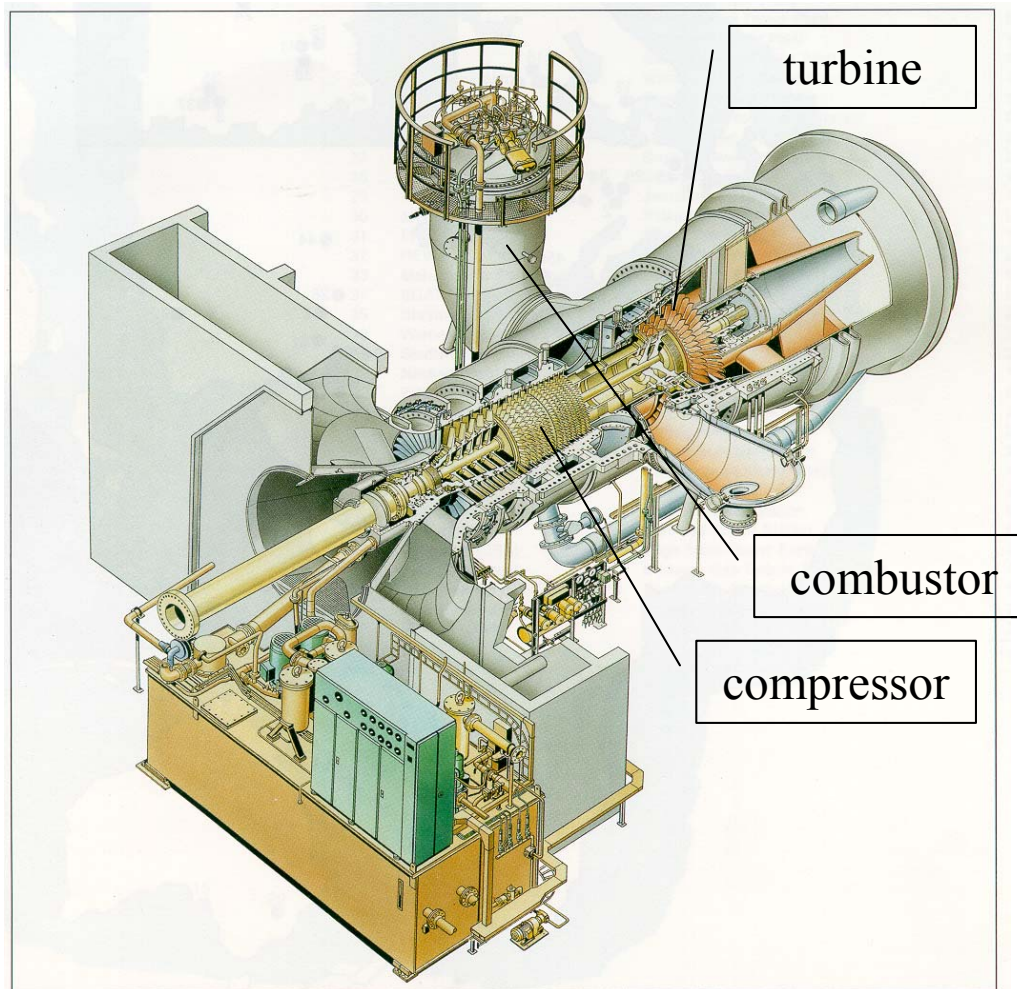


Figure 6 Classification of gas turbines by number of shafts

Figure 8, Figure 9 and Figure 10 viser tre typiske industrielle gassturbiner, henholdsvis Siemens V94.2, General Electric LM5000 og Siemens-Westinghouse 501D5A.



High-reliability heavy-duty Model V94/V84 gas turbine

Figure 7 Siemens V94.2, ca. 160 MW, første gassturbin i 1986 med lav-NOx brennkammer

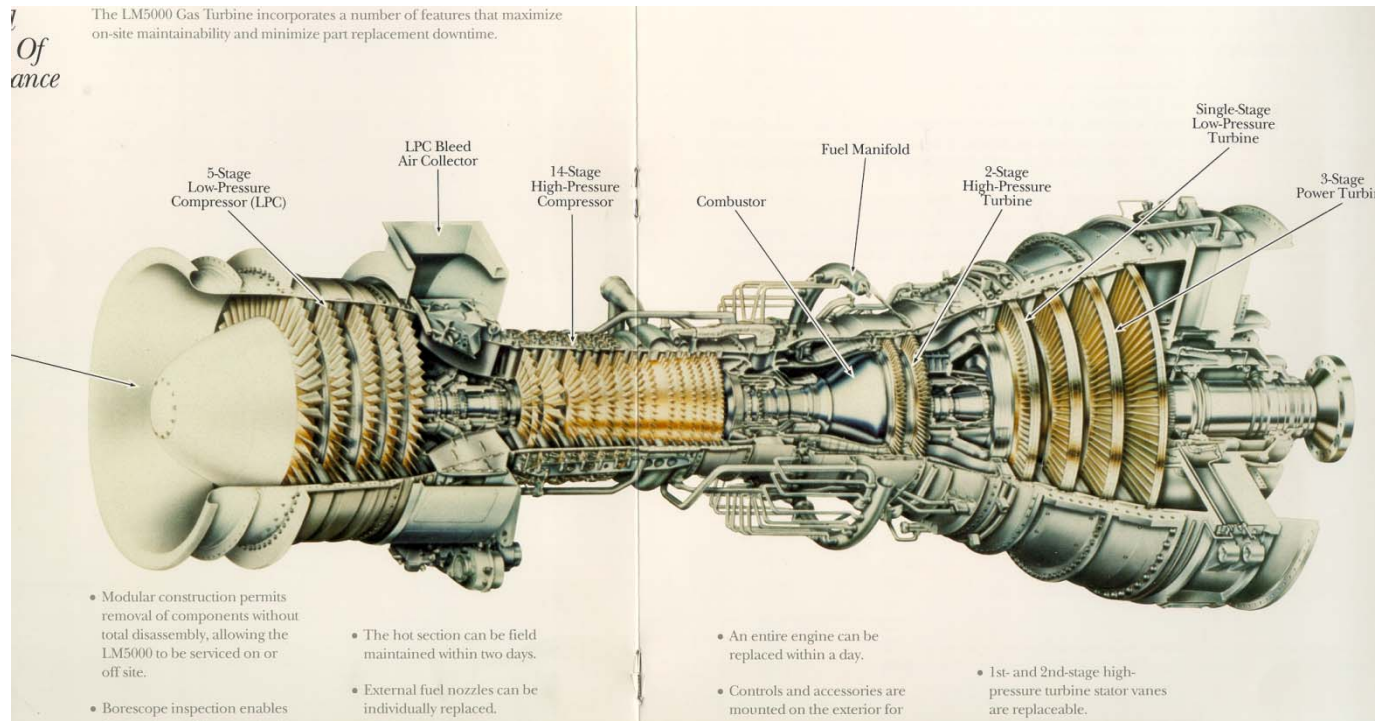


Figure 8 General Electric LM5000, flyderivert gassturbin (tatt ut av produksjon)

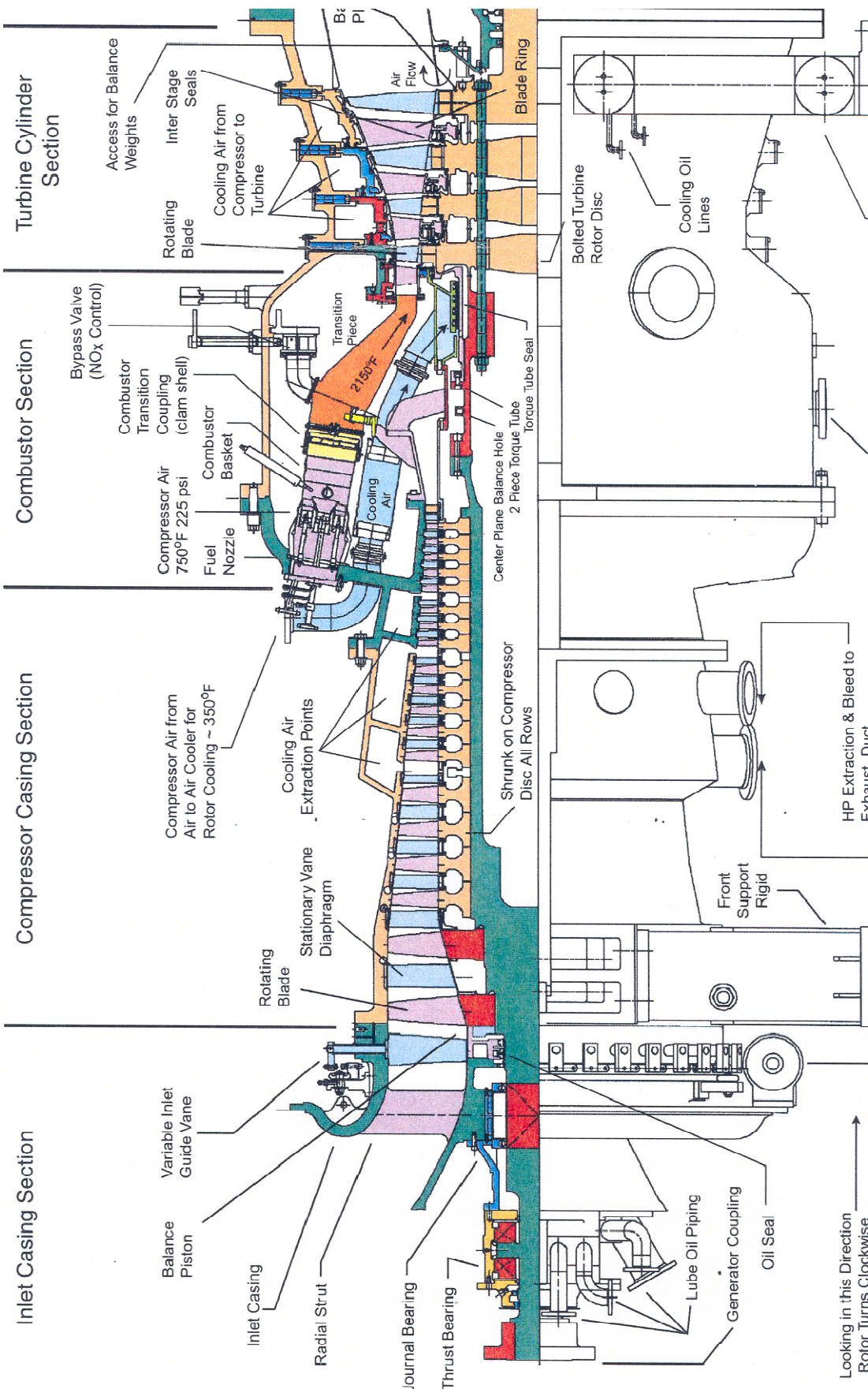


Figure 9 Cutaway diagram of a Westinghouse 50ID5A gas turbine

1.3 Recuperated gas turbines

A recuperated gas turbine uses the exhaust of the turbine to preheat the air entering the combustion section of the turbine (see Figure 10). To do this the full compressor discharge flow is extracted from the turbine and sent to a heat exchanger. The preheated air is then returned to the turbine at the combustor.

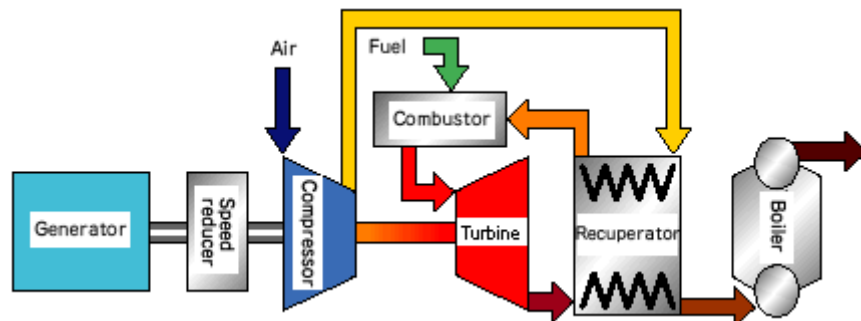


Figure 10 Schematic Diagram of a Recuperated Gas Turbine Cycle²

There are several commercially recuperated gas turbines. Some of them are described in more detail in the following sub-sections, and a summary of these turbines is presented in Table 1.

Table 1 – Comparison of Several Commercially Available Recuperated Gas Turbines

	Power output, MW	Air flow, kg/s	Firing temp. °C	Pressure ratio
Rolls-Royce WR21	25.2	71.5	N/A	16.2
Solar Mercury 50	4.6	17.6	1163	9.9
Heron H-1	1.4	5.1	860	8.9
I-R MT250	0.25	2.0	927	4.1
I-R MT70	0.07	0.7	927	3.0
GE Frame 7B	60.0	238.1	1004	11.5

1.3.1 Rolls-Royce WR21

The Rolls-Royce WR21 has been developed with funding from both the US and UK Navy. The three-shaft design includes a compressor intercooler as well as a recuperator (see Figure 11 and Figure 12). The WR21 has a design power rating of 25 MW at ISO conditions.

² Osaka Gas website: <http://www.osakagas.co.jp/rd/sheet/053e.htm>

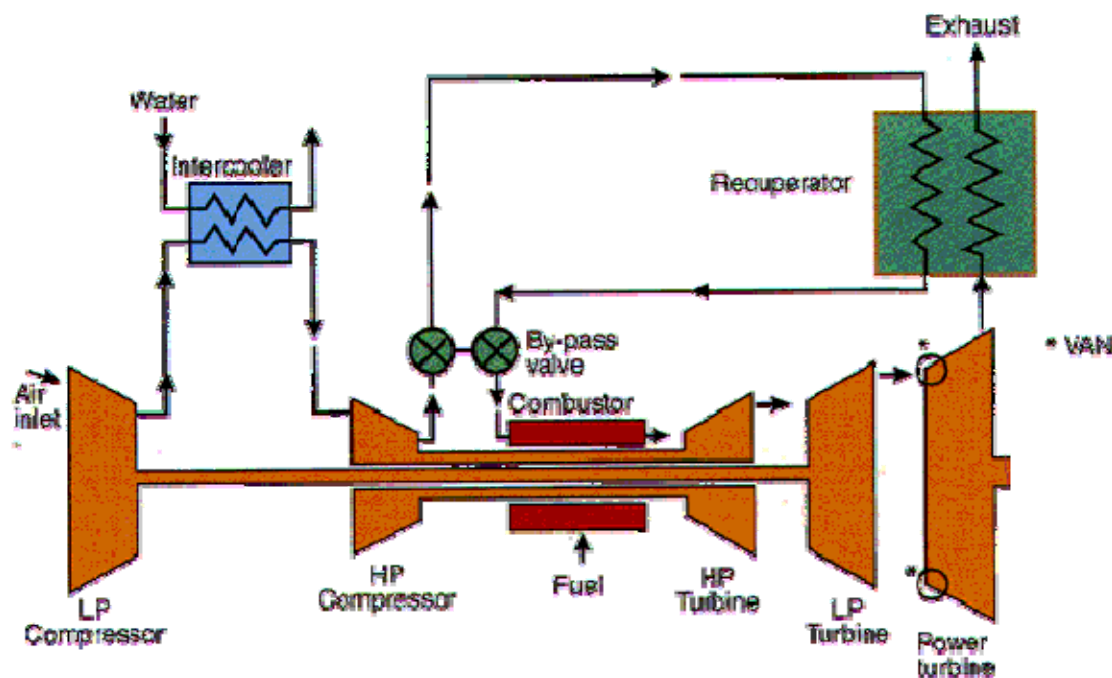


Figure 11 – Schematic Diagram of the Rolls-Royce WR21

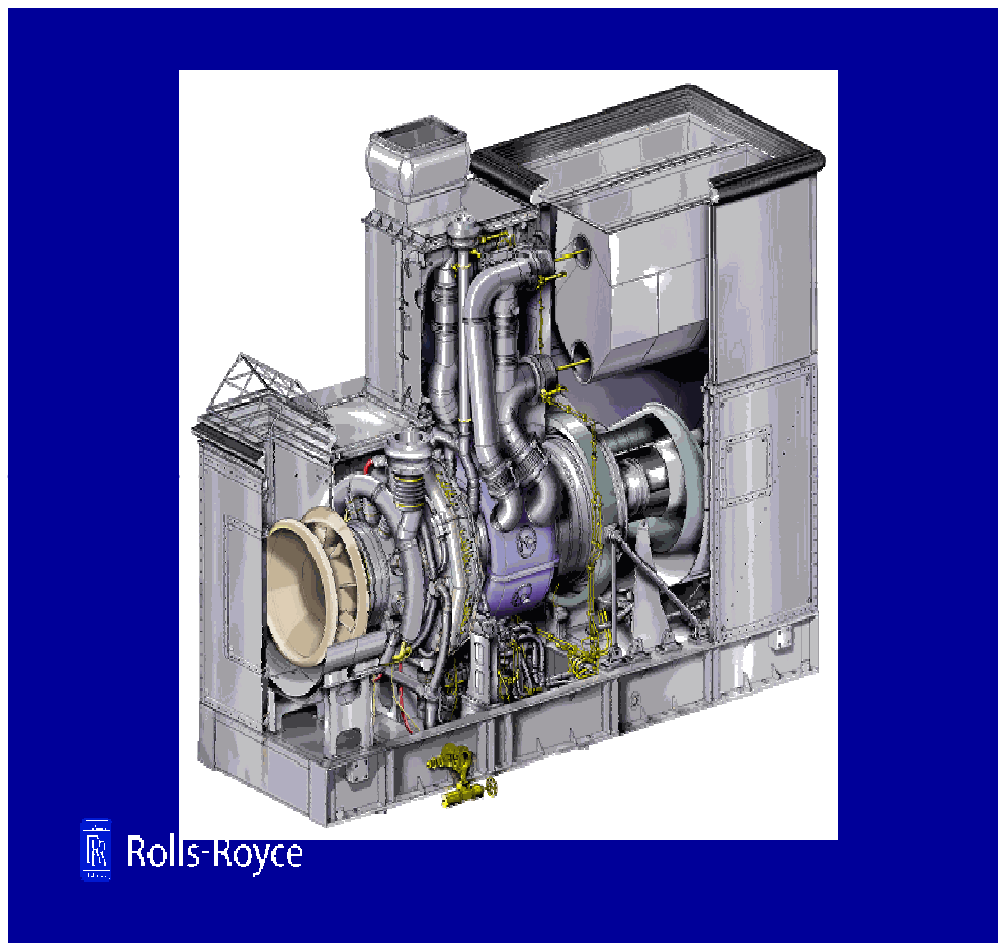


Figure 12 Artist's sketch of a Rolls-Royce WR21 (air intake is on left, exhaust and recuperator on right).

1.3.2 Solar Mercury 50

The Mercury 50 is Solar Turbines' newest gas turbine model. It was developed with funding from the US Dept. of Energy as part of the Advanced Turbine Systems (ATS) program. The ISO power rating of the Mercury 50 is 4.6 MW.

What makes this engine unique among recuperated designs is the engine layout. Instead of the normal compressor-combustor-turbine layout, the Mercury 50 as shown in Figure 13 uses a combustor-turbine-compressor layout.

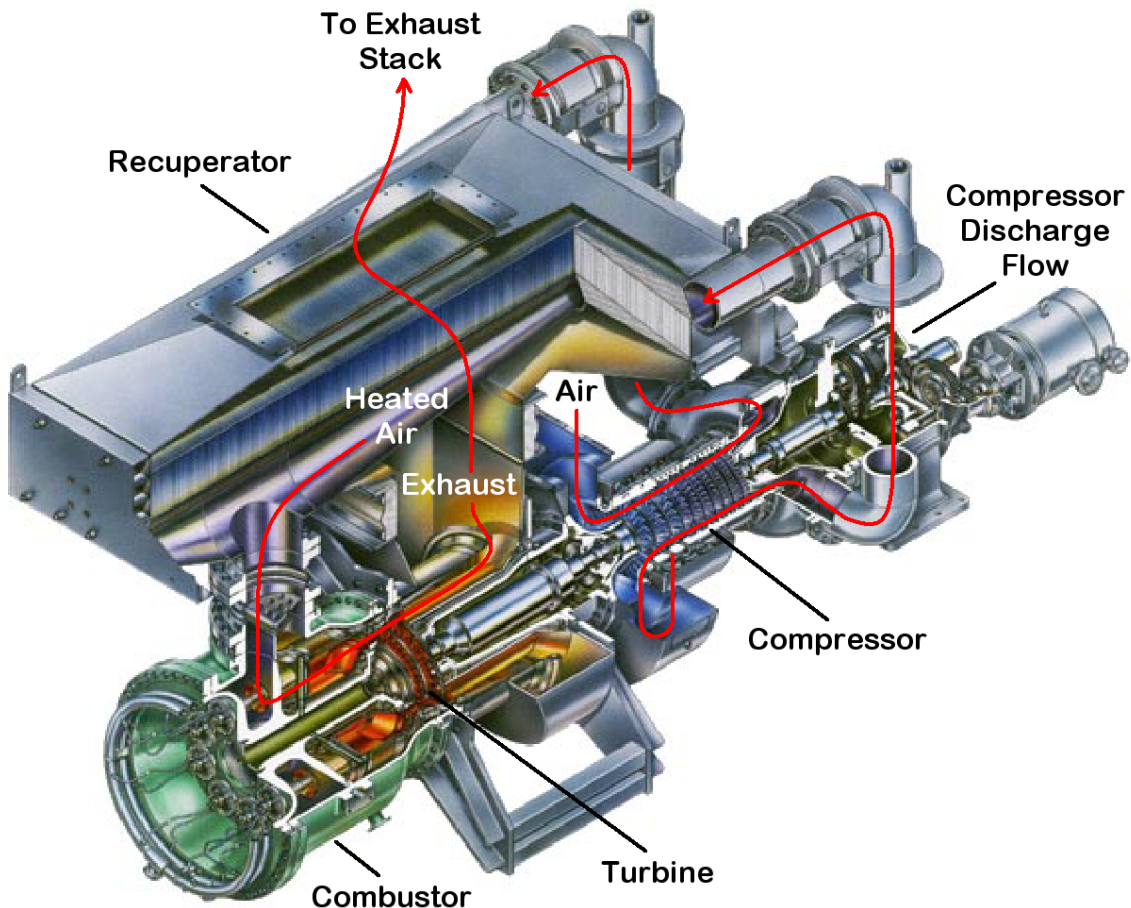
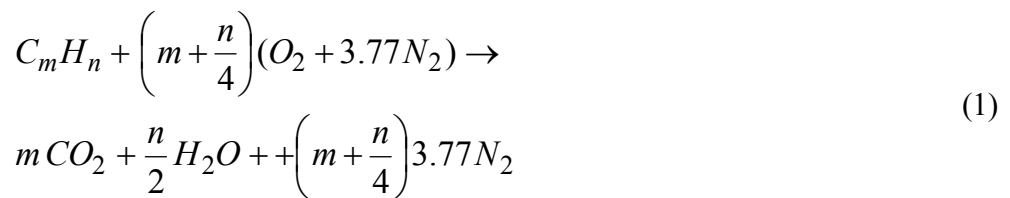


Figure 13 – Cut-away drawing of the Solar Turbines Mercury 50.

1.4 Forbrenning

Forbrenningsligningen for en generell blanding av hydrokarboner (støkiometrisk).



For naturgass som består hovedsaklig av alkaner (metan, etan, butan,...) er relasjonen mellom m og n slik:

$$n=m*2+2 \text{ eller } m=(n-2)/2$$

Forbrenningsligningen med luftoverskudd ser slik ut:

$$\begin{aligned} C_m H_n + \lambda \left(m + \frac{n}{4} \right) (O_2 + 3.77 N_2) &\Leftrightarrow \\ m CO_2 + \frac{n}{2} H_2 O + (\lambda - 1) \left(m + \frac{n}{4} \right) O_2 + \lambda \left(m + \frac{n}{4} \right) 3.77 N_2 \end{aligned} \quad (2)$$

hvor $\lambda = 1/\varphi =$ virkelig luftmengde/støkiometrisk luftmengde

$\lambda =$ ”luftoverskudd

$\varphi =$ ”brenselsfaktor”

En gassturbin har et luftoverskudd på ca. $\lambda = 2.2\text{-}3$, hvilket gir ca. 3-4% CO₂ i eksosen ved forbrenning av naturgass. En moderne gassbrenner i en ovn kan gjerne ha et luftoverskudd ned mot 1.05. Et kullkraftverk har typisk et luftoverskudd på ca. ca. $\lambda = 1.2$, med ca. 12-14% CO₂ i eksosen.

I Tabell 2 er det gitt tre eksempler på bruk av Lign. (2).

Tabell 2 Molbalanser ved forbrenning (metan ved luftoverskudd 3 og 1.05, og propan ved luftoverskudd 3)

$$\begin{array}{ll} m=1 & \text{metan} \\ n=4 & \end{array}$$

Luftoverskudd 3

reaktanter	CmHn	O ₂	N ₂	sum	O ₂ -andel	CO ₂ -andel
antall mol	1	6	22.62	29.62	20.3 %	
produkter	CO ₂	H ₂ O	O ₂	N ₂	sum	
antall mol	1	2	4	22.62	29.62	13.5 %

3.4 %

$$\begin{array}{ll} m=3 & \text{propan} \\ n=8 & \end{array}$$

Luftoverskudd 3

reaktanter	CmHn	O ₂	N ₂	sum	O ₂ -andel	CO ₂ -andel
antall mol	1	15	56.55	72.55	20.7 %	
produkter	CO ₂	H ₂ O	O ₂	N ₂	sum	
antall mol	3	4	10	56.55	73.55	13.6 %

4.1 %

$$\begin{array}{ll} m=1 & \text{metan} \\ n=4 & \end{array}$$

Luftoverskudd 1.05

reaktanter	CmHn	O ₂	N ₂	sum	O ₂ -andel	CO ₂ -andel
antall mol	1	2.1	7.917	11.02	19.1 %	
produkter	CO ₂	H ₂ O	O ₂	N ₂	sum	
antall mol	1	2	0.1	7.917	11.02	0.9 %

9.1 %

Forholdet mellom karbon og hydrogen i brenslet innvirker på hvor mye CO₂ som dannes ved forbrenning. Se Figure 14 for en illustrasjon av dette.

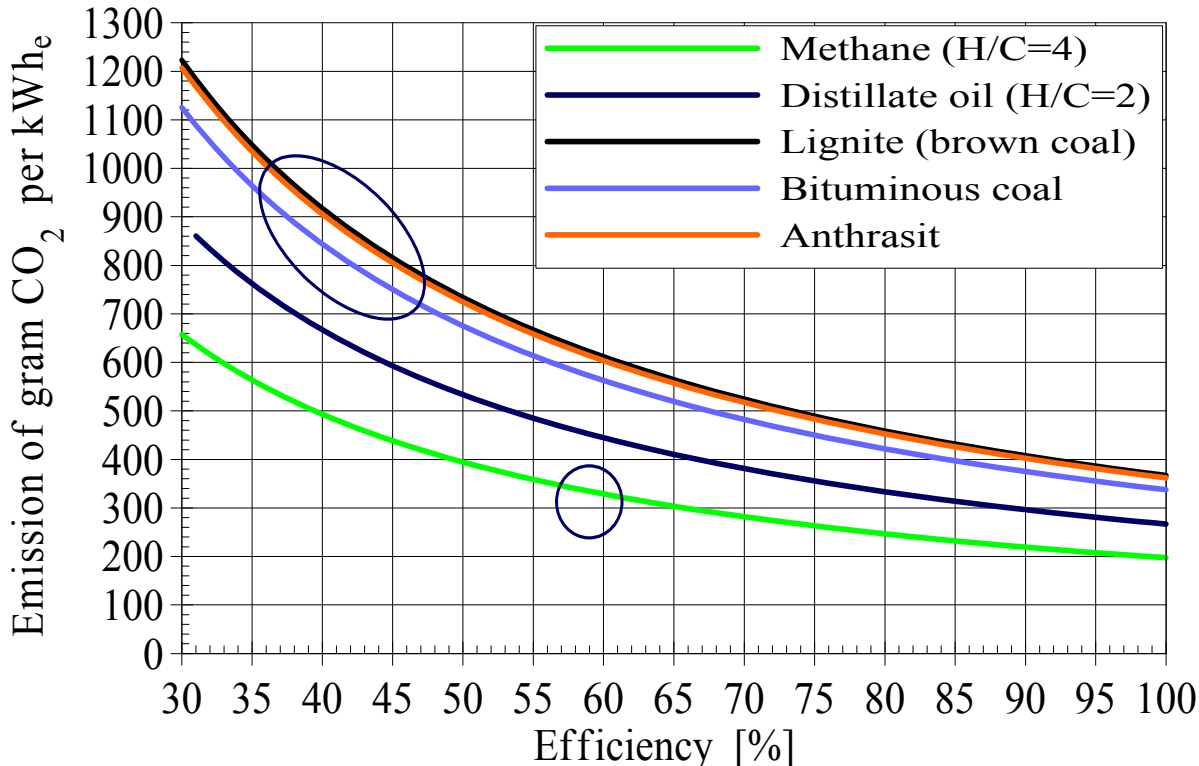
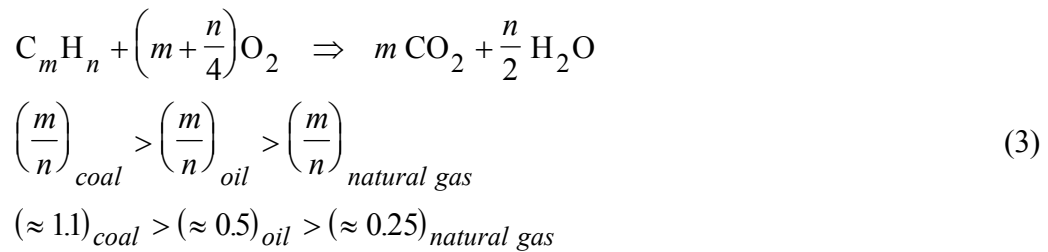


Figure 14 Dannelse av CO_2 ved forbrenning av metan/olje/kull. Verdiene ved 100% virkningsgrad karakteriserer hvor mye CO_2 som dannes på basis av brenslets brennverdi. De to ringene angir hvor mye CO_2 et stort moderne gasskraftverk og typisk godt kullkraftverk gir.

1.5 Brennverdi

Brennverdien for et brensel forteller om hvor mye energi som kan frigjøres ved forbrenning. Det finnes to definisjoner av brennverdien: Øvre og nedre brennverdi (HHV = Higher Heating Value, LHV = Lower Heating Value). Grunnen til at man kan definere to forskjellige brennverdier er at dannelsesentalpien til vann kan ha to verdier: En for væskeform og en for gassform. Hvis førstnevnte brukes får man HHV og sistnevnte gir LHV. Hva man bruker er en definisjonssak. LHV er den mest vanlige innen kraftverksindustrien, spesielt i Europa. I USA benyttes ofte HHV.

Ved å ta utgangspunkt i en enkel forbrenningsreaksjon:



Brennverdien kan beregnes med følgende uttrykk:

$$\begin{aligned}
 Q + \sum_r n_i \bar{h}_i &= \sum_p n_e \bar{h}_e \\
 \sum_r n_i \bar{h}_i &= -74873 + 2 \cdot 0 \\
 \sum_p n_e \bar{h}_e &= -393522 + 2 \cdot -241826_{gas} = -877174 \\
 Q &= -877174 + 74873 = 802301 \text{ kJ/kmol CH}_4 \\
 Q &= 802301 \text{ kJ/kmol CH}_4 = 50009 \text{ kJ/kg CH}_4
 \end{aligned} \tag{5}$$

Dannelsesentalpiene i Lign. (5) er ved 25 °C, 0.1 MPa. Q er her Nedre Brennverdi (LHV) for metan – CH₄, i og med at vi benytter dannelsesentalpien for vann i gassform (-241826 kJ/kmol) i beregningen. Hvis vi hadde benyttet dannelsesentalpien for vann i væskeform (-285830 kJ/kmol), så hadde Øvre Brennverdi (HHV) blitt beregnet til 890.3 MJ/kmol CH₄ eller 55.51 MJ/kg CH₄. For metan er HHV 11% høyere enn LHV. Et kraftverk med 50% virknings basert på LHV vil med metan som brensel ha en virkningsgrad på 45% basert på HHV.

I praksis regner man ikke ut brennverdien slik som vist ovenfor. Brennverdien for forskjellige stoffer er tabulert. Tabell 3 viser en typisk naturgassammensetning fra Kårstøterminalen. Brennverdien for hver komponent er angitt og den totale brennverdien regnes ut som et veid snitt med hensyn på massefraksjonene.

Tabell 3 *Eksempel på sammensetning av naturgass*

		Mol-%	Vekt-%	Nedre brennverdi kJ/kg	Gasskonstant J/(kg·K)	Tetthet kg/Sm ³
Nitrogen	N ₂	0.718	1.09	0.	295.27	1.2563
Karbondioksid	CO ₂	0.604	1.44	0.	188.92	1.9635
Metan	CH ₄	84.220	73.22	50057.4	518.28	0.7157
Etan	C ₂ H ₆	13.522	22.02	47504.3	276.51	1.3415
Propan	C ₃ H ₈	0.823	1.97	46374.2	188.56	1.9673
Isobutan	C ₄ H ₁₀	0.031	0.10	45662.7	143.05	2.5931
Normalbutan	C ₄ H ₁₀	0.052	0.16	45746.4	143.05	2.5931
Total		99.97	100.0	48145.6	450.41	0.8236

Duggpunkt: 40 °C

Svovelinnhold: 1 mg/kg = 0.00012 % (vektbasis)

Sm³ = Standardkubikkmeter (1.013 bar, 15 °C)

1.6 Virkemåte for aksiell kompressor og turbin

Kompressor og turbin er bygget opp av trinn, hvor hvert trinn består av en stillestående rad (tangentiell) av skovler ("stator", "ledeskovl") og en rekke av roterende skovler ("rotor", "løpeskovler"). Skovlene er sammenlignbare med vifteblad. I en kompressor overføres mekanisk arbeid til kinetisk energi på gassen (luft) ved hjelp av bevegelige skovler. I de stillestående skovlene

overføres så kinetisk energi til trykkenergi. I en turbin så skjer denne prosessen i omvendt rekkefølge, hvor hensikten er å lage mekanisk arbeid.

I Figure 15 og Figure 16 er geometri og strømningsbilde vist for et aksialt kompressortrinn. Tilsvarende for et aksialt turbintrinn i Figure 17 og Figure 18.

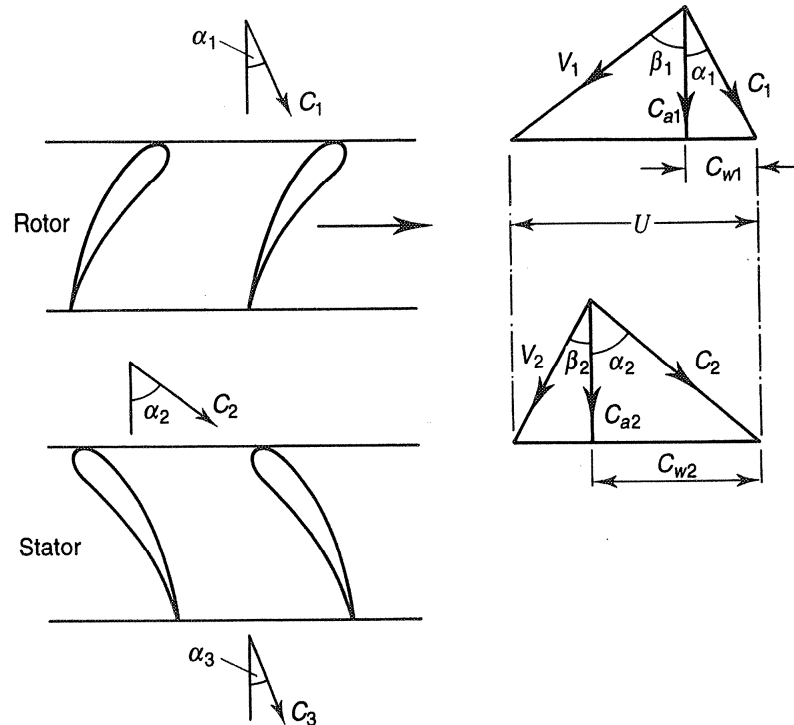


Figure 15 Hastighetsdiagram for et kompressortrinn. Strømningsretningen er vertikal, fra toppen.

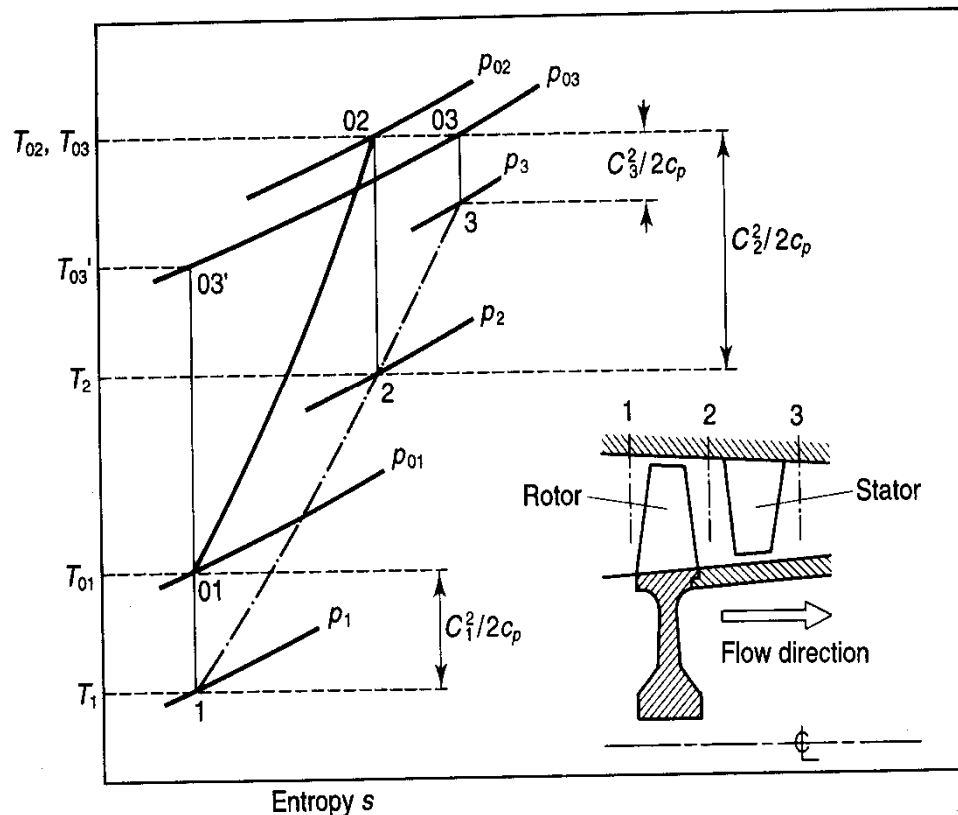


Figure 16 Temperatur-entropidiagram for et kompressortrinn.

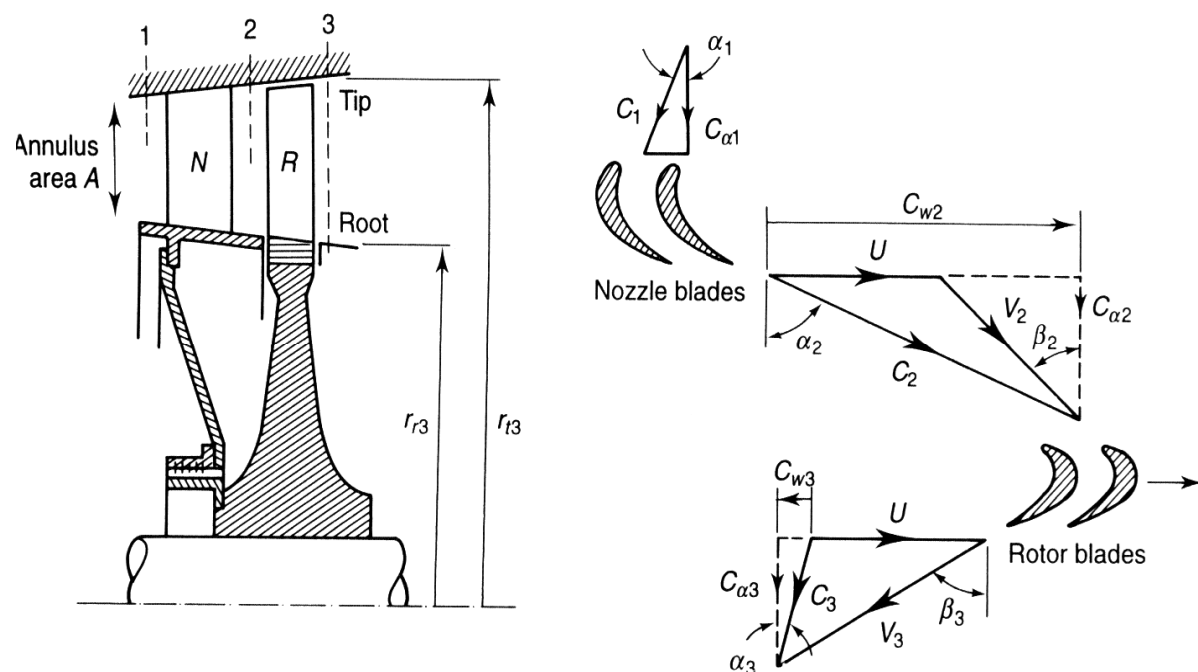


Figure 17 Hastighetsdiagram for et turbintrinn.

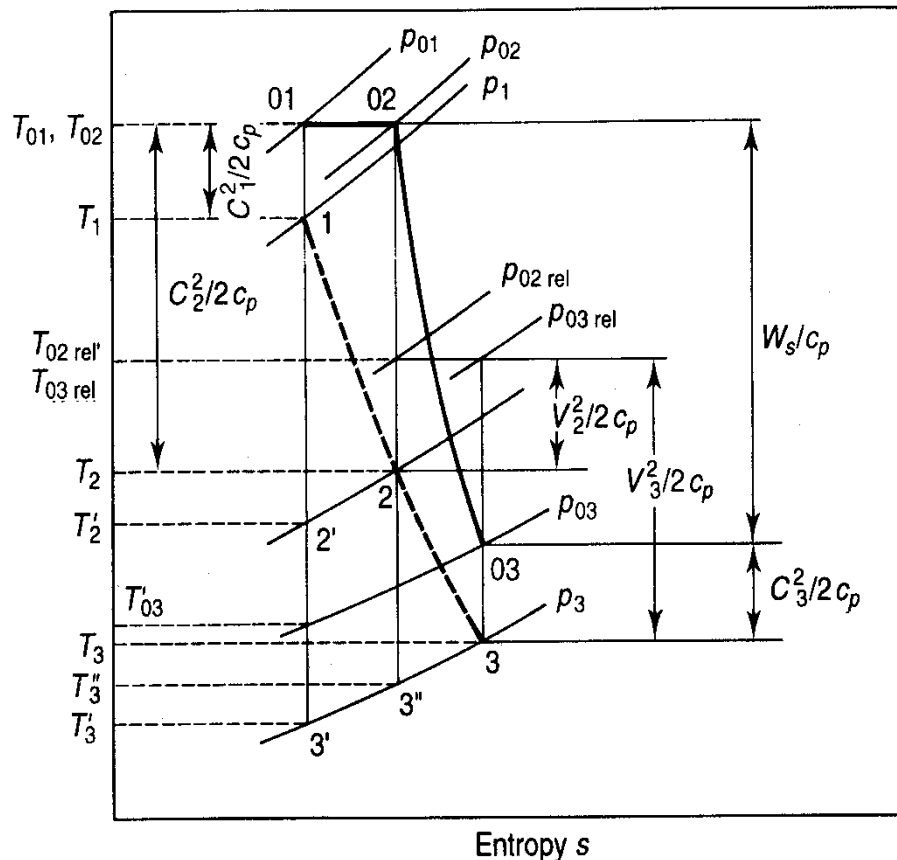


Figure 18 Temperatur-entropidiagramm for et turbintrinn.

1.7 Air intake system

Impurities in inlet air build up on the internal components of the engine. They change the compressor characteristics and can lead to surge conditions. They also reduce the efficiency of the compressor. Coarse dirt in the inlet air erodes the coatings of the components. Poor filtration results in blocking the cooling passages to the rotor blades. Inertial filtration is normally used to remove large particles. It is normally followed by self-cleaning filters, which detect the increase in pressure drop across the filter and release air pulses to remove the dirt. Most filtration systems have a “blow-in” door located downstream of the filter. It opens automatically when the differential pressure between the area downstream of the filter and the outside exceeds a preset value. This door prevents excessive and damaging differential pressure across the filter. However, when the door opens, unfiltered air enters the engine. This increases fouling and possible bug and bird entry into the engine. The ambient air conditions should be evaluated carefully to determine the particle size and concentration in the area before specifying the type of filtration required. Most axial compressor fouling is caused by particles in the 0.3-3 μm range. The filtration system should be specified to remove the whole range of particles encountered. The flexible sealing bands between sections of the intake should be checked routinely for cracks. Unfiltered air enters the engine through such cracks causing damage to the engine.

1.8 Compressor cleaning

Dirt accumulation on the compressor blades changes the compressor characteristics and reduces the output power. The compressor can be cleaned using these five methods:

1. Disassemble the compressor partially to clean the blades of the rotor. This method gives excellent results, but it is very time-consuming.
2. Some manufacturers recommend cleaning the compressor by using ground shell injected into the inlet by a high-velocity air stream. They remove buildup by an abrasive fashion. This method cannot be used with engines having coating on the blades, because they will be eroded. This method is normally done while the compressor is being rotated by the starter. Many users have difficulty with this method because the ground shell enters the hydraulic fluid of the governing system and the pressurizing air for seals and bearings, thus blocking passages. This method cannot be used with units having air-cooled turbine blades (rotating or stationary).
3. Liquid wash while the compressor rotor is on starter. Demineralized water mixed with a detergent is injected to wash the contaminants off the blades. This is followed by a demineralized water rinse and an air-dry cycle while the machine is on starter. Another technique (called soakwash cycle) involves injecting demineralized water while the engine is stopped. The water is allowed to soak to loosen the dirt accumulation before injecting the mixture of demineralized water and detergent into the engine.
4. A “crank cleaning” method involves a soak, followed by an abrasive shell cleaning, a rinse, and a drying cycle.
5. A recent method was developed for on-wing cleaning of aircraft engines (on-line or fired washing). It involves washing the gas generator by spraying a special cleaning liquid into the compressor inlet while the engine is running. The speed of rotation during the cycle and the cleaning liquid are specified by the manufacturer.

1.9 Relation between isentropic and polytropic efficiencies

For compressor and turbine simulation, the polytropic efficiencies are converted into isentropic efficiencies to calculate the exit states. In the generic cooled gas turbine model presented in this report, the so-called ASME method is used for this conversion. The ASME method is described in Section 1.9.2.

However, the ASME method requires that the density (or the specific volume) of the working fluid can be calculated at the inlet state, the isentropic outlet state and the outlet state of the compressor or turbine. If the density is not available, a simplified method using the specific heat ratio, κ , can be employed instead. The simplified method is described in Section 1.9.1. The ASME method is the best choice from a thermodynamic point of view, since it considers real gas effects. The simplified method assumes that the working fluid is ideal gas and the isentropic exit state is not considered. Nevertheless, the difference in the calculated exit temperature and specific work is quite small for the two methods.

For an air compressor with a polytropic efficiency in a range (90-92 %) around the value used in this report (91.5 %), the difference in outlet temperature varies from 0.4-0.5 °C (or 0.12-0.16 %, the unit for temperature is degrees Celsius) for a pressure ratio of 10 to 3-4 °C (or 0.5-0.7 %) for a pressure ratio of 40. For the compressor specific work, the difference is 0.4-0.5 kJ/kg (0.1-0.2 %) for a pressure ratio of 10 and 3.5-4.6 kJ/kg (0.6-0.7 %) for a pressure ratio of 40. With a pressure ratio of 17 and a polytropic efficiency of 91.5 %, the exit temperature difference is 1 °C (0.2 %) and the specific work difference is 1.1 kJ/kg (0.3 %). Low polytropic efficiency results in larger

differences. The simplified method gives higher exit temperature and specific work than the ASME method.

For an air-based turbine with a *TIT* of 1230 °C and a polytropic efficiency in the range (85-87 %) around the value used in this report (85.7 % for the cooled base case turbine), the exit temperature varies between 0.9-1 °C (or 0.13-0.15 %) for a pressure ratio of 10 and 2.9-3.3 °C (or 0.7-0.8 %) for a pressure ratio of 40. The turbine specific work varies with 1-1.2 kJ/kg (or 0.15-0.17 %) for a pressure ratio of 10 and 3.3-3.8 kJ/kg (or 0.3-0.4 %) for a pressure ratio of 40. With a pressure ratio of 17 and a polytropic efficiency of 85.7 %, the exit temperature difference is 1.7 °C (0.3 %) and the specific work difference is 2.0 kJ/kg (0.2 %). Low polytropic efficiency results in larger differences. The simplified method gives lower specific work and higher exit temperature compared with the ASME method.

1.9.1 Simplified method

The relation between the isentropic (η_{is}) and the polytropic efficiency (η_p), assuming ideal gas, are given by Equations (6) and (7). The mean specific heat ratio, κ , is evaluated at the mean logarithmic temperature and pressure, Equations (8) and (9).

$$\eta_{is} = \frac{\frac{p_{out}}{p_{in}}^{\left(\frac{\kappa-1}{\kappa}\right)} - 1}{\frac{p_{out}}{p_{in}}^{\left(\frac{\kappa-1}{\kappa}\eta_p\right)} - 1} \quad (\text{compressor}) \quad (6)$$

$$\eta_{is} = \frac{1 - \frac{p_{out}}{p_{in}}^{\left(\frac{\kappa-1}{\kappa}\eta_p\right)}}{1 - \frac{p_{out}}{p_{in}}^{\left(\frac{\kappa-1}{\kappa}\right)}} \quad (\text{turbine}) \quad (7)$$

$$T_{mean} = \frac{T_{in} - T_{out}}{\ln\left(\frac{T_{in}}{T_{out}}\right)} \quad (8)$$

$$p_{mean} = \frac{p_{in} - p_{out}}{\ln\left(\frac{p_{in}}{p_{out}}\right)} \quad (9)$$

p	pressure	Pa
T	temperature	K
κ	specific heat ratio, c_p/c_v	-
η_p	polytropic efficiency	-, %
η_{is}	isentropic efficiency	-, %
ρ	density	kg/m ³
<i>in</i>	compressor/turbine inlet	
<i>out</i>	compressor/turbine exit	

out,s exit state after isentropic compression/expansion

1.9.2 ASME method

In the ASME method, the relation between the isentropic efficiency (η_{is}) and the polytropic efficiency (η_p) is given by Equation (10) for a compressor and Equation (11) for a turbine. In these relations, the isentropic (n_s) and polytropic coefficients (n) are defined as in Equations (12) and (13). This method is described in the PRO/II manual (version 7, SimSci-Esscor) and the HYSYS manual (Operations Guide, version 3.1, Hyptech).

The Equations (10) and (11) are derived using the expression for the polytropic and isentropic work, Equation (14), where n is a volume exponent that is equal to the isentropic coefficient when the isentropic work is calculated and to the polytropic coefficient when the polytropic work is calculated. CF is a correction factor that allows for real gas effects (Equation (15)); it is usually close to 1. For an ideal gas, CF is exactly 1 and the isentropic coefficient (n_s) is equal to the heat capacity ratio (κ). The polytropic and isentropic efficiencies are related by Equation (16) for a compressor and Equation (17) for a turbine. The correction factor cancels out when the ratio between the polytropic and isentropic works is calculated and the Equations (10) and (11) are the results.

$$\eta_p = \eta_{is} \cdot \frac{\left[\left(\frac{p_{out}}{p_{in}} \right)^{\left(\frac{n-1}{n} \right)} - 1 \right] \cdot \left[\left(\frac{n}{n-1} \right) \cdot \left(\frac{(n_s-1)}{n_s} \right) \right]}{\left[\left(\frac{p_{out}}{p_{in}} \right)^{\left(\frac{(n_s-1)}{n_s} \right)} - 1 \right]} \quad (compressor) \quad (10)$$

$$\eta_p = \eta_{is} \cdot \frac{\left[\left(\frac{p_{out}}{p_{in}} \right)^{\left(\frac{(n_s-1)}{n_s} \right)} - 1 \right]}{\left[\left(\frac{p_{out}}{p_{in}} \right)^{\left(\frac{n-1}{n} \right)} - 1 \right] \cdot \left[\left(\frac{n}{n-1} \right) \cdot \left(\frac{(n_s-1)}{n_s} \right) \right]} \quad (turbine) \quad (11)$$

$$n_s = \frac{\ln\left(\frac{p_{out}}{p_{in}}\right)}{\ln\left(\frac{\rho_{out,s}}{\rho_{in}}\right)} \quad (12)$$

$$n = \frac{\ln\left(\frac{p_{out}}{p_{in}}\right)}{\ln\left(\frac{\rho_{out}}{\rho_{in}}\right)} \quad (13)$$

$$w = \left(\frac{n}{n-1} \right) \cdot CF \cdot \left(\frac{p_{in}}{\rho_{in}} \right) \cdot \left[\left(\frac{p_{out}}{p_{in}} \right)^{\left(\frac{n-1}{n} \right)} - 1 \right], n = n \Rightarrow w_p, n = n_s \Rightarrow w_{is} \quad (14)$$

$$CF = \frac{h_{out,s} - h_{in}}{\left(\frac{n_s}{n_s - 1} \right) \cdot \left(\frac{p_2}{\rho_{out,s}} - \frac{p_1}{\rho_1} \right)} = \frac{h_{out,s} - h_{in}}{\left(\frac{n_s}{n_s - 1} \right) \cdot \left(\frac{p_{in}}{\rho_{in}} \right) \cdot \left[\left(\frac{p_{out}}{p_{in}} \right)^{\left(\frac{n_s-1}{n_s} \right)} - 1 \right]} \quad (15)$$

$$\eta_p = \frac{w_p}{w_{is}} \cdot \eta_{is} \quad (\text{compressor}) \quad (16)$$

$$\eta_p = \frac{w_{is}}{w_p} \cdot \eta_{is} \quad (\text{turbine}) \quad (17)$$

CF	correction factor	-
h	mass specific enthalpy	J/kg
n	polytropic coefficient or polytropic volume exponent	-
n_s	isentropic coefficient or isentropic volume exponent	-
p	pressure	Pa
w_{is}	isentropic work	J/kg
w_p	polytropic work	J/kg
η_p	polytropic efficiency	-, %
η_{is}	isentropic efficiency	-, %
ρ	density	kg/m ³
<i>in</i>	compressor/turbine inlet	
<i>out</i>	compressor/turbine exit	
<i>out,s</i>	exit state after isentropic compression/expansion	

The relations above are illustrated in Figure 19 and Figure 20. Figure 19 was calculated with the compressor inlet pressure 1.01325 bar, no inlet pressure loss and the ambient air defined in this report. Figure 20 was calculated with the turbine inlet temperature and composition from the base case of the cooled generic turbine and the turbine exit pressure was 1.02325 bar. The cooling fraction was the same as in the base case for all polytropic efficiencies.

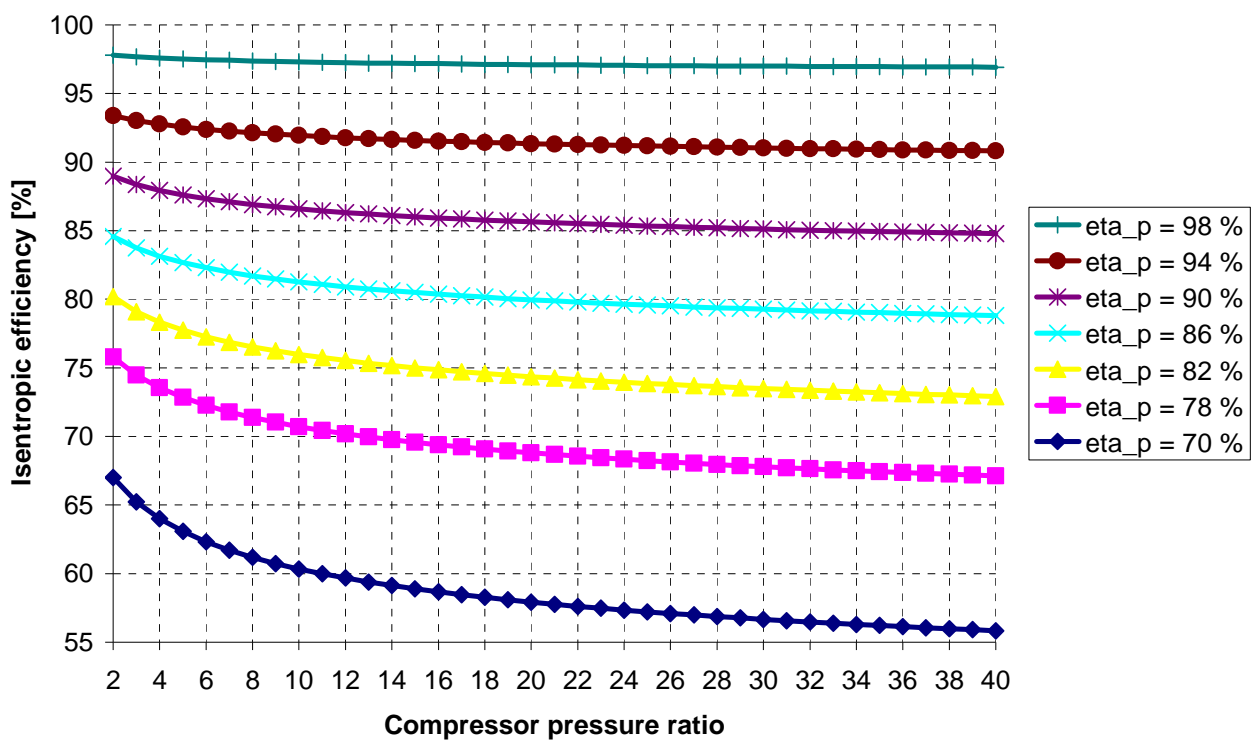


Figure 19 Relation between isentropic and polytropic efficiency for a compressor (ASME method)

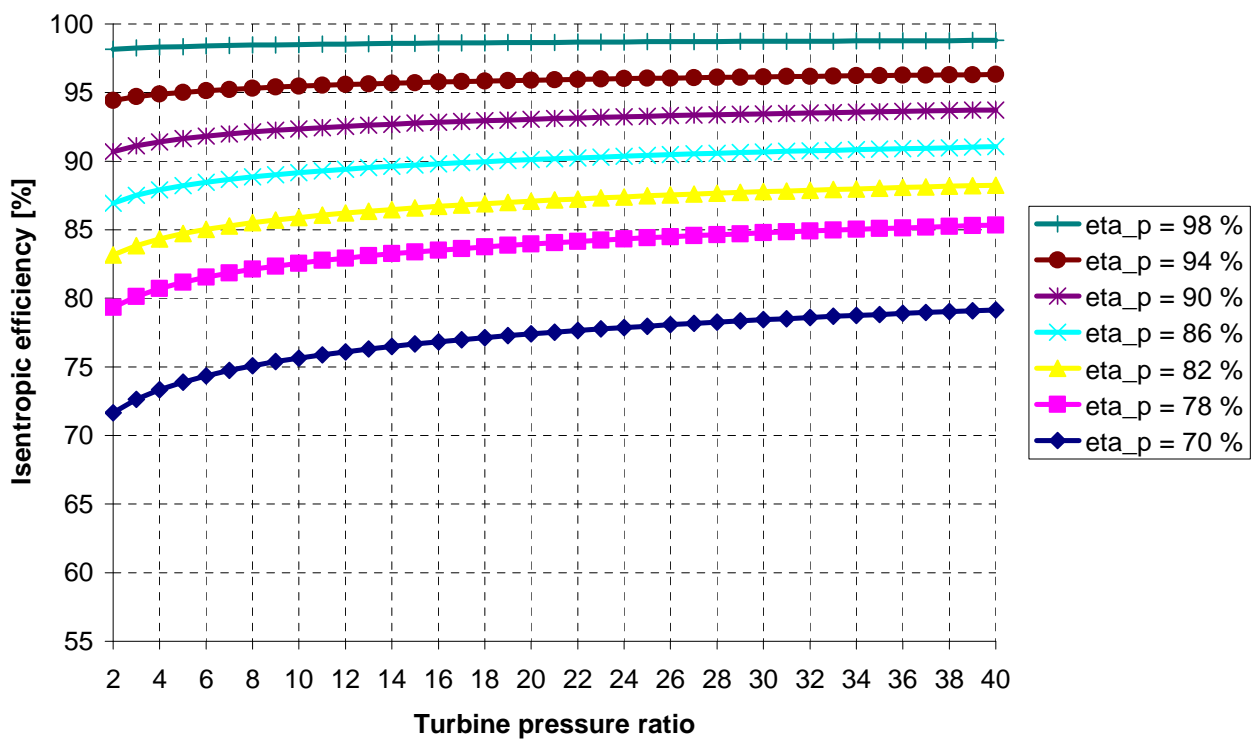


Figure 20 Relation between isentropic and polytropic efficiency for a turbine (ASME method)

1.10 Gassturbinens innløpstemeratur

Innløpstemperaturen på gassturbinen er en viktig størrelse. Virkningsgrad, effekt og trykkforhold influeres av innløpstemperaturen. Dagens utviklingstendens for gassturbiner viser at innløpstemperaturen er det viktigste området for forbedringer av gassturbinens ytelse. Det finnes imidlertid forskjellige måter å definere denne temperaturen på. Tre definisjoner vil her bli gitt. Felles for disse er at temperaturen er ved stagnasjonstilstand. Figure 21 viser en beregningsmodell for energibalansen i gassturbinen. Tabell 4 definerer størrelsene som er benyttet i definisjonen av innløpstemperaturene. Formlene som beskrives i kapittel 1.10.1-1.10.3 viser innløpsentalpien. Denne kan brukes til å beregne innløpstemperaturen.

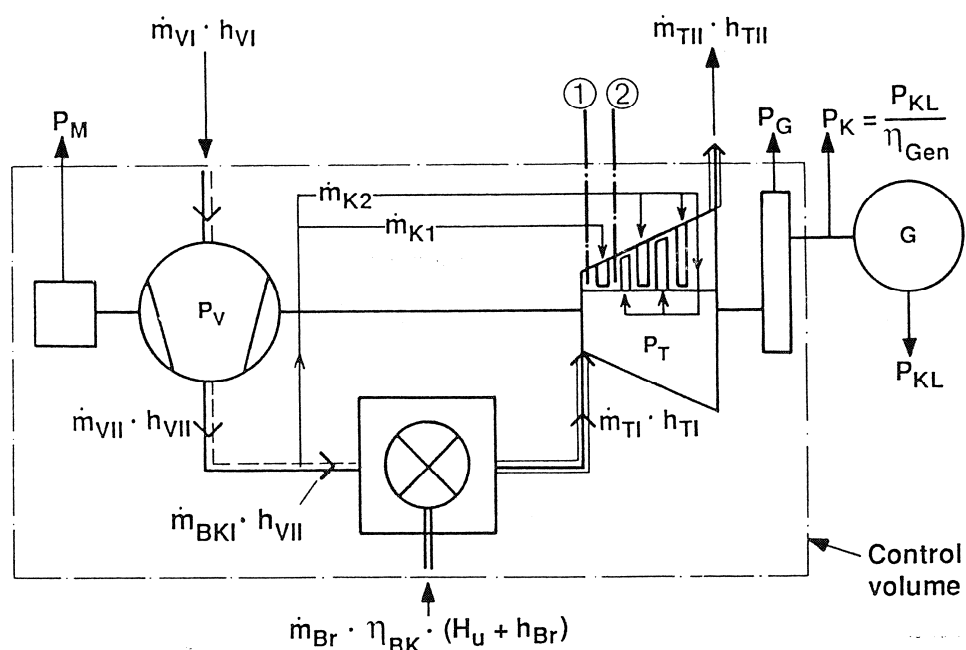


Figure 21 Beregningsmodell

Tabell 4 Definisjoner for beregningsmodell

Symbol	Unit	Definition
\dot{m}_{VI}	kg/s	Flow rate of air entering the compressor
\dot{m}_{VII}	kg/s	Flow rate of air leaving the compressor
\dot{m}_{BKI}	kg/s	Flow rate of air entering the combustion chamber
\dot{m}_{TI}	kg/s	Flow rate of flue gas entering the turbine
\dot{m}_{TII}	kg/s	Flow rate of flue gas leaving the turbine
\dot{m}_{Br}	kg/s	Flow rate of fuel entering the combustion chamber
\dot{m}_{K1}	kg/s	Flow rate of cooling air entering the turbine before the plane 2
\dot{m}_{K2}	kg/s	Flow rate of cooling air entering the turbine behind the plane 2
h_{VI}	kJ/kg	Specific enthalpy of air at the temperature entering the compressor
h_{VII}	kJ/kg	Specific enthalpy of air at the temperature leaving the compressor
h_{TI}	kJ/kg	Specific enthalpy of flue gas at the temperature entering the turbine
h_{TII}	kJ/kg	Specific enthalpy of flue gas at the temperature leaving the turbine

h_{Br}	kJ/kg	Specific enthalpy of fuel at the temperature entering the combustion chamber
H_u	kJ/kg	Lower heating value of the fuel
η_{BK}	%	Combustion chamber efficiency
η_{Gen}	%	Generator efficiency
P_K	KW	Shaft power output
P_{KL}	KW	Generator terminal power output
P_M	KW	Mechanical losses
P_G	KW	Gear friction losses
P_T	KW	Turbine output
P_V	KW	Compressor output

1.10.1 ISO innløpstemperatur

Denne er definert i ISO 3214 "Gas turbines – Acceptance tests" og i DIN 4314.

$$h_{TI\ ISO} = \frac{\dot{m}_{VI}}{\dot{m}_{TI\ ISO}} h_{VII} + \frac{\dot{m}_{Br} \eta_{BK} (h_u + h_{Br})}{\dot{m}_{TI\ ISO}}, \quad \dot{m}_{TI\ ISO} = \dot{m}_{VI} + \dot{m}_{Br} \quad (18)$$

Denne definisjonen gir temperaturen ved blanding av kjøleluft og eksos fra brennkammeret. Denne temperaturen har liten fysisk mening, fordi den ikke finnes på noe sted i gassturbinen. Den beskriver likevel hva man kan kalle "effektiv" innløpstemperatur. Ved håndbergning av gassturbiner ved hjelp av isentropiske relasjoner gir bruk av denne innløpstemperaturen tilnærmet riktig resultat, uten at man behøver å regne i detalj på skovlkjøling.

Denne definisjonen benyttes av leverandører som Siemens og Alstom Power..

1.10.2 "Firing inlet temperature"

Denne definisjonen gir den fysiske stagnasjonstemperaturen etter første ledeskovl. Det betyr blandingstemperaturen av kjøleluft til første ledeskovl og eksos fra brennkammeret.

$$h_{TI,2} = \frac{\dot{m}_{VI} - \dot{m}_{K2}}{\dot{m}_{TI,2}} h_{VII} + \frac{\dot{m}_{Br} \eta_{BK} (h_u + h_{Br})}{\dot{m}_{TI,2}} \quad (19)$$

$$\dot{m}_{TI,2} = \dot{m}_{VI} - \dot{m}_{K2} + \dot{m}_{Br}$$

Dette er den mest brukte definisjonen av innløpstemperatur for gassturbiner. Forskjellen mellom definisjon i seksjon 1.10.1 og 1.10.2 er for dagens gassturbiner ca. 50-70 °C. For neste generasjon av gassturbiner vil denne differansen øke til over 100 °C på grunn av større kjøleluftmengder.

1.10.3 Temperatur foran første ledeskovl – brennkammer utløpstemperatur

Denne definisjonen gir temperaturen gir temperaturen på eksosen fra brennkammeret like før første ledeskovl.

$$h_{TII,1} = \frac{\dot{m}_{VI} - \dot{m}_{K1} - \dot{m}_{K2}}{\dot{m}_{TII,1}} h_{VII} + \frac{\dot{m}_{Br} \eta_{BK} (h_u + h_{Br})}{\dot{m}_{TII,1}} \quad (20)$$

$$\dot{m}_{TII,1} = \dot{m}_{VI} - \dot{m}_{K1} - \dot{m}_{K2} + \dot{m}_{Br}$$

Denne temperaturen brukes ikke av leverandørene i noe særlig grad. I lærebøker og i fag som Termodynamikk og Strømningsslære er denne temperaturen benyttet. Uten kjøling er denne temperaturen lik temperaturene gitt i de to tidligere nevnte definisjonene. Moderne gassturbiner har imidlertid kjøling, noe som fører til at denne temperaturen ikke gir et riktig bilde ved beregning av gassturbinprosessen.

ENGLISH:

The TIT is defined in various ways:

- 1) Combustor exit stagnation (or total) temperature
- 2) Stagnation (or total) temperature after the first row of stator blades and before the first row of rotor blades; ‘first rotor inlet’ temperature’
- 3) Temperature as defined in the ISO 2314:1989, 8.6, which is the mixing temperature (stagnation) of the combustion chamber exit stream and the cooling air streams.

The TIT for a given case is higher for definition 1) compared to definition 2), which is higher than definition 3). The size of the differences depends on how much cooling air is used. If no cooling is applied, all the three definitions give the same temperature.

The historical development of TIT is depicted in Figure 22.

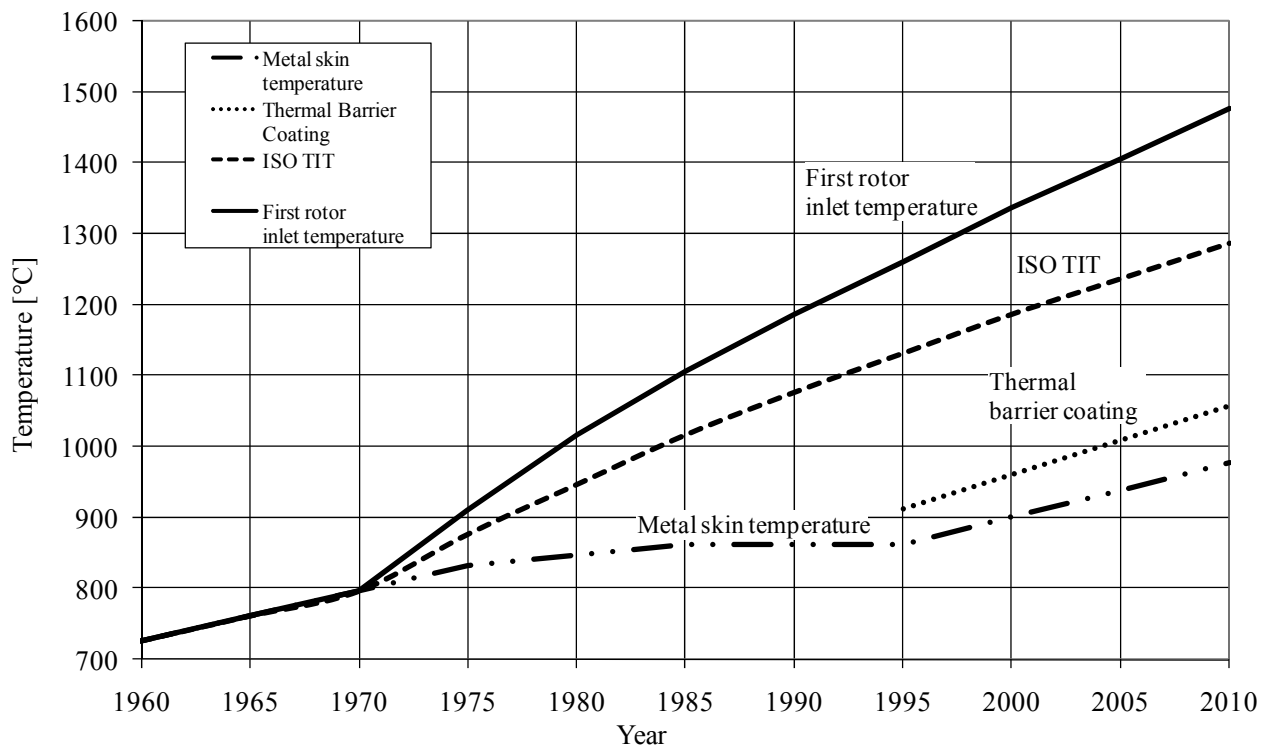


Figure 22 Development of turbine inlet temperature (definition in ISO 2314:1989, 8.6), first rotor inlet temperature and metal skin temperature

A critical factor in the gas turbine development was the rapid adaptation of aero-engine technology (single crystal airfoils, sophisticated cooling techniques, and thermal barrier coatings) in order to operate at the high rotor-inlet temperatures required for high efficiency generation. Early reliability problems have been largely overcome, so that this type of power generation system is now considered to be a mature technology capable of achieving high levels of availability. Current interest in replacing natural gas with gas derived from coal (syngas or hydrogen) in these gas turbine systems focuses attention on implications for the critical turbine components.

When looking at a flow diagram of a gas turbine cycle, one can easily get the impression that a gas turbine is a collection of unit operations connected by flow pipes. However, a gas turbine is a very integrated system. One cannot simply take one compressor here, pick a turbine there, and put in a reactor between them for the combustion of the fuel. A gas turbine must be looked upon as an engine, where the compressor, combustion chamber and turbine are designed to fit each other. If for example the compressor is to be exchanged, this requires a major redesign of the whole gas turbine system. For many advanced gas turbine cycles with CO₂ capture, there may be no existing gas turbines which can be used. Modifying a gas turbine or designing a new one is a major challenge for which the cost and time needed are significant. As a consequence, gas turbine manufacturers hesitate to start modifying their existing models.

1.11 Turbine cooling

1.11.1 Background

High-temperature gas turbines require blade-cooling. In virtually all practical gas turbines, this is accomplished by using air extracted from the gas turbine compressor to flow through the blades, cooling them by convection, then exiting from the blades and mixing with the hot gas flowing through the turbine (convection air-cooling). In some of the more advanced designs, the air exits from the blades through a large number of strategically-placed small holes to form a film of spent cooling air, partially shielding the blades from the hot gases (Film air-cooling). Recently, some new designs of large gas turbines, intended for use in combined cycles, have begun to utilise steam from the bottoming cycle as a gas turbine coolant. This steam is heated as it flows through a closed circuit within the gas turbine blades and is then returned to the steam path of the combined cycle, improving the overall plant efficiency.

Turbine cooling is necessary when using turbine inlet temperatures (TIT) above what is acceptable for blade materials in the turbine. An increase in TIT, matched with an optimised pressure ratio, enables an increase in gas turbine efficiency. The use of cooling fluid causes losses to occur:

- 1) Mixing of hot gas and cooling fluid reduces the temperature of the expanding gas through the turbine, which reduces the turbine work.
- 2) Mixing of the cooling fluid in the hot gas path reduces the momentum of the hot gas as the cooling fluid has to be accelerated up to speed and direction of the hot gas.
- 3) Mixing of the cooling fluid causes disturbances to the flow profile around the blades and increases flow losses.

For a given level of cooling technology, an increase in TIT results in increased efficiency until a point where the gain from increased in TIT is outbalanced by the losses caused by the cooling fluid.

The historical development of TIT is depicted in Figure 22 and Figure 23.

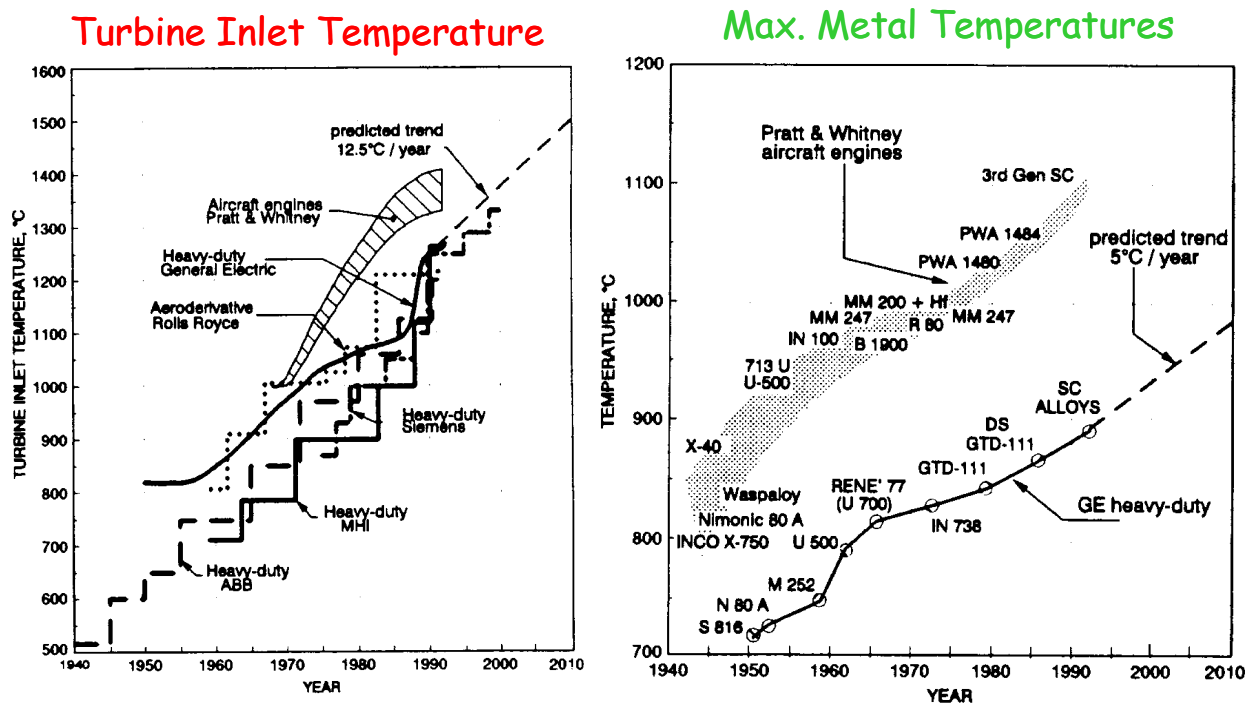


Figure 23 Development of turbine inlet temperature (firing inlet temperature or first rotor inlet temperature) and metal temperature for both aircraft engines and industrial gas turbines.

1.11.2 Typer turbinkjøling

Det finnes mange prinsipper for skovlkjøling. De viktigste er vist i Kombinasjoner av to forskjellige metoder i en og samme gassturbin er vanlig.

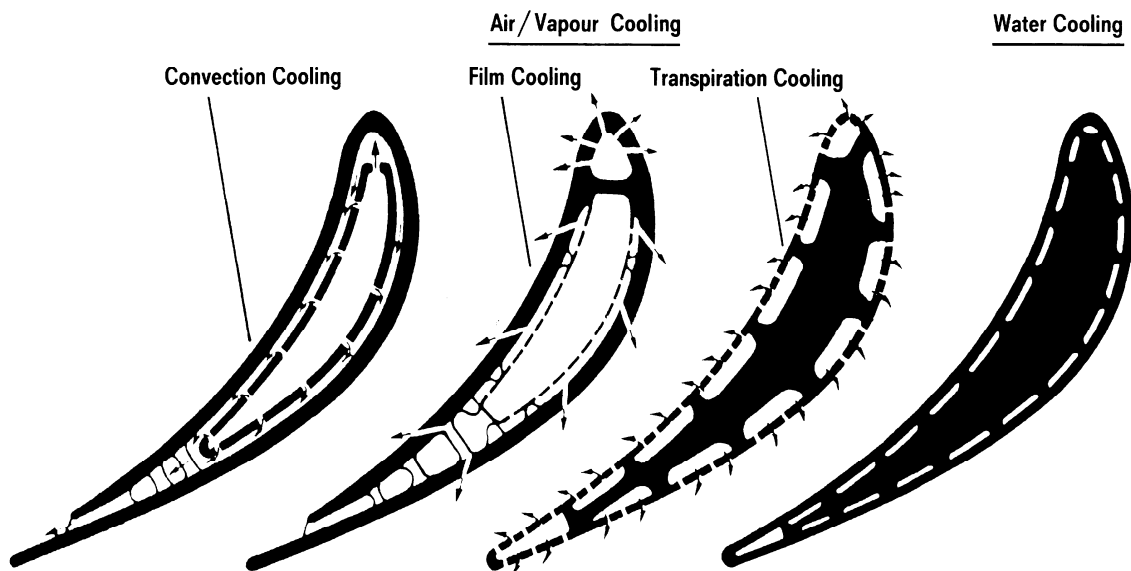


Figure 24 Prinsipper for kjøling av skovler i turbin

1.11.2.1 Konveksjonskjøling

Kjøleluften ledes i hulrom/kanaler i skovlen og varmeoverføringen skjer konvektivt fra veggen i skovlmaterialet (se til venstre i Figure 24). Bedret varmeovergang oppnås ved å bygge inn ribber, finner og geometri som gir turbulent strømning. Kjøleluften ledes vanligvis ut fra skovlens bakkant. viser konveksjonskjøling i et snitt av en skovl.

Prellekjøling eller ”impingement”-kjøling er en form for konveksjonskjøling, hvor man øker varmeovergangen ved å la kjøleluften strømme gjennom ”dyser” vinkelrett og med stor hastighet inn mot skovlveggen. Man unngår oppbygging av grensesjikt. Dette er en vanlig teknikk brukt i soner med stor varmebelastning.

1.11.2.2 Filmkjøling

Ved å lede kjøleluften gjennom skovlveggen i små hull og la den strømme som en film utvendig langs skovflaten oppnåes meget god kjøleeffekt for metalloverflaten (se nr. 2 fra venstre i Figure 24). På utsiden av skovlen får en dermed et grensesjikt som isolerer. Hullene bores gjerne i rekker utover langs skovlen, og slik at kjøleluftstrømmen ledes i gassretningen. En ulempe med filmkjøling er at strømningsforholdene rundt skovlen forstyrres og øker såkalte profiltap. På en annen side er det mulig å benytte meget høy innløpstemperatur som oftest oppveier økte profiltap. Figure 25 viser en filmkjølt skovl.

*(h

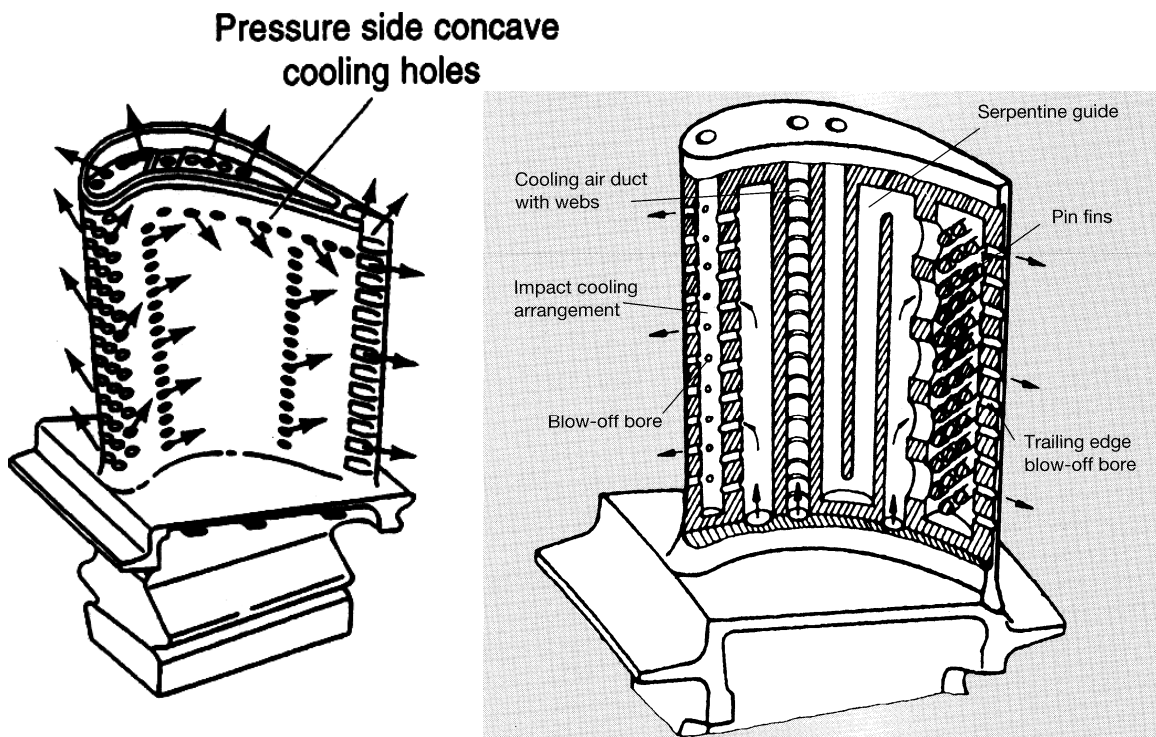


Figure 25 Filmkjøling av turbinskovl

1.11.2.3 Transpirasjonskjøling

Transpirasjonskjøling er en videreutvikling av filmkjøling, hvor man tilstreber at kjøleluften skal transpirere gjennom skovlveggen (se nr. 3 fra venstre i Figure 24). Dette oppnåes ved å øke antall hull og redusere hultverrsnittene, eller ved å benytte et porøst materiale som slipper kjøleluften gjennom. Dette er en avansert kjølemetode som ennå ikke har blitt utprøvd. Utfordringen er å finne et metall/legering som er både sterk og porøs nok.

1.11.2.4 Vann/dampkjøling

Luft har forholdsvis lav varmekapasitet som begrenser varmeovergangen. Vanndamp har ca. dobbelt så stor varmekapasitet som luft, mens vann har ca. 4 ganger varmekapasiteten til luft. Dette tilser at vann kan øke varmeovergangstallet samt transportere mer varme per kg kjølemedium.

Det er forskjellige måter å vannkjøle skovlene på:

- Vannet tilføres ved skovlroten, og konverteres til damp før den når spissen. Der blir den injisert i gasstrømmen.
- Vannet tilføres ved skovlroten, og går via kanaler tilbake til skovlroten og føres vekk.

Vannkjøling er ikke brukt i dagens gassturbiner. Problemene ved å bruke vann i væskeform er for det første vibrasjoner på grunn av at en stor masse væske settes i bevegelse med mulig bobledannelse på grunn av lokal koking, samt store temperaturgradiente i skovlveggene.

Bruk av damp har blitt att i bruk som kjølemedium i gassturbiner. I Figure 26 og Figure 27 er dampkjølingsprinsippet til GE vist. Dampen som benyttes til kjøling går i et lukket system som er koblet til en dampturbinprosess. Kald reheat-damp (ut av høytrykks dampturbin) på ca. 25-30 bar benyttes til kjølingen.

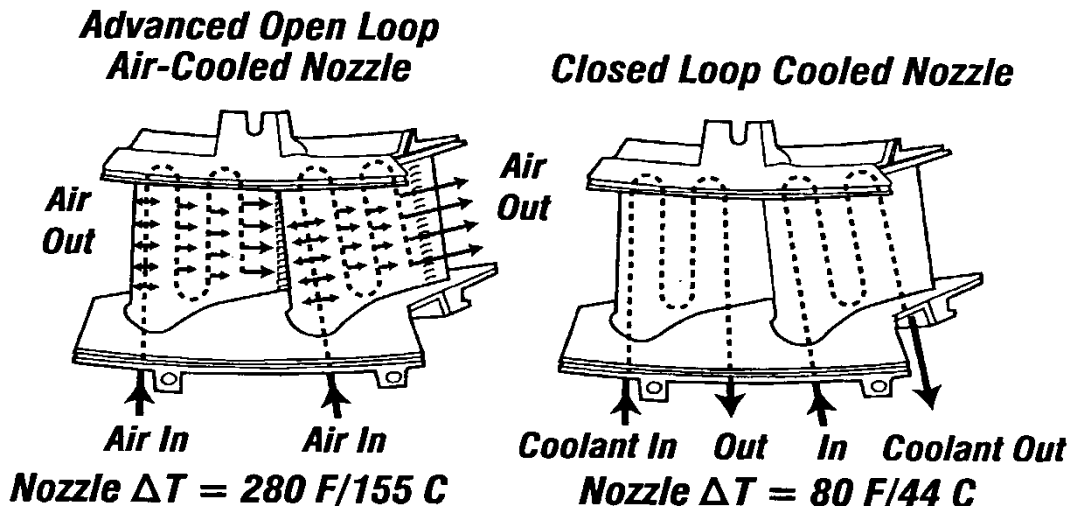
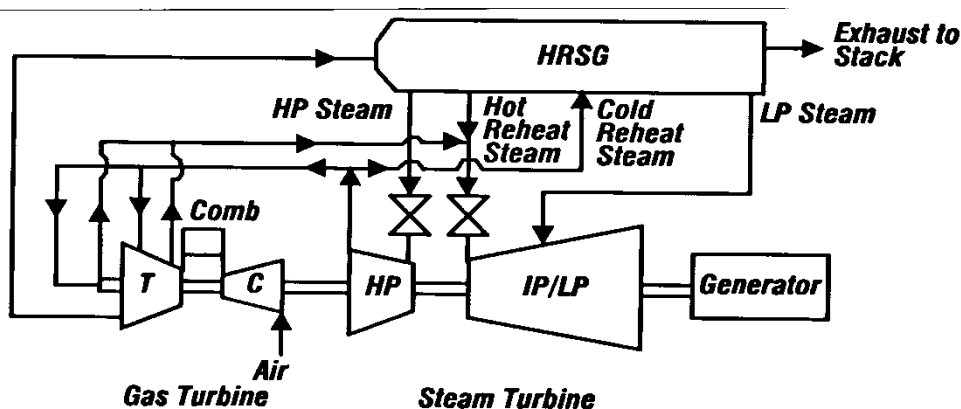


Figure 26 Dampkjøling av turbinskovl. Eksempel fra General Electric hvor luftkjøling og dampkjøling av første ledeskovlrad i turbinen sammenlignes. Ved luftkjøling (filmkjøling) er temperaturfallet fra brennkammerutløp over første ledeskovlrad til første lopeskovlrad på 155 °C. Ved dampkjøling i en lukket sløyfe (konveksjonskjøling) så begrenses temperaturfallet til 44 °C.



System Characteristics

- **Gas Turbine**
 - Scaled Aircraft Engine Compressor
 - DLN Combustor
 - 4 Stage Steam Cooled Turbine
- **Steam Turbine**
 - Reheat 2400 psi/1050 F/1050 F (165 Bar/565 C/565 C)
- **HRSG**
 - 3 Pressure Reheat

Figure 27 Dampkjøling av turbinskovler – integrasjon i kombinert prosess.

I noen gassturbiner kjøles kjøleluften som benyttes i de mest varmebelastede skovler. Det er forskjellige prinsipper som kan benyttes.

- i. Kjøleluften varmeveksles mot brenslet.

- ii. Kjøleluften kjøles eksternt (luft eller vannkjøling)
- iii. I kombinerte prosesser kan kjøleluften brukes til forvarming av kjelvann.
- iv. Kjøleluften kjøles ved vanninjeksjon.

1.11.3 Cooling model concept

A detailed analysis of turbine cooling requires a complex analysis. In particular, this is true for the use of film cooling. In a detailed analysis, a stage-by-stage procedure with rigorous heat transfer calculation inside and outside the blade as well as through the blade wall is necessary. Such a detailed analysis may bring about information about blade surface temperature profiles.

For cycle analysis aiming at efficiency prediction for novel cycles, a simplified procedure is needed in order to be able to carry out a certain number of calculations for various cycle configuration and parameter values. It is here chosen to use a procedure that divides the expansion path into a cooled and an uncooled section.

A model for the calculation of the cooling fluid flow rate, and efficiency reduction is proposed. The structure of a flowsheet model is given in Figure 28. Cooling fluid is bled from the compressor exit and is mixed with the hot combustion products before expansion begins. TIT in this concept, by definition, is the combustor exit temperature. The temperature, at which the expansion begins, is the TIT definition according to the ISO 2314:1989, 8.6. The work of expansion is calculated using the sum of flow rates of combustor exit and the cooling fluid flow.

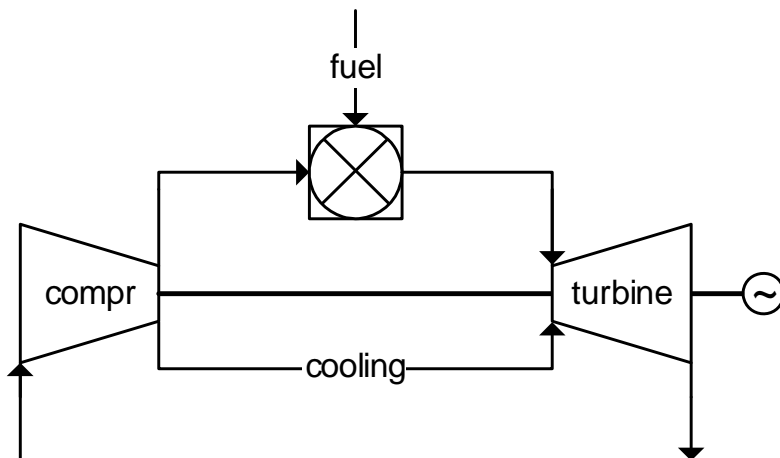


Figure 28 Cooled turbine conceptual model.

1.11.4 Cooling fluid flow rate

The cooling fluid flow rate is calculated using:

$$\frac{\dot{m}_c c_{p,c}}{\dot{m}_g c_{p,g}} = b \left(\frac{T_g - T_b}{T_b - T_{ci}} \right)^s \quad (21)$$

where

\dot{m}_c	cooling fluid flow rate	kg/s
\dot{m}_g	combustor exit flow rate	kg/s

$c_{p,c}$	specific heat capacity, cooling fluid	kJ/(kg K)
$c_{p,g}$	specific heat capacity, combustor exit	kJ/(kg K)
T_g	combustor exit temperature	°C/K
T_b	blade temperature	°C/K
T_{ci}	cooling fluid temperature (compressor exit)	°C/K
b, s	model parameters	

The specific heat capacities, $c_{p,c}$ and $c_{p,g}$, should be evaluated as the average between the temperatures (T_b , T_{ci}) and (T_g , T_b), respectively.

$$c_{p,c} = \frac{h_b - h_{ci}}{T_b - T_{ci}}, \quad c_{p,g} = \frac{h_g - h_b}{T_g - T_b} \quad (22)$$

1.11.5 Turbine efficiency reduction caused by cooling

Mixing of the cooling fluid in the hot gas path reduces the momentum of the hot gas as the cooling fluid has to be accelerated up to speed and direction of the hot gas. This can be expressed as a loss of pressure for the hot gas, which can be converted into a reduction of the polytropic efficiency of the turbine.

$$\frac{\Delta p}{p} = -\frac{\dot{m}_c}{\dot{m}_g} \kappa M^2 \zeta \quad (23)$$

where

\dot{m}_c	cooling fluid flow rate	kg/s
\dot{m}_g	combustor exit flow rate	kg/s
κ	heat capacity ratio	-
M	hot gas Mach number	-
ζ	model parameter	

The model parameter ζ accounts for the direction in which the cooling fluid is injected into the hot gas flow. If the cooling fluid injection is perpendicular to the hot gas flow, ζ is in principle equal to unity.

$$\kappa \approx 1.3 \quad M = 0.6 - 0.8 \Rightarrow M^2 = 0.36 - 0.64 \quad \kappa M^2 \approx 0.5 - 0.8 \quad (24)$$

$$\frac{\Delta p}{p} = -\frac{\dot{m}_c}{\dot{m}_g} \kappa M^2 \zeta = -\frac{\dot{m}_c}{\dot{m}_g} K \quad (25)$$

The value of K is found from real gas turbine data, see below.

The pressure loss information, Δp , can be added to the combustor pressure loss, or it can be converted to a change in turbine efficiency. The latter is given in Eq. (26).

$$\frac{\eta - \Delta\eta}{\eta} = \frac{\ln \frac{p_2}{p_1}}{\ln \frac{p_2}{p_1 + \Delta p}} \quad (26)$$

where

p_1	turbine inlet pressure	bar
p_2	turbine exit pressure	bar
η	turbine polytropic efficiency	-
Δp	pressure drop caused by the cooling air	bar (≤ 0)

Here it should be noted that p_2 can be selected not only as the turbine exit pressure, but can also be an intermediate pressure in the expansion path. It can be convenient to select p_2 as the cooled turbine exit pressure. Observe that higher turbine exit pressures p_2 gives an increase in the calculated efficiency correction, which in general is dependent upon the turbine pressure ratio

$$\frac{p_2}{p_1}.$$

1.11.6 Gas turbine model parameters

Based on information from Siemens and Alstom (within ENCAP), numerical values for the model parameters were found. These values reflect the level of technology found in large modern gas turbines, as for Siemens V94.3 and Alstom KA-26B. This level of technology is also comparable to that of other manufacturer's gas turbines, like GE 9351F and Mitsubishi 701F. The model can be looked upon as a generic gas turbine model that resembles, but do not necessarily replicate, the performance of the above mentioned gas turbines.

Table 5 *Gas turbine parameters*

b	0.15	Δp_{cmb} [%]	3
K	0.051	Combustor heat loss [%]	0.2
s	2	LHV [MJ/kg] (at 10 °C, ideal gas)	46.472
T _b [°C]	860	p _{fuel, inlet} [bar]	70
η_b	1	T _{fuel, inlet} [°C]	10
p _{air, inlet} [bar]	1.01325	$\eta_{p, t, uncooled}$ [%] (turbine efficiency)	86.17
T _{air, inlet} [°C]	15	$\Delta p_{turb, exhaust}$ [mbar]	10
$\Delta p_{compr, inlet}$ [mbar]	10	η_{mech} [%]	99.6
PR _{compr} (base case)	17	η_{gen} [%]	98.5
$\eta_{p, compr}$ [%]	91.5	η_{aux} [%]	100

In the following, computational results are presented in diagram. These diagrams can be used to tune computational models developed by the partners in ENCAP.

- Compressor pressure ratio varied from 10 to 40

- Combustor exit temperature varied from 1000 °C to 1600 °C (1800 °C)
- Specific work = gas turbine gross work / compressor intake mass flow rate
- For the compressor ratio 17, the maximum net efficiency is 38.50 % at a combustor exit temperature of 1425 °C (cooling fraction 22.0 %, cooled turbine inlet temperature 1229 °C, cooled turbine polytropic efficiency 85.7 %, gas turbine specific work 415.5 kJ/kg)

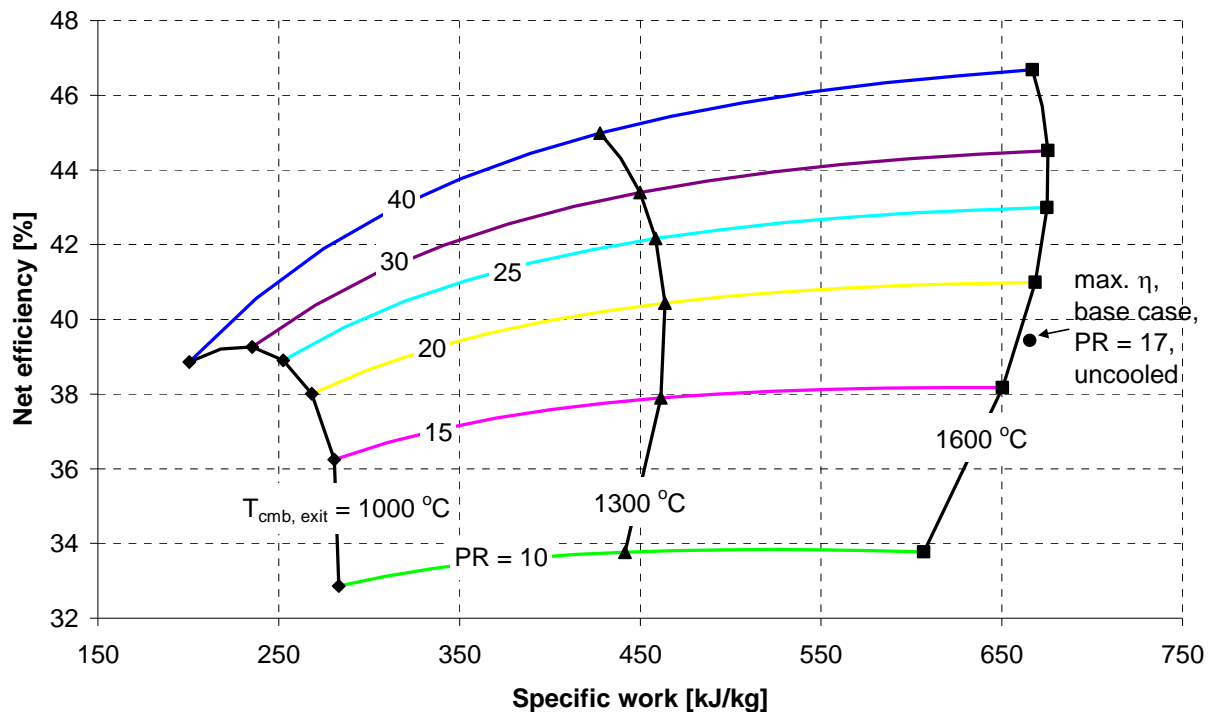


Figure 29 Gas turbine net efficiency versus specific work for the uncooled generic gas turbine. Compressor pressure ratios from 10 to 40 and combustor exit temperatures from 1000 °C to 1600 °C. For the uncooled base case (pressure ratio 17), the net efficiency has a maximum for the combustor exit temperature 1609 °C.

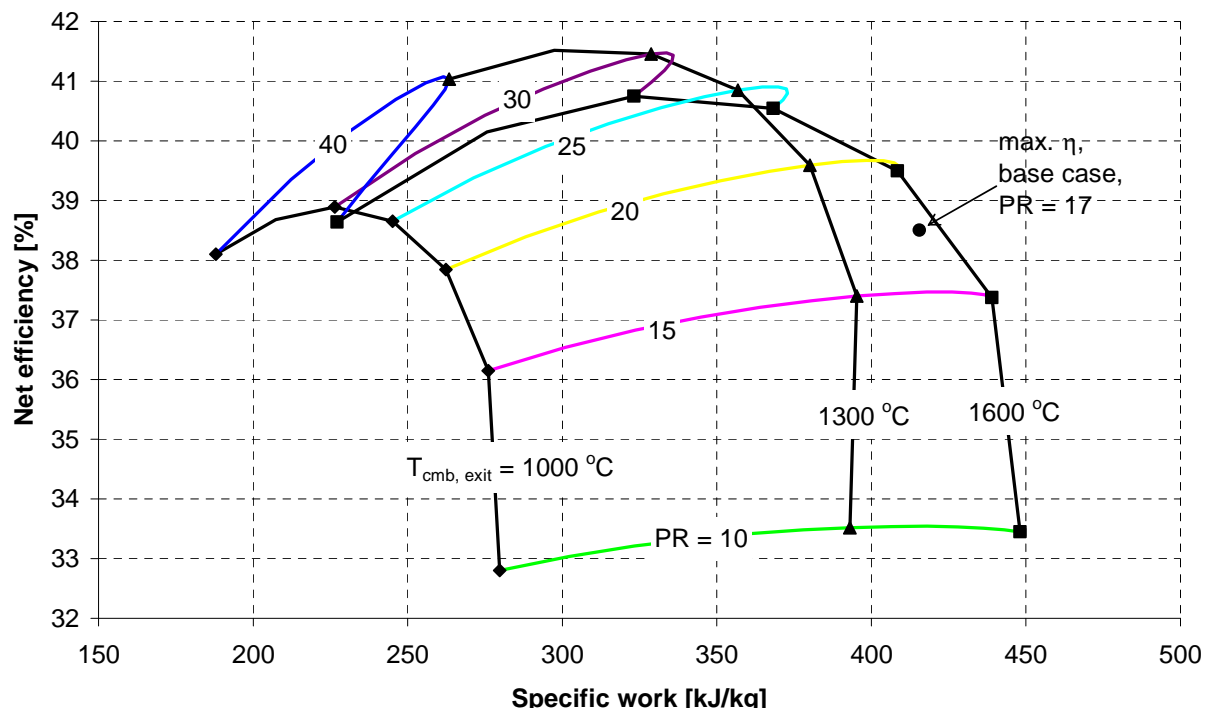


Figure 30 Gas turbine net efficiency versus specific work for the cooled generic gas turbine. Compressor pressure ratios from 10 to 40 and combustor exit temperatures from 1000 °C to 1600 °C. For the base case (pressure ratio 17), the net efficiency has a maximum for the combustor exit temperature 1425 °C.

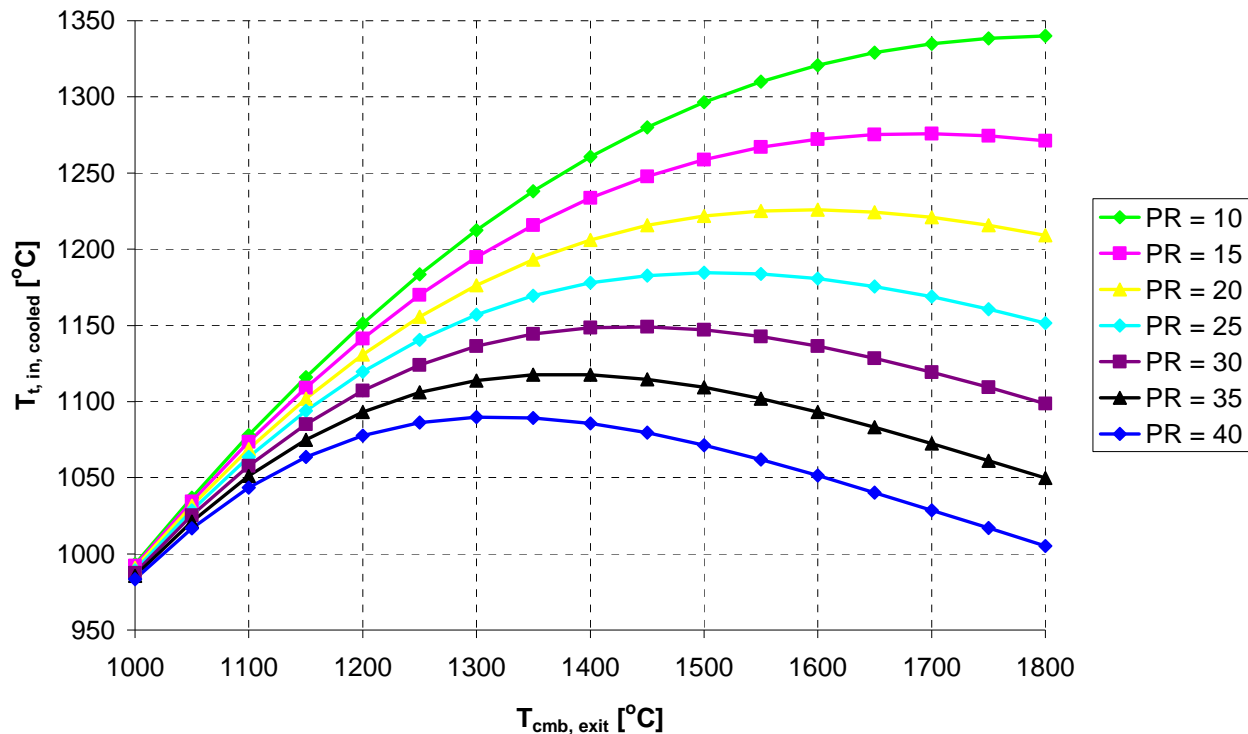


Figure 31 Cooled turbine inlet temperature (definition³) versus the combustor exit temperature for the generic gas turbine.

³ Assumes that all cooling flows and the combustor exit flow are mixed in a single point. The mixing temperature is the so-called ISO turbine inlet temperature.

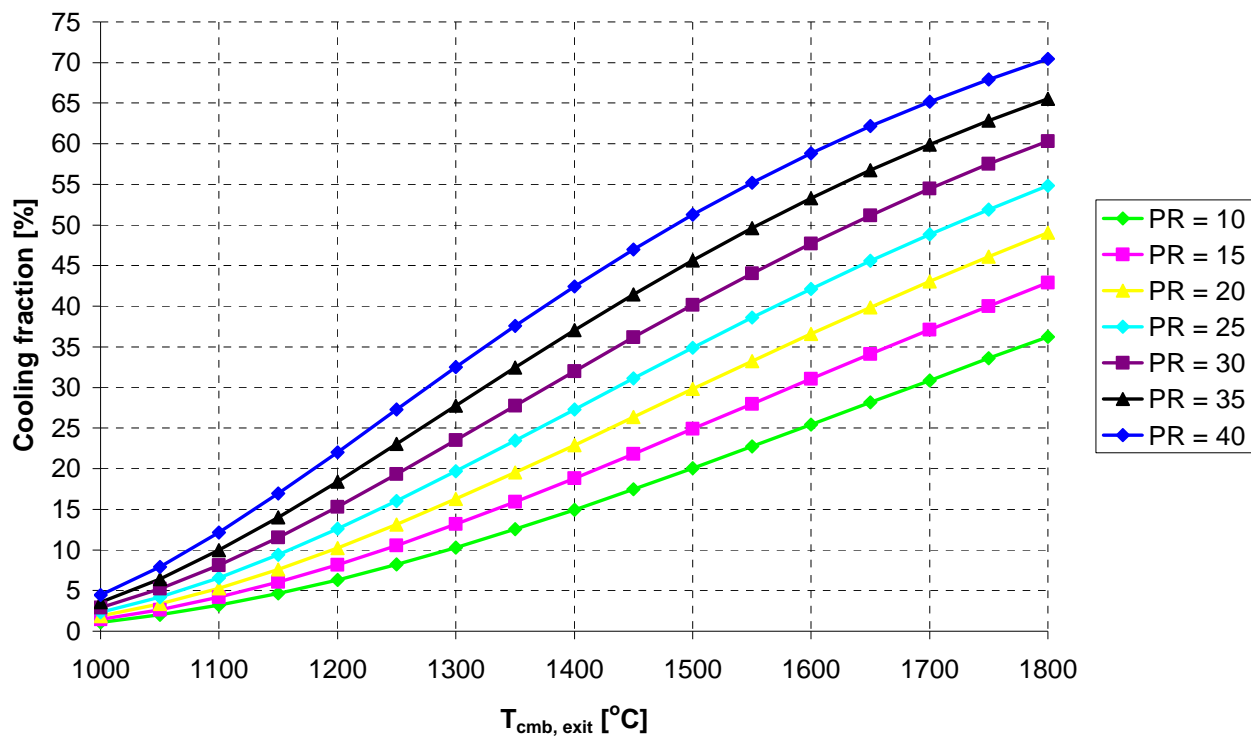


Figure 32 Cooling fraction (that is, the mass flow rate of cooling air divided by the compressor intake mass flow rate) versus the combustor exit temperature for the generic gas turbine.

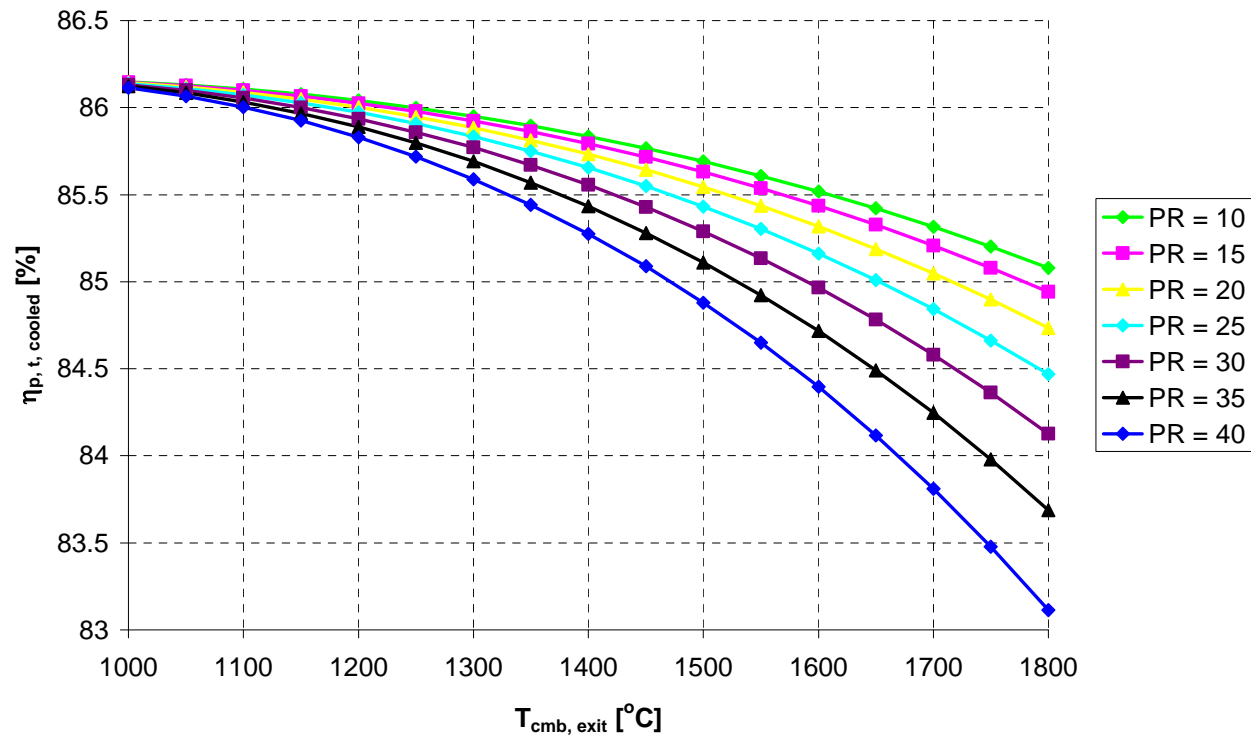


Figure 33 Polytropic turbine efficiency for the cooled generic gas turbine.

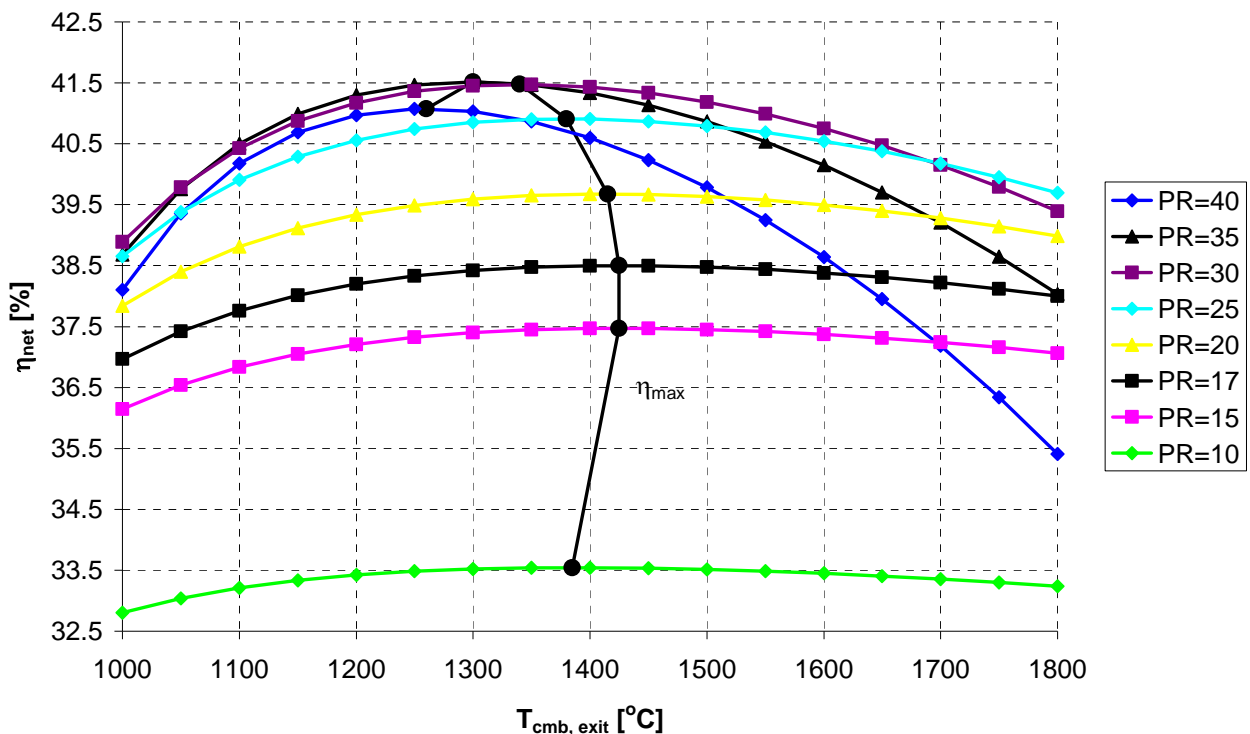


Figure 34 Net efficiency versus the combustor exit temperature for the generic gas turbine.

1.12 Gas turbine combustors

1.12.1 Klassifisering av brennkammer

Det brukes i dag to hovedprinsipper for brennkammere til gassturbiner.

- Eksternt brennkammer:** Forbrenningen foregår i ett eller to store brennkamre utenfor selve ”kroppen” til gassturbinen. Disse kalles ofte for silobrennere eller ”outboard combustors”. Dette prinsippet benyttes stadig sjeldnere. Tidligere benyttet mye og fortsatt litt i dag av leverandører som Siemens og Alstom Power.
- Integrt brennkammer:** Flere brennere (14-16 stk.) eller ”cans” er plassert i ring rundt kompressorutløpet. Prinsippet stammer fra flymotorer. Dette prinsippet dominerer gassturbindesign i dag.

Gassturbinen i Figure 7 på side 13 er eksempel på eksternt brennkammer, mens gassturbinen i Figure 8 er eksempel på integrert brennkammer. Integrerte brennkammere kan videre deles inn i ringbrennkammer (annular combustor) og rørtyppe brennkammer (can combustor).

Fordeler og ulemper:

- Integrerte brennkammer gir en mer kompakt gassturbin
- Større volum i eksterne brennkamre kan gi høyere virkningsgrad for forbrenningen og lavere trykktap.

- Eksterne brennkammer isoleres med keramiske fliser som gir høy levetid og god virkningsgrad for forbrenningen.
- Integrerte brennkammer har kortere avstand og ”direkte kontakt” mellom flammen og første ledeskovl, noe som øker risikoen for skovlbrenning.
- Eksterne brennkammer gir et mer homogent temperaturprofil i innløpet på turbinen.

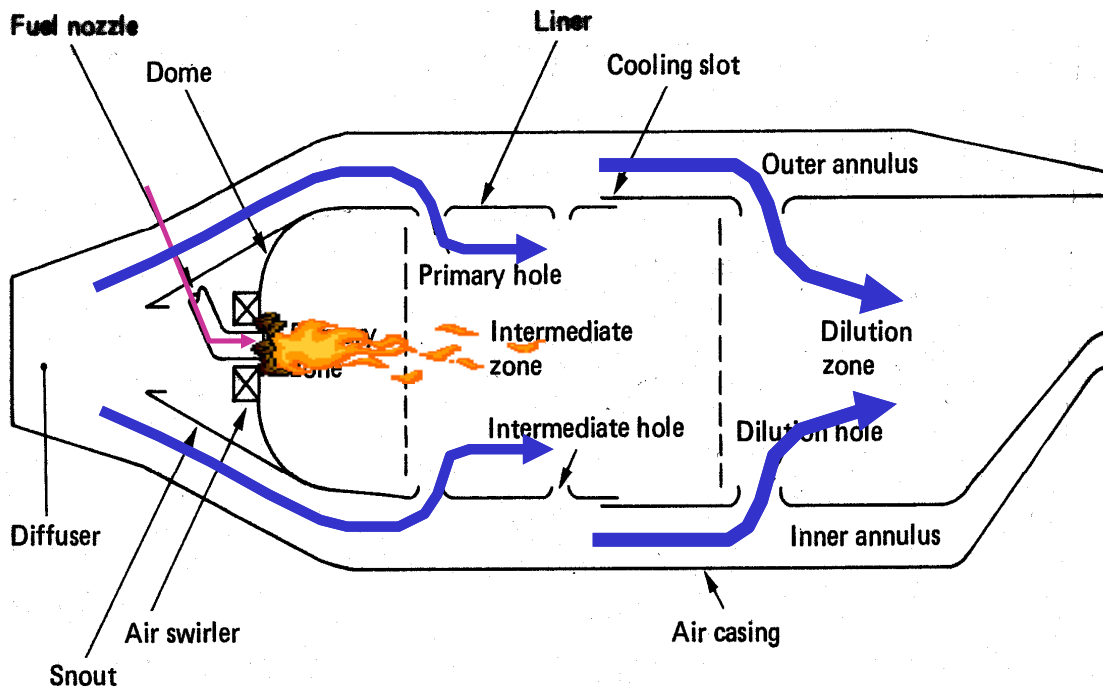


Figure 35 Typical annular combustion system showing addition of dilution air.

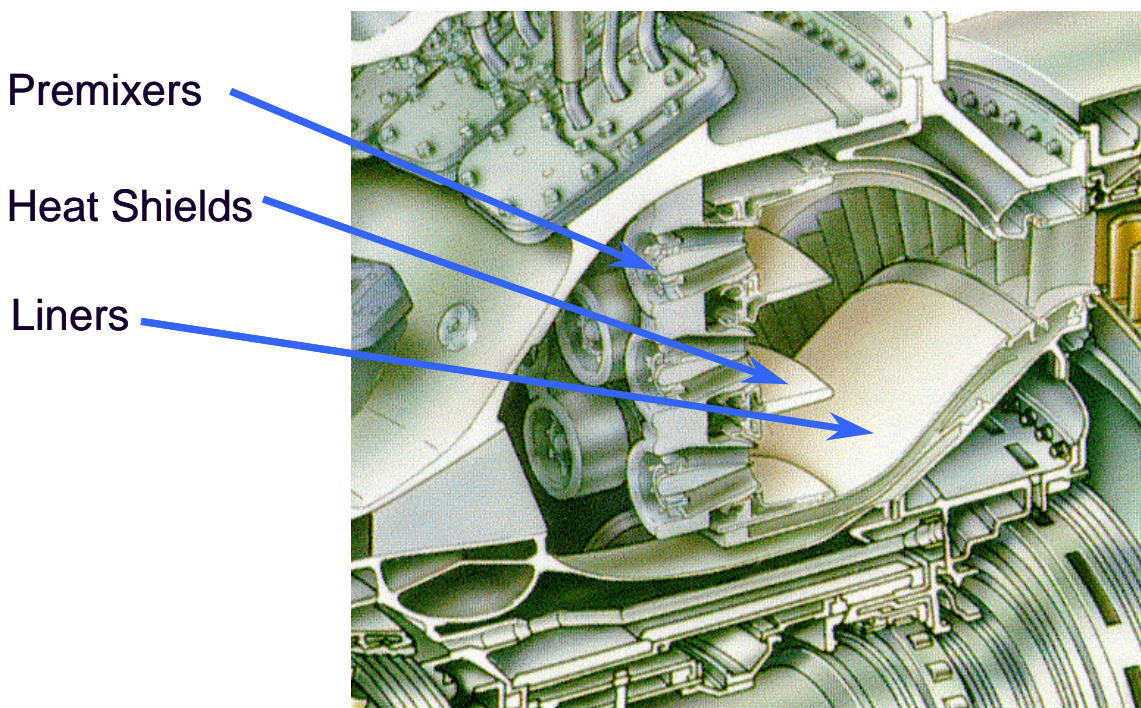


Figure 36 Ringbrennkammer (annular combustor) på General Electric LM2500+. Rommet hvor

forbrenning skjer er sammenhengende rundt "maskinkroppen".

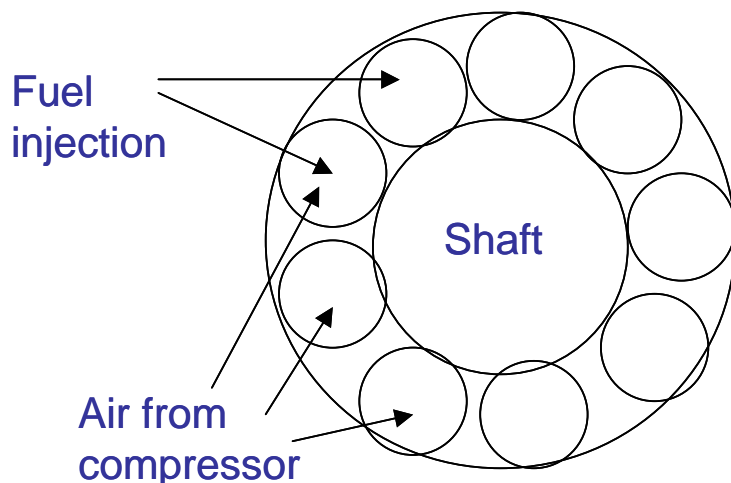


Figure 37 Prinsipp for rørtype brennkammer (can combustor). I hvert rør er det en egen flamme som er i stor grad uavhengig av forbrenningen i de andre rørene.

1.12.2 Low-NOx combustors

Kravene til utslipp av nitrøse gasser ($\text{NO}_x = \text{NO} + \text{NO}_2$) fra termiske kraftstasjoner har i de siste årene blitt skjerpet. De strengeste kravene har man i dag i området rundt Tokyo i Japan, og i California USA. Her er utslippsgrensen satt til under 10 ppm for gassturbinanlegg. Betegnelsen "ppm" betyr "parts per million" og betyr volumandelen av NO_x i eksosen. 1 ppm betyr en milliontedels volumandel av NO_x i eksosen. Angivelse av NO_x gjøres etter en slags "standard", hvor det for gassturbiner er vanlig å benytte "tørr" eksos (uten vanndamp) og 15 vol% O_2 . Dette gjøres for å hindre at uttynningseffekter skal påvirke den oppgitte mengden NO_x . Innen andre områder så benyttes andre prosentsatser for O_2 . Ved en aktuell måling så inneholder eksosen vanndamp, og O_2 -innholdet er normalt ikke akkurat 15%. Den målte verdien for NO_x omregnes da til "standarden".

NO_x bidrar til sur nedbør og dannelse av bakkenær ozon. Norge har forpliktet seg gjennom Göteborg-protokollen til en omfattende reduksjon i utslipp av NO_x i forhold til nivået nå (2003).

I Norge er utslippsgrensen for planlagte gasskraftverk på land vært 10 ppm, og deretter ned til 5 ppm etter 5 år. For gassturbiner offshore så har det ikke vært noe utslippskrav, men myndighetene har "oppfordret" oljeselskapene til å jobbe med saken. Dette har resultert i noe bruk av lav- NO_x -brennkammer.

En av hovedårsakene til dannelse av NO_x er høy temperatur i forbrenningssonene, såkalt "termisk NO_x ". Dannelsen av termisk NO_x er temperaturavhengig, se Figure 38.

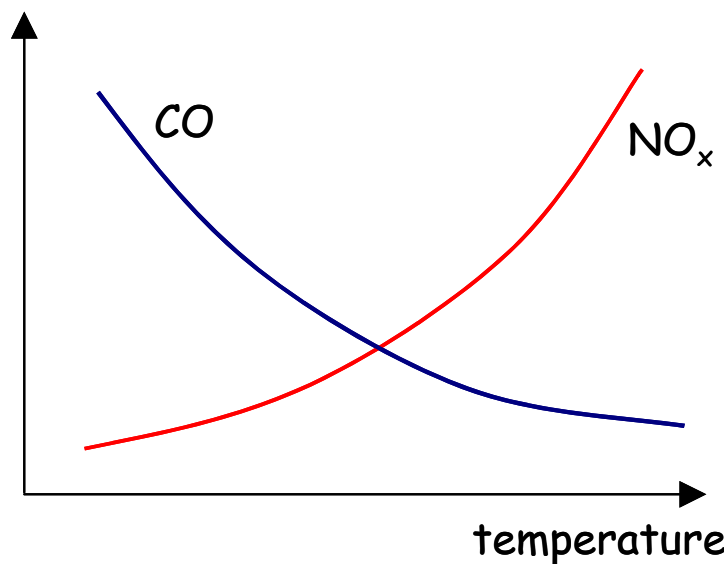


Figure 38 Dannelse av CO og "termisk" NO_x; avhengig av temperatur

Siden ca. 1985 er såkalte lav-NO_x brennere for gassturbiner blitt utviklet. Prinsippet for disse brennerne er å formikse luft og brensel før blandingen går inn i brennkammeret. Dette fører til at forbrenningen skjer ved en lavere middeltemperatur enn uten formiksing. Et av problemene med formiksing er at flammetemperaturen blir så lav at en får stabilitetsproblemer som kan føre til at flammen slokner. Dette er uønsket fordi skovlene i turbinen blir utsatt for store termiske spenninger når gasstemperaturen plutselig går fra ca. 1000 °C ned til 300-400 °C. Dette problemet løses ved at det brukes en såkalt pilotflamme i senteret av brenneren. Pilotflammen fødes med brensel (ikke formikset), mens resten av brenneren fødes med formikset luft og brensel. Med slike brennere får en NO_x-utslipp på ca. 7-25 ppm (gass som brensel). Figure 39 viser brennkammer med lav-NO_x brennere. Figure 40 viser et annet design for lav-NO_x.

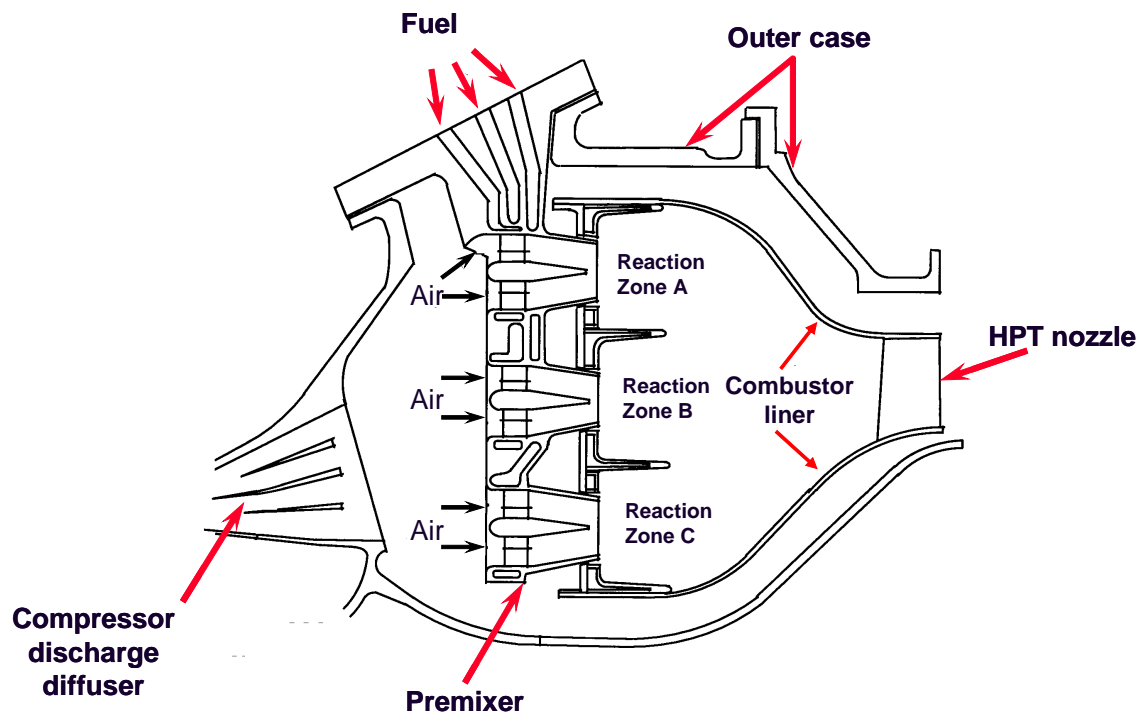


Figure 39 Lav-NOx brennkammer. General Electric LM2500+

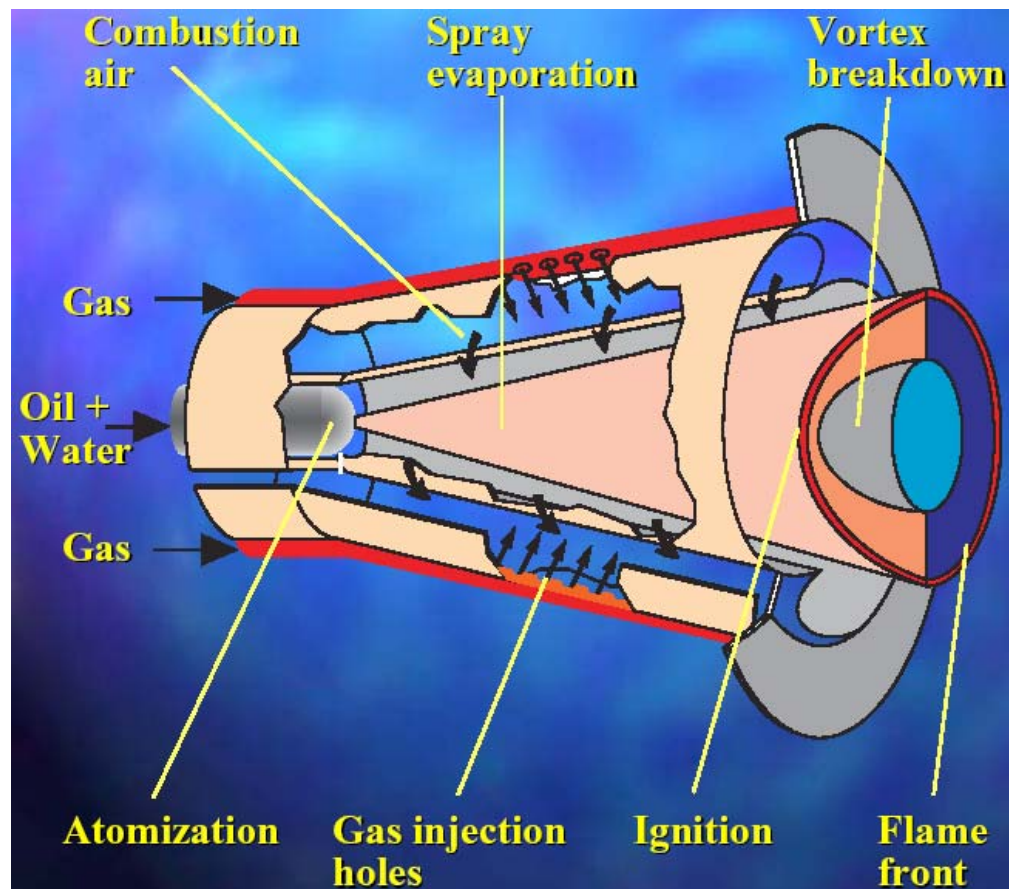


Figure 40 Lav-NOx brenner fra Alstom Power

1.12.3 Other measures for reduction of NOx emissions from gas turbines

- **Water (liquid or steam) injection into the GT combustor**
 - Reduces the flame temperature, and thereby lowers the NOx formation
 - Water/fuel-ratio 1-1.6
 - Below 25 ppmv (natural gas) or 42 ppmv (dist. oil)
- **Selective Catalytic Reduction (SCR)**
 - Use of NH₃ to react with NO₂ (to N₂ and H₂O)
 - Catalyst at appr. 350 °C in the exhaust heat recovery boiler
 - Typically used in oil fired units
 - Below 10 ppmv achievable (typical 80% reduction), 5 ppm possible
 - Ammonia slip → formation of ammonium sulfate & ammonium nitrate
- **Catalytic Combustion**
 - Catalyst in the combustor
 - Tests carried out in a small Gas Turbine, but not commercially available
 - Temperature limitation, life-time limited
 - 3 ppmv demonstrated in test, single-digit emissions achievable
 - Not commercially available yet
- **Catalytic absorption (SCONO_X)**
 - Catalyst in the exhaust gas system (150-370 C)
 - Use of a solid dry catalyst, Potassium Carbonate, to reduce NO₂ (to N₂ and H₂O)
 - The catalyst is first converted Potassium Nitrites and the regenerated by a CO₂/H₂-containing gas
 - Below 3 ppmv NO_x achievable

1.12.4 Combustion of natural gas in a gas turbine – realistic assumptions

Conversion efficiency: $\eta_{\text{comb}} = 100\%$

Combustor pressure drop: $\Delta p/p = 2.5\%$

Heat loss = 0.2%

1.13 Gas turbine performance model

The performance of an existing gas turbine can be predicted rather accurate by matching the characteristics of the compressor and the turbine coupled with a heat balance of the combustor. The characteristics of compressors and turbines are rarely available for people outside the manufacturers. In order to make performance predictions one often has to rely on simplified models. In the following such a simplified model is presented. The model rely on knowing a point of operation; typically the design point. Data for the gas turbine performance in the design point is often publicly known. The model described in the following uses the principle of relating two operating conditions by applying simple laws of physics. A similar approach is presented in (Saravanamuttoo, Rogers et al., 2001).

The following assumptions are made for the model.

- 1) The gas turbine is single-shaft and is coupled to a generator running at constant speed (3000/3600 rpm for 2-pole generators)
- 2) Compresor and turbine efficiencies are constant, independent of load condition
- 3) The lines for constant reduced speed in the compressor diagram are vertical (see Figure 42), which is typical for large axial compressor
- 4) The turbine is assumed to behave like a choked nozzle (see Figure 43)

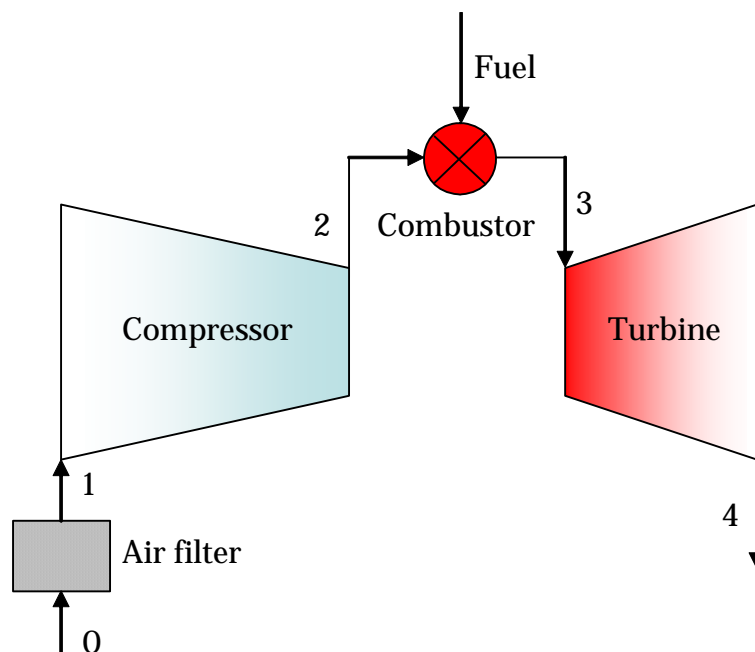


Figure 41 Flow diagram of a gas turbine showing numbers for the indexes used in the model equations.

Compressor:

The assumption 3) above decouples the relation between compressor pressure ratio and compressor flow rate. For constant speed the inlet of the compressor can be assumed to have constant volumetric sucking capacity with respect to velocity v . By combining the equation of continuity and ideal gas law, one obtains a relation between the flow rate \dot{m} and temperature, pressure and gas

constant at the compressor inlet, as well as an equivalent cross-sectional area A_c for the compressor inlet.

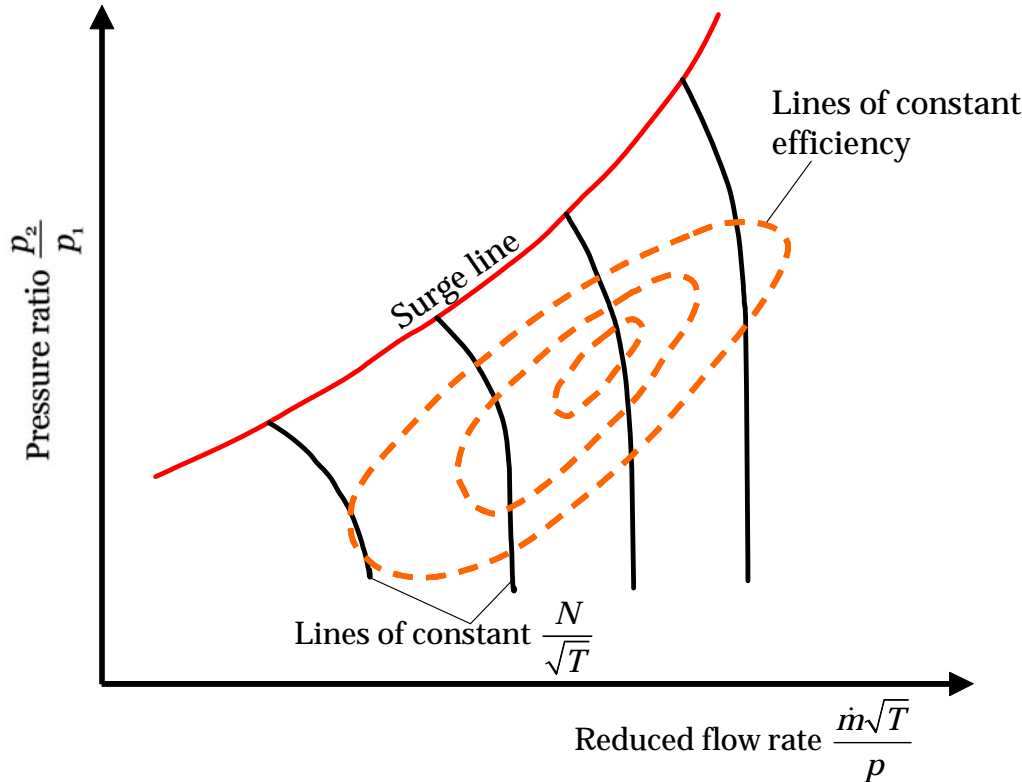


Figure 42 Compressor characteristic.

\dot{m}	= flow rate	[kg/s]
u	= velocity	[m/s]
A_c	= cross-sectiona flow area	[m ²]
R	= gas constant	[kJ/(kg·K)]
P	= ambient pressure	[bar]
ρ	= density	[kg/m ³]
T	= temperature	[K]

$$\dot{m} = \rho u A_c = \rho \dot{V} \quad (27)$$

$$\frac{p}{\rho} = RT \quad (28)$$

$$\dot{m} \sim \frac{p}{R T} A_c \quad (29)$$

By relating a known condition (index ref) and the actual condition (no index), we can write:

$$\frac{\dot{m}}{\dot{m}_{ref}} = \frac{p}{p_{ref}} \frac{R_{ref}}{R} \frac{T_{ref}}{T} \frac{A_c}{A_{c,ref}} \quad (30)$$

The specific gas constant, R , can be replaced by the ratio of the universal gas constant (8314.4) to the molecular weight (MW).

Eq. (30) is important in order to understand the sensitivity of various parameters with respect to the flow rate through the compressor. The power output of a gas turbine is proportional to the flow rate \dot{m} . It can be noted that reduced air pressure at high altitudes reduces the gas turbine flow rate and power output. The same is the case for high ambient air temperatures. The equivalent cross-sectional area A_c can be regarded as a constant, unless variable guide vanes (VGV) are just to control the flow rate through the compressor. VGVs are used quite commonly in most gas turbines, and the air flow rate may typically be reduced to 60-70% of the design flow rate. VGVs are used during start-up, and for optimal control of part-load performance in combined cycle operation.

Air filter:

The pressure drop through the air filter can be predicted based on the same methodology as for the compressor; by relating two operating conditions. The general expression for frictional pressure drop ΔP is:

$$\Delta P = \xi \rho \frac{1}{2} u^2 \quad (31)$$

The friction factor ξ depends on the *Reynolds number* and the *relative roughness* of the surfaces through which the air is flowing. The typical air filter pressure drop is about 10 mbar. There exist a number of equations for calculation of the friction factor, as well as diagrams such as the *Fanning* and *Moody* diagrams. Assuming that the friction factor is constant, one obtains the following relation from Eqs. (28), (27) and (31) for the calculation the pressure drop in an air filter.

$$\frac{\Delta P_{air\ filter}}{\Delta P_{air\ filter,ref}} = \left(\frac{\dot{m}}{\dot{m}_{ref}} \right)^2 \frac{T P_{ref} MW_{ref}}{T_{ref} P MW} \quad (32)$$

This expression is very general and can be used for other types of equipment; like for the gas turbine combustor and the heat recovery system, assuming constant friction factor.

Turbine:

It is very common to have the turbine in a gas turbine operating as choked. The exception is typically at low load. The fact that the turbine is choked is used frequently in performance calculations in order to find the turbine inlet pressure, and thereby the compressor pressure ratio. The so-called *choked nozzle* equation is commonly used. Choked flow is a limiting condition which occurs when the mass flux will not increase with a further decrease in the downstream pressure environment; here meaning that an increased pressure difference over the turbine does not increase the mass flux. It can be derived based on the equation of continuity, the Bernoulli energy conservation equation and a thermodynamic expression stating an isentropic change of state between the stagnation and actual static condition for sonic flow. The equation can also be derived based on the quasi non-dimensional numbers for a turbine commonly used in characteristics, such as in Figure 43.

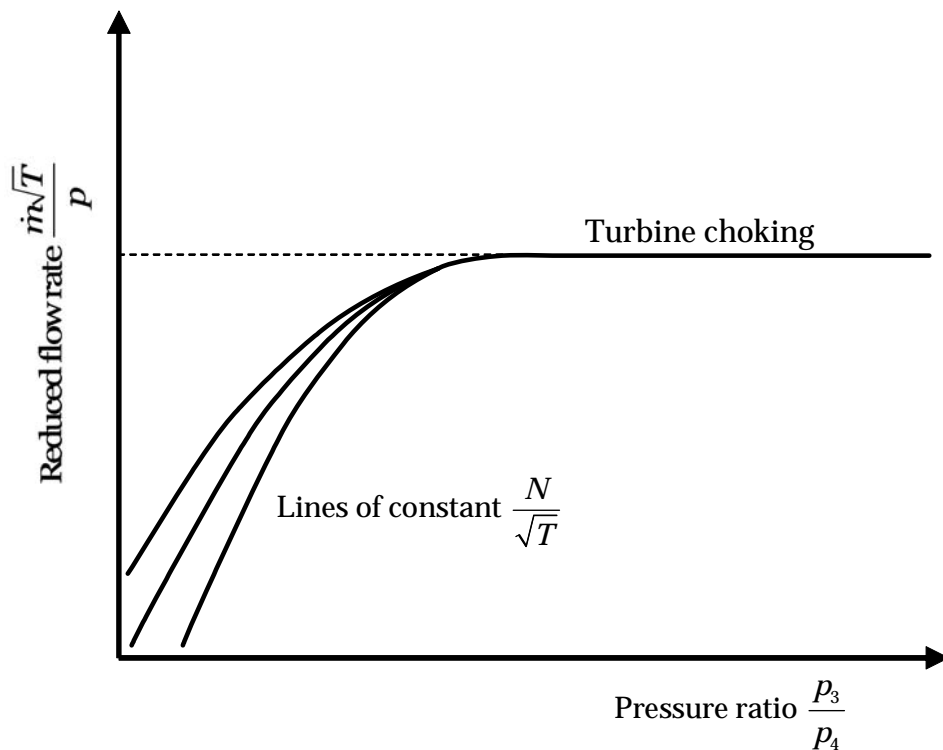


Figure 43 Turbine characteristic.

By setting the reduced flow rate constant, as indicated by the dashed line in Figure 43, we can write:

$$\frac{\dot{m}\sqrt{T_3}}{p_3} = \text{constant}, \quad \frac{\dot{m}\sqrt{T}}{p} \sqrt{\frac{R}{\kappa}} = \text{constant} \Rightarrow \frac{\dot{m}}{p_3} \sqrt{\frac{T_3}{MW_3}} = \text{constant} \quad (33)$$

The left-most expression is a simplified form of the reduced flow rate non-dimensional number, typically used when air is the working fluid, and there is no steam injection in the gas turbine; meaning that the working fluid molecular weight does not change much during operation. In cases where the working fluid composition changes quite a lot, it may be more appropriate to also include the molecular weight in the reduced flow rate expression; as is done in the right-most expression above.

By relating two different operating conditions using Eq. (33), the choked nozzle equation is established:

$$\frac{p_3}{p_{3,\text{ref}}} = \frac{\dot{m}_3}{\dot{m}_{3,\text{ref}}} \sqrt{\frac{T_3}{T_{3,\text{ref}}} \frac{MW_{3,\text{ref}}}{MW_3}} \quad (34)$$

The above equation states that the pressure in front of the turbine is proportional to the inlet flow rate and to the square root of the temperature, and inversely proportional to the square root of the molecular weight. A more general description of this relation also includes the non-choked regime (Traupel, 1966).

1.14 Off-design calculation of a single-shaft gas turbine

1.14.1 Procedure

Assumptions:

- 1) Single-shaft constant speed operation
- 2) Large axial compressor with vertical speed lines in the compressor map
- 3) Constant compressor and turbine efficiency
- 4) The turbine operates as choked

\dot{m}	flow rate	[kg/s]
T	temperature	[K]
p	pressure	[bar]
MW	molecular weight	[kg/kmol]
c_{pk}	specific heat	[kJ/(kgK)]
η_p	polytropic efficiency	[-]
W	power	[kW]

Index r means reference condition for \dot{m} , T , p and MW

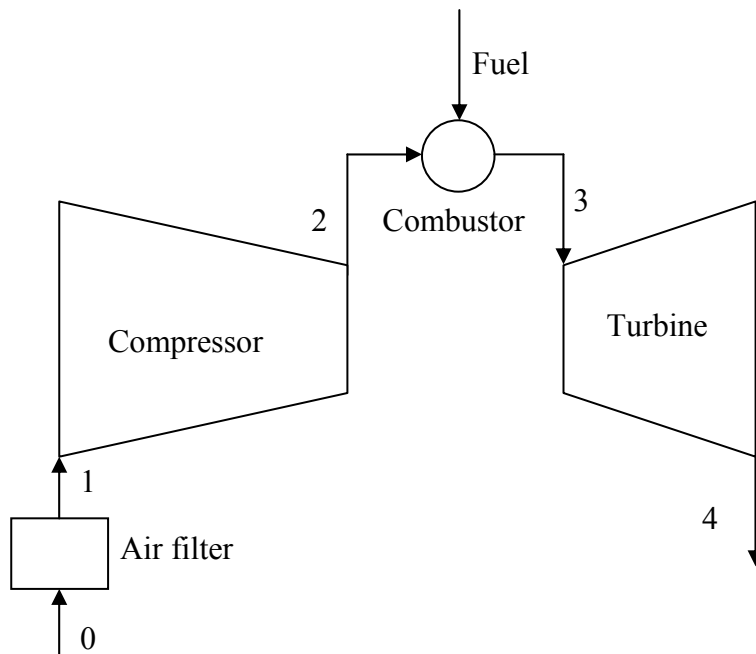


Figure 44 Gas turbine cycle with cycle point indexes

- 1) Compressor flow rate

$$\frac{\dot{m}_1}{\dot{m}_{r,1}} = \frac{T_{r,1}}{T_1} \quad (35)$$

- 2) Air filter pressure drop

$$\frac{\Delta P_{af}}{\Delta P_{r,af}} = \left(\frac{\dot{m}_1}{\dot{m}_{r,1}} \right)^{1.8} \left(\frac{T_1 P_{r,1}}{T_{r,1} P_1} \right)^{0.8} \quad (36)$$

3) Compressor work

$$P_1 = P_0 - \Delta P_{af} \quad (37)$$

Guessing P_2 , and then;

$$\frac{T_2}{T_1} = \left(\frac{P_2}{P_1} \right)^{\frac{R}{C_{pk} \eta_p}} \quad (38)$$

$$W_{compr} = \dot{m}_1 C_{pk} (T_2 - T_1) \quad (39)$$

4) Combustor

$$(\dot{m}_1 + \dot{m}_{fuel}) C_{Pt} (T_3 - T_0) = \dot{m}_1 C_{Pt} (T_2 - T_0) + \dot{m}_{fuel} LHV \quad (40)$$

Estimating combustor pressure drop (neglecting the fundamental loss)

$$\frac{\Delta P_c}{\Delta P_{r,c}} = \left(\frac{\dot{m}_3}{\dot{m}_{r,3}} \right)^{1.8} \left(\frac{T_3 P_{r,3}}{T_{r,3} P_3} \right)^{0.8} \quad (41)$$

5) Turbine inlet (the choked condition)

$$\frac{P_3}{P_{r,3}} = \frac{\dot{m}_3}{\dot{m}_{r,3}} \sqrt{\frac{T_3}{T_{r,3}} \frac{MW_{r,3}}{MW_3}} \quad (42)$$

$$\dot{m}_3 = \dot{m}_1 + \dot{m}_{fuel} \quad (43)$$

$$P_3 = P_2 - \Delta P_c \quad (44)$$

Check the value of P_2 compared to that guessed before Eq. (38). If different, choose value of P_2 and go back to Eq. (38).

6) Turbine work

$$\frac{T_4}{T_3} = \left(\frac{P_4}{P_3} \right)^{\frac{R \eta_p}{C_{pt}}} \quad (45)$$

$$W_{turb} = \dot{m}_3 C_{Pt} (T_3 - T_4) \quad (46)$$

7) Gas turbine work and efficiency

$$W_{GT} = W_{turb} - W_{compr} \quad (47)$$

$$\eta_{GT} = \frac{W_{GT}}{\dot{m}_{fuel} LHV} \quad (48)$$

1.14.2 Example - gas turbine calculation - design

In the following (see Table 6) an example of a heat and mass balance calculation for a gas turbine (uncooled) is given. The numbers in *italic* are calculated values, while the others are input values. A pressure ratio of 16, a compressor inlet flow rate of 630 kg/s, and a turbine inlet temperature of 1250 °C are chosen as the main design parameters. The temperature ratios over the compressor and turbine are calculated using Eq. (38) and (45).

The specific heat capacity is assumed to be constant, and is calculated using the gas constant R and the specific heat capacity ratio κ, as:

$$c_p = \frac{R \kappa}{\kappa - 1} \quad (49)$$

Table 6 Gas turbine heat and mass balance

		Design
0	Ambient temperature	°C
0	Ambient pressure	°C
	Fuel LHV	MJ/kg
	Air gas constant	kJ/(kg K)
	Air "kappa"	-
	<i>Specific heat capacity air</i>	<i>kJ/(kg K)</i>
1	Compressor flow rate	kg/s
	Air filter pressure drop	mbar
	Compressor pressure ratio	-
	Compressor efficiency, polytropic	%
	<i>Compressor efficiency, isentropic</i>	<i>89.4 %</i>
1	<i>Compressor inlet pressure</i>	<i>bar</i>
1	<i>Compressor inlet temperature</i>	<i>C</i>
2	<i>Compressor outlet pressure</i>	<i>bar</i>
2	<i>Compressor outlet temperature</i>	<i>°C</i>
2	<i>Compressor outlet temperature, ideal</i>	<i>°C</i>
	<i>Compressor specific work</i>	<i>kJ/kg</i>
	<i>Compressor work</i>	<i>MW</i>
3	Turbine inlet temperature	°C
	Combustor pressure drop	%
3	<i>Turbine inlet pressure</i>	<i>bar</i>
	Exhaust gas constant	kJ/(kg K)
	Exhaust "kappa"	-
	<i>Specific heat capacity exhaust</i>	<i>kJ/(kg K)</i>
	<i>Fuel flow</i>	<i>kg/s</i>
3	<i>Turbine inlet flow rate</i>	<i>kg/s</i>
	Turbine polytropic efficiency	%
	Turbine exit pressure drop (HRSG)	mbar
4	<i>Turbine exit pressure</i>	<i>bar</i>
	<i>Turbine pressure ratio</i>	-
	<i>Turbine isentropic efficiency</i>	%
4	<i>Turbine exit temperature</i>	<i>°C</i>
	<i>Turbine specific work</i>	<i>kJ/kg</i>
	<i>Turbine work</i>	<i>MW</i>
	<i>Gas turbine backwork ratio (gross)</i>	<i>-</i>
	Mechanical efficiency	%
	Generator efficiency	%
	Auxiliary power	%
	<i>Gas turbine gross work</i>	<i>MW</i>
	<i>Gas turbine shaft work</i>	<i>MW</i>
	<i>Generator terminal output</i>	<i>MW</i>
	<i>Plant net output</i>	<i>MW</i>
	<i>Gas turbine gross efficiency</i>	%
	<i>Gas turbine shaft efficiency</i>	%
	<i>Generator terminal efficiency</i>	%
	<i>Plant net efficiency</i>	<i>36.5 %</i>

The key numbers from the calculation are also showed in the flowsheet below, Figure 45.

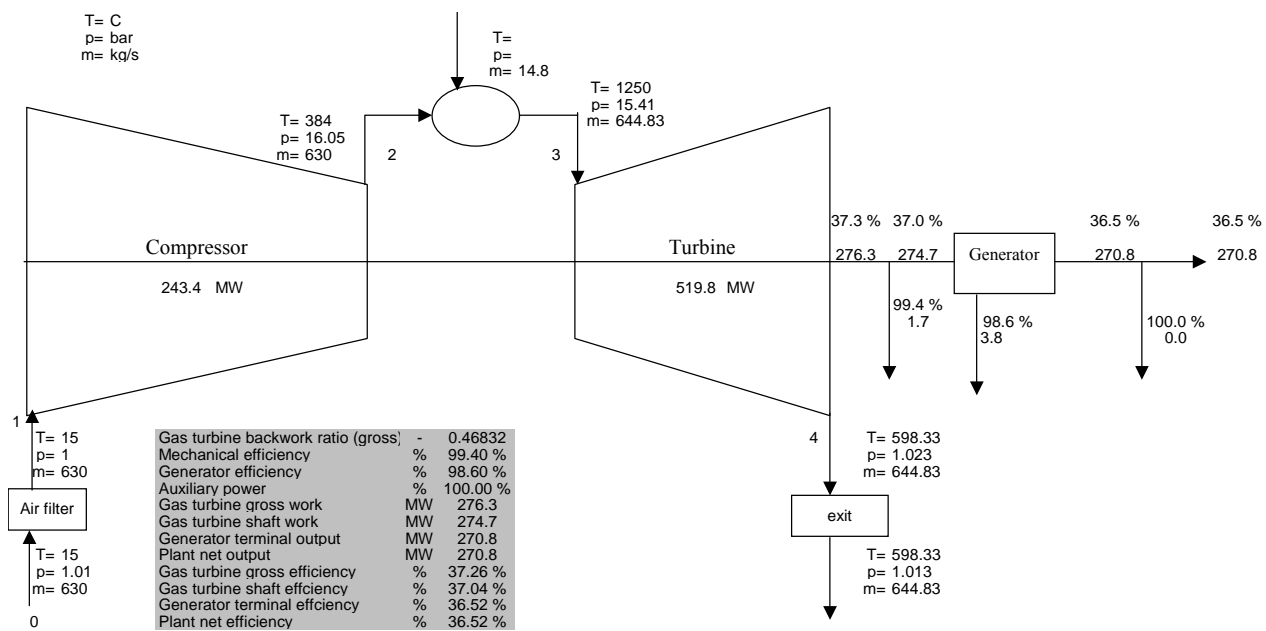


Figure 45 Key numbers from the gas turbine calculation

1.14.3 Example - gas turbine calculation – off-design/operation

In this example the same gas turbine as in section 1.14.2 is assumed. In the following, it is assumed that the gas turbine hardware is fixed, so that we look at how this gas turbine performs when exposed to other operating conditions. The basis for the following is the procedure including the assumptions given in section 1.14. Four different off-design conditions are calculated:

- 1) Reducing the ambient temperature from 15 °C to 0 °C.
- 2) Increasing the ambient temperature from 15 °C to 30 °C.
- 3) Reducing the turbine inlet temperature from 1250 °C to 1200 °C.
- 4) Increasing the turbine inlet temperature from 1250 °C to 1300 °C.

The results of the calculations are shown in Table 7 and Figure 46. The empty spaces in the off-design columns in Table 7, means that the value in the design column is used at off-design.

Table 7 Gas turbine off-design calculation

		Design	Off-design	Off-design	Off-design	Off-design
Ambient temperature	°C	15	0	30	15	15
Ambient pressure	°C	1.013	1.013	1.013	1.013	1.013
Fuel LHV	MJ/kg	50.01				
Air gas constant	kJ/(kg K)	0.288				
Air "kappa"	-	1.38				
Specific heat capacity air	kJ/(kg K)	1.0459				
Compressor flow rate	kg/s	630	664.23	599.12	630.00	630.00
Air filter pressure drop	mbar	10	10.55	9.51	10.00	10.00
Compressor pressure ratio	-	16	16.93	15.17	15.70	16.29
Compressor efficiency, polytropic	%	92.5 %				
Compressor efficiency, isentropic	%	89.4 %	89.3 %	89.4 %	89.4 %	89.3 %
Compressor inlet pressure	bar	1.0030	1.0025	1.0035	1.0030	1.003
Compressor inlet temperature	C	15	0	30	15	15
Compressor outlet pressure	bar	16.05	16.97	15.22	15.75	16.34
Compressor outlet temperature	°C	384.4	361.2	408.5	381.4	388.6
Compressor outlet temperature, ideal	°C	345.1	312.9	377.3	345.1	345.1
Compressor specific work	kJ/kg	386.4	377.8	395.8	383.2	390.7
Compressor work	MW	243.4	250.9	237.1	241.4	246.1
Turbine inlet temperature	°C	1250	1250	1250	1200	1300
Combustor pressure drop	%	4.0 %	4.2 %	3.8 %	3.9 %	4.1 %
Turbine inlet pressure	bar	15.41	16.25	14.64	15.13	15.68
Exhaust gas constant	kJ/(kg K)	0.2927				
Exhaust "kappa"	-	1.310				
Specific heat capacity exhaust	kJ/(kg K)	1.237				
Fuel flow	kg/s	14.8291	16.0132	13.7510	14.0490	15.5964
Turbine inlet flow rate	kg/s	644.83	680.25	612.87	644.05	645.60
Turbine polytropic efficiency	%	87.0 %				
Turbine exit pressure drop (HRSG)	mbar	10	10	10	10	10
Turbine exit pressure	bar	1.023	1.023	1.023	1.023	1.023
Turbine pressure ratio	-	15.06	15.89	14.31	14.79	15.32
Turbine isentropic efficiency	%	90.3 %	90.4 %	90.3 %	90.3 %	90.3 %
Turbine exit temperature	°C	598.33	588.79	607.49	572.83	623.73
Turbine specific work	kJ/kg	806.05	817.85	794.71	775.74	836.48
Turbine work	MW	519.76	556.34	487.06	499.61	540.03
Gas turbine backwork ratio (gross)	-	0.4683	0.4510	0.4869	0.4832	0.4558
Mechanical efficiency	%	99.40 %	99.40 %	99.40 %	99.40 %	99.40 %
Generator efficiency	%	98.60 %	98.60 %	98.60 %	98.60 %	98.60 %
Auxiliary power	%	100.00 %	100.00 %	100.00 %	100.00 %	100.00 %
Gas turbine gross work	MW	276.35	305.42	249.91	258.21	293.89
Gas turbine shaft work	MW	274.69	303.59	248.41	256.66	292.12
Generator terminal output	MW	270.84	299.34	244.93	253.07	288.03
Plant net output	MW	270.84	299.34	244.93	253.07	288.03
Gas turbine gross efficiency	%	37.3 %	38.1 %	36.3 %	36.8 %	37.7 %
Gas turbine shaft efficiency	%	37.0 %	37.9 %	36.1 %	36.5 %	37.5 %
Generator terminal efficiency	%	36.5 %	37.4 %	35.6 %	36.0 %	36.9 %
Plant net efficiency	%	36.5 %	37.4 %	35.6 %	36.0 %	36.9 %

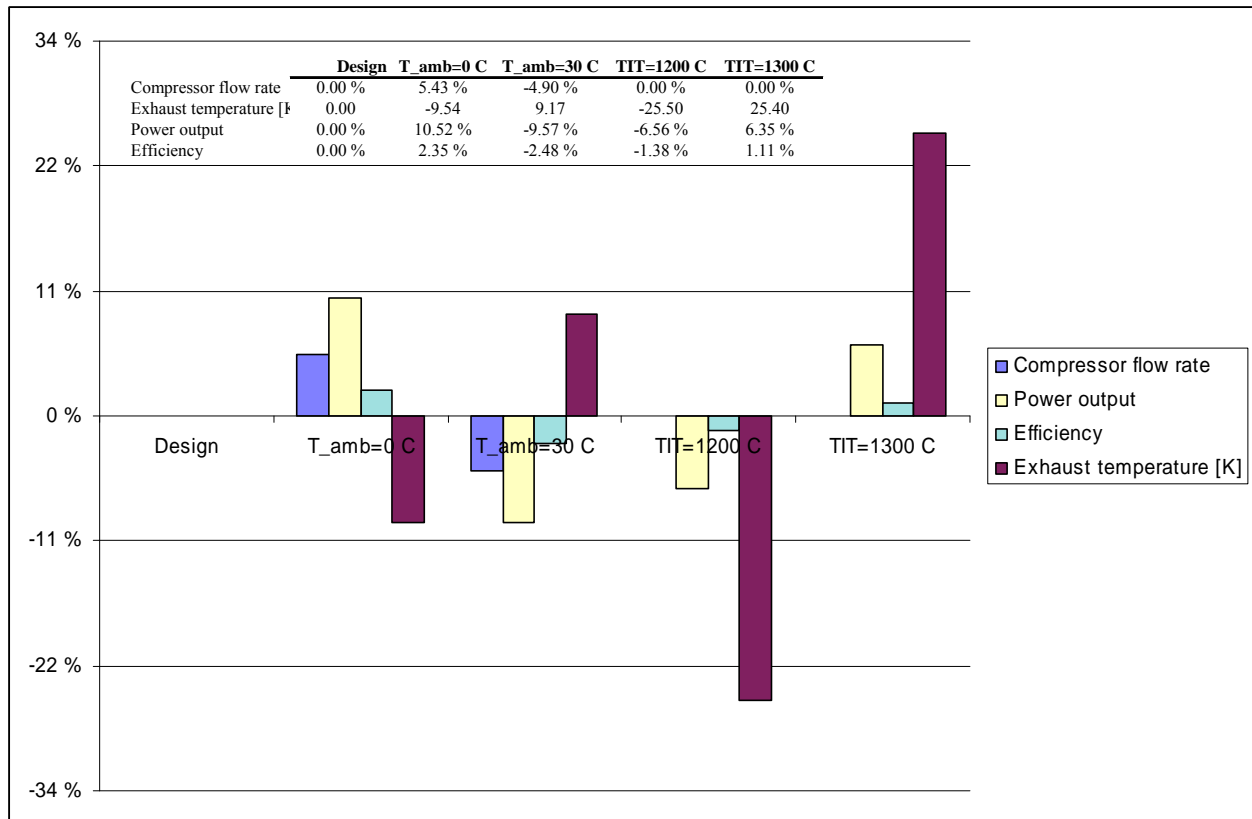


Figure 46 Changes in selected parameters from the gas turbine calculation shown in Table 7

1.15 Part-load performance of a gas turbine in a combined cycle

There are two principles being used for reducing the load of a gas turbine. One is to simply reduce the fuel input, and the other one is to combine reduction of fuel flow and active reduction of air flow capacity of the compressor. The former is typically used in simple cycle plants, and provides the highest efficiency of the gas turbine. The latter is commonly used in combined cycles, as it provides a higher part-load efficiency of the combined cycle compared to that of the former principle.

When reducing the fuel flow of the gas turbine, the flue gas temperature at the turbine exit decreases. A reduced turbine exit temperature causes a reduction of the steam temperature obtained in the HRSG, which implies a reduction of the steam cycle efficiency. When combining a reduction of the fuel and air flows, it is possible to maintain a high turbine exit temperature which enables high steam cycle efficiency. The turbine exit temperature is mainly determined by the turbine inlet temperature and the turbine pressure ratio. The relation between these three parameters is given by Eq. (33). The air flow through the compressor is determined by ambient air condition, as related in Eq. (30), and by the use of variable guide vanes. The ability to reduce compressor flow rate by using variable guide vanes varies between the different types of compressor. The lower limit is typically in the range 70-85% air flow rate.

For a certain power output of a gas turbine and combined cycle, there is a range of fuel flow and air flow combinations that can be used. This means that the turbine exit temperature can be controlled within a certain range for a given power output. This is used in order to maximize the combined

cycle efficiency at part load. The various manufacturers have their own turbine exit temperature control procedures. In the following this is illustrated for four anonymous gas turbines in a combined cycle configuration, by turbine exit flue gas flow rate (

Figure 47), turbine inlet temperature (Figure 48), turbine exit temperature (Figure 49), and efficiencies for gas turbine, steam cycle and combined cycle (Figure 50 and Figure 57). There are three F-type gas turbines (F1-F3) and one E-type gas turbine (E), used to produce the results.

The relevance of these performance data to CO₂ capture is mainly the reduction of flue gas flow rate, and the change in concentration of CO₂ in the flue gas. The latter is depicted in Figure 58. The change in flue gas flow rate and concentration of CO₂ will influence the performance of a post-combustion process, like in an absorption column.

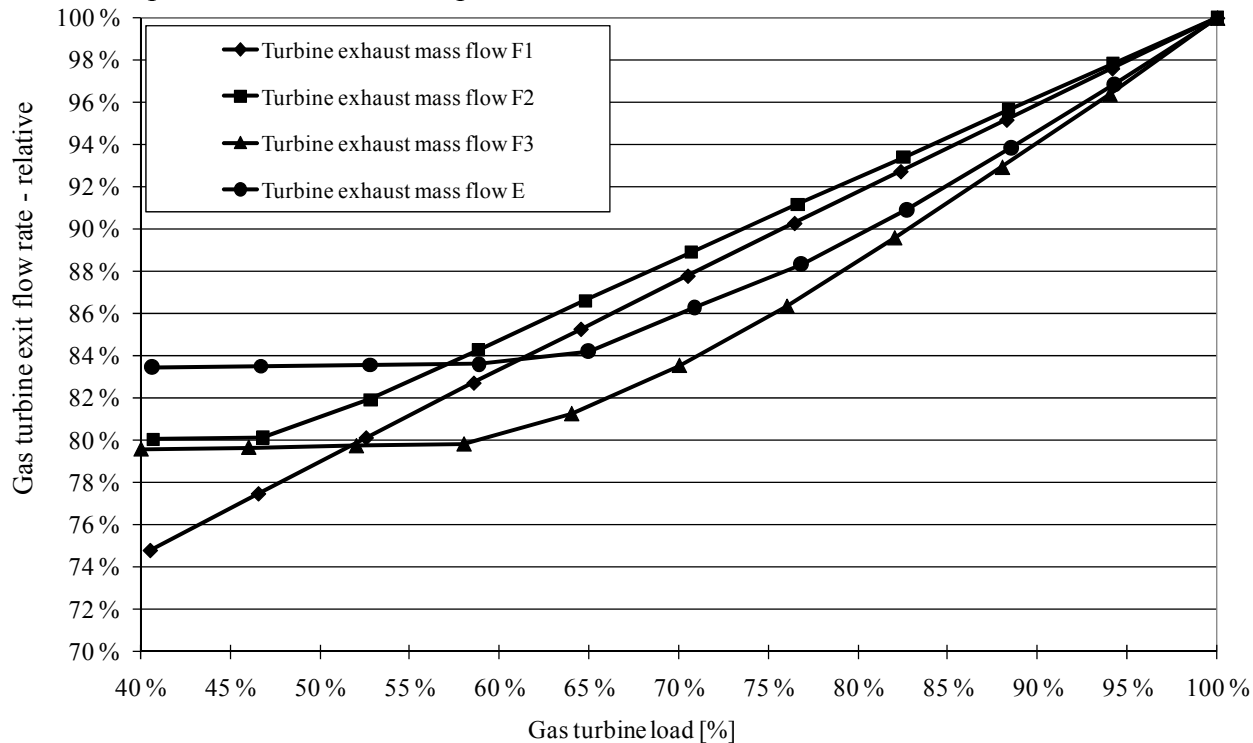


Figure 47 Gas turbine exit flow rate for a combined cycle where a combination of reduced air flow and fuel flow is used to obtain a specific power output and a turbine exit temperature.

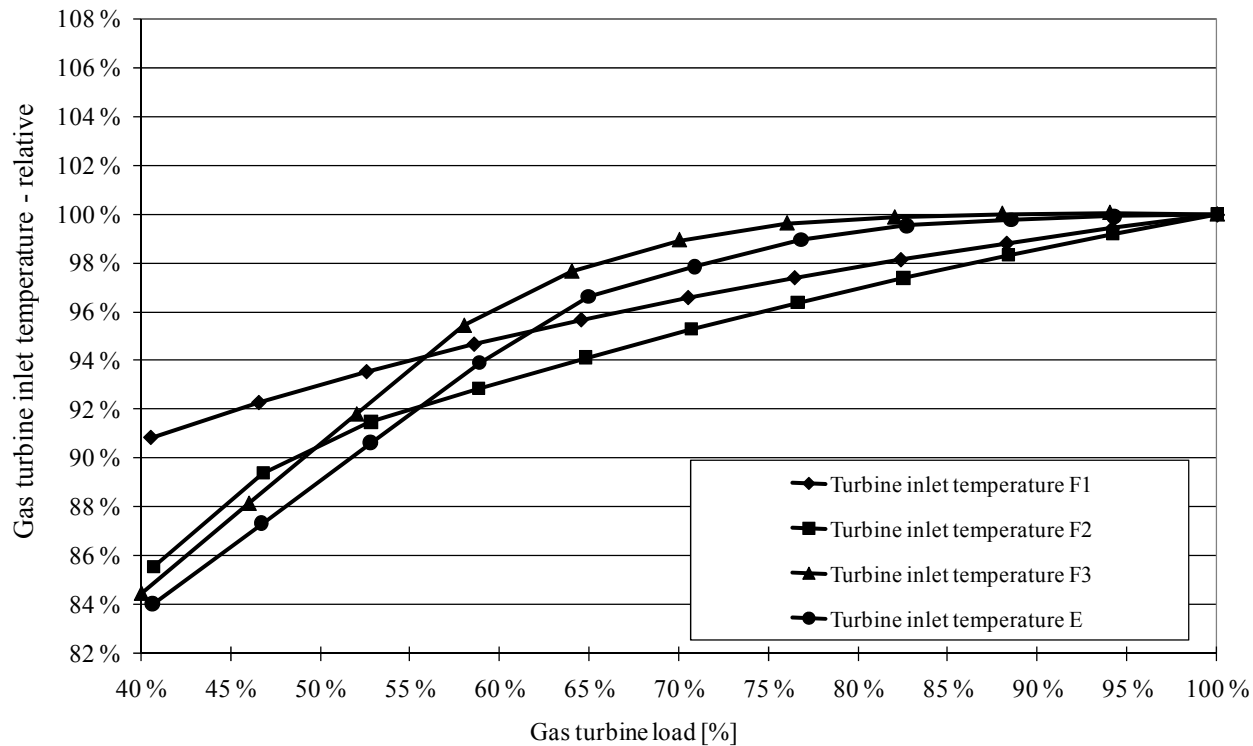


Figure 48 Gas turbine inlet temperature (TIT) for a combined cycle where a combination of reduced air flow and fuel flow is used to obtain a specific power output and a turbine exit temperature. The TIT reduction is moderate as long as air flow reduction can be used to reduce the power output.

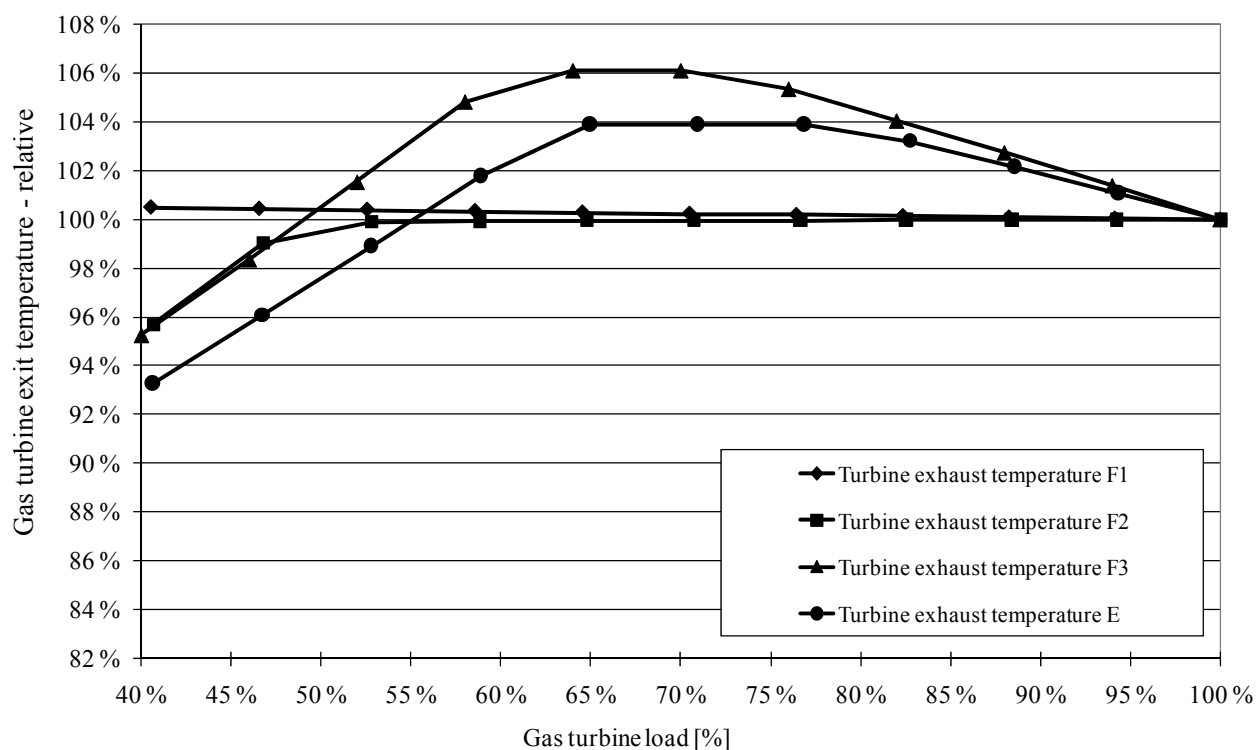


Figure 49 Gas turbine exit temperature for a combined cycle where a combination of reduced air flow and fuel flow is used to obtain a specific power output and a turbine exit temperature. Note that the temperature may increase for some part load levels.

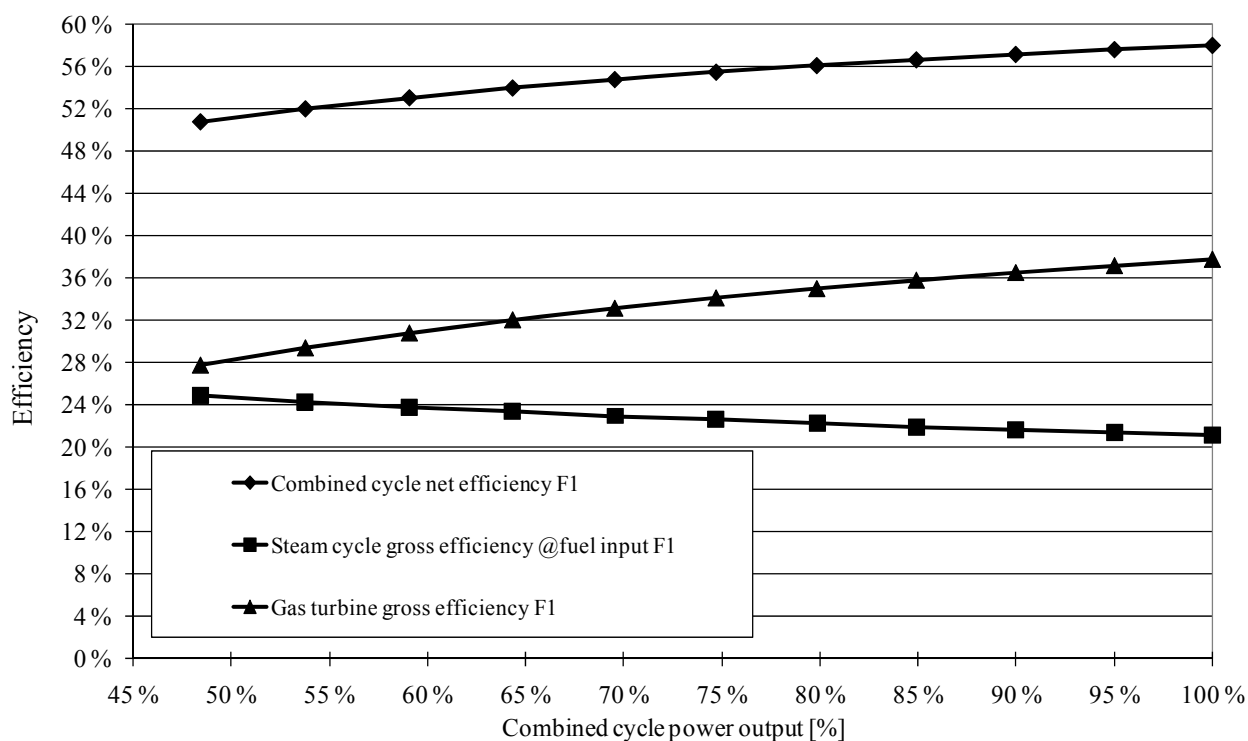


Figure 50 Gas turbine, steam cycle and combined cycle efficiencies for a modern F-type gas turbine. The efficiency of the steam cycle is based on the fuel used in the gas turbine.

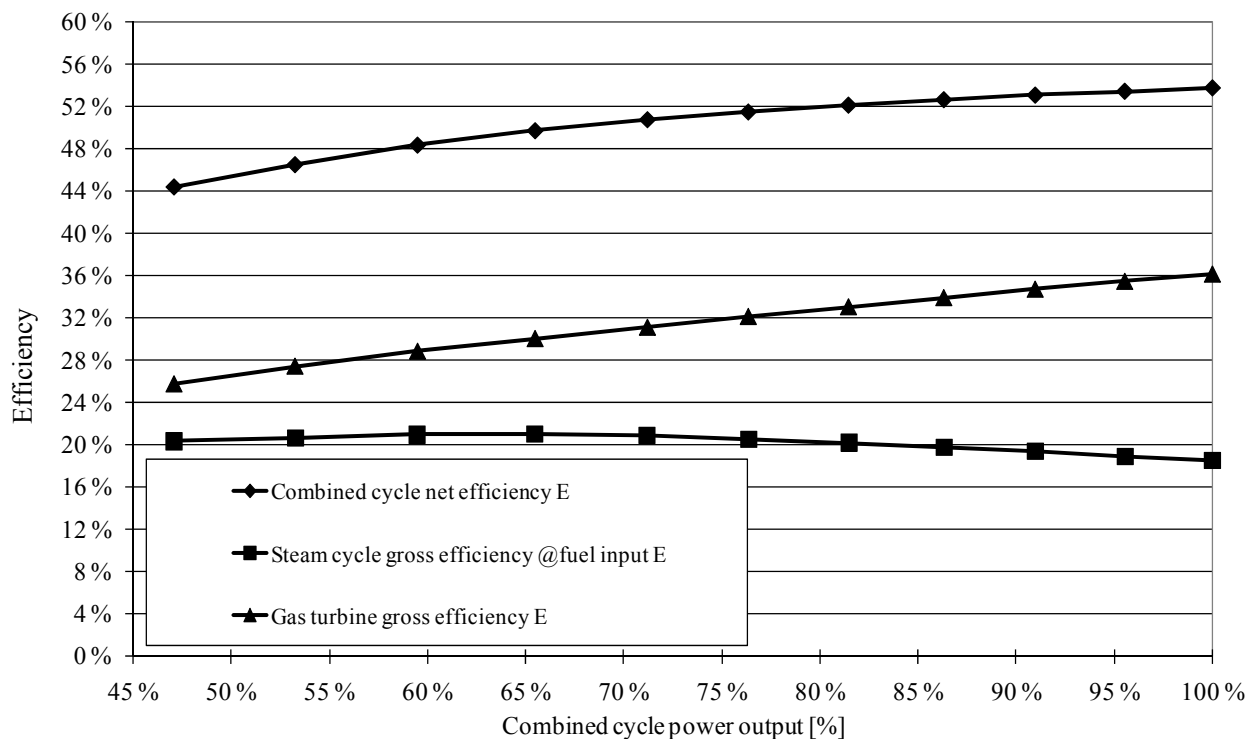


Figure 51 Gas turbine, steam cycle and combined cycle efficiencies for an E-type gas turbine. The efficiency of the steam cycle is based on the fuel used in the gas turbine.

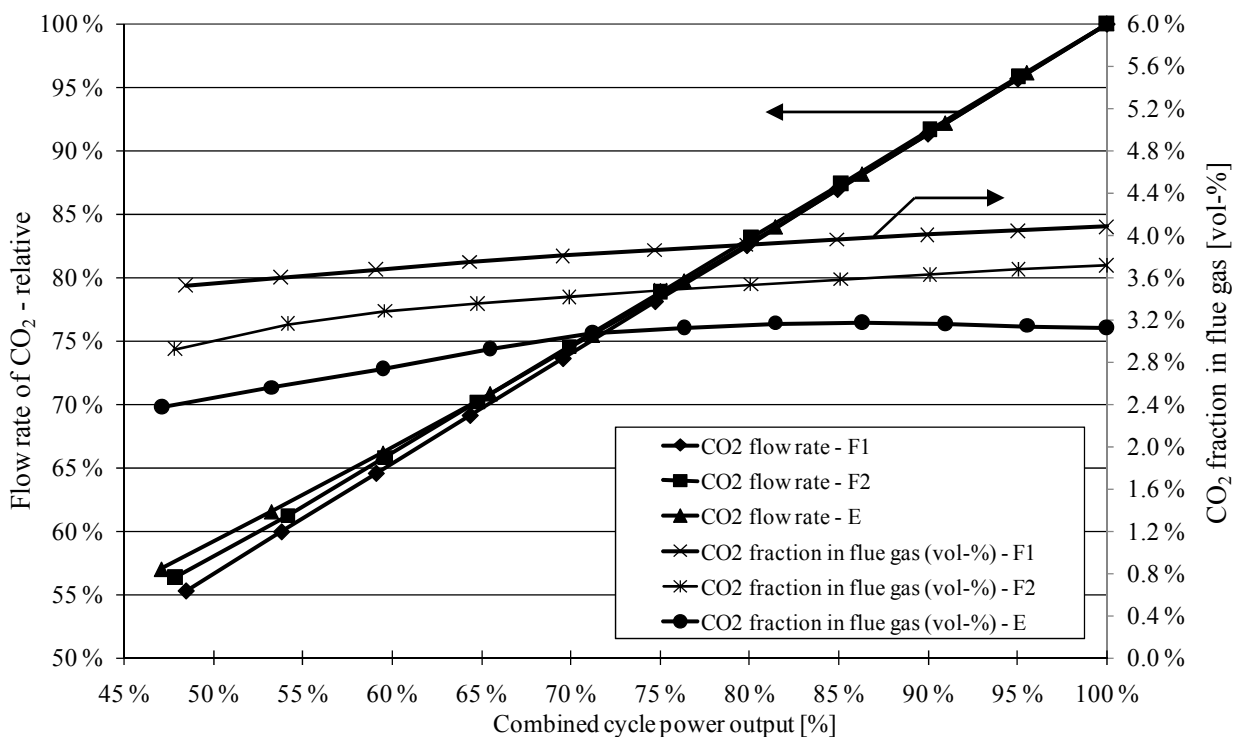


Figure 52 The relative flow rate of CO₂ (left) as a function of the combined cycle power output, and the volumetric fraction of CO₂ in the flue gas (right).

1.16 Air filter and exhaust duct pressure drop

The gas turbine is exposed to pressure drop both in the intake air filter and ducting, as well as for the exhaust gas in the ducting, heat recovery equipment and stack. A typical value of air filter and ducting pressure drop is 10 mbar. The value may vary both with design specifications and clogging caused by impurities in the air. Behind the gas turbine, the exhaust is exposed to many types of components that may vary a lot between plants. Such equipment may comprise the exhaust gas ducting, heat recovery equipment, gas cleaning equipment, duct burners. A HRSG will typically be the dominating cause of exhaust gas pressure drop, with about 20-35 mbar. For the total pressure drop behind a gas turbine, values ranging from 5-40 mbar are usual.

In Figure 59 the effects on power output and efficiency are depicted from variations in inlet filter pressure drop (a reduction of the pressure in front of the compressor) and exhaust gas duct pressure (increase of the turbine exit pressure).

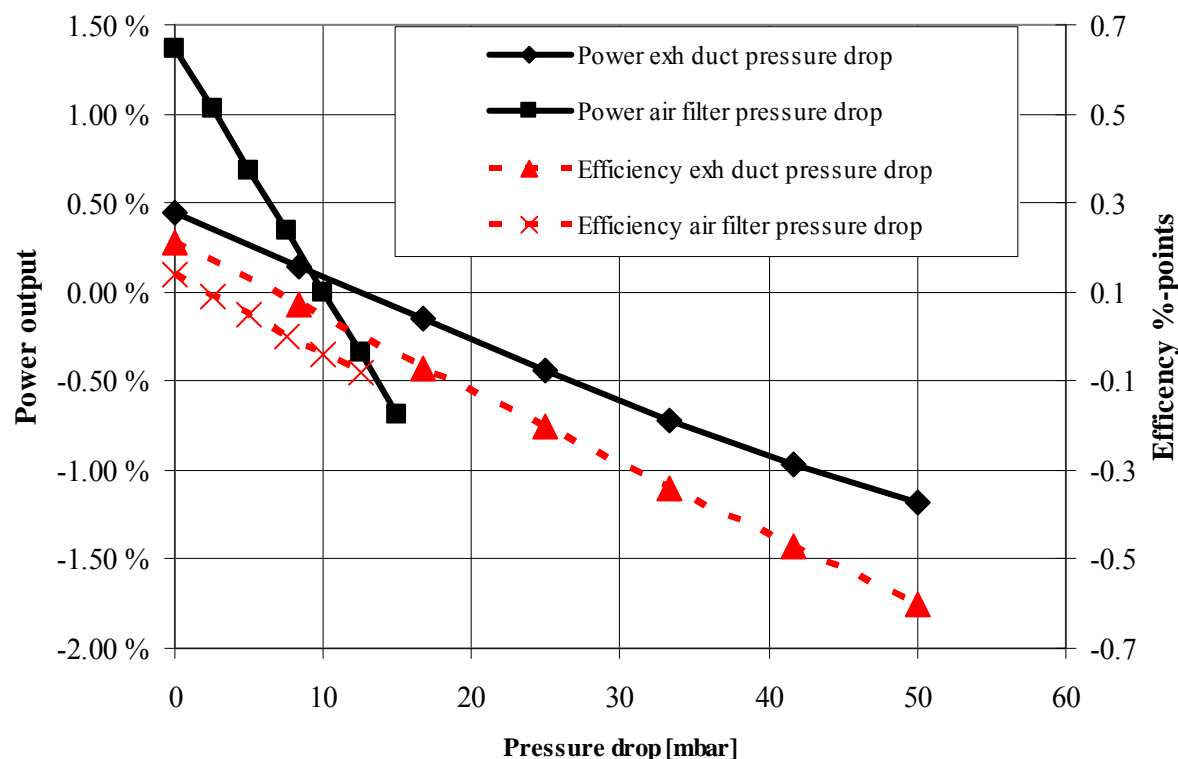


Figure 53 Influence of air filter and exhaust gas ducting pressure drop on gas turbine power output and efficiency. The right-hand side axis is showing changes in efficiency points, where 0 means a net gas turbine efficiency of about 38%.

1.17 Gas turbine instrumentation and control system

Modern gas turbine instrumentation and control systems provide advanced monitoring and diagnostics designed to prevent damage to the unit and to enable it to operate at its peak performance. The following sections describe the various measurements and instrumentation used in gas turbines.

1.17.1 Vibration measurement

Machine vibration is monitored using:

- Displacement probes
- Velocity pickup detectors
- Accelerometers (measurement of acceleration)

Displacement probes are used to measure the movement of the shaft in the vicinity of the probe. They cannot measure the bending of the shaft away from the probe. Displacement probes indicate problems such as unbalance, misalignment, and oil whirl.

Velocity pickup detectors have a flat response of amplitude as a function of frequency. This means that their alarm setting remains unchanged regardless of the speed of the unit. Their diagnostic role is somewhat limited. The velocity pickup detectors are very directional. They provide different values for the same force when placed in different directions.

Accelerometers are normally mounted on the casing of the machine. They pick up the spectrum of vibration problems transmitted from the shaft to the casing. Accelerometers are used to identify problems having high frequency response such as blade flutter, dry frictional whirl, surge, and gear teeth wear.

1.17.2 Pressure measurement

Pressure transducers consist of a diaphragm and strain gauges. The deflection of the diaphragm is measured by strain gauges when pressure is applied. The output signal varies linearly with the change in pressure over the operating range. Transducers having an operating temperature below 350°F (177°C) are located outside the machine due to temperature constraints. In these cases, a probe is installed inside the machine to direct the air to the transducer. Most modern gas turbines provide probes to measure the compressor inlet and outlet pressure, and turbine exhaust pressure. These probes are normally installed along the shroud of the unit. Some gas turbines have probes installed in each bleed chamber in the compressor and on each side of the inlet air filter. Figure 54 illustrates the locations of pressure and temperature probes in a typical gas turbine.

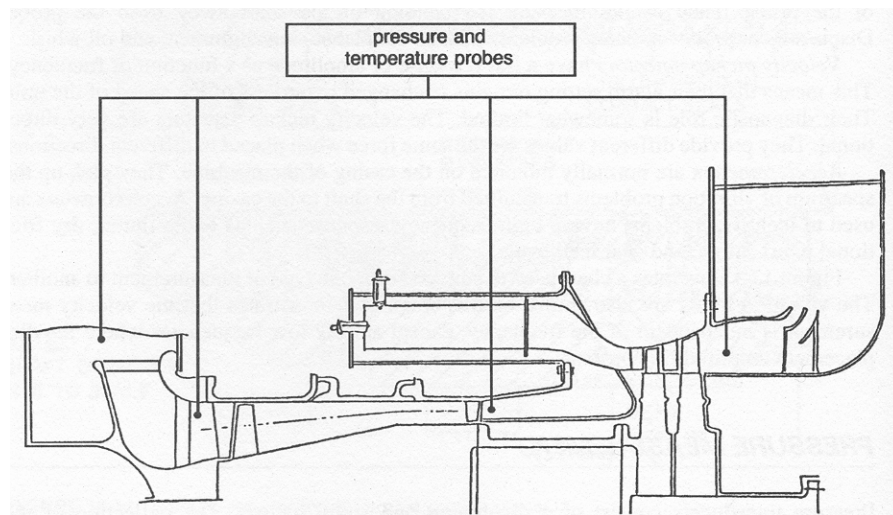


Figure 54 Locations of pressure and temperature probes on a typical gas turbine.

1.17.3 Temperature measurement

Temperature detectors such as thermocouples (used for high-temperature measurement) and resistive thermal detectors (RTDs) are installed in the following locations in a typical gas turbine:

1. Turbine exhaust temperature. Thermocouples are installed around the periphery at the exhaust of the turbine. Two thermocouples are installed at each location to improve the reliability of the measurements. Some gas turbines install thermocouples in two different planes at the turbine exhaust. The first set of thermocouples (e.g., 16) is installed, about 0.5 in (1.3 cm) downstream of the last-stage blades of the turbine. These thermo-couples measure the *blade path* temperature of the turbine. Differences between the readings obtained between thermocouples located at different locations around the periphery indicate differences in air temperature leaving the combustors. This differential temperature between the combustors creates significant thermal stresses on the blades of the turbine. Most control systems reduce the load or trip the gas turbine when the differential temperature readings exceed predetermined values.

2. The second set of thermocouples (e.g., 16) are installed at the exhaust of the gas turbine, a few meters downstream of the blade path thermocouples. They measure the air temperature leaving the machine. In heat recovery applications (e.g., cogeneration and combined cycle plants), this is the air temperature entering the heat recovery steam generators (HRSG). This temperature is monitored to prevent overheating of the turbine components. The temperature inside the combustors (firing temperature) is not normally monitored due to the following constraints:
 - Thermocouples that are able to detect a temperature around 2400 to 2600°F (1315 to 1427°C) are very expensive. ,
 - Turbine damage could occur if a thermocouple were to break and pass through the turbine blades.

Thus, the firing temperature is normally obtained by measuring the exhaust temperature of the turbine and calculating the firing temperature based on the design characteristic (expected temperature drop) of the turbine.

3. Redundant RTDs are embedded in the babbitt (white metal) of the bearing to monitor the oil temperature in the bearings. The unit is tripped on high lube oil temperature. It is also prevented from starting on a low lube oil temperature.
4. The compressor inlet and discharge temperatures are measured to evaluate the compressor performance.

Thermocouples and RTDs are used as temperature detectors. Each one of them has advantages and disadvantages. The following paragraphs describe the features of each type of temperature detectors.

Thermocouples

Thermocouples provide transducers used for measuring temperatures from -330 to 5000 F (-200 to 2760°C). Figure 55 shows the useful range of each type of thermocouples. They operate by producing a voltage proportional to the temperature difference between two junctions of dissimilar metals. Thermocouples measure this voltage to determine the temperature difference. The temperature at one of the junctions is known. Thus, the temperature at the other junction can be determined. Since they produce a voltage, there is no need for an external power supply.

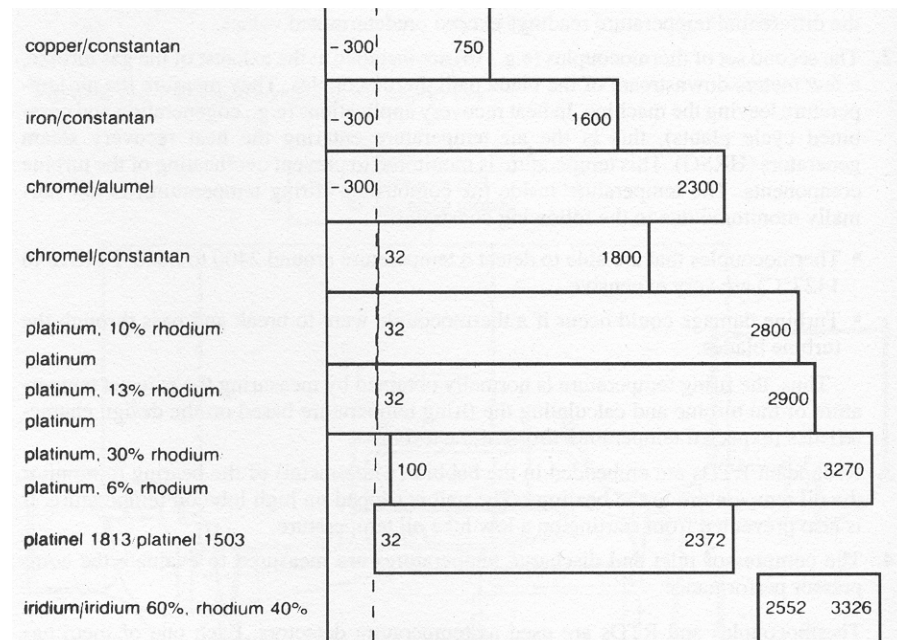


Figure 55 Ranges of various thermocouples, in Fahrenheit. Conversion to Celcius is $(F-32) * 5/9$.

Resistive Thermal Detectors

Resistive thermal detectors (RTDs) determine the temperature by measuring the change in resistance of an element due to a change in temperature. Platinum is normally used in RTDs due to its mechanical and electrical stability. Platinum RTDs are used for measuring temperatures from -454 to 1832 F (-270 to 1000°C). The RTD requires an electrical current source to operate. Its accuracy is within $\pm 0.02^\circ\text{F}$ ($\pm 0.01^\circ\text{C}$).

1.17.4 Control systems

The control system of a gas turbine performs the following functions:

- Provides speed and temperature control in the machine
- Control the unit during normal operation
- Provide protection to the gas turbine
- Perform start-up and shutdown sequence of events

Speed Control

Magnetic transducers measure the speed of the shaft at a toothed wheel mounted on the shaft. The transducers provide an output in the form of AC voltage having a frequency proportional to the rotational speed of the shaft. A frequency-to-voltage converter is used to provide a voltage proportional to the speed. This measured value of the speed is then compared to the desired value of the speed (speed setpoint). The difference between these two values is called the *error*. If there is an error, the control system will adjust the opening of the fuel valve to eliminate it. It relies on a proportional-integral-derivative (PID) algorithm (mathematical expression) to eliminate the error within minimal time and without instabilities (oscillations in the speed).

Temperature Control

A series of thermocouples mounted around the periphery at the exhaust of the turbine provides an input to the control system. They are normally made from iron-constantan or chromel-alumel fully enclosed in magnesium oxide sheaths to prevent erosion. Two thermocouples are frequently

mounted for each combustion can. The redundancy improves the reliability of the control system. The output of the thermocouples is generally averaged. . . . The control system compares this measured value of the turbine exhaust temperature with the desired value of *setpoint*. The difference between these values is called the *temperature error*. If the temperature error is different from zero, the control system will adjust the opening of the fuel valve to eliminate it. It relies also on PID algorithm to eliminate the error within minimal time and without instabilities.

Protective Systems

The protective systems provide protection during the following events:

- Overspeed
- Overtemperature
- Vibration
- Loss of flame
- Loss of lubrication

The overspeed protection relies on a transducer mounted on the accessory gear or shaft. It trips the unit at around 110 percent of the operating speed. The overtemperature protection system relies on thermocouples similar to the ones used for temperature control. The flame detection system consists of at least two ultraviolet flame detectors that provide the status of the flame in the combustion cans. In gas turbines having multiple-combustor cans, the flame detectors are mounted in cans, which are not equipped with spark plugs (igniters) to ease the propagation of the flame between cans during the ignition phase. During normal operation, a detector indicating a loss of flame in one can will only annunciate an alarm in the control room. At least two detectors must indicate a loss of flame to trip the machine. The vibration protection system normally relies on velocity transducers to provide a constant trip setpoint throughout the complete speed range. Two transducers are normally installed on the gas turbine with additional transducers on the driven equipment (e.g., generator). Vibration monitors provide an alarm at a specified level and a trip at a higher level. Most control systems provide a warning in the event of an open-circuit, ground, or shortcircuit fault.

1.17.5 Start-up sequence

The gas turbine control system performs the start-up sequence. It consists of ensuring that all subsystems of the gas turbine perform satisfactorily, and the turbine rotor temperature does not increase too rapidly or overheat during start-up. The control system is designed to start the unit remotely, accelerate it to operating speed, synchronize it automatically with the grid, and increase the load to the desired setting. The start-up sequence for a typical large gas turbine includes the following.

Starting Preparations

The following steps are required to prepare the equipment for a typical start-up:

- Close all control and service breakers.
- Close the computer breaker if it has been de-energized, and enter the time of day. Under normal conditions, the computer operates continuously.
- Acknowledge any alarms.
- Confirm that all lockout relays are reset.
- Place the “Remote-Local” switch to the desired position.

Start-up Description

When all the preparations to start the unit are complete and the unit is ready to go through the start-up process, the “Ready to Start” lamp will energize. At this stage, the operation of the start-up push button will initiate the start-up sequence. Following are the initial steps in the start-up sequence:

1. Energizing the auxiliary lubrication oil pump (see note)
2. Energizing the instrument air solenoid valve

Note: The auxiliary lubricating oil pump is normally powered from an AC power supply. It is used during the start-up and shutdown phase to provide lubrication to the machine. The main lubricating oil pump is normally shaft driven. It provides lubrication to the unit during normal operation. However, some units use two fully redundant lubricating oil pumps powered from an AC power supply. An emergency DC oil pump is also used in most gas turbines. It relies on power from a battery bank to provide sufficient lubrication for safe shutdown and turning gear operation when the normal AC power fails.

When the pressure downstream of the auxiliary lubricating oil pump reaches a predetermined value, the turbine turning gear is started. If the pressure downstream of the auxiliary lubricating oil pump does not reach the predetermined value within 30 s, the unit is shut down. When the signal indicating adequate operation of the turning gear is received, the start-up sequence continues.

At this stage, the starting device (e.g., starting motor) is activated if the lubricating oil pressure is sufficient (above the predetermined value). The turning gear motor is de-energized at around 15 percent of the operating speed. When the turbine reaches the firing speed (when ignition should start), the turbine overspeed trip solenoid and vent solenoid are energized to reset. When the oil pressure is sufficient, the overspeed trip bolts will be reset. These bolts are used to trip the unit at around 12.5 percent overspeed. They initiate the trip when the governing system fails to limit the overspeed to a lower value. When the overspeed trip bolts are reset, the ignition circuit is energized. It will initiate or energize the following:

- Ignition transformers.
- Ignition timer. (The unit is allowed 30 s to establish the flame on both detectors; otherwise, the unit will shut down after several tries.)
- Appropriate fuel system (depending on the type of fuel selected—liquid or gas).
- Atomizing air.
- Timer to de-energize the igniters at the proper time.

At around 50 percent of the operating speed, the starting device is stopped. This is called the *self-sustaining speed* of the gas turbine. At this stage, the turbine is generating enough power to drive the compressor and continue the increase in speed. The bleed valves, which bleed air from the compressor during start-up to prevent surge, close around 92 percent of the operating speed.

Following fuel injection and confirmation of ignition, the speed reference (known as the *no-load speed setpoint*) is increased. The fuel valve will open further to increase the speed of the unit. The shaft is accelerated at a desired rate that is limited by the maximum permissible blade path and exhaust temperatures. The unit is tripped if the desired acceleration is not maintained due to the following reasons:

- If the acceleration is high, compressor surge could occur, leading to extensive damage in the machine.

- If the acceleration is high, the rotor could overheat at a much higher rate than the stator. The rotor blades would expand at a higher rate than the stator blades. This could lead to rubbing between the blades, resulting in a significant damage to the turbine.

When the unit reaches the operating speed, it can be synchronized manually or automatically. Following synchronization, the speed reference becomes a load reference. In other words, since the speed of the unit cannot increase while the unit is synchronized, an increase in speed reference will result in an increase in the load. The speed/load reference is increased at a predetermined rate. This leads to further opening in the fuel valve until the desired load is reached. The computer will store the number of starts and operating hours at various loads. This information is used for maintenance scheduling.

Shutdown

Following a local or remote shutdown request, the fuel is reduced at a predetermined rate until zero load is reached. At this stage, the main circuit breaker connecting the unit to the grid and the circuit breaker connecting it to its own auxiliary loads (*field circuit breaker*) are opened and the fuel valves are tripped. During an emergency shutdown (e.g., a load rejection following a fault on the grid), the circuit breakers and fuel valves are tripped immediately without waiting for the load to be reduced. The turbine speed and the oil pressure from the motor-driven pump will drop. The DC auxiliary lubricating oil pump will start. At around 15 percent of the operating speed, the turning gear motor will be restarted. When the unit reaches the turning-gear speed (around 5 rpm), the turning-gear overrunning clutch will engage the shaft to rotate the rotor slowly.

The unit must be purged completely of any fuel before it can be restarted. This is done by moving air through it. The air flow must be greater than five times the volume of the turbine. The unit must be left on turning gear for up to 60 h. At this stage, sagging and hogging are no longer a concern due to low rotor temperature. The turning gear and auxiliary lube oil pump are stopped and the shutdown sequence is complete. The computer stores all the contact status and analog values. They can be displayed if required.

1.17.6 Gas turbines and fuel quality

Gas turbines can burn a wide range of fuels including various gas mixtures and distillates. Even crude oils and heavy fuel oils can be used as fuel, but then with some sort of fuel treatment and regularly maintenance. Regardless of the fuel employed, it must be supplied to the gas turbine within a certain specification of cleanliness in order to prevent high temperature corrosion, ash deposition and fuel system problems. Such specifications are made by the gas turbine manufacturers. It is important to take into account these specifications when dealing with non-conventional fuels.

High temperature corrosion in gas turbines can result from the presence of trace metals in the fuel. These are notably; sodium, potassium and vanadium which form compounds which melt on the turbine hot gas path components, dissolve the protective oxide coatings, and leave metal surfaces open to corrosive sulphidation attack.

Ash forming impurities may be present in the fuel as oil soluble organometallic compounds, water soluble salts and solids. Ashes formed during combustion may be deposited on hot gas path components causing a deformation of the optimum profile, a gradual decrease in the cross-sectional area of the gas path resulting in a power loss of the turbine.

The most critical components are the first stage vanes (high temperature) and first stage rotor blades (high temperature and high mechanical stress). These components are made of complex alloys with high mechanical strength at elevated temperature. They have a complex cooling structure, but the aggressiveness of the environment may be of such nature that the related corrosion phenomena become the limiting factor for component lifetime. It is therefore important to control degradation caused by corrosive substances in the combustion products.

Fuel system problems can result from the presence of water and solids such as sand, rust, scale and dirt as well as microorganisms. These cause clogging of filters and fuel distributors and erosion of fuel pumps.

Hot-corrosion problems have been encountered in modern gas turbines. Techniques have been developed to detect and control the parameters that cause these problems. They include the monitoring of the water content and corrosive contaminants in the fuel line. Any changes in the quality of the fuel can be identified and corrective measures taken. This technique relies on monitoring the water content in the fuel. Since sodium (Na) contaminants in the fuel are caused by external sources such as seawater, monitoring the water content will indicate the sodium content in the fuel. This on-line technique is used for lighter distillate fuels. For heavier fuels, a complete analysis of the fuel should be performed at least monthly using the batchtype system. The results of the analysis should be stored in the computer. The turbine efficiency should be determined with the aid of a fuel Btu (heat content) meter. A water capacitance probe is used to detect water in the fuel line. The corrosive condition of the fuel is monitored by a corrosion probe, which operates based on detecting metal in the fuel.

1.18 Dampinjiserte gassturbiner/Steam-injected gas turbines

1.18.1 Innledning

Dampinjeksjon i gassturbiner har lenge vært brukt til å senke dannelsen av nitrøse gasser. For dette formålet injiseres dampmengder i størrelsesorden med brenselmengden. Formålet med dette kapittelet er å se på dampinjeksjonsmengder som er betydelig større, og som hovedsakelig har andre formål.

Dampinjeksjon i gassturbiner har i prinsipp vært kjent lenge, men det er først i de siste årene at utviklingen har skutt fart. Et generelt navn på denne type prosess er "Cheng-cycle", oppkalt etter Dah Y. Cheng som er innehaver av den mest omfattende patentrettigheten på dette området. Et annet navn på denne typen prosesser er STIG (Steam Injected Gas Turbines). Gassturbin med dampinjeksjon kan en si er en kombinasjon av en Brayton- og Rankine-prosess.

Anvendelsesområdet for dampinjiserte gassturbiner er i hovedsak på små kraft/varme-kraftverk, som et alternativ til kombinerte kraftverk eller 'simple-cycle gassturbiner'. Det er spesielt i Nord-Amerika at installasjoner har blitt gjort.

Det er i første rekke såkalte flyderivert gassturbiner som egner seg for dampinjeksjon i større mengder. Det er fordi disse gassturbinene har en større evne til å ta en stor økning i massestrøm gjennom turbinen sammenlignet med de såkalt industrielle gassturbinene. Dette har sammenheng

med at de flyderiverte gassturbinene har større ”surge margin”. Her er noen eksempler på gassturbiner som egner seg for dampinjeksjon:

- Allison 501-KB
- UTC FT4C
- Garrett IE990
- Garrett 831
- General Electric LM2500 STIG 40
- General Electric LM2500 STIG 80
- General Electric LM2500 STIG 120
- General Electric M7652
- General Electric MS5002
- Solar Saturn
- Solar Centaur
- BBC Type 11

Maksimal mengde av dampinjeksjon ligger normalt i området 8-10 % av massestrømmen av luft inn i kompressor. Unntaket er gassturbinen Allison 501-KB som kan ta opp til 15-17 %.

1.18.2 Virkning av dampinjeksjon i gassturbiner

Hvis en ser på hva som skjer med en gassturbin når en injiserer damp, kan dette enkelt sammenfattes i følgende punkter:

- 1) Turbinen tilføres ekstra masse, som er ”gratis” på grunn av lavt pumpearbeid for vann sammenlignet med kompresjon av luft. Den økte massen fører til større avgitt arbeid fra turbinen.
- 2) Den ekstra massen (dampen) må tilføres energi for å bringes opp til temperaturen i innløpet av turbinen. Dette gjøres delvis ved hjelp av røykgass fra gassturbinen og delvis fra økt brennstofftilførsel i brennkammeret. Dette senker virkningsgraden.
- 3) Det økte dampinnholdet i gassen som ekspanderes gjennom turbinen får økt spesifikk varmekapasitet, og dette fører til økt avgitt arbeid.
- 4) For en gitt gassturbin øker trykkforholdet når damp injiseres.

Den totale virkning av de nevnte punktene er både økt effekt og virkningsgrad for gassturbinen. Sammenlignet med en gassturbin uten dampinjeksjon, senkes røykgasstemperaturen og trykkforholdet øker.

1.18.3 Fordeler og ulemper ved dampinjeksjon

Fordeler ved dampinjeksjon:

- Turbin innløpstemperatur kan holdes konstant ved dellast, ved at injisert dampmengde reduseres for å oppnå lavere last. Dette har stor betydning for levetid og driftsikkerhet på turbinen.
- Dannelse av nitrøse gasser (NOx) minskes ved dampinjeksjon.

- Driftserfaringer tyder på at tilgjengelighet og pålitelighet ikke reduseres ved dampinjeksjon.
- I kraft/varme-kobling kan behov for kraft og varme som varierer i motfase dekkes i større grad sammenlignet med gassturbin uten dampinjeksjon. Med dampinjeksjon blir området for fleksibilitet i denne sammenhengen betydelig utvidet.
- Variasjon av lufttemperatur gir mindre innvirkning på prosessen med dampinjeksjon
- Vannforbruket for en dampinjisert gassturbin er litt mindre enn for en kombinert prosess med vått kjøletårn.
- Sammenlignet med kombinerte anlegg er størrelsen på investeringsbeløpet mindre. Dette betyr mindre økonomisk risiko ved endring av markedsforhold.

Ulemper ved dampinjeksjon:

- Økt vannforbruk sammenlignet med en gassturbin uten dampinjeksjon. Vannforbruket ligger i området 1-1.6 kg/kWh.
- Høyere dannelse av nitrøse gasser ved lav dampinjeksjon. Dette fordrer muligen installasjon av katalysator selv om dette ikke er nødvendig ved full dampinjeksjon.
- På grunn av høyt vanndampinnhold i røykgassen, kan røykgassen ut av pipa bli meget synlig. Synlige utslipp fra kjøletårn blir ofte forbundet med forurensning, selv om det ikke er det. Utslipp fra kjøletårn er urettmessig nærmest blitt et symbol på forurensning fra kraftverk. Det foregår idag forskning på å unngå synlige utslipp. Her kan en nevne utvikling av hybrid-kjøletårnet.
- Større krav til kjøling av turbinblad, på grunn av ekspansjonsgassens økte spesifikke varmekapasitet og derved bedrede varmeovergangstall til metaloverflaten på turbinbladene.

1.18.4 Sammenligning med kombinert prosess

Den kombinerte prosess (som vil bli forklart senere) med kondenserende dampturbin har vist en unik fleksibilitet mellom produksjon av kraft og varme. Denne fleksibiliteten er større enn for dampinjiserte gassturbiner i kraft/varme-kobling. Når det gjelder virkningsgrad er den kombinerte prosessen med kondenserende dampturbin uten konkurranse fra dampinjiserte gassturbiner. Dette gjelder særlig for store anlegg i området over 50-100 MW.

Når det gjelder mindre anlegg hvor den kombinerte prosess ofte har mottrykks dampturbin, blir forholdene annerledes. Kombinerte prosesser med mottrykks dampturbin har liten grad av fleksibilitet mellom produksjon av kraft og varme. Her kan dampinjiserte gassturbiner konkurrere både i virkningsgrad og særlig i fleksibilitet.

Kombinert prosess med kondenserende dampturbin og vått kjøletårn har også meget god fleksibilitet, men forholdsvis lav virkningsgrad. Her kan dampinjiserte gassturbiner i kraft/varme-kobling konkurrere i økonomi. Dette er særlig interessant i områder hvor tilgangen på kjøling (vann) er begrenset.

1.18.5 Miljømessige konsekvenser av dampinjeksjon på gassturbiner

Utslipp av nitrøse gasser (NOx) kan begrenses i betydelig grad med dampinjeksjon, slik at typiske europeiske utslippskrav kan overholdes. Som nevnt får man her et problem hvis det under spesielle driftsforhold ikke injiseres så mye damp. Dette kan bety at installasjon av katalysator er nødvendig uansett.

Utslipp av karbonmonoksyd (CO) øker med økende dampinjeksjon i brennkammeret. Dette er særlig et problem under drift med en lavere innløpstemperatur enn normalt. Dette problemet kan løses med en større del av dampinjeksjonen i selve turbinen eller i utløpet av kompressoren.

Utslippen av uforbrente hydrokarboner øker når mengden av damp injisert i brennkammeret øker over en viss verdi. Dette kan delvis avhjelpes med de samme metodene som for reduksjon av CO nevnt ovenfor.

Tester utført på gassturbinen General Electric LM5000 viser at en ved full last kan oppnå utslipp av både NOx og CO under 25 ppm (basert på 15 % O₂).

1.18.6 Beregningseksempler for dampinjiserte gassturbiner

Tabell 8 viser noen beregninger for gassturbiner med og uten dampinjisering. Her ser en tydelig hvordan både effekt og virkningsgrad forbedres ved injisering av damp.

Tabell 8 *Gassturbiners effekt og virkningsgrad med og uten dampinjeksjon (foreldet!)*

Type gassturbin	Uten dampinjeksjon		Med dampinjeksjon	
	Effekt MW	Virkningsgrad %	Effekt MW	Virkningsgrad %
Solar Saturn	1.03	22.2	1.17	24.1
Allison 501-KB	3.6	27.6	4.1	29.5
G.E. LM2500 STIG40	21.2	35.4	26.1	39.6
UT FT4C-3F	28.5	30.2	32.6	31.8
G.E. LM5000 STIG80	32.2	35.3	44.4	40.8
G.E. LM5000 STIG120	32.2	35.3	49.0	42.2

1.19 Gas turbine database

In the following, data from the gas turbine data base of GTPRO (Thermoflow, Inc. – www.thermoflow.com) are presented; see Table 9, Table 10 and Table 11.

In Figure 56-Figure 62 the same information is presented in graphs.

In the following diagrams, performance data are presented for most gas turbines in the market in the range 0.5-330 MW. The performance values are taken at the reference conditions of the air entering the gas turbine set by ISO 2314:1989, 6.6.2:

- total pressure of 1.013 bar
- total temperature of 15 °C

- relative humidity of 60 %

Further, no-loss conditions are assumed, which means that there is no air filter pressure drop in front of the compressor inlet, and there is no pressure loss after the turbine. The compressor inlet pressure and the turbine exit pressure are consequently the same as the ambient air pressure of 1.013 bar.

Table 9 Gas turbine data – 0.5-25 MW - updated per 2008

	shafts	Speed	Pressure	TIT	Exhaust	Air flow	Power	Efficiency	Cost
		rpm	ratio	°C	°C	kg/s	MWe	%LHV	\$/kW
P+W ST6L-721	2	33000	6.9	888	513	3	0.486	22.2	1235
Vericor VPS1	1	41730	10.6	937	496	4	0.514	18.7	1362
P+W ST6L-795	2	33000	7.4	1004	589	3	0.65	23.2	1077
P+W ST6L-813	2	30000	8.5	1004	561	4	0.808	24.6	1238
Turbomeca M	2	22000	9.6	988	505	5	1.086	26	1197
Solar Saturn 20-T1600	1	22516	6.6	899	512	7	1.21	24.3	1074
Kawasaki GPB15	1	22000	9.4	991	520	8	1.48	24.2	878
Kawasaki GPB15D	1	22000	9.6	1002	530	8	1.48	24	946
P+W ST18A	2	18900	13.9	1093	532	8	1.826	28	986
Rolls-Royce 501-KB3	2	12850	8	1066	566	13	2.675	25	636
Kawasaki GPB30	1	22000	9.4	991	520	16	2.915	23.9	686
Kawasaki GPB30D	1	22000	9.6	1002	530	16	2.92	23.8	719
Vericor VPS3	2	15400	8.8	1104	601	13	3.089	26.5	712
Solar Centaur 40-T4700	1	14950	10	916	443	19	3.51	27.8	712
Vericor VPS4	2	16000	10.6	1232	560	14	3.815	30.1	629
P+W ST40	3	14875	16.9	1204	544	14	3.824	31.2	680
Rolls-Royce 501-KB5S	1	14200	10	1057	560	15	3.915	29.1	639
Solar Centaur 50	1	14950	10.7	1054	517	19	4.6	29.3	587
Solar Mercury 50	1	14180	9.9	1093	374	18	4.6	38.5	761
Rolls-Royce 501-KB7S	1	14600	13.9	1057	498	21	5.235	31.4	554
Siemens SGT-100-1S	1	17384	14.4	1110	531	20	5.29	30.3	586
Kawasaki GPB60D	1	14000	12.9	1093	542	22	5.398	29.2	537
Solar Taurus 60-T7800	1	14950	12.3	1093	508	21	5.5	31.4	509
GE5	1	16630	14.8	1232	574	19	5.5	30.6	527
Kawasaki GPB60	1	14000	12.7	1104	545	22	5.533	29.6	506
Solar Taurus 60-T7900	1	14950	12.3	1093	511	21	5.67	31.5	582
Rolls-Royce 501-KH5	1	14600	13.5	1052	535	15	6.1	38.1	623
Solar Taurus 65-8400	1	14950	15.4	1218	549	21	6.29	32.7	588
Kawasaki GPB70D	1	13790	15.9	1104	513	27	6.744	30.6	549
Siemens SGT-200-1S	1	11053	11.9	1024	466	29	6.745	31.3	563
Kawasaki GPB70	1	13790	15.9	1121	522	27	6.93	30.7	505
Solar Taurus 70-T10302S	1	10800	16.6	1121	494	26	7.305	33.5	520
Solar Taurus 70-T10300	1	10800	16.9	1121	486	26	7.515	34.1	519
Siemens SGT-300	1	14010	13.5	1110	538	29	7.969	31.1	540
MAN TURBO THM 1304-10	2	7556	10	982	495	44	9.31	28	580
Solar Mars 90-T13000	2	8568	16.3	1066	466	40	9.44	31.8	646
Solar Mars 100-T15000	2	8568	17.4	1104	487	41	10.68	32.6	655
MAN TURBO THM 1304-11	2	8600	11	996	487	48	10.76	29.8	586
GE10	1	11000	15.6	1077	481	47	11.25	31.1	569
MAN TURBO THM 1304-12	2	8600	11	1010	494	48	11.52	30.6	573
GE10	2	7900	15.6	1077	482	47	11.7	32	564
Siemens SGT-400	2	9500	16.3	1249	543	40	12.76	34.4	603
GE LM1600	3	7000	21.5	1232	488	46	13.7	35.4	474
Rolls-Royce Avon-2648	2	5500	9	893	438	77	14.61	28.7	534
Mitsubishi MF111B	1	9660	14.6	1135	526	56	14.838	31.3	553
Solar Titan 130-T20500	1	11170	17	1149	496	49	14.995	35.5	507
Hitachi H15	1	9710	14.6	1177	546	52	15.086	32	550
Siemens SGT-500	3	3600	12.1	863	374	92	17.015	31.8	523
GE LM2000	2	3600	15.6	1121	474	62	17.558	35.5	484
GE LM2000	2	3000	16	1121	479	63	17.639	34.9	482
Kawasaki GPB180D	1	9420	18	1249	544	58	17.72	33.3	525
GE LM2500PH	2	3600	17.6	1296	531	64	21.626	36.6	573
GE LM2500PE	2	3000	19.5	1296	529	68	21.822	35.5	509
GE LM2500PE	2	3600	19.5	1296	524	68	22.775	36.8	487
Siemens SGT-600	2	7700	14	1182	542	78	24.63	34.2	512

Table 10 Gas turbine data – 25-50 MW - updated per 2008

	shafts	Speed	Pressure	TIT	Exhaust	Air flow	Power	Efficiency	Cost
		rpm	ratio	°C	°C	kg/s	MWe	%LHV	\$/kW
P+W FT8 Swift Pac 25	3	3000	19.3	1160	463	82	25.048	37.7	551
P+W FT8 Swift Pac 25	3	3600	19.3	1160	463	82	25.048	37.7	551
Rolls-Royce RB211-6556	3	4950	20.8	1171	487	91	25.15	34.1	457
GE 5371PA	1	5100	10	963	485	123	26.555	28.9	471
P+W FT8 Swift Pac 25	3	3600	20.2	1221	480	85	27.555	38.1	559
P+W FT8 Swift Pac 25	3	3000	20.2	1221	480	85	27.555	38.1	559
Hitachi H25	1	7280	14.2	1177	547	89	27.69	33.8	401
Rolls-Royce RB211-6562	3	4800	20.8	1227	491	93	28.54	36.1	456
GE LM2500+PK	2	3000	24.5	1260	521	87	29.276	37.2	400
GE LM2500+PR	2	3000	25	1260	528	87	29.846	37.1	436
GE LM2500+PY	2	6100	23.3	1260	501	83	30.054	39.7	433
GE LM2500+PV	2	6100	23.3	1260	500	83	30.34	39.9	386
GE LM2500+PR	2	3600	24.4	1260	516	86	30.44	38.6	427
GE LM2500+PK	2	3600	24.3	1260	516	86	30.651	38.7	382
Rolls-Royce RB211-6761	3	4850	21.5	1260	504	93	31.57	37.7	494
GE LM2500+RD	2	3000	23	1288	526	90	32.606	38.3	451
GE LM2500+RB	2	6100	23.3	1260	511	88	32.686	39.7	450
GE LM2500+RC	2	3000	23	1288	524	90	32.835	38.4	396
GE LM2500+RD	2	3600	23	1288	526	90	33.104	38.9	444
GE LM2500+RA	2	6100	23.3	1260	524	90	33.337	39	390
GE LM2500	2	3600	23	1288	524	90	33.337	39	390
GE 6581B	1	5160	12.3	1135	546	145	42.1	32.2	375
GE LM6000 PD	2	3000	29.1	1260	452	125	42.751	41.4	426
GE LM6000 PF	2	3000	29.1	1260	452	125	42.751	41.4	444
GE LM6000 PD	2	3600	30	1260	456	124	42.916	41.7	424
GE LM6000 PF	2	3600	30	1260	456	124	42.916	41.7	443
GE 6591C	1	7100	19	1327	568	117	42.95	36.4	393
GE LM6000 PC	2	3000	28.9	1260	451	128	43.517	41.5	404
GE LM6000 PC	2	3600	30	1260	454	125	43.574	41.8	404
GE LM6000 PC	2	3600	28.9	1260	453	126	43.758	41.8	402
Siemens SGT-800	1	6600	19	1288	544	129	47	37.5	391
GE LM6000 PC SPRINT	2	3600	30.1	1260	449	129	47.125	41.7	386
GE LM6000 PC SPRINT	2	3600	30.1	1260	449	129	47.157	41.7	386
GE LM6000 PC SPRINT	2	3000	30.1	1260	448	130	47.179	41.5	386
GE LM6000 PC SPRINT	2	3000	30.1	1260	448	131	47.182	41.4	386
GE LM6000 PD SPRINT	2	3600	30.8	1260	448	130	47.265	41.7	400
GE LM6000 PD SPRINT	2	3000	30.8	1260	447	131	47.333	41.5	399
GE LM6000 PF SPRINT	2	3000	31	1260	450	131	47.958	41.6	409
GE LM6000 PF SPRINT	2	3600	31	1260	452	130	48.003	41.8	408
Siemens SGT-900	1	5400	15.3	1149	514	172	49.5	32.9	341
P+W FT8 Swift Pac 50	3	3600	19.3	1160	463	165	50.3	37.9	388
P+W FT8 Swift Pac 50	3	3000	19.3	1160	463	165	50.3	37.9	388

Table 11 Gas turbine data – 52-334 MW - updated per 2008

	shafts	Speed	Pressure	TIT	Exhaust	Air flow	Power	Efficiency	Cost
		rpm	ratio	°C	°C	kg/s	MWe	%LHV	\$/kW
Rolls-Royce TRENT 60 DLE	3	3000	35	1288	444	154	51.89	42.1	389
Rolls-Royce TRENT 60 DLE	3	3600	35	1288	440	154	52.157	41.9	387
P+W FT8 Swift Pac 50	3	3600	20.2	1221	480	170	55.406	41.9	383
P+W FT8 Swift Pac 50	3	3000	20.2	1221	480	170	55.406	38.4	383
ALSTOM GT8C2	1	6220	17.6	1177	508	194	56.46	34.3	377
Rolls-Royce TRENT 60 WLE	3	3600	36	1288	432	157	58.296	40.9	381
Rolls-Royce TRENT 60 WLE	3	3000	36	1288	424	160	58.296	40.7	381
Siemens SGT-1000F	1	5400	15.8	1310	583	188	67.4	35.3	369
GE 6111FA	1	5100	15.5	1327	594	210	78.3	35.7	332
GE 7121EA	1	3600	12.6	1113	534	297	85.99	33	280
GE 7121EA	1	3600	12.6	1113	534	297	86.67	33.2	280
ALSTOM GT11NM	1	3600	13.5	1146	503	315	89.6	34	288
GE LMS100PA	2	3600	37.4	1399	416	203	98.338	45	404
GE LMS100PA	2	3600	37.4	1399	416	203	98.338	45	417
GE LMS100PA	2	3000	37.4	1399	417	203	98.487	45.1	403
GE LMS100PA	2	3000	37.4	1399	417	203	98.487	45.1	416
ALSTOM GT11N2	1	3000	15.5	1146	526	393	113.58	33.3	271
ALSTOM GT11N2	1	3600	14.5	1146	532	392	113.9	33.3	263
ALSTOM GT11N2	1	3600	15.5	1149	526	393	115.395	33.8	263
Siemens SGT6-3000E	1	3600	14.2	1177	543	376	121.7	34.7	244
GE 9171E	1	3000	12.4	1129	540	414	127.6	34.2	243
Siemens SGT5-2000E (41MAC)	1	3000	11.9	1121	529	526	163.8	34.9	230
Siemens SGT5-2000E (33MAC)	1	3000	12	1149	539	525	167.7	35	228
GE 9231EC	1	3000	14.2	1204	553	515	172.985	35.5	234
ALSTOM GT24	1	3600	32	1260	615	421	173.35	35.7	256
GE 7241FA	1	3600	15.5	1327	597	449	174.56	36.8	253
GE 7241FA	1	3600	15.5	1327	599	448	174.6	36.7	246
ALSTOM GT13E2	1	3000	16.5	1149	510	554	180.16	36.9	251
GE 7251FB	1	3600	18.5	1371	626	445	186.6	37.2	258
Mitsubishi 501 F	1	3600	16	1399	614	462	188.29	37.2	242
Siemens SGT5-3000E (41MAC)	1	3000	13.4	1260	578	507	190.8	36.9	221
Siemens SGT5-3000E (33MAC)	1	3000	14	1288	587	507	201	37.2	220
Siemens SGT6-5000F	1	3600	14	1349	579	507	204.1	38.2	249
GE 9351FA	1	3000	15.8	1327	606	636	259.73	37.5	260
GE 9351FA	1	3000	15.8	1327	600	654	260.7	37.2	267
Mitsubishi 501 G	1	3600	20	1500	592	589	264.57	39.4	236
Siemens SGT6-6000G	1	3600	20.1	1427	598	588	266.3	39.3	239
ALSTOM GT26	1	3000	32	1260	616	626	276.2	37.4	281
Mitsubishi 701 F	1	3000	17	1399	588	655	278.84	39.3	266
Siemens SGT5-4000F	1	3000	17.2	1316	573	678	288	39.8	254
GE 9371FB	1	3000	18.2	1427	637	649	291.485	38.3	268
GE 9001H	1	3000	23.2	1427	621	685	331	39.5	279
Mitsubishi 701 G	1	3000	21	1427	587	737	334	39.5	276

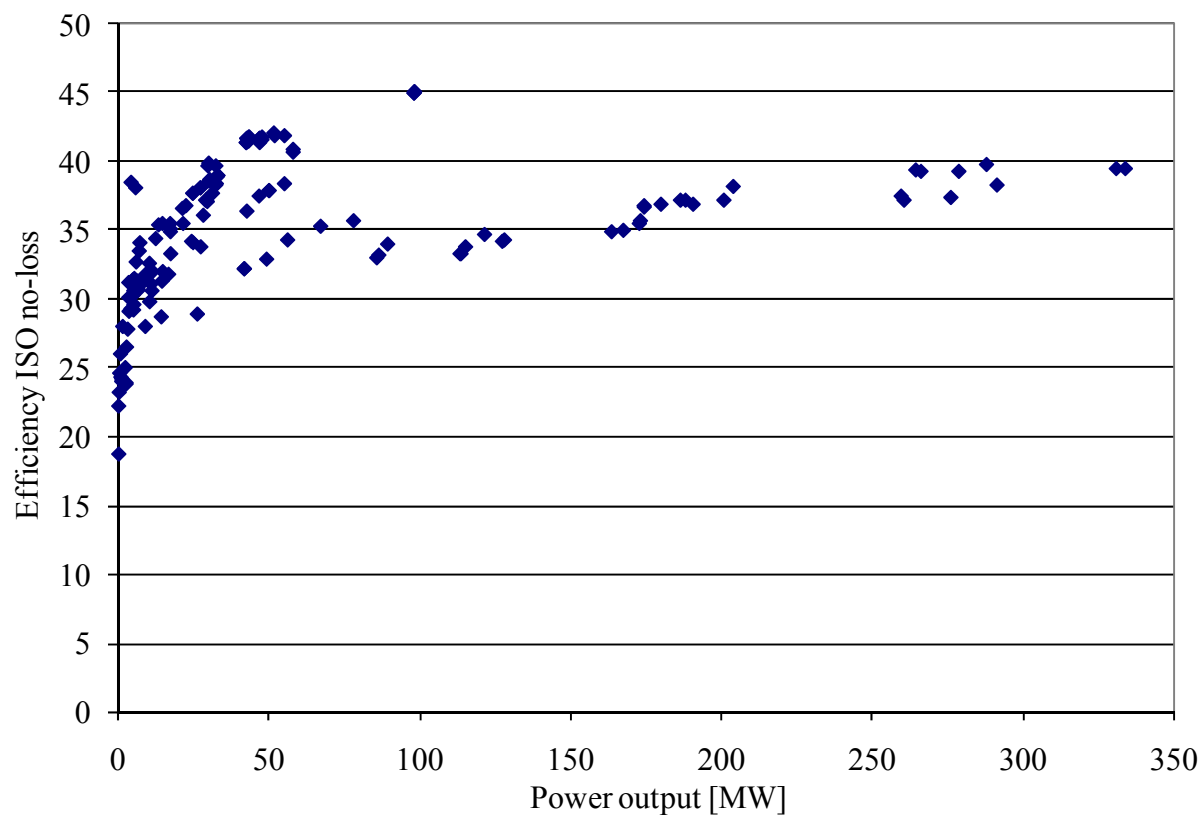


Figure 56 Gas turbine efficiency (no-loss, ISO conditions) vs. power output

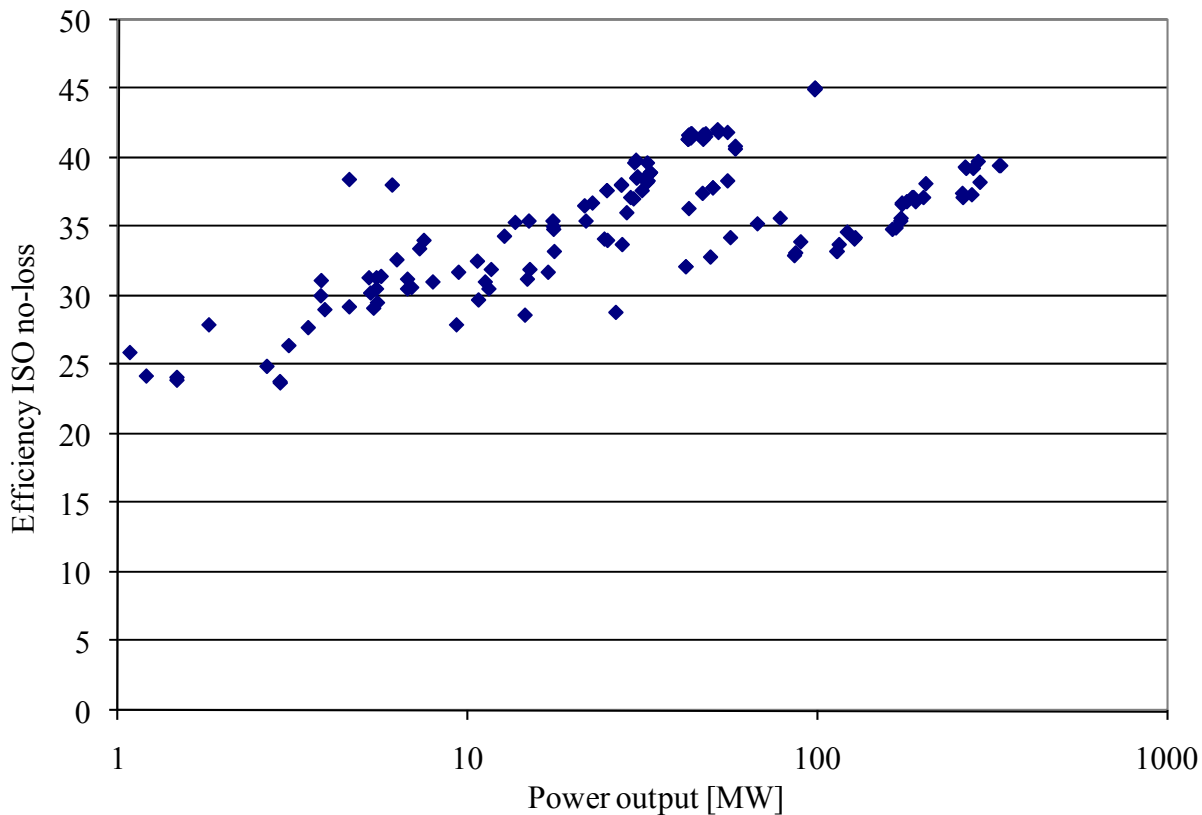


Figure 57 Gas turbine efficiency (no-loss, ISO conditions) vs. power output (logarithmic scale)

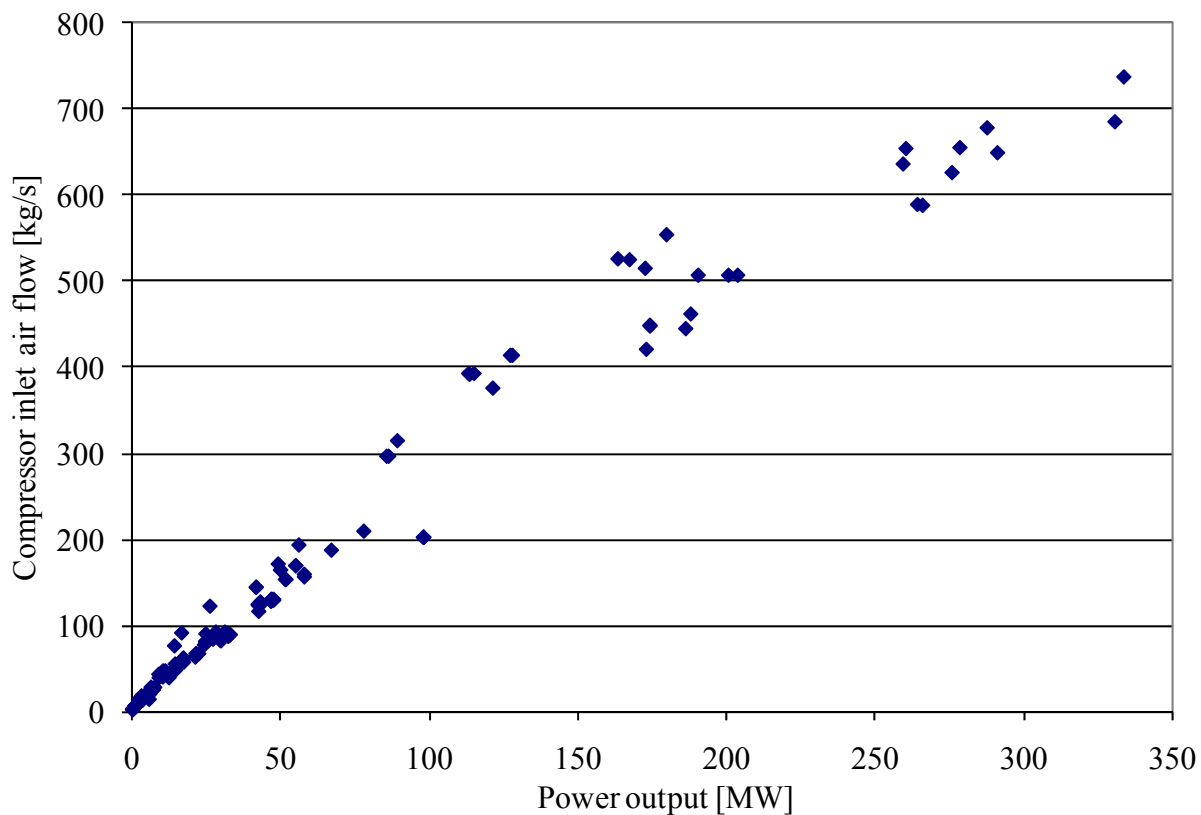


Figure 58 Gas turbine compressor inlet flow rate vs. power output

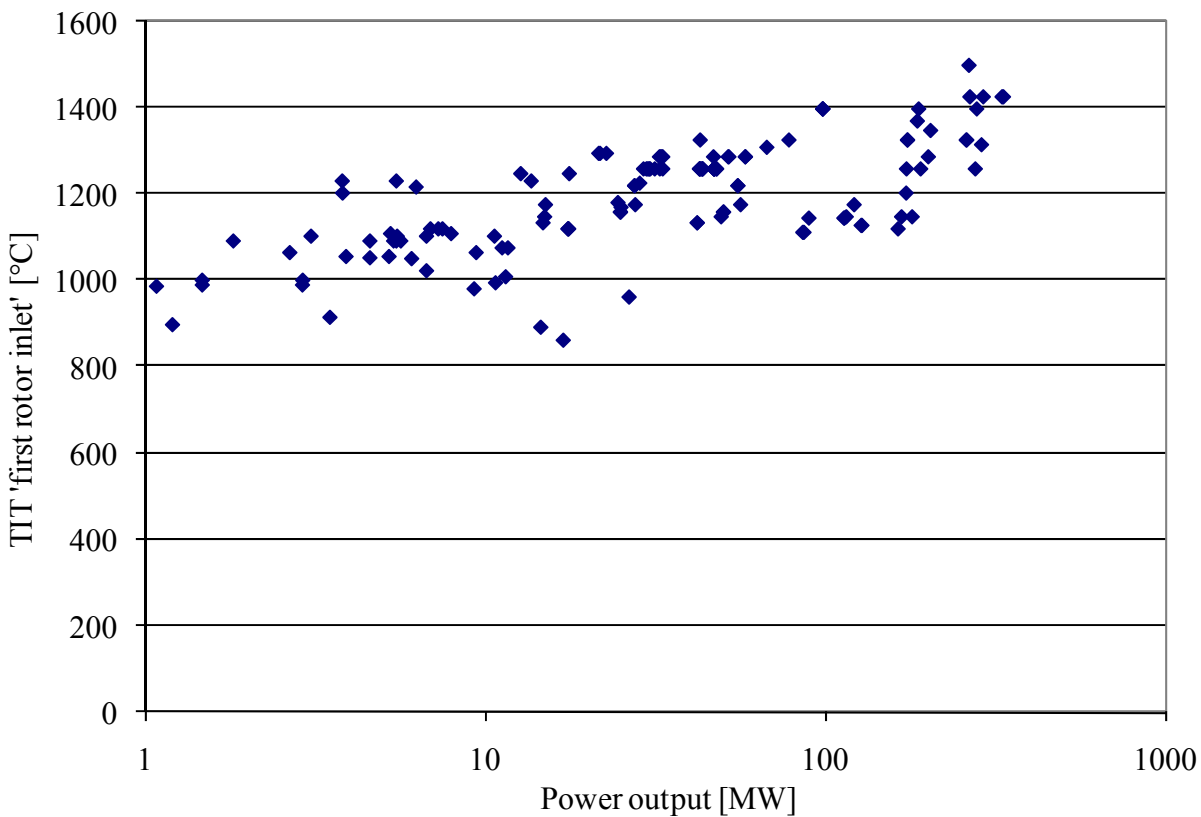


Figure 59 Gas turbine inlet temperature (first rotor inlet) vs. power output (logarithmic scale)

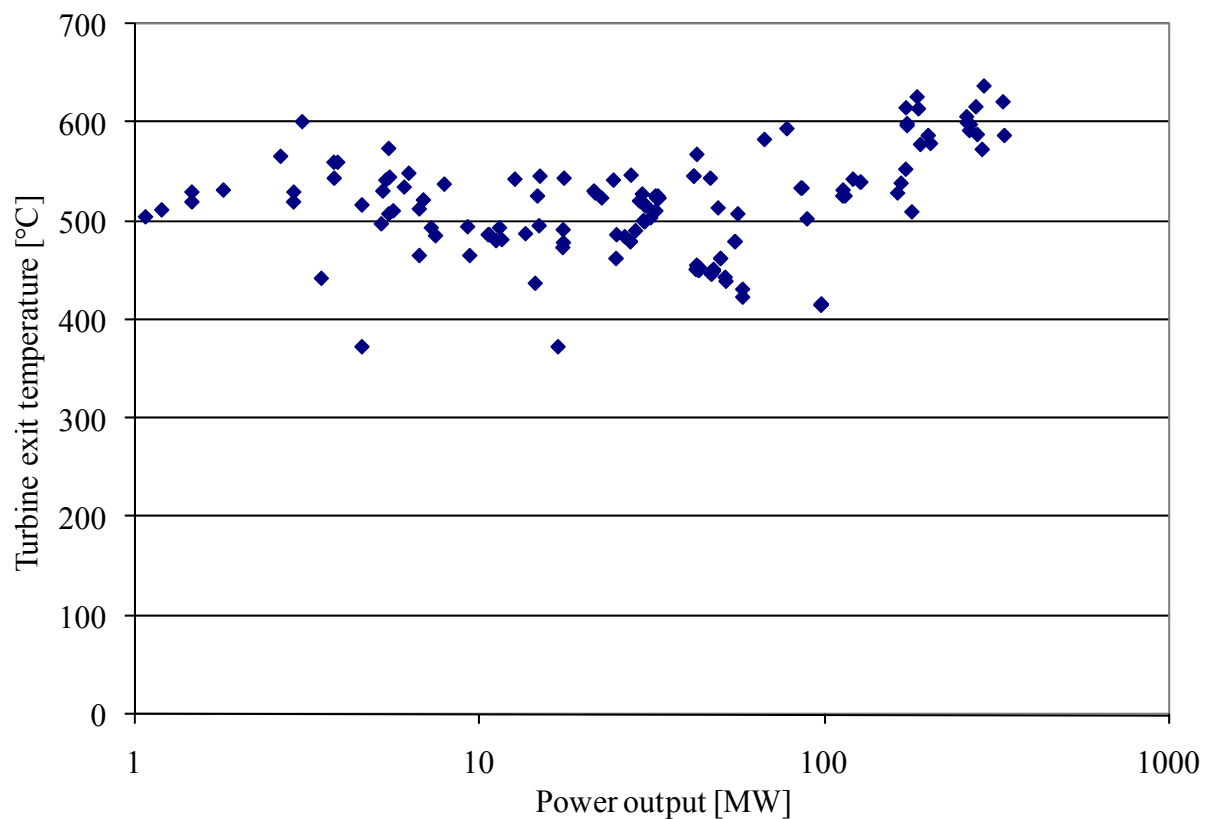


Figure 60 Gas turbine exhaust temperature vs. power output (logarithmic scale)

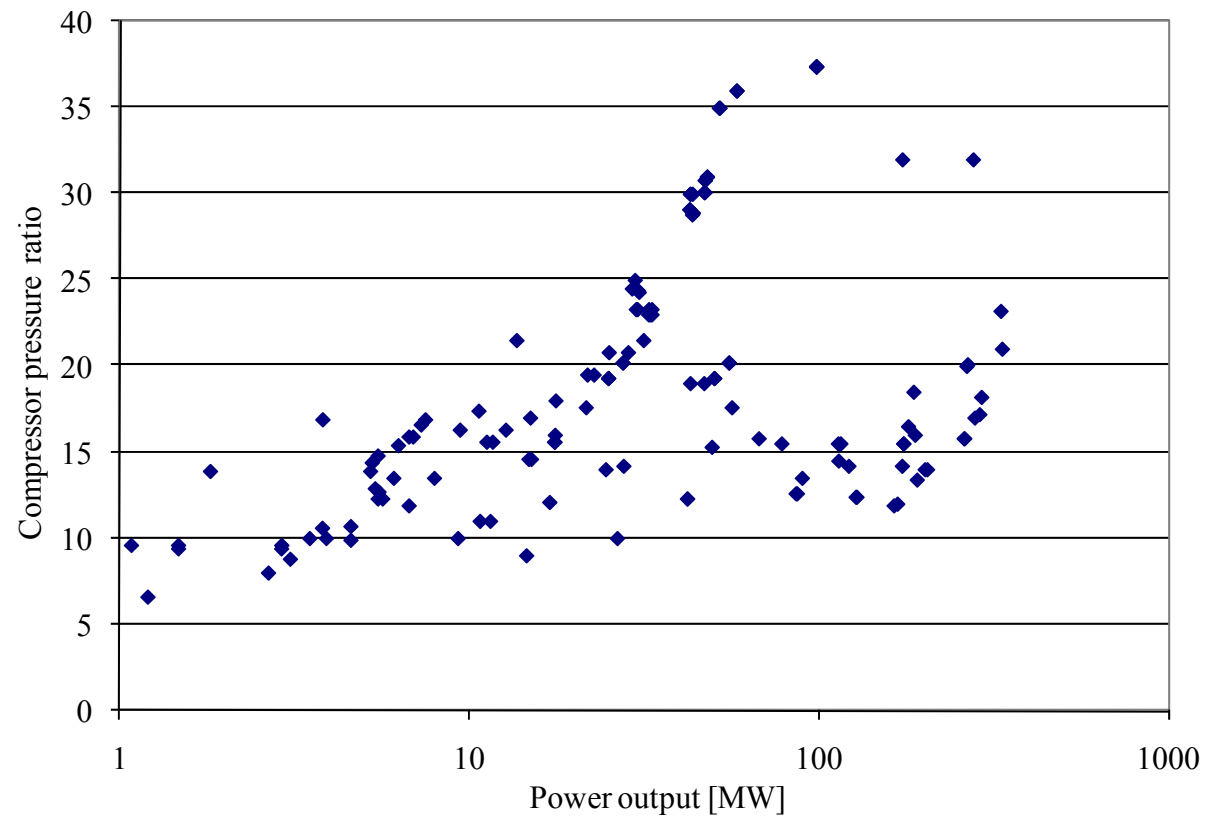


Figure 61 Gas turbine pressure ratio (compressor) vs. power output (logarithmic scale)

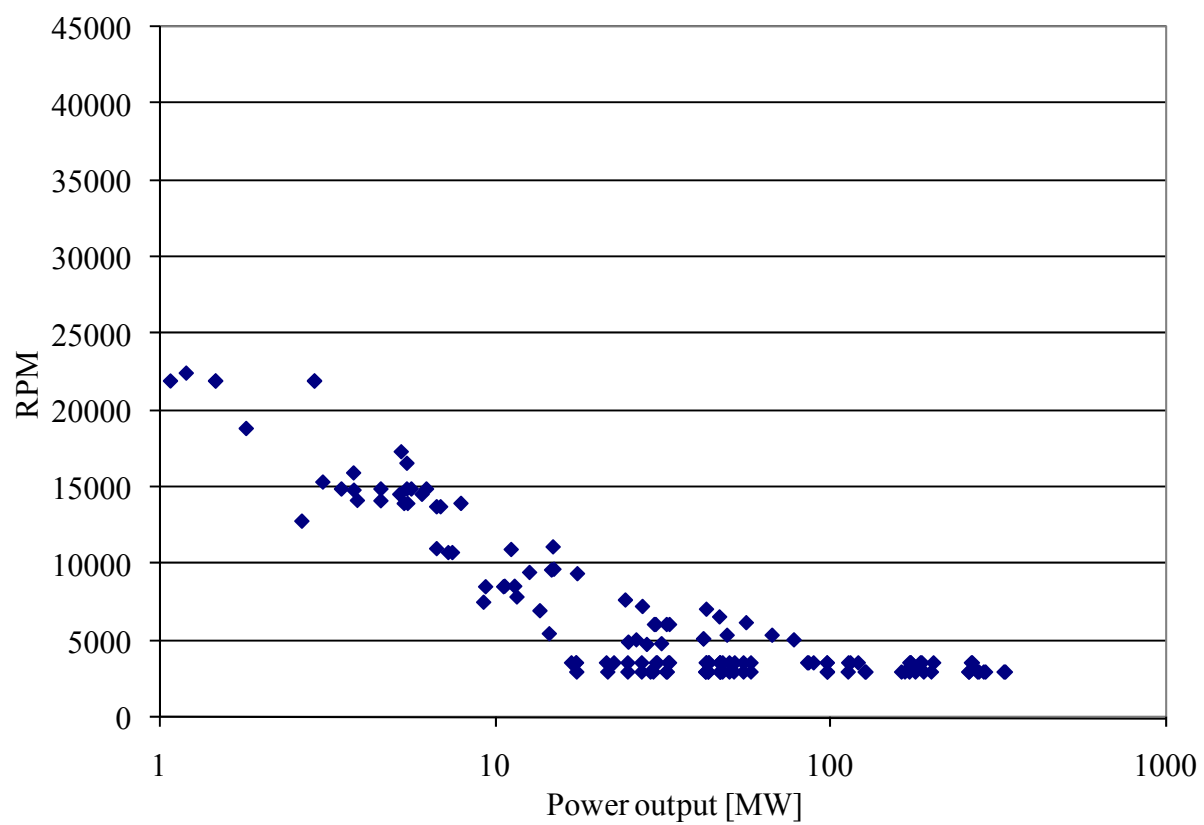


Figure 62 Gas turbine speed vs. power output (logarithmic scale)

2 Gas turbine fuels

2.1 Introduction

The gas turbine plants that have been installed over last years are mostly operated on natural gas (80%), while approximately 18% are operated on light oil and distillates, and 2% are operated on residual oil (ABB, 1994a; Siemens, 1994).

For gas turbine power plants, gaseous hydrocarbon fuels are better than available liquid fuels from a technical point of view, with respect to plant performance, plant availability and pollution emission levels. Natural gas with little sulphur and no fuel-bound nitrogen can be regarded as the best in this respect. A gas turbine plant is normally designed for use of a liquid fuel as backup (⌚ 2 days) in case of unavailability of gas. However, there are reasons for gas turbine power plants being able to burn different kinds of liquid fuels including low quality liquid fuels. These reasons may be the ability to better negotiate the price of natural gas, or to be able to produce in periods of time when the availability of natural gas, for some reason, is poor.

2.2 Why fuel specifications for gas turbines

Gas turbines can burn a wide range of fuels including distillates, crude oils and heavy fuel oils. Regardless of the fuel employed, it must be supplied to the gas turbine within a certain specification of cleanliness in order to prevent high temperature corrosion, ash deposition and fuel system problems.

High temperature corrosion in gas turbines can result from the presence of trace metals in the fuel. These are notably, sodium, potassium and vanadium which form compounds which melt on the turbine hot gas path components, dissolve the protective oxide coatings, and leave metal surfaces open to corrosive sulphidation attack.

Ash forming impurities may be present in the fuel as oil soluble organometallic compounds, water soluble salts and solids. Ashes formed during combustion may be deposited on hot gas path components causing a deformation of the optimum profile, a gradual decrease in the cross-sectional area of the gas path resulting in a power loss of the turbine.

The most critical components are the first stage vanes (high temperature) and first stage rotor blades (high temperature and high mechanical stress). These components are made of complex alloys with high mechanical strength at elevated temperature. They have a complex cooling structure, but the aggressiveness of the environment may be of such nature that the related corrosion phenomena become the limiting factor for component lifetime. It is therefore important to control degradation caused by corrosive substances in the combustion products.

Fuel system problems can result from the presence of water and solids such as sand, rust, scale and dirt as well as microorganisms. These cause clogging of filters and fuel distributors and erosion of fuel pumps.

2.3 ISO-specifications for gas turbine fuels

There exist ISO specifications for gas turbine fuels (ISO 4261, 1993; ISO 3977, 1991). This standard sets out the properties of fuels at the time and place of transfer of custody to the user. The turbine user should confirm that arrangements are made to ensure that the fuel entering the combustor meets the manufacturer's requirements. This may include transportation arrangements with the fuel supplier, particular care in fuel storage, quality control at the point of use and fuel purification procedures. One should note that trace contamination may occur during transportation and storage. For trace metals in the fuel, the ISO 4261 gives guidelines on limits, but the user should take advice from the gas turbine manufacturer. The guideline limits in ISO-4261 are:

Vanadium	0.5 milligrams/kg (or ppm)
Sodium + Potassium	0.5 milligrams/kg
Calcium	0.5 milligrams/kg
Lead	0.5 milligrams/kg

2.4 Significance of specifications for gas turbine fuels

The properties selected in the ISO specifications, are those that are considered to be of most importance in determining the characteristics of fuels used in various gas turbine applications, and are chosen to ensure that adequate care has been taken in the handling of these fuels prior to the transfer of custody to the user. In general, these specifications are the same as those required for fuels used in industrial and marine engines and boilers, but gas turbine experience has shown that additional controls on the chemical nature of the fuel ash are desirable to restrict the corrosion potential of certain slag-forming substances which can be deposited on those turbine parts which may operate above 590 °C.

Flash point

The flash point is a guide to the fire hazard associated with the storage and use of gas turbine fuels. Specification of minimum flash point temperature is usually mandatory.

Viscosity

Viscosity is a measure of the resistance of the fuel to flow. For gas turbine fuels it is extremely important, as it is a measure of how well the fuel will flow or can be pumped and also of the ease of atomization at the fuel nozzles.

A minimum viscosity is specified, as some fuel pumps may not operate satisfactorily if the viscosity is below this figure. A maximum viscosity is specified for these fuels to prevent excessive pressure losses in the system, pumping problems and poor atomization.

Low-temperature operability

A number of test methods for assessing low temperature operability of gas turbine fuels are available. The method chosen will depend on the category of fuel and on local practice. There are several different methods for assessing low-temperature properties of gas-oil type fuels.

- a) Cloud point (for determination see ISO 3015) i.e. the temperature, expressed to the nearest 1 °C, at which a cloud or haze of wax crystals appears at the bottom of the test jar when the oil is cooled under specified conditions. It is the most restrictive method of low temperature performance assessment. Most gas-oil type fuels are still capable of flow at temperatures somewhat below their cloud point, but at such temperatures any fine filters in the fuel line may become obstructed and restrict or prevent flow.
- b) Pour point (for determination see ISO 3016), i.e. the lowest temperature at which movement of the oil is observed, when the sample is cooled under prescribed conditions and examined at intervals of 3 °C for flow characteristics. Pour point can be reduced significantly by the use of certain types of additives.
- c) Cold filter plugging point, i.e. the highest temperature, expressed to the nearest 1 °C, at which the fuel, when cooled under the prescribed conditions, either will not flow through a fine mesh filter or a nominal aperture width of 45 µm or will require more than 60 s for 20 ml fuel to pass such a filter or aperture when subjected to a vacuum of 2.0 kPa.

Carbon residue

The Ramsbottom test for carbon residue measures the amount of carbonaceous residue formed during the evaporation and pyrolysis of a petroleum product when burnt with limited excess air. It is intended to provide some indication of the relative coke-forming tendency, content of aromatic compounds and smoke forming in the exhaust. Further, coke particulates may lead to increased erosive impact on turbine blading. The residue is not entirely formed of carbon but is a coke which can be changed further by pyrolysis. Petroleum products containing naturally occurring ash-forming constituents or additives will have an erroneously high carbon residue when measured by the test, depending on the amount of ash which can be formed.

Ash and trace metal contaminants

The test (ISO 6245) measures material remaining after combustion at 775 °C, from ash-forming constituents naturally present in the fuel or from additives or inorganic contaminants.

Ash results from the non-combustible material in a fuel. Ash-forming contaminants occur in liquid fuels in three forms; suspended solid particulates, dispersed salt water and oil-soluble compounds. The solid particulate and salt water can cause maintenance problems in the fuel system. A greater concern is the formation of fouling and corrosive combustion ash deposits from all three of ash-forming contaminants when the fuel is burned. With distillate-type fuels, these potential problems can be avoided or minimised by maintaining strict cleanliness of the fuel.

The primary condition for corrosion of a metal surface in a hot gas path by an overlying ash deposits is that the metal temperature be higher than the melting point of the ash. A melted ash can dissolve a protective oxide layer and attack the metal substrate, whereas a dry ash could be inert or interact with the underlying metal at a much slower rate. Different compounds present in the combustion ash have different melting points, depending on the specific chemical composition of the ash and the local turbine environment. The major metallic elements occurring in fuel which contribute to corrosion are sodium, potassium, vanadium and lead.

Even very small concentrations of corrosive contaminants in the fuel can form significant ash deposits. As an example, at a fuel consumption rate of 25 t/h, each 1 mg of ash per kilogram of fuel means 25 g of ash passing through the turbine each hour.

The total ash in distillate fuels is usually very small and the results of salt water or gasoline contamination during fuel transportation, handling and storage. Residual fuels (and crude oils) have much higher ash contents due to a higher retention of dispersed water and solids and to the presence of soluble organometallic compounds of vanadium, nickel and possibly iron. The ash content of distillate fuels is normally less than 100 mg/kg fuel, and is typically 2-10 mg/kg for a clean fuel. Residual fuels on the other hand, may contain several hundred milligrams of ash per kilogram, usually necessitating complete fuel treatment; desalting and vanadium inhibition by an additive, usually magnesium- and sometimes silicon-based.

Ash-forming contaminants may also enter the gas turbine in the turbine inlet air, particularly in marine and industrial environments. Unless removed by proper inlet air filtration, these airborne contaminants by themselves, or in combination with fuel ash, may also cause corrosion of hot metal parts.

Corrosive fuel ash

Corrosive combustion ash will form whenever there are significant contaminant levels of vanadium, sodium, potassium or lead in a liquid fuel.

Vanadium

Vanadium occurs as an oil-soluble organometallic compound in crude oils, varying in concentration from less than 1 mg/kg to over 100 mg/kg depending largely on the geographic origin of the crude oil. During petroleum refining, the vanadium concentrates in the residual oil, the distillates being virtually vanadium-free. Vanadium cannot be economically removed from crude oils or residual oils to produce vanadium-free fuels.

During combustion, vanadium is converted to vanadium pentoxide, melting at 675 °C. If sodium is present with vanadium, sodium vanadates with melting points as low as 535 °C can form.

The melting point of the ash can be raised by adding a magnesium compound to the fuel (dosage ratio magnesium to vanadium is 3:1). Excess sodium content will counteract this reaction, so consequently the lower the sodium content, the better the response to the magnesium additive. Silicon compounds exert a physical dilution effect, reducing the corrosive action of sodium/vanadium complexes. Whenever additives are used, fouling but nonaggressive ash deposits will build up in the turbine hot gas path and reduce the output of the turbine. They have to be removed periodically to maintain turbine performance. Calcium can act as an effective inhibitor for vanadium corrosion, but its deposition tendencies have precluded its use (forming hard insoluble deposits resulting in permanent loss of power and efficiency).

Sodium and potassium

Sodium and potassium are components of salt water, a common contaminant in liquid petroleum fuels. The sodium concentration in salt water is several times the concentration of potassium, and both are capable of forming highly corrosive combustion ash.

Sodium sulphate is formed when liquid fuels are burned; it melts at 884 °C, causing "sulphidation" attack.

Sodium- and potassium-caused corrosion is usually controlled by removal of salt water from the fuel by settling, centrifuging or electrostatic separation, or coalescing filtration. Careful design and management of storage facilities, combined with adequate settling times, will contribute to fuel cleanliness, thus significantly reducing the effects of water-soluble contaminants, and may reduce the need for further separation techniques. Chromium-based additives have been reported to be effective in combatting the corrosive action of sodium.

Lead

The presence of lead in gas turbine distillate fuels is usually the results of the fuel being contaminated with leaded gasoline or used lubricating oils during transportation and handling. Lead contaminants are oil-soluble and cannot be removed by fuel cleaning. During combustion lead is converted to lead oxide or lead sulphate. These compounds have fairly high melting points, but the presence of minor amounts of sodium will lower the ash melting point to around 600 °C.

Strict fuel management during transportation, handling and storage is best way to avoid lead contaminants. Some success has been reported using additives based on magnesium and chromium to increase the ash melting point of a lead-containing fuel.

Other elements

Nickel, zinc, arsenic and other heavy metals which are sometimes present in category 4 fuels may form low-melting eutectic with metals and cause corrosion.

A summary of the effects on the turbine and possible treatment of fuel trace metal contamination is shown in Table 12.

Table 12 *Trace metals in gas turbine fuels: effects and treatment*

Trace metal	Effect on turbine	Type of treatment
Sodium	High temperature	Fuel washing
+ Potassium	Corrosion Deposition	(settling, centrifuging electrostatic separation coalescing filtration) Turbine washing
Calcium	Hard deposits	Fuel washing Turbine washing
Lead	High temperature corrosion	Inhibited by Mg and Chromium addition
Vanadium	High temperature corrosion Deposition	Inhibited by Mg or silicon compound additions
Magnesium	Inhibits vanadium but forms deposits	Magnesium sulphonate, magnesium oxide or magnesium sulphate

Ash content

The amounts of all harmful elements should be kept as low as possible in a gas turbine fuel. However, the ash content has a great influence on the corrosive effect of these elements. The effect of 1 mg sodium and 1 mg vanadium per kilogram fuel can have different significance depending on the total ash content. This is illustrated as follows:

Table 13 *Significance of ash content in conjunction with sodium and vanadium*

	Fuel A	Fuel B
Sodium content	1 mg/kg fuel	1 mg/kg fuel
Vanadium content	1 mg/kg fuel	1 mg/kg fuel
Ash content	10 mg/kg fuel	100 mg/kg fuel
Na + V as % of total ash content	20% (wt.)	2% (wt.)
Influence on ash melting point	Great	Small

Fuel A can be corrosive in the gas turbine while Fuel B can be acceptable, despite the fact they have the same sodium and vanadium contents (see Table 13). The behaviour of the ash of Fuel A can be converted into that of the ash of Fuel B by adding an additive that contributes a further 90 mg/kg fuel of inert or high melting point material to the ash.

Fouling ash deposits

The combustion ash may be harmless due to its high melting point, but accumulation of fouling deposits will disturb blade and vane efficiency and reduce throughput area, resulting in decreased power and increased fuel consumption. The rate of buildup of fouling deposits is a function of many factors, such as total fuel ash content and composition, particle capture efficiency, turbine operating temperature, turbine design and size.

Additive combinations, like magnesium + silicon, can significantly reduce the fouling rate. The turbine manufacturer should always be consulted for recommendations for the use of such additive combinations.

The use of high ash content fuel of category 3 or 4 may result in fouling to such a degree that periodic ash removal from the turbine hot gas path is required.

Calcium in a fuel is not harmful from a corrosion standpoint; in fact, it serves to inhibit the corrosive action of vanadium. However, calcium can lead to hard-bonded deposits difficult to remove even with water washing. Calcium is not a problem with distillate type of fuels, but may occur for heavier fuels/residual oil. Fuel washing systems, normally required for heavier fuels/residual oil, also reduce the calcium contaminant level.

Fuel ash evaluation

A fuel ash evaluation should provide information on, both the amount of ash formed during fuel combustion and the potential corrosiveness of this ash. The total amount of ash is determined by carefully burning a measured volume of fuel in the laboratory and weighing the residue obtained from ashing the combustion residue.

Two methods are available for assessing the potential corrosiveness of the combustion ash. The first is the determination of the trace metallic element concentrations in the fuel. The second is a melting point measurement of a fuel ash prepared in the laboratory. Turbine manufacturers set limits on trace metal contents or ash melting point (ash sticking temperature may be used in place of ash melting point) based on correlations with turbine performance experience. Both ash evaluation methods have an uncertainty because the ash deposit formed at a given point in the turbine hot gas path may not have the same composition as the ash produced outside the turbine in the laboratory. Ash-forming elements may not deposit in the turbine in the same proportions in which they are present in the fuel. Composition of turbine deposits can differ at different deposition sites, and given deposits may not be homogeneous.

Low ash content distillate fuels require very careful burning and subsequent ashing of large quantities of fuel to provide the minimum amount of ash required for ash content determination and for ash melting point tests.

Water and sediment

The limits for this adventitious contamination are set at the lowest level consistent with normal transport and handling procedures and which the propensity of a particular category of fuel to hold these materials in suspension. Sediment is defined for this purpose as material insoluble in toluene.

Water and sediment in a fuel oil tend to cause fouling of the fuel handling facilities and the gas turbine fuel system. The sediment in fuel can be gums, resins, asphaltic materials, carbon, scale, sand or mud. It is mainly a problem in residual oils. Very few distillate fuels leave the refinery with more than 0.05% water and sediment.

Fuel storage tanks should be designed with floating suctions that are equipped with low level bottom limits.

Sulphur

Sulphur is present to some degree in all petroleum fuels. Sulphur occurs in fuels as combustible organic compounds yielding sulphur oxides on combustion. These combine with any traces of sodium or potassium present to form alkali sulphates; a principal source of hot corrosion. The sulphur level in a fuel cannot be lowered enough by refining to avoid the formation of alkali sulphates, so that they must be controlled by limiting the sodium and potassium levels in the fuel.

Gas turbine installations utilising exhaust heat recovery equipment could have metal temperatures below the dewpoint of sulphuric acid, and in these cases it is necessary to know the sulphur level in the fuel to avoid acid corrosion of heat transfer surfaces. The maximum allowable sulphur to avoid sulphuric acid condensation will depend on the specific heat recovery equipment used. For fuels exceeding this maximum level, the operating temperature of the heat recovery equipment could be changed accordingly to avoid condensation of acid products.

The sulphur level of liquid fuels is regulated in many localities as a means of controlling the emission of sulphur oxides in the exhaust gas.

Crude oils burned directly as fuels may also contain active sulphur in the form of hydrogen sulphide or mercaptans. These substances, especially in the presence of water, may cause corrosion to fuel system components. For this reason, the water content of such fuels should be kept as low as possible.

2.5 Non-fuel contaminants

Contaminants harmful to gas turbines, in excess to those that are in the fuel, can be air-borne, water-borne and brought in by inhibitor dosing.

In the case where contaminants are present in air, water/steam and/or inhibitor, the total limits in the fuel should be controlled such that the total concentration equivalent in the fuel (from all sources) conforms to the given limits for a specific gas turbine.

Air-borne contaminants

Contaminants in air can cause erosion, corrosion and fouling of the compressor. These contaminants can also contain the same trace metals as found in fuels and which cause corrosion to the hot section of the gas turbine.

Compressor erosion can be caused by sand or flyash; compressor corrosion by noxious fumes such as HCl and H₂SO₄; compressor fouling by liquid or solid particles which adhere to the compressor blading. Hot section corrosion can be caused by sodium from, e.g., sea salt, salt particles, carry-over of treatment chemicals used in evaporative coolers, chemical process effluents; potassium from flyash or fertilizers; lead from automobile exhausts; and vanadium from residual fuel fired steam plants.

Specifically, with respect to hot section corrosion, the total of Na, K, V and Pb should not exceed 0.005 ppm by weight in air. If it is anticipated that this level will be exceeded, special care should be taken with respect to air filtration.

Water-borne contaminants

Water or steam injection is used for NO_x control or steam that is injected to augment power output should not contain impurities which cause hot section deterioration or deposits. Specifically, the total of Na + K + V + Pb should not exceed 0.5 ppm by weight in the water or steam.

2.6 Fuel treatment technology

2.6.1 Introduction

Fuel oils are complicated mixtures of hydrocarbons categorized for marketing convenience by specifications. The fuel specification will largely determine the type of fuel treatment system which must be supplied in order to prevent costly operating problems, such as hot corrosion and the clogging, erosion and corrosion of the fuel systems in liquid fired gas turbines. Guidance for fuel treatment system selection is given in Table 14.

Table 14 *Fuel treatment system selection (after Alfa Laval)*

Type of fuel oil	Fuel treatment system
Distillate	Single-stage centrifugal separation without water washing
Light Crude	
Heavy crude	Two-stage centrifugal separation with water washing
Residual or blended residual	

Since alkali metals are present as water soluble salts, they can be extracted from the oil by water addition. Especially the elements sodium and potassium, which are harmful to the gas turbine components, are removed by separation of the water phase to an acceptable remaining level. Simultaneously, also solid foreign matter is efficiently removed by this separation process. This "water washing" is done with demineralized water.

The essential steps in a two-stage fuel treatment system for heavy fuel oil is shown in Figure 63. The major functions of the system are:

- Pumping
- Demulsifier dosing
- Heating
- Mixing
- Water/oil separation
- Vanadium inhibitor dosing
- Waste water treatment

The corrosive action of vanadium is inhibited by an additive, usually magnesium- and sometimes silicon-based. Siemens (1994) has developed a process for vanadium inhibition, based on socalled EPSOM salt ($MgSO_4 \cdot 7H_2O$). The cost of EPSOM salt consumed during operation is approximately 5.5-6.5% to that of AMERGY 5800 and KL-200. EPSOM salt has the advantage over AMERGY 5800 and KL-200 that the deposit layer is softer.

Clogging of filters in the fuel system should be expected when using a residual oil. These filters are arranged in a parallel manner such that one is in operation while another is being cleaned. Normally $10\mu m$ filters are used, but for residual oil $25\mu m$ is used. Bottom cleaning of the fuel storage tanks must be carried out from time to time.

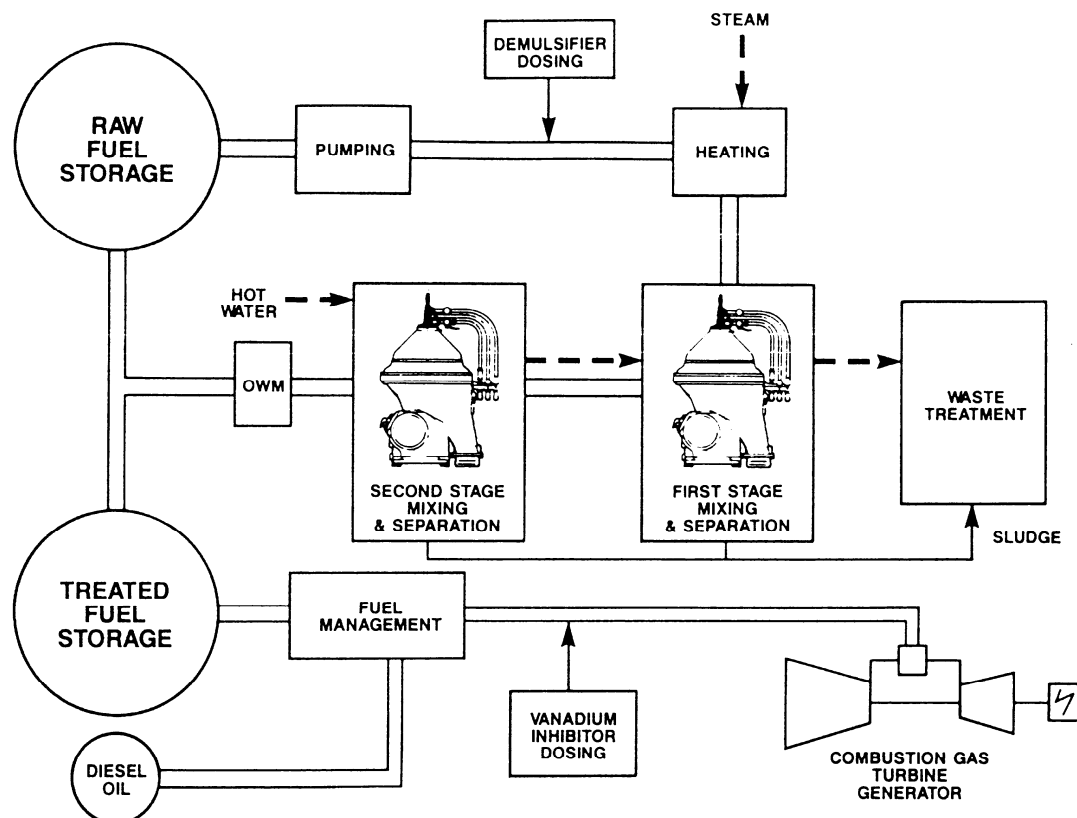


Figure 63 Block flow diagram - heavy fuel oil treatment

There are some expenses that have to be considered for a fuel treatment process. These are:

- demineralized water is required
- high wash water consumption (10% of oil)
- spent wash water polluted by oil
- chemical demulsifier needed
- residual water in the washed oil

2.7 Natural gas composition - example

$$P = 70 \text{ bar}$$

$$T = 10 \text{ }^{\circ}\text{C}$$

Table 15 *Composition*

N ₂ (mole %)	0,89
CO ₂ (mole %)	2,0
C1 (mole %)	89,0
C2 (mole %)	7,0
C3 (mole %)	1,0
C4-i (mole %)	0,05
C4-n (mole %)	0,05
C5-i (mole %)	0,005
C5-n (mole %)	0,004
C6 (mole %)	0,001

Table 16 *Calculated heating values*

	10 °C	15 °C	25 °C
Lower Heating Value (LHV) [kJ/m ³]		35447	34258
Lower Heating Value (LHV) [kJ/kg]	46472	46482	46503
Higher Heating Value (HHV) [kJ/kg]	51629	51639	51474

m³ is defined at 15°C and 1.01325 bar (which is different from Normal cubic metres, Nm³, defined at a reference condition of 0°C and 1.01325 bar).

Sensible heat of the fuel is to be included in calculations (of particular importance for low calorific value fuels).

Table 17 *Other properties*

Molecular weight [kg/kmole]	18,02
Density [kg/m ³]	0.76212

3 HRSG design

3.1 Introduction

Heat Recovery Steam Generators (HRSGs) recover energy from gas turbine exhaust to produce steam. When the HRSG is part of a combined cycle system, the steam conditions are defined by the steam turbine requirements and by cost/efficiency optimization of the plant. When used in a CHP (Combined Heat and Power, or cogeneration) application, it is the process requirements that define the amount of steam needed, as well as the steam pressure and steam temperature. When steam flow is critical to the process, redundancy in the HRSG design is also specified in the form of multiple HRSGs and/or fresh air firing capability.

Because the requirements at every plant or site are unique to that site, each application is unique and requires a different HRSG design. For CHP applications, it is usual to find steam conditions ranging from about 7 bar saturated steam to over 80 bar/530°C superheated steam. As well as different steam conditions, process or permit requirements may demand the addition of a duct burner or emissions control equipment.

In order to respond to the many different requirements, HRSG designers need to ensure boiler components have the appropriate amount of surface area and to incorporate a variety of auxiliary equipment into the system. Auxiliaries could include burners, dampers, pumps, fans, de-aerators, CO catalysts, selective catalytic reduction (SCR) catalysts, etc.

For the customer to obtain an HRSG system that meets their needs for the lowest cost, it is essential to specify the performance requirements. Because processes differ from plant to plant, it is impossible to define all possible requirements, but some are common for all projects. These are listed below:

- static gas side pressure drop
- steam flow – nominal, maximum, and required steam turndown
- steam temperature
- steam pressure at the header
- expected cycling operation of the HRSG
- is a bypass system required for the gas turbine to operate in simple-cycle duty?
- emissions limits
- noise limits from – the casing, safety relief valves, and steam vents
- required response of the HRSG when there are variations in steam header pressure from:
 - changes in steam demand
 - loss of steam supply from another source
- is fresh air firing required?
 - forced draught (draft)
 - induced draught
- steam demand that requires supplemental firing when the gas turbine is operated at part load.

The starting point in the design of all HRSGs is determining the optimum heat transfer surface area required to meet the steam requirements and the gas side static pressure drop.

3.2 Properties of water/steam

Computational procedures for boilers and steam turbines based on ideal gas are rarely used, simply because steam at the conditions typically found in a steam turbine or in boiler, behaves as a real gas. That means density and enthalpy values deviates from that of ideal gas. Water/steam is perhaps the fluid for which the properties are most known. There is an international organisation, IAPWS that defines the equations which describes the various properties. The latest formulation, IAPWS-97, is described in the following paper:

W. Wagner et al., "The IAPWS Industrial Formulation 1997 for the Thermodynamic Properties of Water and Steam," ASME J. Eng. Gas Turbines and Power, 122, 150-182 (2000).

The properties are available either in printed steam tables or in various computer codes.

For more details on HRSG design, see
<http://www.hrsgdesign.com/>

3.3 Tubes and tube arrangement

An HRSG (Heat Recovery Steam Generator) is normally designed with water/steam inside pressurised steel tubes, and with the exhaust gas on the outside of the tubes at close to atmospheric pressure. The tube outer diameter is normally either 1.5 or 2 inches.

The heat transfer coefficients on the cold and hot side are quite different. On the inside of boiler tubes the heat transfer coefficient may be around 3000-5000 W/(m² K) for an economiser, 4000-8000 W/(m² K) for an evaporator, and 500-2000 W/(m² K) for a superheater. For exhaust gas at atmospheric pressure (outside the tubes), the heat transfer coefficient may be around 30-50 W/(m² K). In order to compensate for the big difference in heat transfer coefficient between the hot and the cold side, the heat transfer surface on the hot side/outside (exhaust gas) is extended by so-called fins. The geometry of finned tubes is depicted in Figure 64, with some terms given.

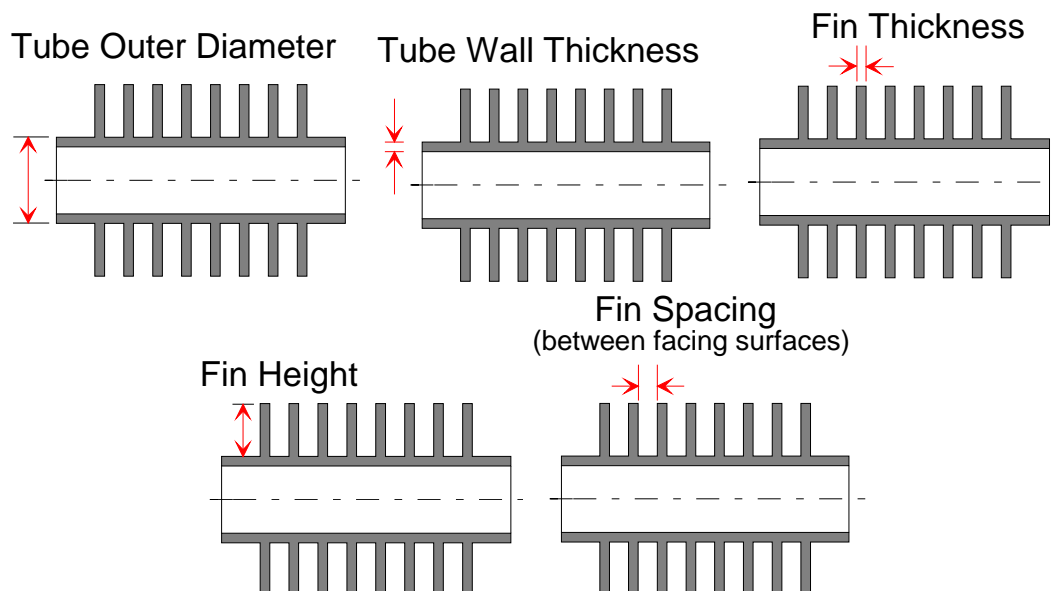


Figure 64 *Finned tube. Main design hardware parameters given.*

The fins may be either ‘solid fins’ or ‘serrated fins’, see Figure 65. In some cases a design with bare tubes (no fins) are selected.

Solid Fin Serrated Fin

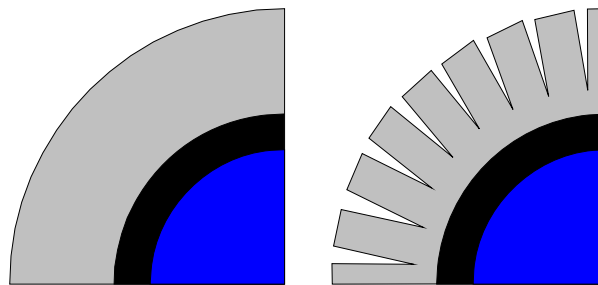


Figure 65 Solid (left) and serrated (right) fins

The arrangement of the tubes in the HRSG is shown in Figure 66. The tubes are spaced in both transverse and longitudinal direction, with a number of tube rows longitudinal (N_r) and a number of tube rows transverse (N_t). The distance between the tubes, ‘pitch’, is explained in Figure 67. The cross-sectional area of the HRSG is given by a length (L) and width (W). One can say that the heat transfer of the HRSG determines how many tubes are required, as the heat transfer area is proportional with the number of tubes. Further, the allowed exhaust gas pressure drop across the HRSG in the longitudinal direction, gives the **cross-sectional area** ($LW=A$) because the exhaust gas velocity is inversely proportional to the cross-sectional area, and the pressure drop is proportional to the velocity squared. This means that an HRSG with a small pressure drop allowed, will have a large cross-sectional area and a short length in the longitudinal direction. On the other hand, an HRSG with a large pressure drop allowed, will have a small cross-sectional area and is long in the longitudinal direction.

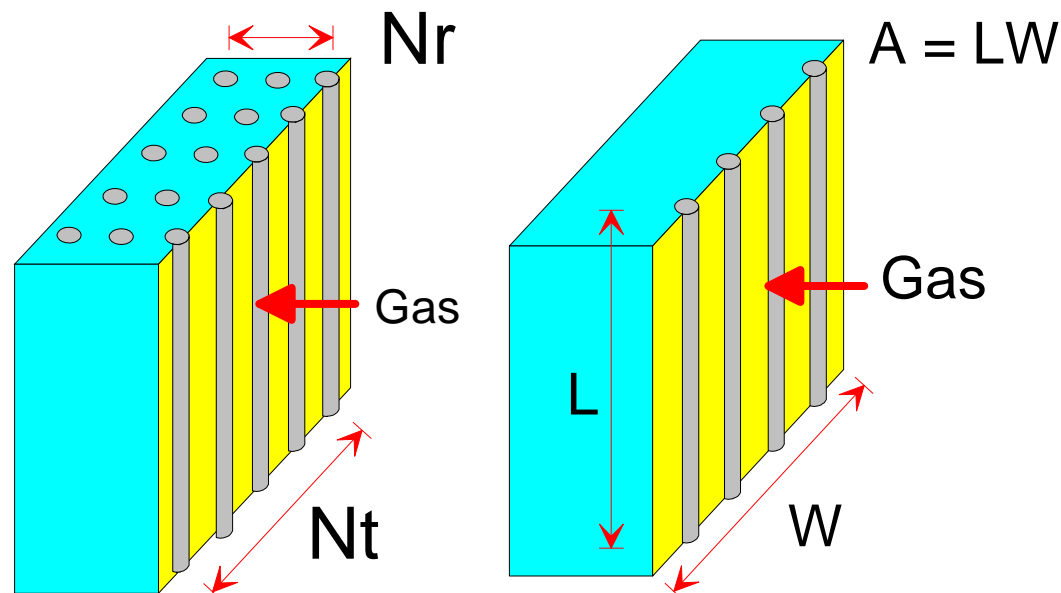


Figure 66 Arrangement of tubes in HRSG. There are rows of tubes in both transverse and longitudinal direction.

In the longitudinal direction, there are two ways of arranging the rows relative to each other. One is the so-called ‘in-line’ arrangement, where the tube rows follow straight lines in the longitudinal direction. The other arrangement is the so-called ‘staggered’, where the rows are displaced with a certain angle.

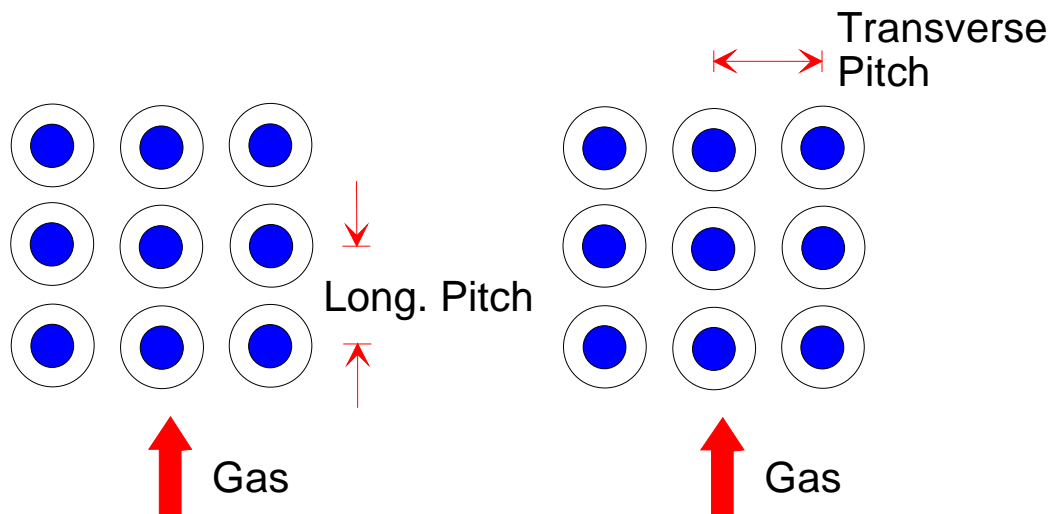


Figure 67 *Tube spacing*

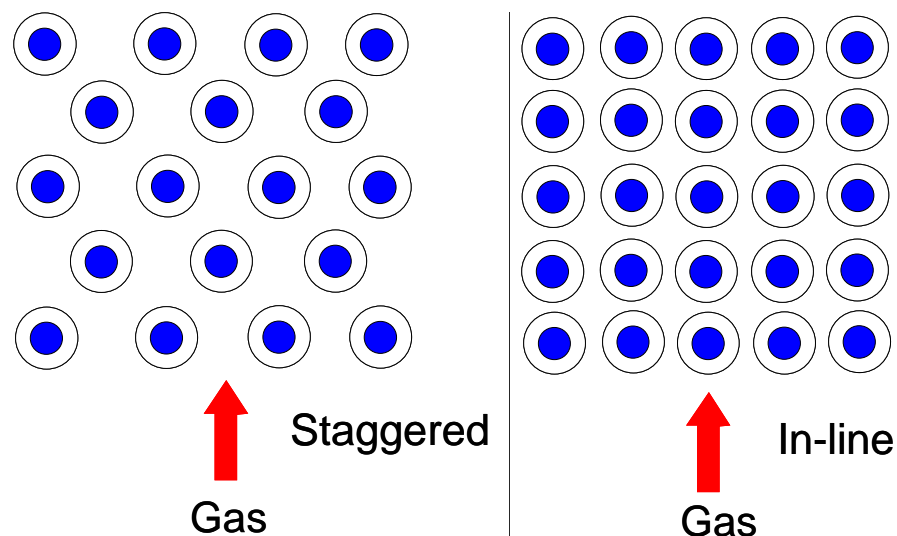


Figure 68 *Tube row arrangement in the longitudinal direction.*

The flow direction of the exhaust gas may be either horizontal or vertical, meaning that the HRSG is either a horizontal HRSG (see Figure 69) or a vertical HRSG (see Figure 70). Worldwide, there is about a 50/50 split between horizontal and vertical HRSG design.

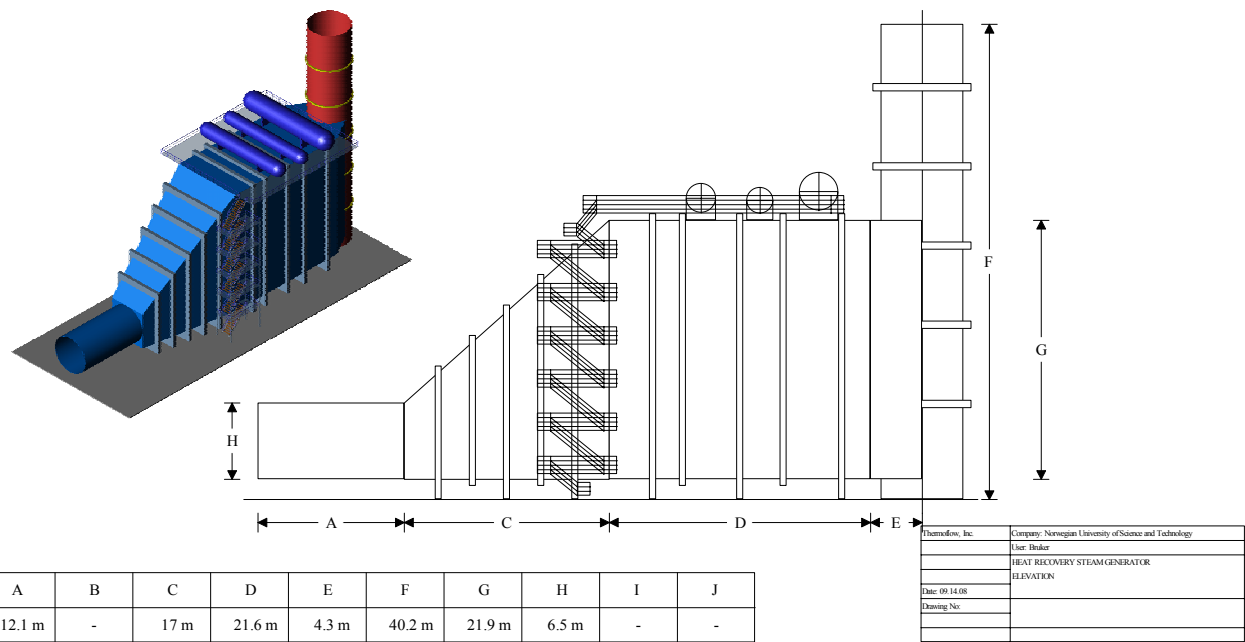


Figure 69 Horizontal HRSG, dimensions relevant for a 270 MW gas turbine (Thermostream 2008)

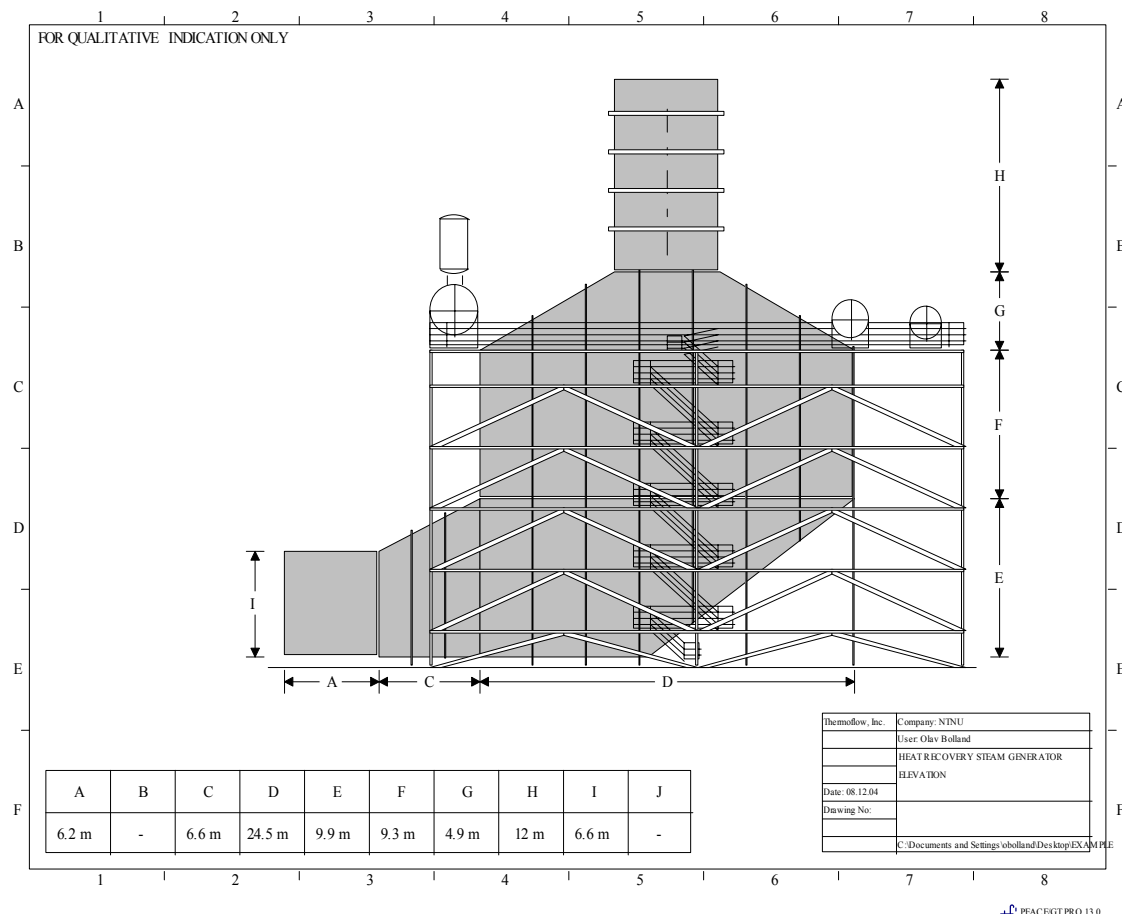


Figure 70 Vertical HRSG, dimensions relevant for a 270 MW gas turbine

3.4 Tube material and selection

Selecting the tube material and size to use in an HRSG design is really a matter of experience. As you work with different HRSGs for different services, you develop knowledge of what fit before in a similar design, so you know where to start with a new design. But a few general rules can be used to start the selection.

In addition to the pressures and temperatures the tube materials will be exposed to, designers also need to take into account the potential for corrosion due to condensation from water condensing on the outside surfaces. In the case of oil firing, there is also the problem of acid condensing on the outside tube surfaces. There is also the issue of flow-assisted corrosion (FAC) in certain areas of the HRSG. FAC is a significant problem with carbon steel components handling rapidly moving water or water/steam mixtures in the power generating industry. The mechanism of FAC can be described in terms of a mixture of surface dissolution and erosion controlling the thickness of the protective oxide. Erosion is influenced by the combined action of flow-induced mechanical forces (shear stresses, pressure variations by high flow velocity and particle impact in multi-phase flows) and dissolution by electrochemical processes.

In all cases, the appropriate selection of materials will minimize the loss of tube material.

For the typical, general purpose HRSG, using standard tubing sizes, the 2" tube size will normally work out to be the most economical tube size. The cost will generally go up with a smaller or larger tube size. Most HRSG units recover heat from a relatively low temperature gas, i.e., less than 550 °C. Of course, many of the modern HRSG's are supplementary fired to achieve even greater efficiencies. But, with the exception of the superheater, you can normally assume that carbon steel tubes will work for the evaporator and the economizer. If the superheater outlet temperatures are low, such as 350 °C and below, you should be able to assume carbon steel tubes to start. If higher than 350 °C, you may want to start with T11 tubes.

In a similar manner, you can make some preliminary estimates to determine what the design metal temperature for the HRSG tubes need to be. With this temperature, you would select the least material that is good for the temperature. Eventual analysis may show that a higher alloy and a thinner wall may be more economical, so running calculations with several materials is always wise.

Table 18 *Typical tube materials in HRSG*

Tube material (ASME designation) and usual location in HRSG	
SA 178A (carbon steel)	Superheaters
	Boilers
	Economizers
	Feedwater heaters
SA 213 T11 (1.25 Cr – 0.5 Mo)	Superheaters
	Boilers (if flow-assisted corrosion is a concern)
	Economizers (if flow-assisted corrosion is a concern)
SA 213 T22 (2.25 Cr – 1 Mo)	Superheaters
SA 213 T91 (9 Cr – 1 V)	Superheaters
SA 268 TP439 (18 Cr – 1 Si – 1 Mn)	Feedwater heaters
SA 789 S31803 (22 Cr – 1 Si – 2 Mn – 3 Mo)	Feedwater heaters

Table 19 *Typical generic, pipe and tube specifications used for HRSG tubes*

Generic Specification	Pipe Specification	Tube Specification
Carbon Steel	SA 106 Gr B	SA 178 A
1¼ Cr ½ Mo	SA 335 Gr P11	SA 213 T11
2½ Cr 1 Mo	SA 335 Gr P22	SA 213 T22
5 Cr ½ Mo	SA 335 Gr P5	SA 213 T5
9 Cr 1 Mo	SA 335 Gr P9	SA 213 T9
18 Cr 8 Ni	SA 312 TP 304	SA 213 TP 304
16 Cr 12 Ni 2 Mo	SA 312 TP 316	SA 213 TP 316
18 Cr 10 Ni Ti	SA 312 TP 321	SA 213 TP 321
18 Cr 10 Ni Ti	SA 312 TP 321H	SA 213 TP 321H

3.5 Feedwater tank/deaerator

3.5.1 Introduction

The removal of dissolved gases from boiler feedwater is an essential process in a steam system. The presence of dissolved oxygen in feedwater causes rapid localized corrosion in boiler tubes. Carbon dioxide will dissolve in water, resulting in low pH levels and the production of corrosive carbonic acid. Low pH levels in feedwater causes severe acid attack throughout the boiler system. While dissolved gases and low pH levels in the feedwater can be controlled or removed by the addition of chemicals, it is more economical and thermally efficient to remove these gases mechanically. This mechanical process is known as deaeration and will increase the life of a steam system dramatically.

Deaeration is based on two scientific principles. The first principle can be described by Henry's Law. Henry's Law asserts that gas solubility in a solution decreases as the gas partial pressure above

the solution decreases. The second scientific principle that governs deaeration is the relationship between gas solubility and temperature. Easily explained, gas solubility in a solution decreases as the temperature of the solution rises and approaches saturation temperature. A deaerator utilizes both of these natural processes to remove dissolved oxygen, carbon dioxide, and other non-condensable gases from boiler feedwater. The feedwater is sprayed in thin films into a steam atmosphere allowing it to become quickly heated to saturation. Spraying feedwater in thin films increases the surface area of the liquid in contact with the steam, which, in turn, provides more rapid oxygen removal and lower gas concentrations. This process reduces the solubility of all dissolved gases and removes it from the feedwater. The liberated gases are then vented from the deaerator.

The principle flow diagram for deaeration si shown in Figure 71, while the internal design of an deaerator is shown in Figure 72.

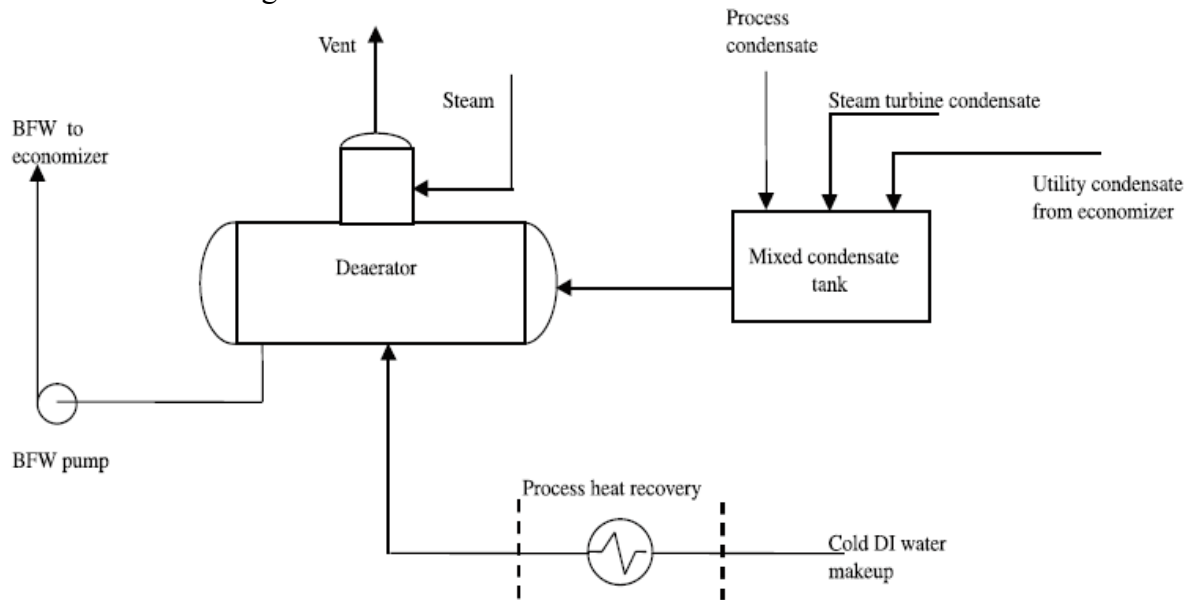


Figure 71 *Schematic of Degaerator and auxiliary equipment. Water from steam turbine condenser, process return condensate and makeup is collected and mixed before it enters the deaerator. Steam is added in order to reach saturated condition for the water entering the tank. Preheating of the water 7-10 K below the boiling point is normal, and contributes to small steam consumption. In a power plant, the deaerator pressure is typically between 0.2-1.2 bar.*

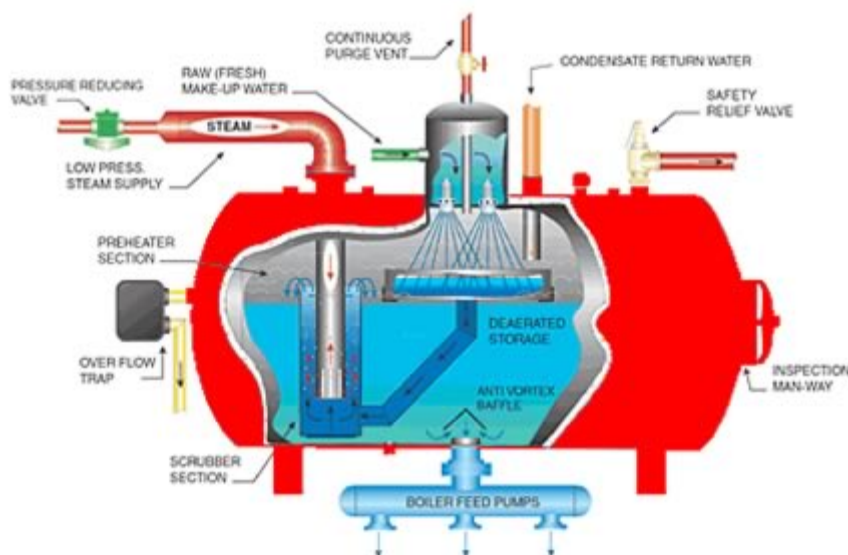
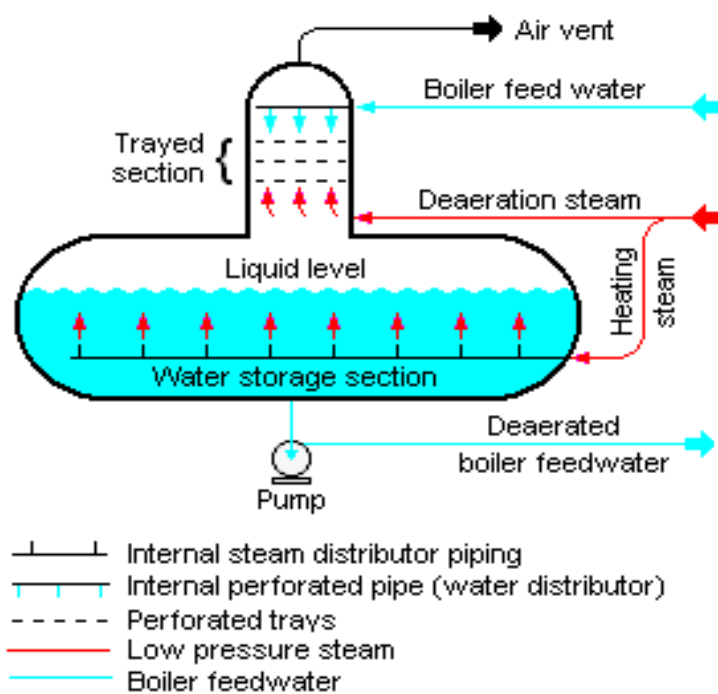


Figure 72 Example of internal design of a deaerator

The atomized water presents a tremendous amount of surface exposure to the violent scrubbing action of the high velocity steam and accomplishes the complete removal of dissolved gases. The deaerated water passes from the atomizing section to the storage tank, and the steam flows counter-currently from the deaerating section to the pre-heating section.

The steam jet atomizing valve is spring loaded and adjustable. It maintains a substantially constant pressure differential on the steam supply, regardless of the load at which the deaerator is operated and regardless of the temperature at which water is received by the deaerator.

Under variable load conditions with substantially constant water inlet temperature, the spring-loaded, steam jet atomizing valve maintains continuous high velocity and uniform energy application to the deaerating process. The spring loading on the atomizing valve is adjusted to the exact requirements of the particular installation operation conditions. All steam used to heat the incoming water and substantially all the steam used in both the heating and deaerating processes pass through the deaerating stage and provides a volume of scrubbing vapours 100 to 150 times the volume of the water being deaerated.

3.5.2 Why deaerate

Degaeration of boiler feedwater is almost universally practiced. There are very strong reasons for doing so. Water fed to boilers consists of raw make-up water and condensate returns, most commonly a mixture of the two. Both contain oxygen and carbon dioxide in solution in varying amounts. These gases, particularly at the elevated temperatures encountered in modern boilers, greatly accelerate the rate of corrosion of the steel surfaces within the boiler, as well as piping and other plant apparatus in contact with the condensing steam.

While oxygen and carbon dioxide could be removed by the addition of scavenging chemicals to the feedwater alone, this practice is extremely costly in all but the smallest plants. Generally speaking, plants generating in excess of 5000 kg/hr. of steam can justify the installation of a deaerator. If the percentage of make-up to the system is above 50% and/or the CO₂ content or alkalinity of the feedwater is high (CO₂ + HCO₃ exceeding 100 ppm.) the use of a deaerator will result in worthwhile savings even below 5000 kg/hr. boiler capacity.

Although deaerators are capable of reducing oxygen and carbon dioxide to very low levels, they should not be considered as a substitute for proper internal boiler feedwater treatment. They are not an alternative to proper softening and dealkalinization of the make-up feedwater. They will, however, greatly reduce the amount of "scavenging chemicals" which must be fed to maintain proper residuals with the boiler.

3.5.3 A Deaerator will accomplish the following:

Oxygen Removal is the primary reason for deaerating water and is the first thing most individuals think about when they begin to consider the application or need for a Deaerator. Oxygen in feedwater will cause the following problems and this is why oxygen must be removed.

Oxygen is extremely corrosive to boilers. We are all well aware of how corrosive oxygen in water is to an iron pail, or any other iron container at natural temperatures. When heat is added to water, dissolved oxygen becomes even more corrosive. The maximum safe figure for most boilers is approximately .005 cc/liter (7 parts per billion).

As steam condenses, any oxygen that is carried over with the steam will be highly corrosive to the condensate lines and the process equipment. Carbon Dioxide may also be present in the steam and condensate. Carbon Dioxide is corrosive when it condenses and combines with water, but when oxygen is also present, the condensate becomes approximately four times more corrosive than when only oxygen, or only carbon dioxide is present by itself. In order to protect the process equipment and condensate lines the oxygen must be removed.

Where there is condensate being returned to the boiler, the condensate should be deaerated for removal of all oxygen that may have been drawn into the system or into the condensate receiver. If condensate is not deaerated a recycling of oxygen and carbon dioxide may occur in the system.

Carbon Dioxide Removal

Most raw waters contain free carbon dioxide which is very corrosive when combined with water to form carbonic acid. Carbon dioxide in its free state requires all of the mechanical requirements of good deaeration for removal. In steam, carbon dioxide is not corrosive, but when the steam condenses, the carbon dioxide combines with water and forms very corrosive carbonic acid, which will dissolve return lines and process equipment rapidly. Of course, carbon dioxide alone is not as dangerous as it is when there is a small amount of oxygen present in the system, but it should be removed when possible. When combined with dissolved oxygen, carbon dioxide is considerably more corrosive.

Improve Heat Transfer

Air or non-condensable gases in steam cause losses as high as four times in thermal efficiency. Air or non-condensable gases in steam cause a thermal blanket which reduces the heat transfer across the tube wall. It is a well recognized fact that steam that is high in non-condensable gases retards heat transfer because it acts as an insulating blanket. The gases (primarily oxygen and carbon dioxide) that cause this decrease in heat transfer are removed when proper deaeration is employed.

3.6 Dew point of exhaust gas – possible corrosion

There are two types of dew points to consider for a boiler/HRSG:

- a) sulphur dew point
- b) water dew point

The sulphur dew point must be considered for sulphur-containing fuels. Normally, natural gas contains so little sulphur that the dew point is far below any exhaust gas temperatures. For oil and solid fuels, depending on the sulphur content, the dew point is typically in the range 100-165 °C. The stack temperature has to be kept above the sulphur dew point temperature in order to avoid corrosion on metal surfaces in the boiler/HRSG and stack.

The significance of the water dew point, is that a liquid phase is formed, which contains acid components. These components may contain sulphur or nitric acid (HNO_3). The latter is formed from NO/NO_2 originating from the combustion. The presence of water may cause corrosion.

The water dew point of gas turbine exhaust gas is typically around 40 °C. It is rare that bulk exhaust temperatures become even close to that in power plants. A typical exhaust gas stack temperature in a high-efficiency plant is about 80-100 °C. (It is common for some domestic boilers, 2-5 kW, to deliberately design for exhaust temperature below the dew point in order to utilise some of the latent heat of the exhaust gas.) Even if the bulk exhaust temperature is above the dew point, it may be below the dew point near a cold surface. This is depicted in Figure 73.

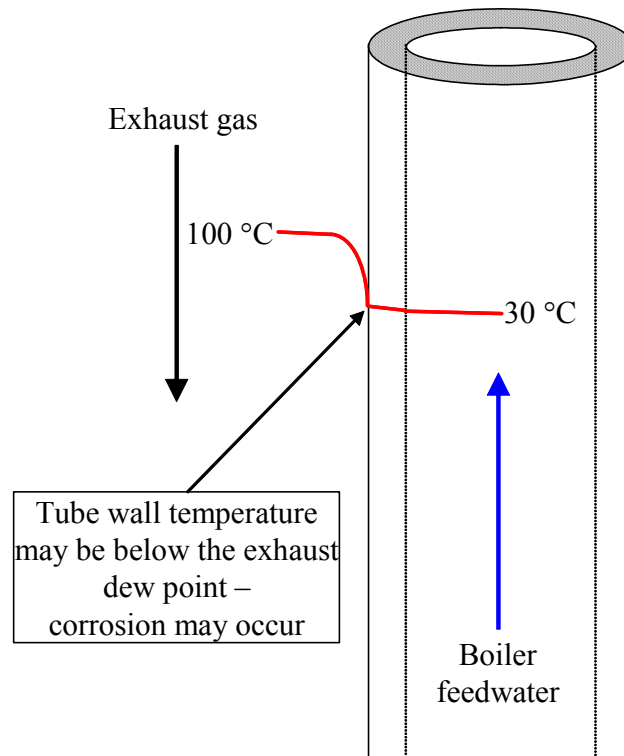


Figure 73 Illustration of a typical temperature profile from the hot exhaust gas, through the tube wall and to water flow inside the tube. The heat transfer coefficient is much high on the inside of the tube compared to the outside, so that the outside tube wall temperature is close to the inside water temperature.

In order to avoid condensation of water at the tube wall surface, it is in power plant industry a rule of thumb to require the boiler/HRSG feed water to enter with a minimum temperature of 60 °C. This means that some kind of preheating normally is required from the condenser temperature up this minimum.

Corrosion may also be avoided by using stainless steel, or coating of the tubes with a non-corroding material. Both these options are very expensive in a boiler/HRSG, so the preheating option is preferred.

3.7 Drum

A drum or steam drum connects the economiser, evaporator and the superheater in an HRSG. There is a drum for every pressure level in the HRSG (not for reheating, if regarding that as a pressure level). The cross-section of the drum is circular, with a diameter in the range 1-2m. The length depends on the size of the plant, may be up to 15 m. The drum is filled about 50% with liquid water, where the water at the surface is at the boiling point. The hot water from the economiser is entering the drum and is distributed in the water volume. A sketch of a drum is given in Figure 74.

The drum is a pressure vessel with two main functions:

- Separating liquid water and saturated steam
- Remove impurities in the feed water

From the drum, water is led to the evaporator. Back from the evaporator a two-phase mixture is returned to the drum, above the water volume. This two-phase mixture goes normally through hydro cyclones, where the steam and the liquid water are separated. The steam leaves at the top of the drum for the superheater, while the liquid water returns down into the water volume. The steam/liquid water in the drum is at the saturation state, ensured by heat and mass transfer between the saturated steam in the upper half of the drum, and the liquid water at the boiling point in the lower half of the drum.

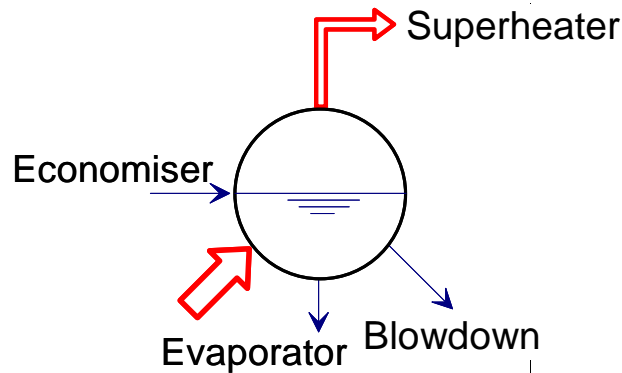


Figure 74 *Steam drum in an HRSG.*

In the upper half of the drum, steam is condensing, and likewise in the lower half of the drum, water is evaporating. Impurities in the steam have the tendency of being nuclei for the condensation of steam. This has a cleansing effect on the steam, and the impurities are accumulated in the water volume of the drum. In order to remove the impurities, liquid water is either continuously or batchwise extracted from the bottom of the drum. This is called **blowdown**.

The flow from the drum through the evaporator back to the drum, may be either **forced circulation** or **natural circulation**.

A **forced circulation** system uses a pump to maintain circulation in all the tubes of the evaporator tube bundle. A typical forced circulation system is shown to the left in Figure 75. The water is distributed within an inlet header to the various parallel circuits and the steam and water mixture is collected in an outlet header. The mixture is returned to a drum for separation of the steam and water.

The tubes may have any orientation but are generally horizontal with an upward water flow to improve stability between the parallel channels. The forced circulation evaporator will generally have more flow resistance than a natural circulation evaporator. In low pressure drop tube bundles, inlet orifices may be required to provide for better distribution to the parallel circuits. When designing the circulation rate for these HRSGs, these factors must be weighed against the cost of the pump and the pumping energy. Experience in steam boilers has shown that the "danger" zone in which film boiling can be expected to occur is between 20 and 25 percent steam generation by weight. This has led to the rule of thumb for a 5:1 circulation ratio. This is in fact on the borderline and does not allow sufficient conservatism for unusual or extreme cases. For instance, an HRSG with a very long horizontal tube length (some units have been manufactured with tubes as long as 30m).

Also, the relation of the drum to the evaporator coil needs to be considered. As an example a steam coil in a fired heater may have the steam separation drum located 30 m away and at the ground, where the coil may be 15m up on top of the heater. In this case, the water pressure in the evaporator may be such that instead of total vaporization occurring in the coil, the temperature rises instead,

and the major vaporization occurs at the inlet separators in the steam drum. In these cases, a 3 : 1 circulation ratio may be sufficient.

Conventional, vertical tube boilers are generally designed for **natural, "thermosyphon"**, **circulation**. This means the water and steam/water circuits are arranged so that the two phase mixture in the steam generating tubes rises to the steam drum by thermal lift of differential density and is replaced by water from the drum by gravity flow. However, it should be noted that many horizontal tube natural circulation boilers have been successfully used for years.

Although the nature of a thermosyphon circulation boiler is quite simple, the calculation procedure to check the design to see what the circulation ratio is, can become very complicated. Most designs are such that each row of tubes have a different circulation than all the other rows, but some actually have a different circulation ratio for every tube in the evaporator, which would be difficult to determine.

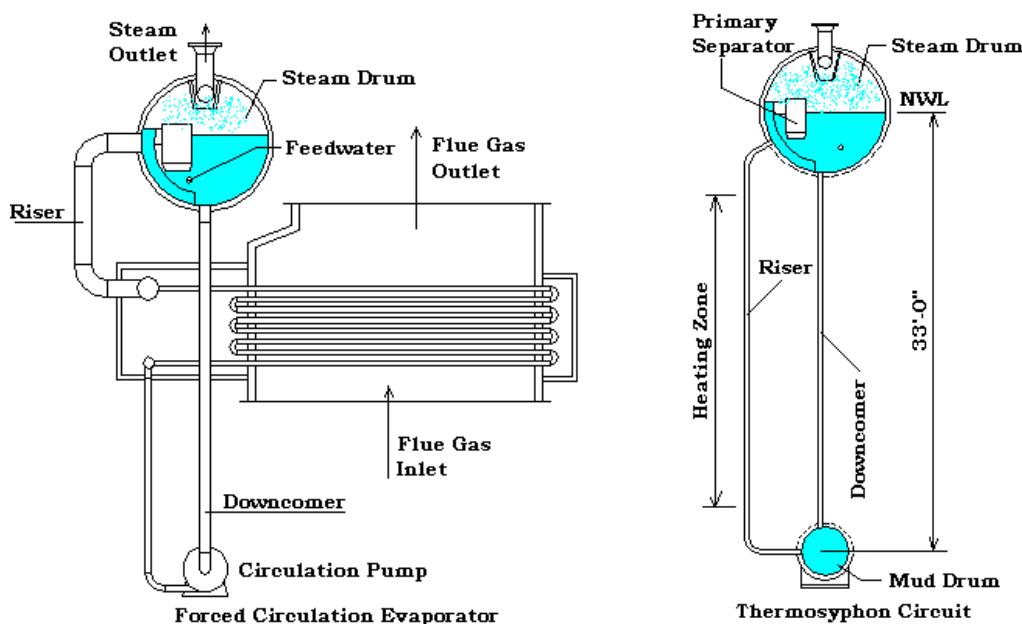


Figure 75 *Steam drum system in an HRSG. Left: forced circulation. Right: natural circulation*

3.8 TQ-diagram of a HRSG

In order to illustrate and also as a help in calculations, it is common to use the so-called TQ-diagram. It shows profiles for the heat transfer process between exhaust gas and water/steam, using temperature on the ordinate axis and heat transferred on the abscissa axis. An example of a TQ-diagram is given in Figure 76.

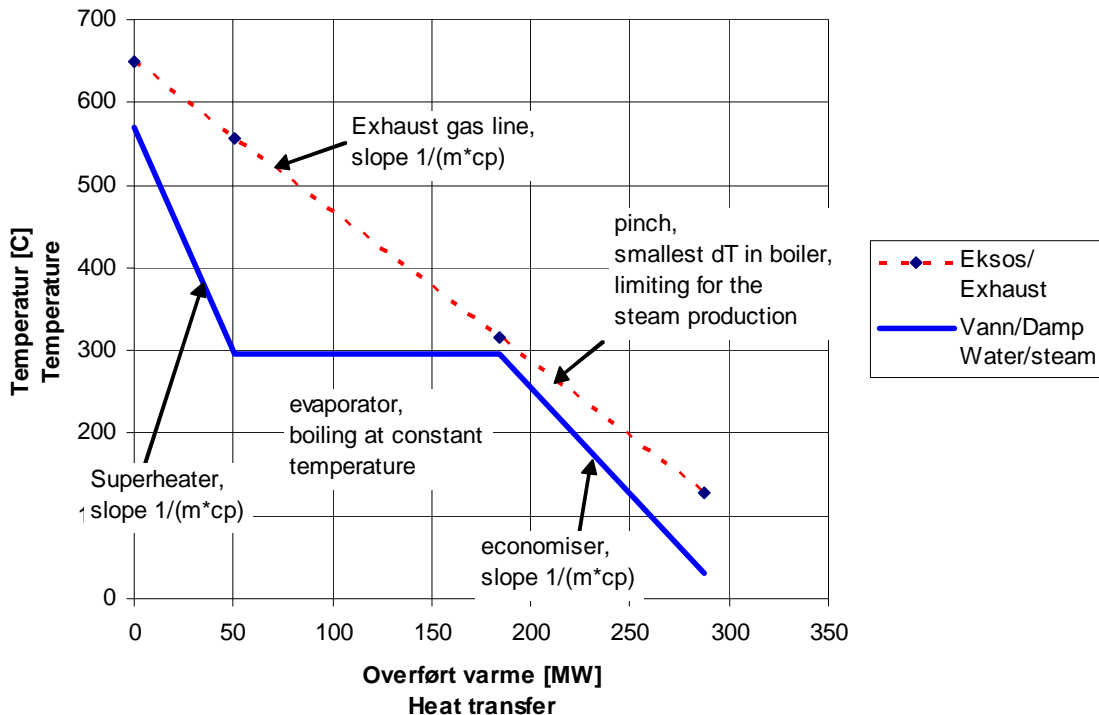


Figure 76 *TQ-diagram, showing the heat transfer process between exhaust gas and water/steam for a single-pressure HRSG.*

For the water/steam, there are three different zones. Starting from the lowest temperature, the first zone is heating of liquid water to close to the boiling temperature. The next zone is horizontal, and is water boiling at constant temperature. The third zone is superheating of steam. The three zones are commonly described as ‘**economiser**’, ‘**evaporator**’ (or boiler) and ‘**superheater**’. The term ‘**preheater**’ is also used for heating of liquid water; typically in cases with condensing steam as heat source.

The heat balance of an element in one of the streams in a TQ-diagram can be written as:

$$\Delta Q = \dot{m} c_p \Delta T \quad (50)$$

Rearranging, results in an expression for the slope of the lines in the TQ-diagram.

$$\frac{\Delta Q}{\Delta T} = \frac{1}{\dot{m} c_p} \quad (51)$$

An important term for HRSG design is the ‘**pinch**’ or ‘**pinch-point**’. This is the location in the HRSG with the smallest temperature difference. One can say that this location is limiting how much

steam that can be produced. As one can imagine from Figure 76, much of the heat transfer area of the HRSG is located near the pinch point, because the heat transfer area is inversely proportional to the temperature difference. Typical values for the pinch temperature difference in an HRSG vary from 8-35 K. The lower value (8-12 K) is applied in high-efficiency plants, while the upper number may be found in cases where the investment cost and/or weight is more important than efficiency; for example combined cycles operating on oil platforms in the North Sea, or in power plants with limited time of operation (peaking units).

In Figure 76 a single-pressure process is shown. It is common to design with 1-3 pressure levels. In the case of triple-pressure systems, reheat is normally included. As a rule of thumb, one can say that single-pressure systems are preferred in small plants or in cases where investment cost is more important than efficiency. Triple-pressure reheat systems are chosen for large plants (400-500MW Combined Cycle power output) where high efficiency is of importance. In between, dual pressure systems are also quite common. Flowsheet of these options are given in section 5.4.

If supplementary firing is used to increase the temperature of the gas turbine exhaust, the location of the pinch point may move from between the evaporator and economiser, and to the cold end of the economiser. This is depicted in *Figure 77*.

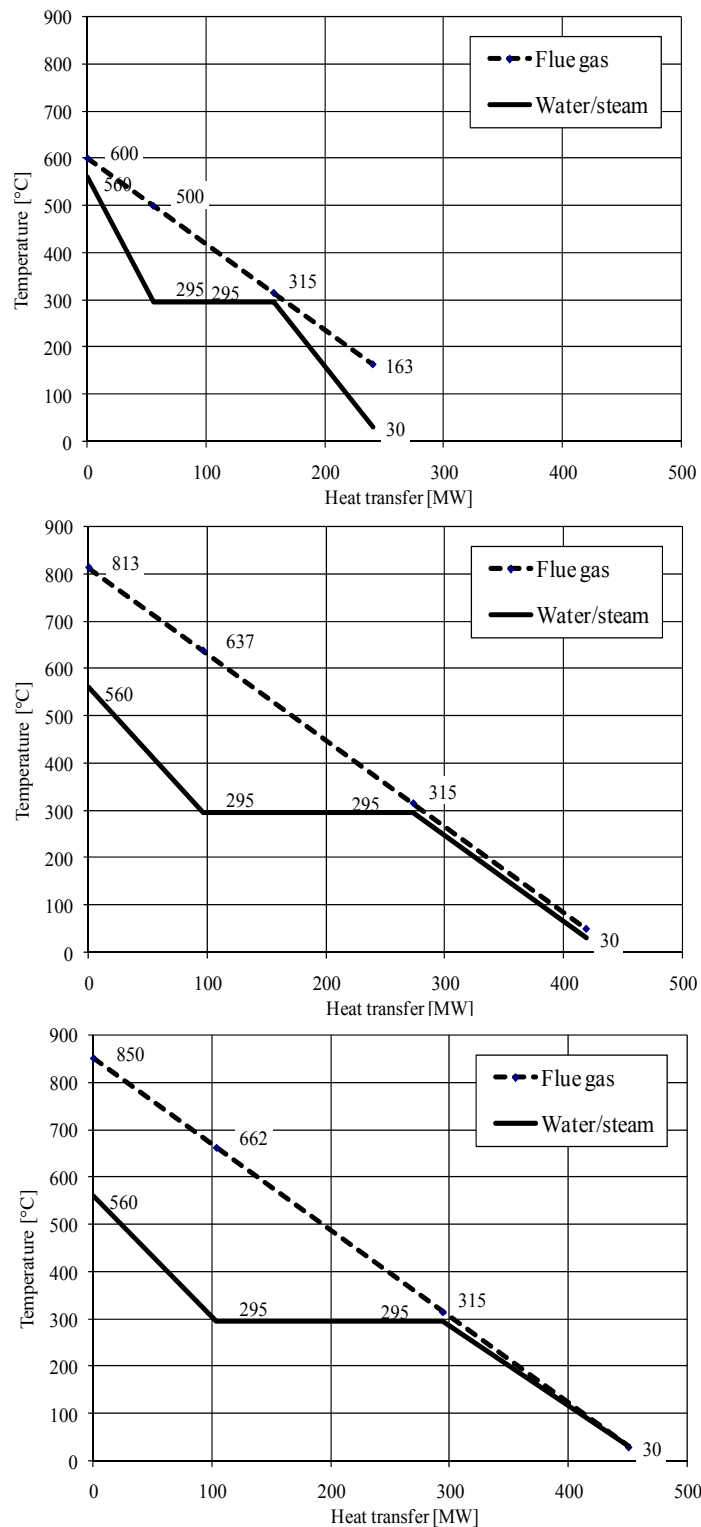


Figure 77 TQ-diagrams for various exhaust gas temperatures, keeping the pinch temperature and exhaust gas flow rate constant. The left diagram shows the location of pinch between the evaporator and economiser. The diagram in the middle shows a case where the exhaust gas line and the economiser line are parallel. The right diagram shows that the exhaust gas stack temperature and the economiser water inlet temperature are equal, which from a design point of view means that the pinch temperature difference must be increased.

3.9 Computational procedure for a pressure level in a HRSG

This is a computational procedure in order to determine the flow rate of steam (\dot{m}_{steam}), given an exhaust gas temperature, flow rate and composition. In the following, the abbreviations ECO, EVA, SUP are used for Economiser, Evaporator and Superheater. The procedure is simplified with the assumptions of no pressure losses or heat losses. See Figure 78 for symbol clarification.

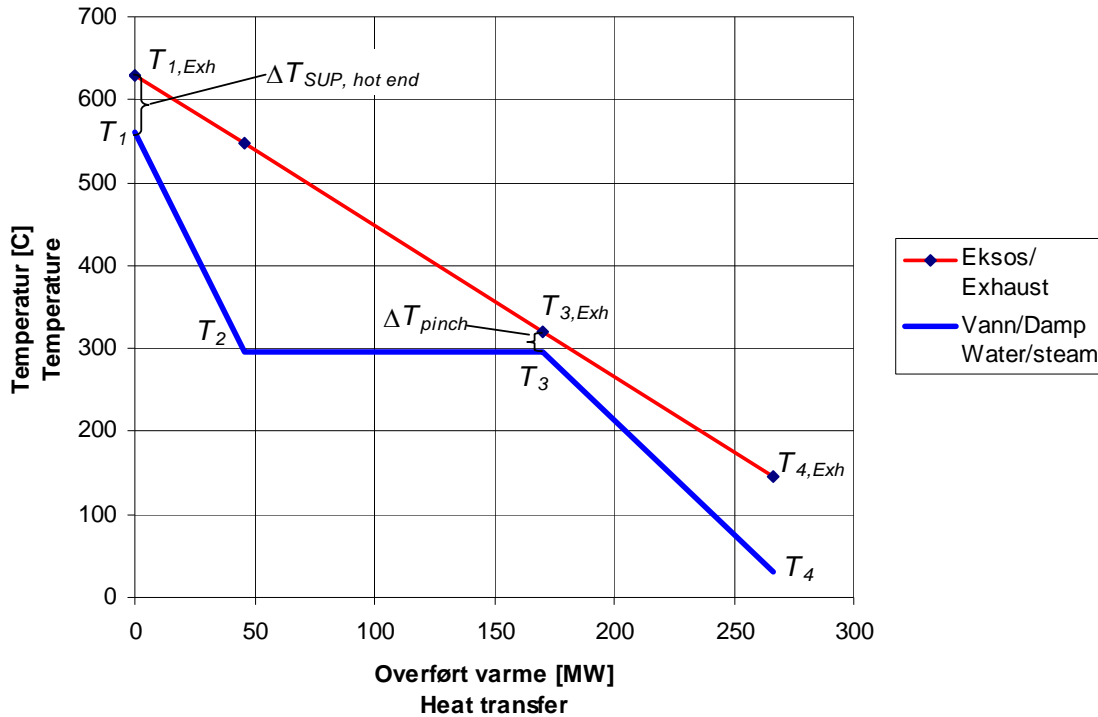


Figure 78 *TQ-diagram with symbols used in the computational procedure given in section 3.9.*

This

- 1) Determine/choose the live steam pressure (superheater exit), P_{SUP} . Without pressure loss this equals the evaporator pressure, P_{EVA} .
- 2) Find the saturation temperature for P_{EVA} , $T(P_{EVA})=T_2=T_3=T_{EVA}$, from a steam table
- 3) Choose ΔT_{pinch} , normally 8-20 K
- 4) Calculate the exhaust gas temperature at the pinch; $T_{3,Exh} = T_{EVA} + \Delta T_{pinch}$
- 5) Choose the temperature difference/'approach' at the superheater hot end, $\Delta T_{SUP,hot end}$, normally 20-40 K. $\Delta T_{SUP,hot end} = T_{1,Exh} - T_1 \Rightarrow T_1 = T_{1,Exh} - \Delta T_{SUP,hot end}$
If T_1 by this procedure exceeds the maximum steam temperature allowed, T_1 is then set equal to the maximum steam temperature.
- 6) Find the enthalpy of steam at the superheater hot end $h_1 = h(T_1, P_{SUP})$
- 7) Find the enthalpy of saturated water at the evaporator pressure, $h_3 = h'(P_{EVA})$

The economiser water exit temperature is in a real case 2-10K below the saturation temperature (economiser ‘approach’). This may be taken into account by setting the h_3 equal to that of the economiser exit (subcooled water).

- 8) Calculate the flow rate of steam by using an energy balance between the exhaust gas and the water/steam above the pinch, including the evaporator and the superheater.

$$\begin{aligned}\dot{m}_{steam} (h_1 - h_3) &= \dot{m}_{Exh} c_{p,Exh} (T_{1,Exh} - T_{3,Exh}) \\ \Rightarrow \dot{m}_{steam} &= \frac{\dot{m}_{Exh} c_{p,Exh} (T_{1,Exh} - T_{3,Exh})}{(h_1 - h_3)}\end{aligned}\quad (52)$$

- 9) Find the enthalpy of water entering the economiser , $h_4 = h(T_4, P_{ECO})$
 10) Calculate the exhaust gas temperature at the economiser cold end with an energy balance, Eq. (53), between the exhaust gas and the water for the economiser (or alternatively, as in Eq. (54), a balance for superheater, evaporator and economiser):

$$\begin{aligned}\dot{m}_{steam} (h_3 - h_4) &= \dot{m}_{Exh} c_{p,Exh} (T_{3,Exh} - T_{4,Exh}) \\ \Rightarrow T_{4,Exh} &= T_{3,Exh} - \frac{\dot{m}_{steam} (h_3 - h_4)}{\dot{m}_{Exh} c_{p,Exh}}\end{aligned}\quad (53)$$

$$\begin{aligned}\dot{m}_{steam} (h_1 - h_4) &= \dot{m}_{Exh} c_{p,Exh} (T_{1,Exh} - T_{4,Exh}) \\ \Rightarrow T_{4,Exh} &= T_{1,Exh} - \frac{\dot{m}_{steam} (h_1 - h_4)}{\dot{m}_{Exh} c_{p,Exh}}\end{aligned}\quad (54)$$

In the following an example of this procedure is given. Assumptions are as follows:

$T_{1,Exh}$	= 630 °C
\dot{m}_{Exh}	= 500 kg/s
$C_{p,Exh}$	= 1.1 kJ/(kg K)
P_{SUP}	= 80 bar ($P_{EVA}=P_{ECO}=P_{SUP}$)
$T_{1,max}$	= 560 °C
ΔT_{pinch}	= 20 K
T_4	= 30 °C

This

- 1) Determine/choose the live steam pressure (superheater exit). $P_{SUP} = 80$ bar
- 2) Find the saturation temperature for P_{EVA} , $T'(P_{EVA})=T_2=T_3=295$ °C
- 3) Choose ΔT_{pinch} : 20 K
- 4) Calculate the exhaust gas temperature at the pinch; $T_{3,Exh} = 295 + 20 = 315$ °C
- 5) Choose the temperature difference/’approach’ at the superheater hot end, $\Delta T_{SUP,hot end} = 30$ K

$$T_1 = 630 - 30 = 600 \text{ °C} > 560 \text{ °C} \Rightarrow T_1 = 560 \text{ °C}$$

- 6) Find the enthalpy of steam at the superheater hot end

$$h_1 = h(560 \text{ } ^\circ\text{C}, 80 \text{ bar}) = 3543.75 \text{ [kJ/kg]}$$

- 7) Find the enthalpy of saturated water at the evaporator pressure

$$h_3 = h'(80 \text{ bar}) = 1318.19 \text{ [kJ/kg]}$$

Note that the average specific heat capacity of the steam in the superheater is 2.96 kJ/(kg K).

- 8) Calculate the flow rate of steam by using an energy balance between the exhaust gas and the water/steam above the pinch, including the evaporator and the superheater.

$$\dot{m}_{steam} = \frac{500 \cdot 1.1 \cdot (630 - 315)}{(3544 - 1318)} = 77.9 \text{ [kg/s]} \quad (52)$$

- 9) Find the enthalpy of water entering the economiser

$$h_4 = h(30 \text{ } ^\circ\text{C}, 80 \text{ bar}) = 132.99 \text{ [kJ/kg]}$$

Note that the average specific heat capacity of the water in the economiser is 4.47 kJ/(kg K).

- 10) Calculate the exhaust gas temperature at the economiser cold end with an energy balance between the exhaust gas and the water for the economiser:

$$T_{4,Exh} = 315 - \frac{77.85 \cdot (1318 - 133)}{500 \cdot 1.1} = 147.2 \text{ } ^\circ\text{C} \quad (53)$$

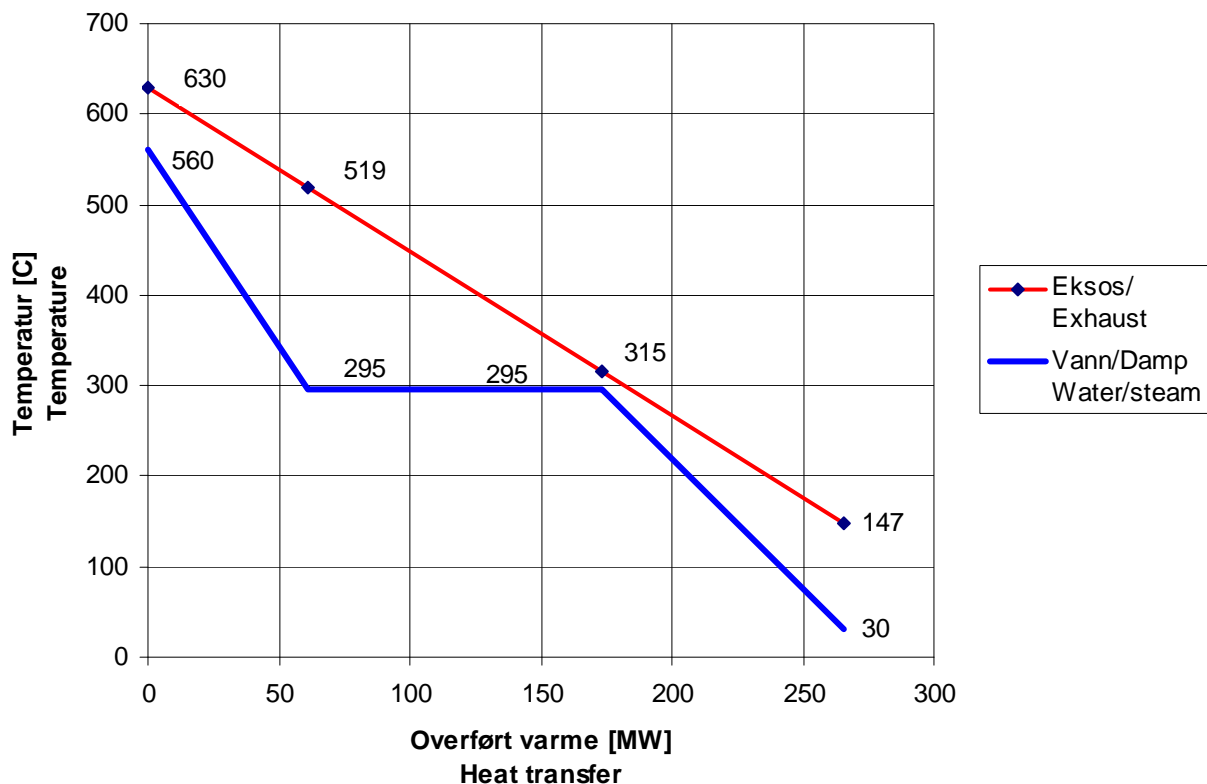


Figure 79 TQ-diagram illustrating the example above

4 Steam turbines

4.1 Principles of impulse and reaction stages

In a steam turbine, high-enthalpy (high pressure and temperature) steam is expanded in the nozzles (stationary blades) where the kinetic energy is increased at the expense of pressure energy (increase in velocity due to decrease in pressure). The kinetic energy (high velocity) is converted into mechanical energy (rotation of a shaft — increase of torque or speed) by impulse and reaction principles. The impulse principle consists of changing the momentum of the flow, which is directed to the moving blades by the stationary blades. The jet's impulse force pushes the moving blades forward. The reaction principle consists of a reaction force on the moving blades due to acceleration of the flow as a result of decreasing cross-sectional area.

Figure 80 illustrates a turbine with impulse blading. It has one velocity-compounded stage (the velocity is absorbed in stages) and four pressure-compounded stages. The velocity is reduced in two steps through the first two rows of moving blades. In the moving blades, velocity decreases while the pressure remains constant.

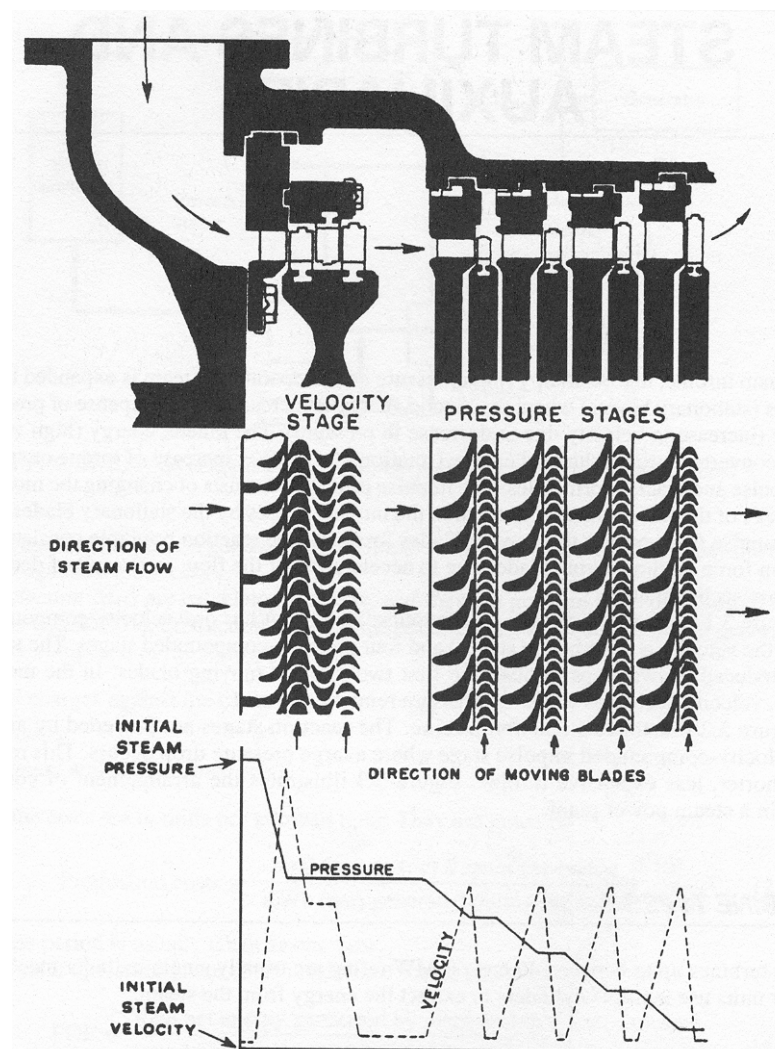


Figure 80 *Turbine with impulse blading. Velocity compounding is accomplished in the first two stages by two rows of moving blades between which is placed a row of stationary blades that*

reverses the direction of Steam flow as it passes from the first to the second row of moving blades. Other ways of accomplishing velocity compounding involve redirecting the steam jets so that they strike the same row of blades several times with progressively decreasing velocity.

Many moderate-pressure plants have added high-pressure noncondensing turbines to increase capacity and improve efficiency. High-pressure boilers are added to supply steam to the noncondensing turbines, which are designed to supply the steam to the original turbines. These high-pressure turbines are called superposed, or topping, units. Mixed-pressure turbines are designed to admit steam at low pressure and expand it to a condenser. These units are used mainly in cogeneration plants.

Figure 81 illustrates a reaction turbine. The reaction stages are preceded by an initial velocity-compounded impulse stage where a large pressure drop occurs. This results in a shorter, less expensive turbine. Figure 82 illustrates the arrangement of components in a steam power plant. An example of a steam turbine is given in

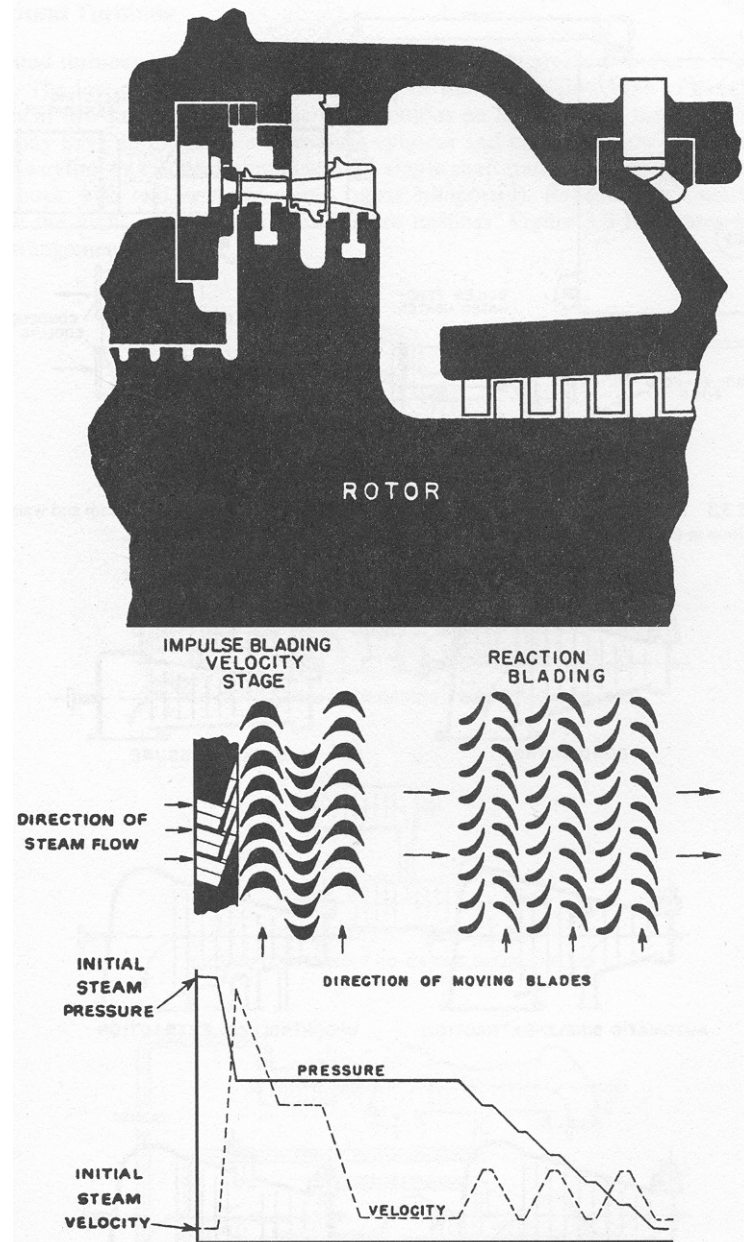


Figure 81 Reaction turbine with one velocity—compounded impulse stage. The first stage of this turbine is similar to the first velocity-compounded stage of Figure 80. However, in the reaction blading of this turbine, both pressure and velocity decrease as the steam flows through the blades. The graph at the bottom shows the changes in pressure and velocity through the various stages.

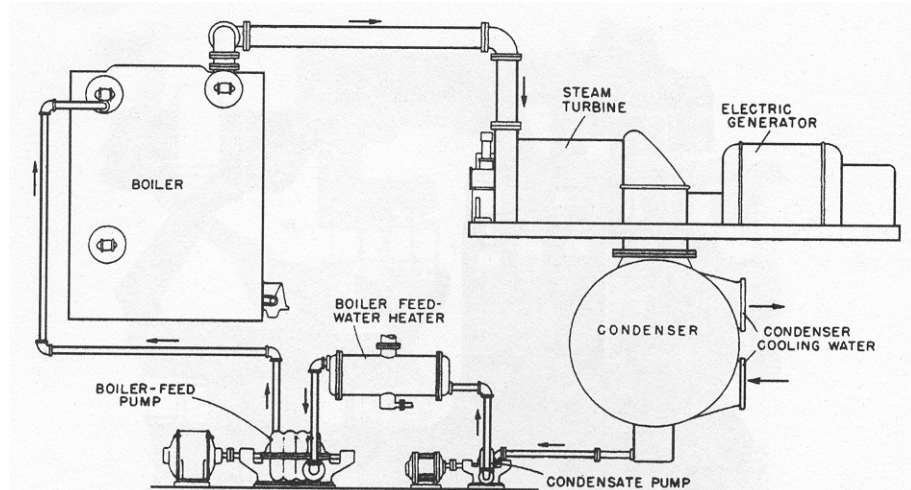


Figure 82 Simple power plant cycle. This diagram shows that the working fluid, steam and water, travels a closed loop in the typical power plant cycle.

4.2 Turbine types

Steam turbines up to between 40 and 60 MW rating are usually single-cylinder machines. Larger units use multiple cylinders to extract the energy from the steam.

4.2.1 Single Cylinder Turbines

The two types of steam turbines are condensing and back-pressure (noncondensing). Figure 83 illustrates these types and some of their subclassifications. Back-pressure turbines exhaust the steam at the pressure required by the process, see example of such a steam turbine in Figure 84. Automatic extraction turbines allow part of the steam to be withdrawn at an intermediate stage (or stages) while the remainder of the steam is exhausted to a condenser. These turbines require special governors and valves to maintain constant pressure of the extraction steam while the turbine load and extraction demand are varying. Uncontrolled extraction turbines are used to supply steam to feedwater heaters, since the pressure at the extraction points varies with the turbine load.

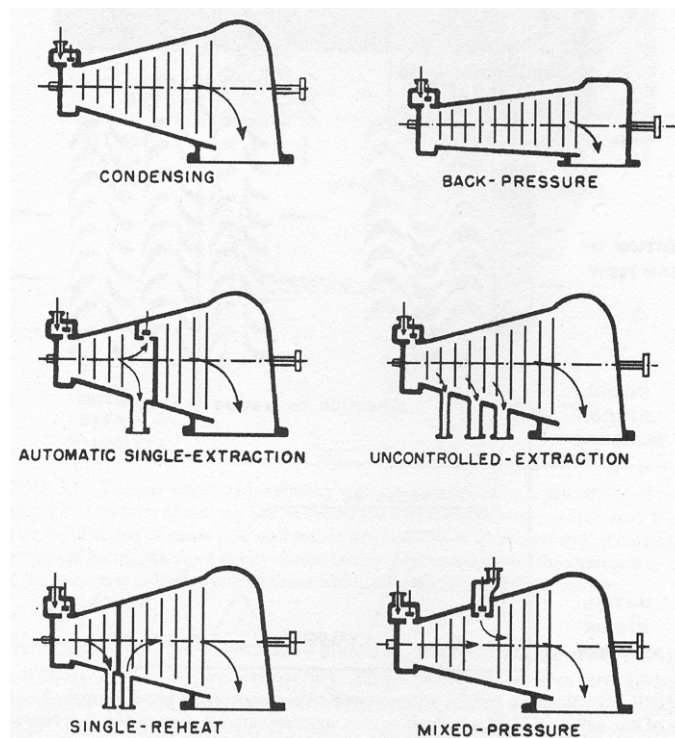
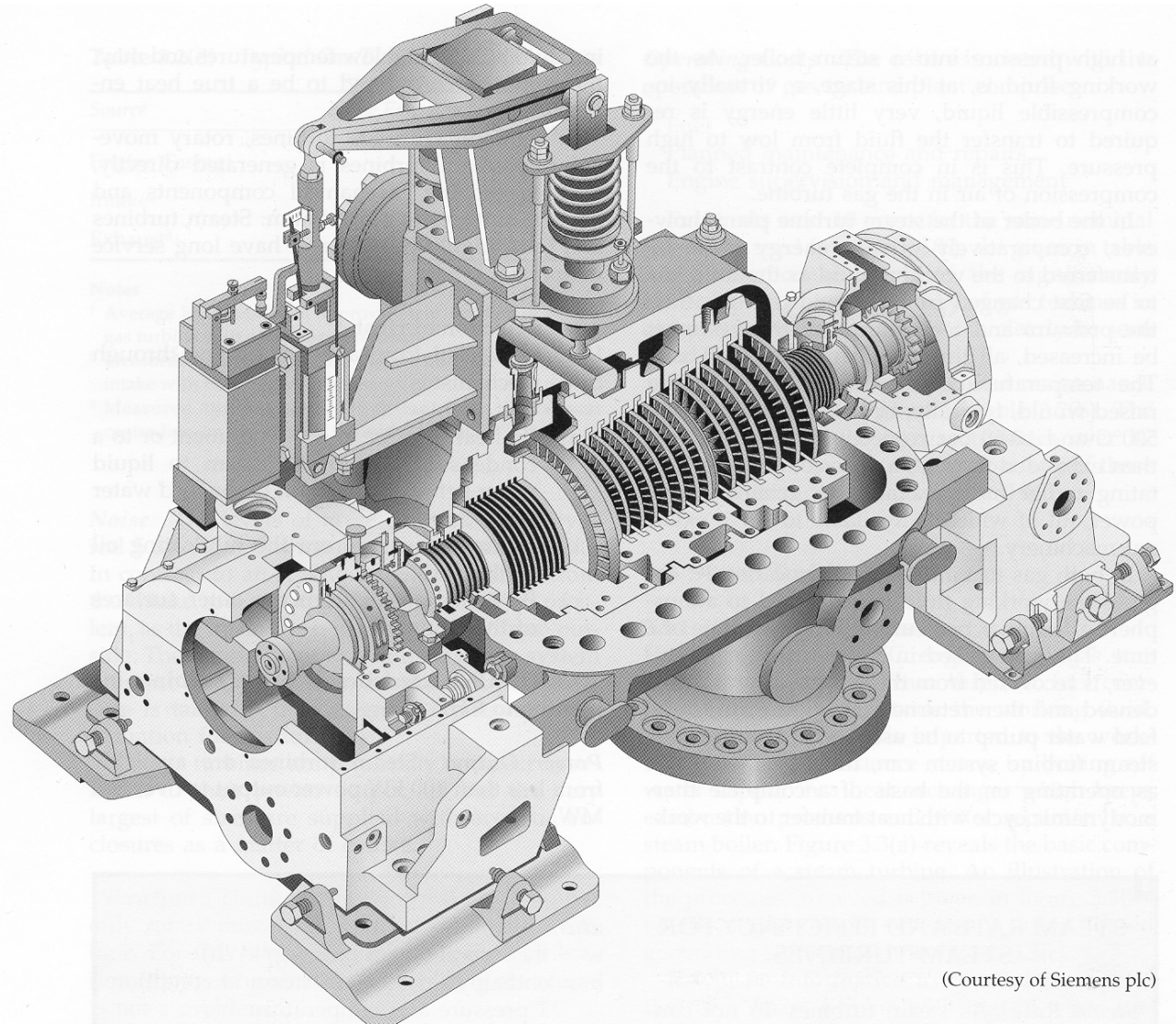


Figure 83 Single-cylinder turbine types. Typical types of single-cylinder turbines are illustrated. As shown, condensing turbines, as compared to back-pressure turbines, must increase more in size toward the exhaust end to handle the larger volume of low-pressure steam.



(Courtesy of Siemens plc)

Figure 84 Steam turbine – backpressure

4.2.2 Compound Turbines

Compound turbines have more than one cylinder: a high-pressure and a low-pressure turbine. The low-pressure cylinder is usually of the double-flow type to handle large volumes of low-pressure steam (due to limitations on the length of the blades). Large plants may have an intermediate pressure cylinder and up to four low-pressure cylinders. The cylinders can be mounted along a single shaft (tandem-compound), or in parallel groups with two or more shafts (cross-compound). Reheating is usually done between the high- and intermediate-pressure turbines. Figure 85 illustrates some of these arrangements.

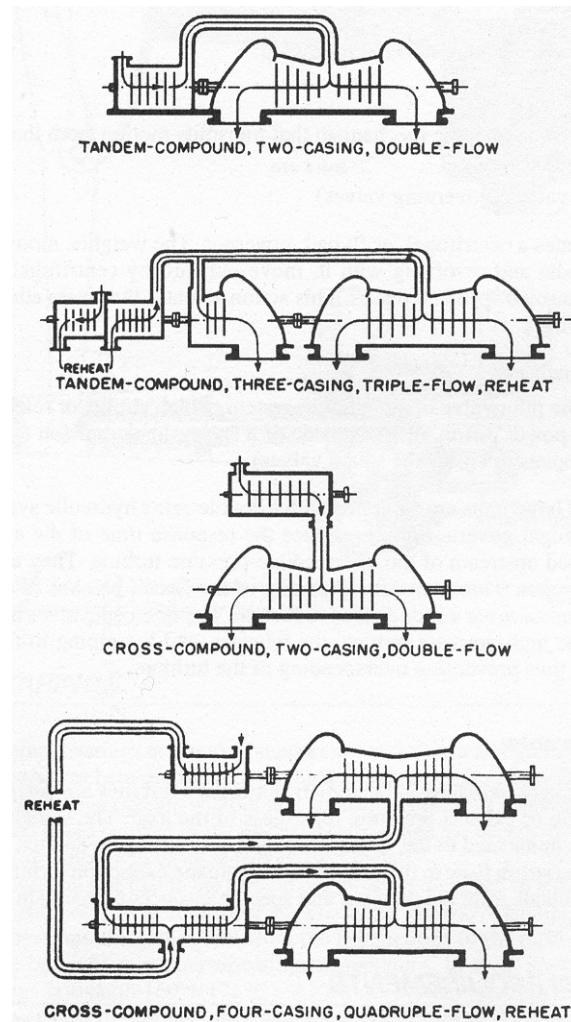


Figure 85 Some arrangements of compound turbines. While many arrangements are used, these diagrams illustrate some of the more common ones.

4.2.3 Casing design

Depending upon the the pressure the turbine is designed for, various principles are used. For high-pressure turbines (>150 bar) it is common to use single-casing turbines, but for lower pressure a horizontally split casing is normally used (see Figure 87).

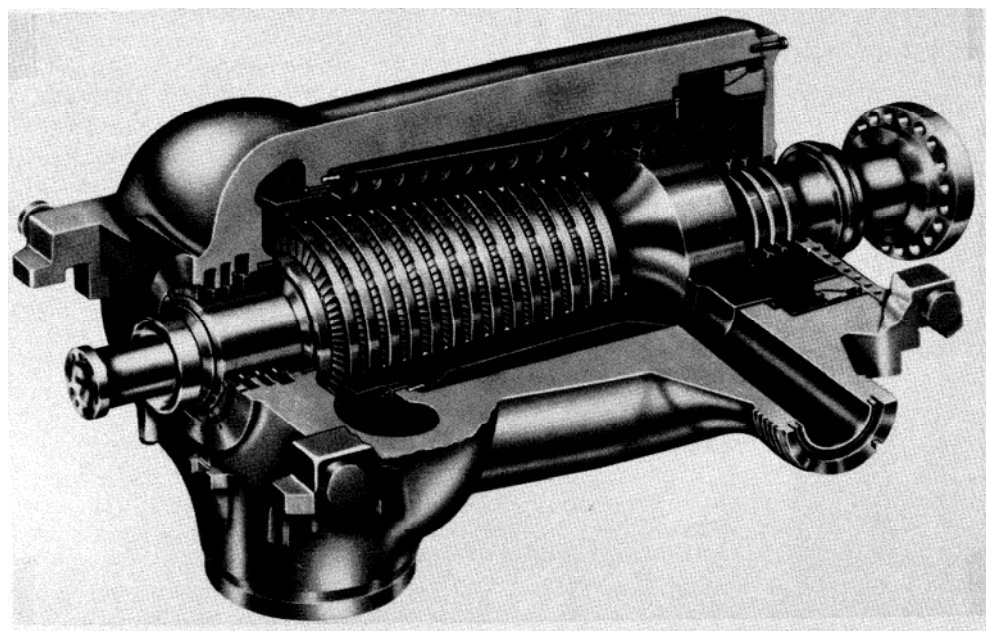


Figure 86 *High-pressure turbine with single casing*

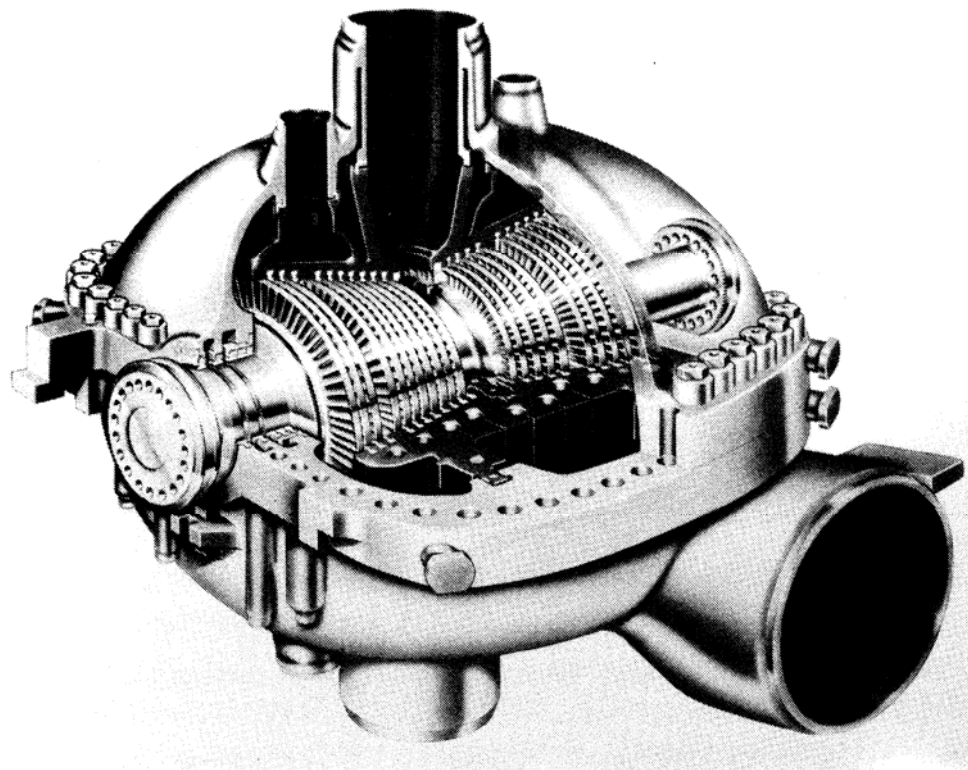


Figure 87 *Intermediate-pressure turbine with single casing*

4.3 Steam turbine expansion path

4.3.1 Enthalpy/entropy-diagram

The performance calculation for steam turbine is based on enthalpy values for steam and/or liquid water. A methodology – we doing a hand calculation - is to use an enthalpy/entropy-diagram. Using such a diagram is common for illustrating the expansion path of a steam turbine. An advantage for this type of diagram is that the vertical height is proportional to the work of the steam turbine.

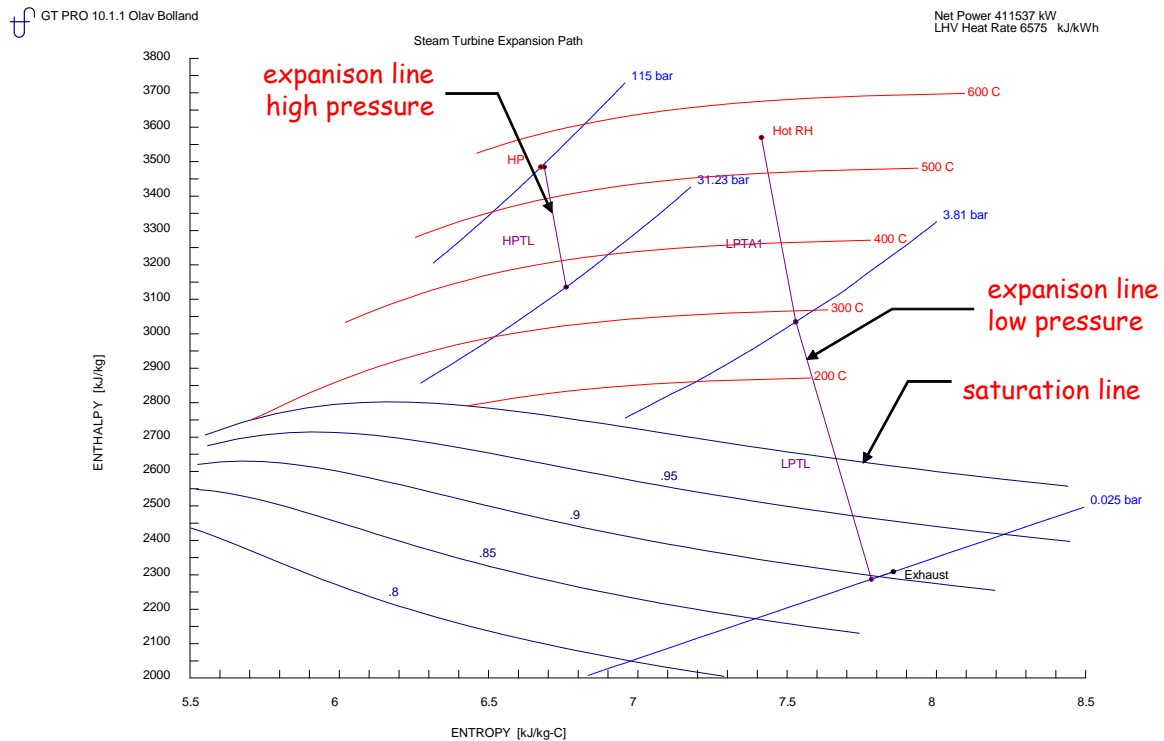


Figure 88 Enthalpy/entropy-diagram for the expansion path of steam turbine in triple pressure reheat steam cycle. High pressure steam is first expanded, and then the steam is reheated in the HRSG, and then further expanded in 'LPTA1'. After that, the expansion continues in the low pressure turbine. The expansion path crosses the saturation line and ends up in the two-phase area, in this case with a steam quality of about 0.9. Along the isobar 0.025 bar, the leaving loss is depicted, see section 4.3.3. The diagram is made with the computational program GTPRO (Thermoflow, Inc.).

4.3.2 Wet steam expansion

When the expansion path crosses into the wet region, condensation does not occur as expected from the equilibrium conditions in an enthalpy/entropy diagram. When crossing the saturation line the steam becomes subcooled, at a rather small rate of formation of small water drops. The drops are in an equilibrium state with a temperature that corresponds to the saturation pressure, while the steam is colder than the drops. As the steam expands the growth in drop size will then be opposed by evaporation from the drop surface. According to Traupel (1988), the growth rate of the drops is an exponentially increasing function of the steam subcooling, ΔT_{sub} . The steam subcooling for a given pressure is the difference between the actual steam temperature and the temperature at which the steam is in an equilibrium state. The steam subcooling for a given pressure designated by subscript 1, is according to Dietzel (1980):

$$\Delta T = T_{\text{sat}}(P_1) - T_1 \quad (55)$$

Where T_1 is given by

$$T_1 = T_G - \frac{(\kappa - 1)(h_G - h_1)}{\kappa R} \quad (56)$$

G designates the state where the expansion path crosses the saturation line. The isentropic exponent of wet steam is in general (Traupel, 1988),

$$\kappa \equiv -\frac{v}{p} \left(\frac{\partial P}{\partial v} \right)_s \quad (57)$$

where the last term denotes the partial derivative with constant entropy. A simple correlation for the isentropic exponent of wet steam is given by Dietzel (1980),

$$\kappa = 1.035 + 0.1 x \quad (58)$$

where x is the steam quality. The maximum subcooling of the steam depends on the "speed of expansion" given by Eq. (2.5) (Dietzel, 1980),

$$S = \frac{1}{P} \frac{dP}{dt} = \frac{u_{ax}}{p} \frac{\partial P}{\partial a} \quad (59)$$

where a = steam path length in axial direction

u_{ax} = steam velocity in axial direction

For large values of S the rate of formation and growth of drops will be small and imply a large subcooling of the steam. At the maximum subcooling of the steam the drop size will have reached a critical value where the temperature difference between the drops and the subcooled steam cannot oppose a further growth in drops size. A spontaneous condensation then takes place and the steam will come into an equilibrium state. If the points at which this spontaneous condensation takes place for different expansion paths and with different speeds of expansion are drawn in an enthalpy-entropy diagram, lines for constant steam quality can be obtained from these points. These lines are designated "Wilson-lines", and for practical applications these lines can be regarded as parallel with lines of constant steam quality in an enthalpy-entropy diagram (Traupel, 1988). This is shown in Figure 89. According to Dietzel (1980) the location of the Wilson-line will typically be in the range given in Table 20.

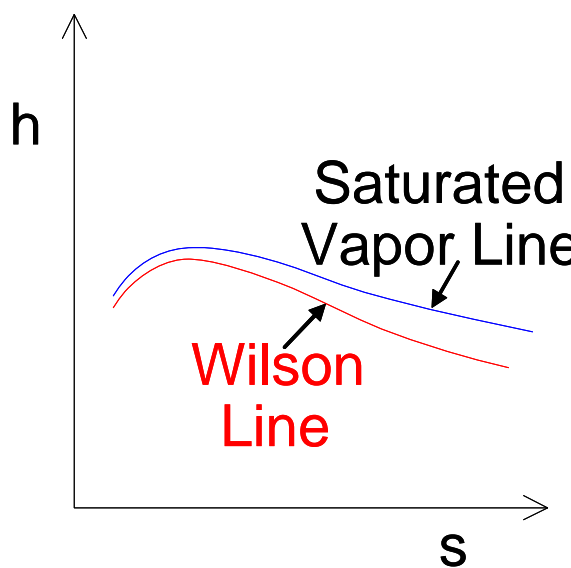


Figure 89 Schematic of enthalpy-entropy diagram with approximate location of Wilson-lines

Table 20 *Location of Wilson-line as function of expansion velocity (Dietzel, 1980)*

Speed of expansion S [1/s]	Quality x [kg _{steam} /kg _{total}]
10	0.977
100	0.974
1000	0.970
10000	0.963

As shown in Table 20, the range of steam quality in which the spontaneous condensation takes place is rather narrow, and it is common in analysis to fix the occurrence of the Wilson-line to a specific steam quality.

The efficiency for the low pressure section of the steam turbine may be corrected for moisture if the expansion crosses the Wilson line. The efficiency degradation is a function of steam quality, and can be found by using the so-called Baumann's formula:

$$\eta_{is} = \eta_{is,dry} (1 - \alpha (1 - x_{mean})) \quad (60)$$

$\eta_{is,dry}$ = isentropic efficiency for dry steam

α = Baumann coefficient

x_{mean} = mean steam quality for the actual computational step

Considerable differences in opinion exist in regard to the value of the Baumann coefficient. According to Gyarmathy (Ojala, 1968) α varies in the range 0.4-0.9 on analysis of the expansion path within the whole wet region, dependent upon the type of turbine and the drainage devices. However, Gyarmathy has also indicated that appreciable differences may occur in these values in the examination of individual stages. Wood (Ojala, 1968) has compared results from several researchers in this field, and concludes that $\alpha \approx 1$. A study of Smith (Traupel, 1988) on a high-speed, low pressure test turbine shows that $\alpha \approx 1.2$. According to Rukes (1988) the mean α for large steam turbines is in the range 0.5-0.8, and depends on the turbine exit steam quality which means that the Baumann coefficient is not constant along the expansion path but is depending on steam quality. Traupel (1988) suggests to use a variable α , as a declining function of $(1-x)$.

An alternative to the Baumann's formula, is to correct the efficiency in the wet region below the Wilson-line for each computational step with an exponential type of function,

$$\eta_{is} = \eta_{is,dry} (1 - (1 - x_{mean})^c) \quad (61)$$

where c is the efficiency moisture correction factor

If $c = 1$, Eq. (61) is identical to Eq. (60) for $\alpha = 1$. Table 21 shows the efficiency correction in the wet region and the Baumann coefficient as functions of $(1-x)$ for different values of the efficiency correction factor, c .

Table 21 *Steam turbine efficiency correction for moisture*

	$c=1.1$	$c=1.1$	$c=1.2$	$c=1.2$	$c=1.3$	$c=1.3$
$1-x$	$\eta_{is}/\eta_{is,dry}$	α	$\eta_{is}/\eta_{is,dry}$	α	$\eta_{is}/\eta_{is,dry}$	α
0.05	0.963	0.741	0.973	0.549	0.980	0.407
0.07	0.946	0.766	0.959	0.588	0.968	0.450
0.09	0.929	0.786	0.944	0.618	0.956	0.486
0.11	0.912	0.802	0.929	0.643	0.943	0.516
0.13	0.894	0.815	0.914	0.665	0.930	0.542

Some steam turbines have water drainage devices located at the low-pressure section of the LP-turbine, see Figure 90. When steam condenses along the expansion path, small drops are formed and existing drops continue to grow. Most of the drops are small and can be characterized as fog. According to Dietzel 60-90 % of the drops at the last stage are of that size. These drops have a velocity close to that of the steam and follow the steam flow well. Another fraction of the drops (10-30 %) has a much lower velocity than the steam and causes erosion when hitting the rotor blades. 0-10 % of the drops are centrifugated toward the casing of the turbine by forming a film on the rotor blades. The centrifuged water may be drained from the turbine through small holes in the casing and be led to the condenser. The typical location of these holes is close behind the rotor rows (Traupel, 1988). There are also examples of drainage through holes in the last stage stator blades (Rukes, 1988).

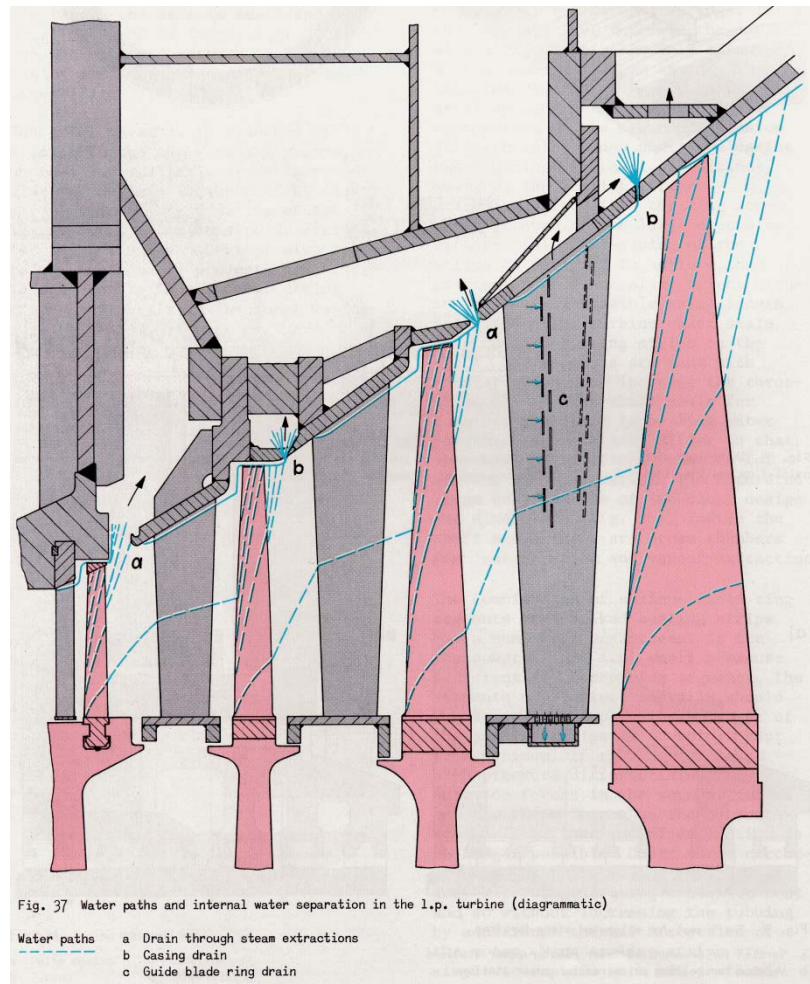


Fig. 37 Water paths and internal water separation in the l.p. turbine (diagrammatic)

Water paths
 a Drain through steam extractions
 b Casing drain
 c Guide blade ring drain

Figure 90 Cut of the low pressure section of a steam turbine. The figure shows how water can be drained from the expansion path; either through steam extraction points (a), or drain holes right behind the rotot blades (b), or through suction slits on the surface of the last stator blade (c).

La Roche (Traupel, 1988) has examined the question of how much water that is drained from a steam turbine for different pressures and steam qualities. The result of this work is shown in Figure 91. The drainage effectiveness is defined as

$$\varepsilon = \frac{m_w}{m_1 (1 - x_1)} \quad (62)$$

where

- m_w = amount of drained water
- m_1 = total mass flow in expansion path before drainage
- x_1 = steam quality in expansion path before drainage

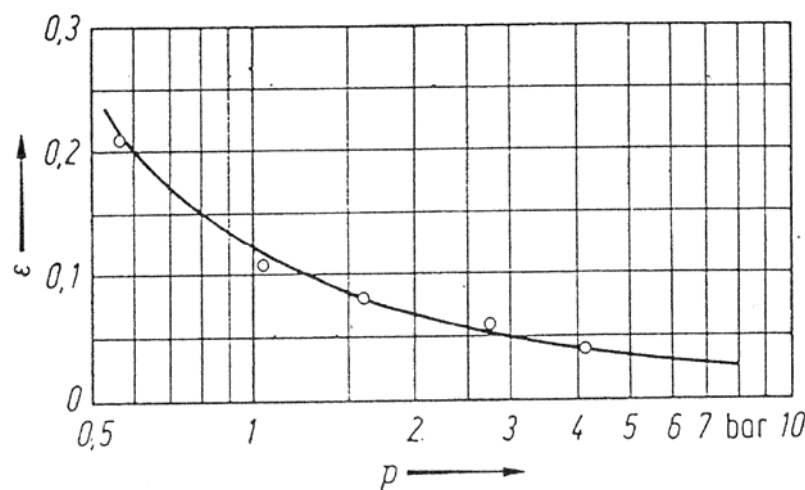


Figure 91 Moisture drainage effectiveness ϵ after La Roche (Traupel, 1980).

4.3.3 Turbine leaving loss

Condensing steam turbines have a considerable leaving loss. The axial velocity behind the last stage is typically in the range 200-270 m/s. The kinetic energy corresponding to this range of velocities amounts to 20-36 kJ/kg. The absolute velocities behind the last stage may be higher than the axial component. In most cases steam turbines have a diffuser located behind the LP-turbine exit. The diffuser increases the static pressure and enables expansion of the steam to a static pressure which may be below that of the condenser. In this way some of the leaving loss can be regained. It is common in most cycle analysis to assume the leaving loss is as a constant, even if it varies depending on the steam velocity, see Figure 92.

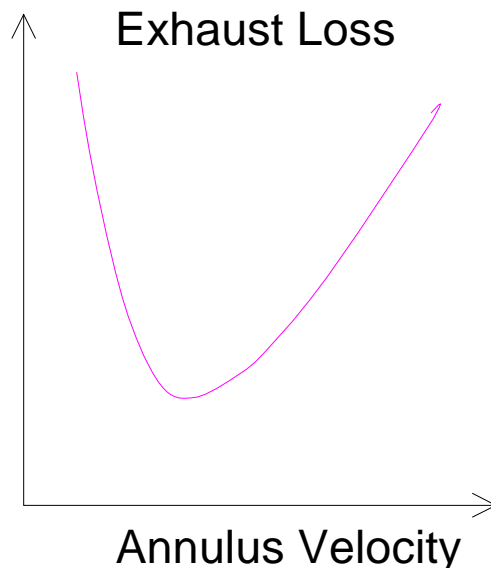


Figure 92 General exhaust loss curve for a steam turbine.

5 Combined Cycle

5.1 What is a Combined Cycle

The idea of combining power cycles with different working fluids, heat supply and heat rejection temperatures, was developed in the early twentieth century (Horlock, 1995). The motivation was to increase the thermal efficiency. The development of the combined gas turbine and steam turbine cycles came somewhat later. By 1970 there were a number of plants in operation. Throughout the 1980s the technology developed with larger gas turbines and the introduction of pre-mixed combustion for low NO_x emissions. Around 1990 the net plant efficiency of combined cycles passed 50% (LHV). Throughout the 1990s a large number of combined cycle power plants were built, and many of them in base load operation. Around 1995 a new generation of large gas turbines came on the market, bringing the block⁴ size of combined cycle power output to 350-400MW and efficiency up to 57-58%. As of 2008 the power output may be up to about 500MW and efficiency close to 60%.

A combined gas turbine and steam turbine cycle, or simply combined cycle (Kehlhofer, 1999), is the two cycles connected by the heat recovery steam generator (HRSG). A simplified diagram is shown in Figure 93. The HRSG is further discussed in Chapter 3. The gas turbine flue gas temperature is within the range 450-650 °C. The energy contained in the flue gas amounts the fraction of the fuel energy that is not converted to power by the gas turbine. This energy is used to raise steam and to produce power by the steam turbine. Depending upon type of HRSG the flue gas temperature is reduced to 80-200 °C, where the lower value is typical for large modern combined cycle burning a fuel with no or very little sulfur. The steam is produced with a temperature in the range 450-560 °C, and a pressure in the range 30-170 bar. Steam may be produced at multiple pressure levels. The use of super-critical steam pressure (>220.64 bar) has been suggested (Bolland, 1991), (Dechamps, 1998). Super-critical steam pressure gives the combined cycle potentially higher efficiency, but it depends on size of the steam turbine and dependence of pressure on the steam turbine efficiency.

Supplementary firing can be applied to produce additional steam using the flue gas as combustion air, as it contains typically 12-13% by volume of oxygen. Supplementary firing is not common.

⁴ A combined cycle block consists of one gas turbine, one HRSG and one steam turbine. It is common to have the gas turbine and steam turbine on a common shaft, sharing one generator.

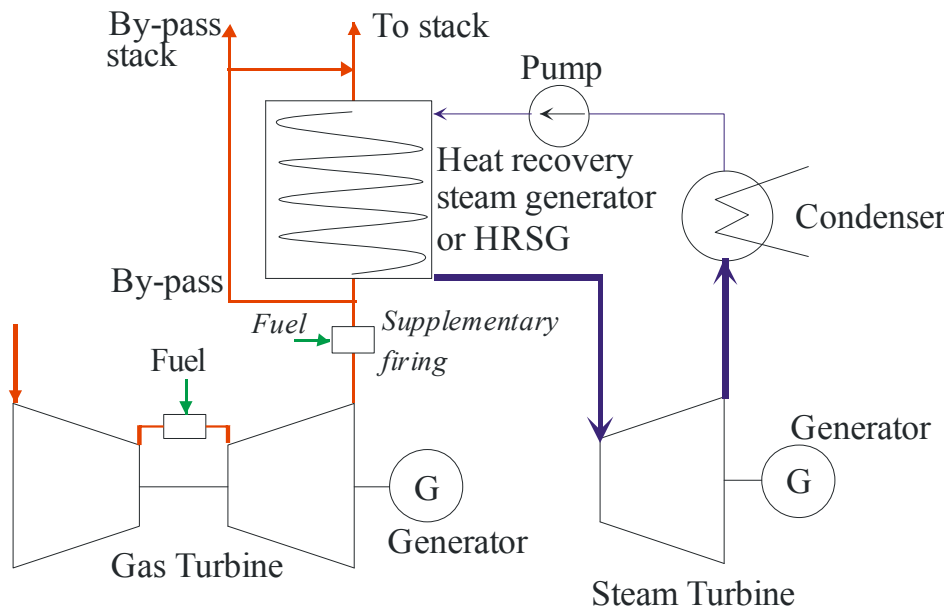


Figure 93 Combined gas turbine and steam turbine cycle – ‘combined cycle’. Supplementary firing can be used to augment steam production

5.2 Virkningsgrad for kombinerte prosesser

I dampturbinprosessen så konverteres ca. 30-40% av varmen i eksosen til arbeid. Det betyr at dampturbinprosessen kan bidra med ca. 20 % -poengers økning i anleggets totale virkningsgrad. Et kombinert anlegg kan ha en virkningsgrad i området 45-60%, avhengig av anlegges størrelse og hvor mye investeringer som er myntet på å oppnå høy virkningsgrad. En virkningsgrad på nærmere 60% er ca. 10-15%-poenger høyere enn andre kommersielle teknologier for elektrisitetsproduksjon.

Hvorfor gir så kombinasjonen av en gassturbinprosess og en dampturbinprosess en så høy virkningsgrad. Vi kan benytte en enkel forklaringsmodell ved å se på den såkalte Carnot-virkningsgraden:

$$\eta_C = 1 - \frac{T_l}{T_h} \quad (63)$$

Carnot-virkninggraden kan benyttes som en kvalitativ beskrivelse av virkningsgrad for andre kraftprosesser forskjellig fra Carnot-prosessen. T_l er temperatur for varmeavgivelse fra prosessen, mens T_h er temperatur for varmetilførsel for prosessen. I Figure 94 og Figure 95 nedenfor er det vist for en gassturbin- og en dampturbinprosess hvor T_l og T_h ligger. Disse reelle prosessene er til forskjell fra Carnot-prosessen slik at varme tilføres og fjernes ved glidende temperatur, og ikke ved konstant temperatur som i Carnot-prosessen. Analogien med Carnot-prosessen kan selvsagt likevel benyttes. En ser at begge prosessene har enten høy temperatur for varmeavgivelse (gassturbin) eller lav temperatur for varmetilførsel (dampturbin); noe som er negativt for virkningsgraden. På en annen side har begge prosessene sitt fortrinn med tanke på virkningsgrad gjennom høy temperatur for varmetilførsel (gassturbin) eller lav temperatur for varmeavgivelse (dampturbin). Når disse prosessene kombineres oppnår en å beholde fordelene mens ulempene i denne sammenheng forsvinner (se Figure 96). En kan legge til at ved kombinasjonen av de to prosessene så innføres en

termodynamisk “straff” ved at varme må overføres mellom de to prosessene (i dampkjelen) med en viss temperaturdifferanse.

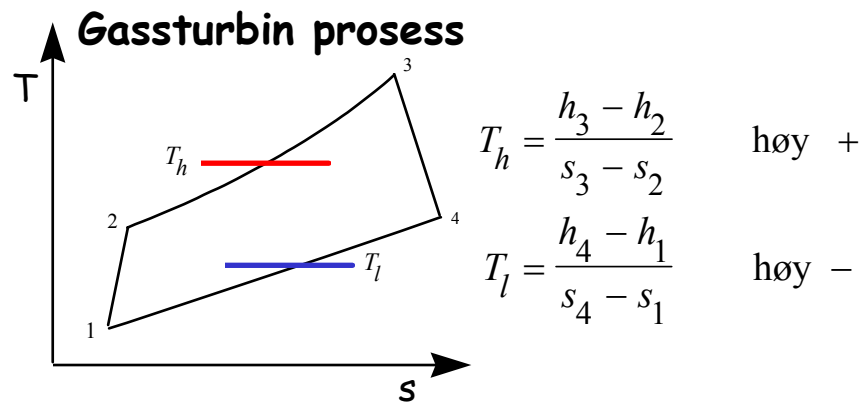


Figure 94 Temperatur-entropi-diagram for en gassturbinprosess (h er entalpi, s er entropi).

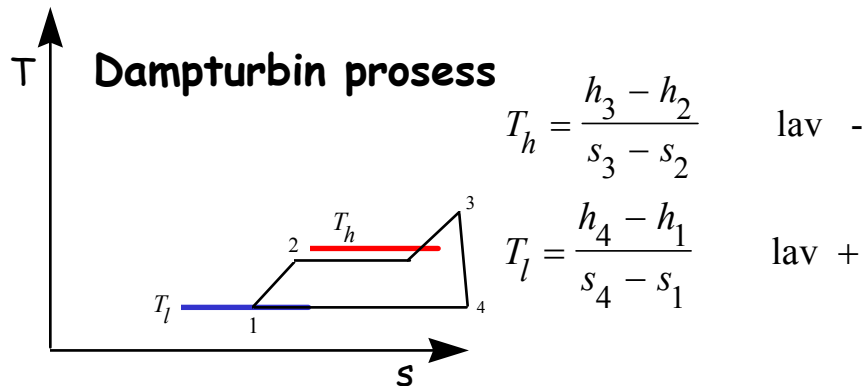


Figure 95 Temperatur-entropi-diagram for en dampturbinprosess.

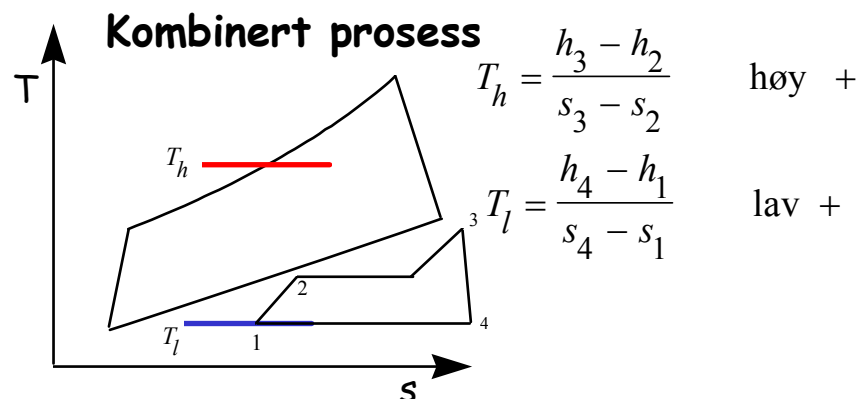


Figure 96 Temperatur-entropi-diagram for en kombinert gassturbin og dampturbinprosess.

5.3 Alternatives to the steam cycle

A lot of work has been done in order to find an alternative to the steam cycle in a combined cycle. The disadvantage with steam as a working fluid is the high heat of evaporation which implies relatively high losses of exergy in the heat transfer between the gas turbine and the steam turbine cycle. This is illustrated by the mismatch between the flue gas temperature line and that of the evaporating water and superheating of steam in Figure 76. Another disadvantage is the low saturation pressure at low temperatures. The condensation of steam following the expansion in the steam turbine takes place at a pressure typically in the range 0.02-0.12 bar. At these pressures the specific volume is large. The low-pressure section of the steam turbine may be very large with blades slightly exceeding 1m. Inleakage of air is a challenge to avoid as well as to remove dissolved oxygen in the condensate which may cause high-temperature corrosion in the steam boiler.

A number of alternative working fluids to steam have been suggested (Vijayaraghavan and Goswami, 2005), (Devotta and Holland, 1985), (Saleh, Koglbauer et al., 2007). A mixture of ammonia and water (Kalina cycle) has been suggested for heat source temperatures up to that of gas turbine flue gas (Kalina and Leibowitz, 1987). Halogenated hydrocarbons have interesting thermodynamic properties for low-temperature heat sources, but are hampered with a number of disadvantages; such as toxicity and ozone depletion effects. Alkanes are being used in some low-temperature applications (geothermal). Helium and CO₂ have been suggested for use in closed Brayton cycles at high temperatures, such as that of gas turbine flue gas and nuclear reactors (Chen, Zheng et al., 2003), (Dostal, Hejzlar et al., 2006). CO₂ has also been suggested for use in Rankine cycles for low-temperature heat sources (Zhang, Yamaguchi et al., 2007). Air has been suggested as a working fluid in open Brayton cycles with compressor intercooling, the Air Bottoming Cycle (Guo and Wang, 1992), (Hirs, Wagener et al., 1995), (Bolland, Førde et al., 1996), (Spector and Patt, 1997), (Heppenstall, 1998), (Korobitsyn, 2002).

During the 1980s and early 1990s there was a lot of interest in developing the steam injected gas turbine cycle, in which the gas turbine flue gas energy is used to raise steam and to inject it into the gas turbine (Tuzson, 1992), (Bolland and Stadaas, 1995), (Poullikkas, 2005). The amount of steam injected is above that commonly used for NO_x control (about 2% weight steam compared to compressor inlet air flow). A typical range is 5-17% weight of steam to air. A steam injected gas turbine can be regarded as an integrated Brayton and Rankine cycle. A rough estimation is that 30-50 plants were built.

Despite all the work that has been done to find alternatives, the steam cycle still remains the obvious choice as the bottoming cycle for gas turbines. The temperature profile mismatch in the HRSG, which has been used as the main argument against the steam cycle by those searching for alternatives, has been reduced by introduction of multiple (2 or 3) pressure levels and steam reheat.

5.4 Cycle configurations

The steam cycle in a combined cycle is designed in various configurations in order to optimise with respect to cost, type of application, performance and efficiency. The three most important design criteria are:

- Number of pressure levels in the steam cycle. By increasing number of pressure levels, a smaller average temperature difference between the flue gas and the water/steam is obtained.

Consequently, the boiler efficiency may be increased to the cost of increased complexity. The benefit of added number of pressure levels decreases as the flue gas temperature increases. As an example, in fired boilers (coal, oil or natural gas) the flue temperature may be over 1000 °C. In such application single pressure steam cycle including reheat is used. For gas turbine flue gas (450-650 °C), dual-pressure and triple-pressure cycles are most common. In large combined cycle power plants (400-500 MW), it is common to design it with a triple-pressure reheat steam cycle.

- Type of steam turbine: This depends on the usage of the generated steam. In cases where the utilisation of heat is most important and power generation is of secondary interest, back-pressure turbines are chosen. In other cases, power generation is more important than heat, condensing steam turbines are chosen.
- Reheat. After expansion of steam in the high-pressure steam turbine, the steam may be reheated in the HRSG before further expansion in the intermediate- and low-pressure turbines. Reheat increases the low-pressure turbine exit steam quality, and enables a higher steam pressure (HP) to be used.

The gas turbine and the steam turbine may be connected on a common shaft, driving the same generator. It has become very common to design a combined cycle with 1 gas turbine, 1 HRSG and 1 steam turbine; a block. However, there are many examples where the steam from multiple gas turbines/HRSGs is fed to one large steam turbine. There are also a few examples where the flue gas from two gas turbines is passed on to one HRSG. In some plants a by-pass of flue gas is used, which imply that the flue gas can be diverted by a damper to go in a ducting outside the HRSG. The flue gas may then be taken to a separate by-pass stack or into the stack connected to the HRSG.

In the following, examples are shown for combined cycle configurations that are used in plants, see Figure 97-Figure 100. The efficiency of combined cycles is increased when adding pressure level and introducing reheat. Comparisons between the various configurations can be found in (Bolland, 1991), (Dechamps, 1998).

Terms:

HRSG=Heat Recovery Steam Generator.

HP=High Pressure

IP=Intermediate Pressure

LP=Low Pressure

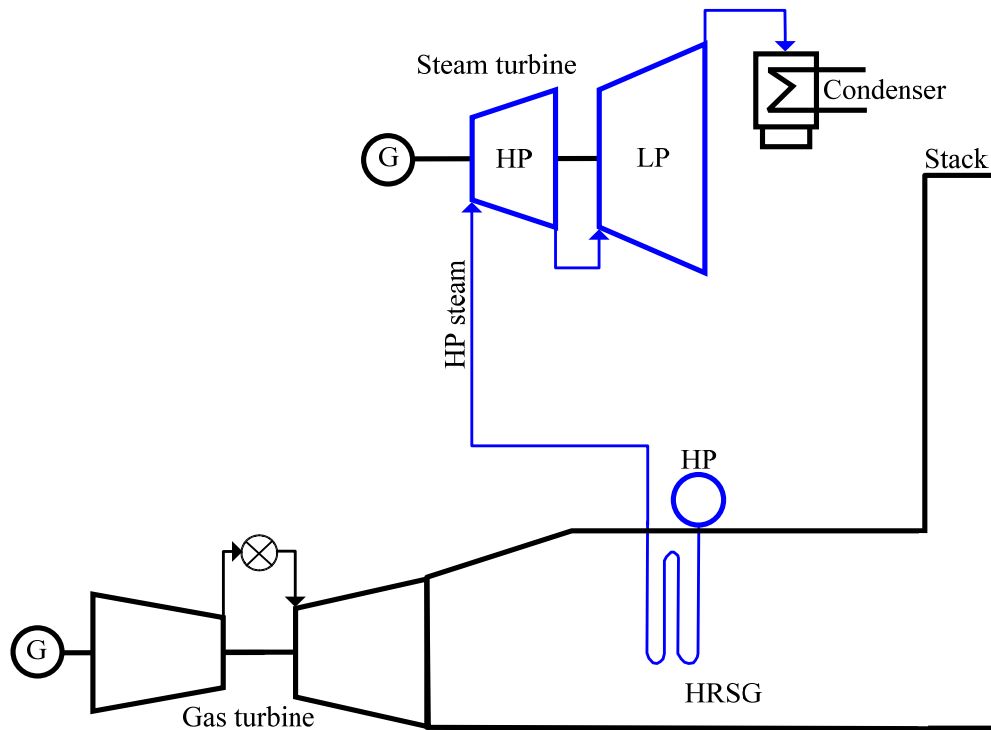


Figure 97 Combined cycle with a single pressure steam cycle.

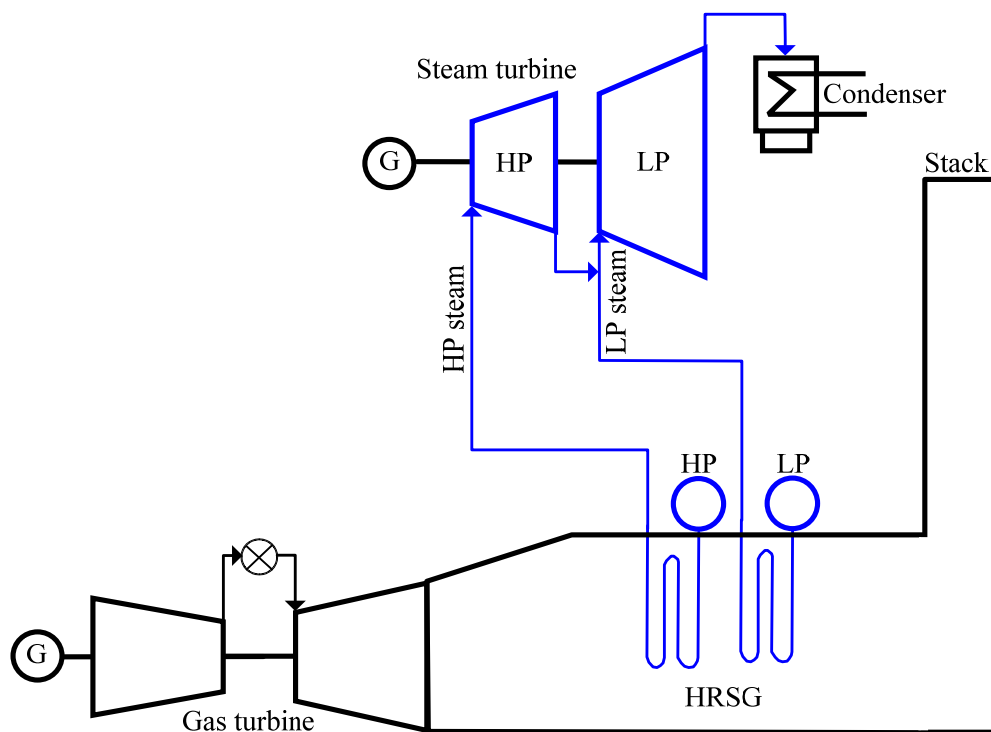


Figure 98 Combined cycle with a dual-pressure steam cycle.

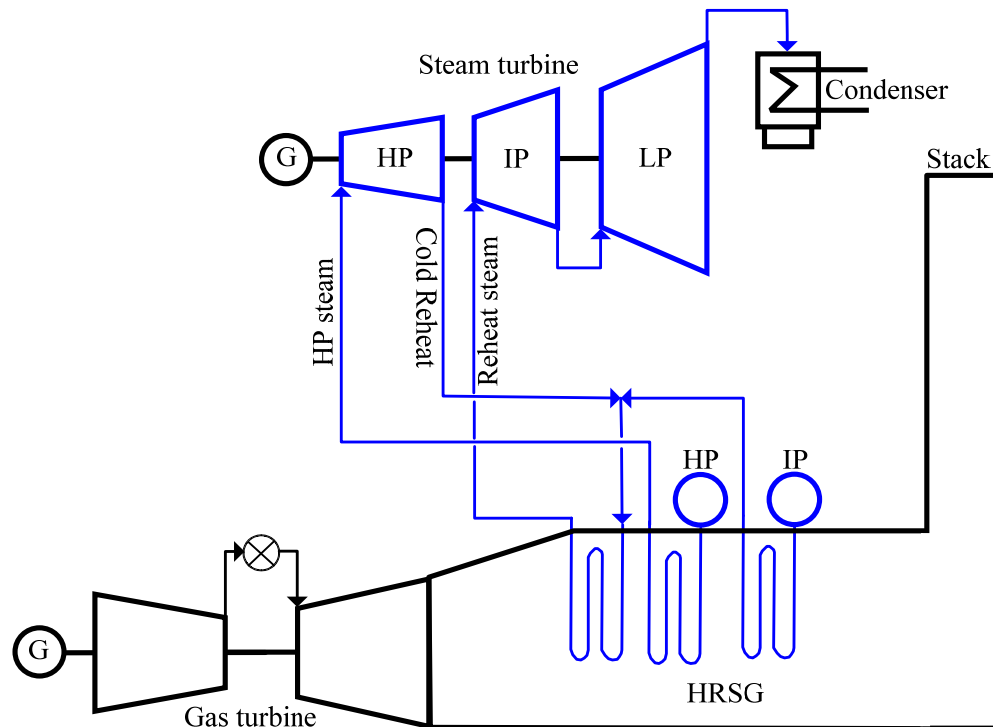


Figure 99 Combined cycle with a dual-pressure reheat steam cycle

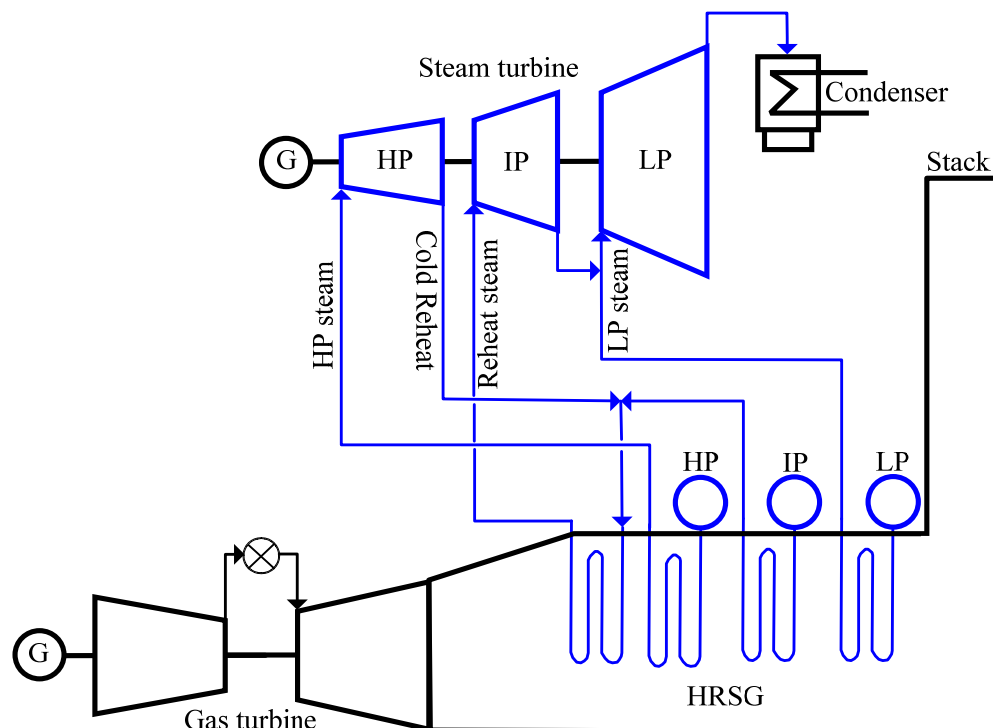


Figure 100 Combined cycle with a triple-pressure reheat steam cycle

5.5 Miljøutslipp fra en kombinert prosess

Ved produksjon av termisk kraft basert på naturgass er det i hovedsak utslipp av CO₂ og NO_x (NO og NO₂) som er av betydning i miljøsammenheng. Utslipp av svoveldioksid SO₂ er minimale på grunn av at naturgass normalt sett inneholder lite svovel, typisk for Nordsjøgass er fra 1 mg svovel per Sm³. Partikulære utslipp er helt neglisjerbare ved forbrenning av naturgass.

I Tabell 22 er eksossammensetning fra et gasskraftverk (gassturbin og dampeturbin) gitt. Brennkammeret i gassturbinen er et såkalt "tørt lav NO_x" brennkammer, og leverandøren garanterer en NO_x andel i eksosen på 25 ppmv ved tørr avgass og 15 volum-% oksygen (15 % O₂, tørr)⁵. Ved den aktuelle eksossammensetningen tilsvarer dette et NO_x innhold på 0.00234 volum-% (23.4 ppmv). De forskjellige komponentene i eksosen er også angitt i vektenheter i forhold til energiinnhold i brensel (g/MJbrensel) og kraftproduksjon (g/MJel) (kg/kWhel).

Tabell 22 Typisk eksossammensetning for kombinert gassturbin-/dampeturbinprosess.

Komponent	Symbol	Volum fraksjon volum-%	Utslipp Virkningsgrad ^a 58%		
			g/MJbrensel	g/MJel	kg/kWhel
Nitrogen	N ₂	74.94	723.9	1248	4.49
Argon	Ar	0.90	12.4	21.4	0.08
Oksygen	O ₂	12.91	142.4	246	0.88
Karbondioksid	CO ₂	3.84	58.3	101	0.36
Vann	H ₂ O	7.40	46.0	79.3	0.29
Nitrogenokside ^b	NO _x	0.00234	0.0371	0.0640	0.00023
Trykk		1.013 bar			
Temperatur ut av skorstein		90 °C			
Duggpunkt		40 °C			
Molvekt		28.5 kg/kmol			

^a Virkningsgrad for ren elektrisitetsproduksjon

^b Utslippet er beregnet for aktuell gassammensetning basert på 25 ppmv ved 15 volum-% O₂ og tørr gass

I en gassturbin vil det foregå en tilnærmet fullstendig forbrenning slik at knapt noe kullos (CO) eller uforbrente hydrokarboner (UHC) vil finnes i avgassen. CO-konsentrasjonen i eksosen vil typisk ligge under 10 ppmv (15 % O₂, tørr). Ved døllast vil utslippet av CO øke noe.

Når det gjelder utslipp til vann, slippes store mengder kjølevann ut fra kombinerte anlegg. Kjølevannet benyttes til å kondensere damp etter dampeturbinen. Ca. 33% av energien i brenslet kommer ut i form av lavtemperatur kjølevann fra et kombinert gassturbin/dampeturbin kraftverk (antar 58% virkningsgrad for elektrisitetsproduksjon, ingen utnyttelse av varme fra kraftverket til f.eks. fjernvarme). Hvis en antar at kjølevannet (typisk sjøvann) øker sin temperatur med 10 °C

⁵Standard måte for å angi NO_x utslipp fra gassturbiner

gjennom kraftverket, så betyr dette en mengde på $5\text{-}6 \text{ m}^3/\text{s}$ kjølevann for et gasskraftverk på 400 MW_{el}.

Når det gjelder utslipp av støy er dette ikke ansett som noe problem fra et teknisk synspunkt. Med dagens akustiske isolasjonsteknologi er støydemping et spørsmål om kostnader.

6 Coal power plants

For coal as fuel, it is by far most common to use conventional steam plants. The boiler, where combustion and heat transfer to the working fluid take place, may be of various designs. A special case is IGCC (Integrated Gasification Combined Cycle), in which coal is gasified and where the gaseous fuel is used in a gas turbine process. For natural gas as fuel, most plants use gas turbines, in which the fuel is burned, and often combined with a steam cycle where steam is generated utilising exhaust gas from the gas turbine.

6.1 Coal fired power plants

In general, a number of methods for large-scale coal-fired power generation are well established and widely used. Others are used only in a few plants. In Figure 101 these methods are depicted. Coal can either be combusted or gasified. The different methods are explained later. For more in-depth information on coal power plants, refer to (Miller, 2005) and (Woodruff, Lammers et al., 2004).

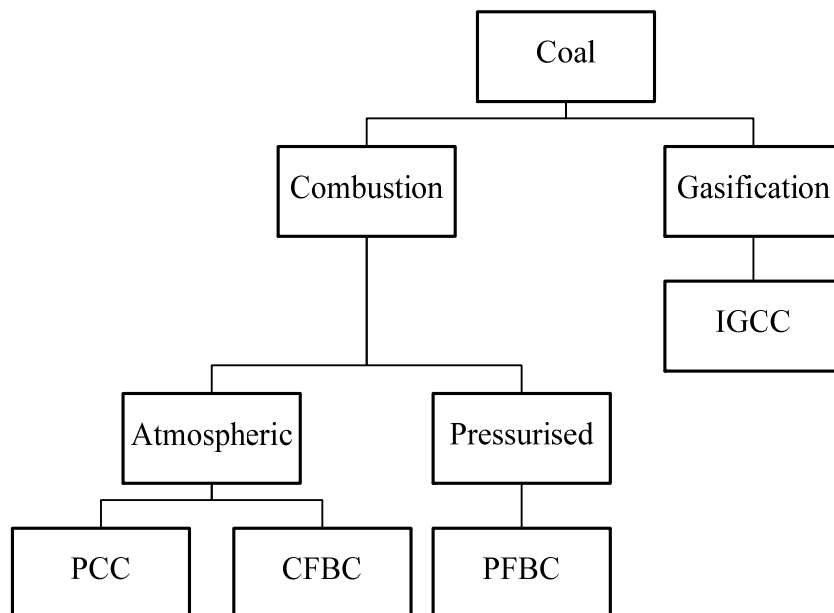


Figure 101 Coal conversion for power generation

Common for all coal fired power plant is a coal handling system. The coal is crushed, pulverised, sometimes dried, sometimes cleaned, and then fed to the combustion device either pneumatically or as a coal-water slurry.

6.1.1 The steam cycle in a coal power plant

A steam cycle is a so-called Rankine cycle for which the main characteristics are:

- compression of the working fluid in the liquid phase

- the working fluid is changing between liquid and gas phase through the cycle
- the working fluid is in a closed loop in the cycle

With only a very few exceptions, the working fluid of Rankine cycles is water/steam. An example of steam cycle in a coal power plant is shown in Figure 102, including some typical key data.

The main components in a steam cycle are:

1. Heat supply, either by combustion or by sensible heat of a hot gas, which is transferred to generate steam using pressurised water. The various combustion methods are discussed in the following chapters.
2. The high-pressure steam is expanded in a steam turbine, where the energy of the steam is partly converted to work. The work is transferred via a rotating shaft, and is converted to either electricity by a generator or to pressure energy by a pump or compressor.
3. The steam from the steam turbine condenses in a heat exchanger called a condenser, in which the heat of condensation is rejected from the cycle, using a cooling system. A special case is when the steam is utilised for a purpose outside the power plants, e.g. steam network in a refinery, or a paper mill, and the amount of condensate coming back to the power plant may vary from 0-100%. The steam turbines in power plants giving off useful heat by steam from the steam turbine exit, are often referred to as back-pressure turbines. Heat can also be given off to external demands using steam extractions from the steam turbine, which is similar to the extractions discussed in point 5 below. When either or both of these methods for giving useful heat off to external demands, the power plant is referred to as a Combined Heat and Power (CHP) plant or a cogeneration plant.
4. The cooling system may be of various designs, depending upon the available sink for the rejected heat.
 - a. Water cooled condenser with a once-through open loop water system, when there is sufficient access to cold water; either sea water, river water or water from a cooling pond.
 - b. Water cooled condenser, with cooling tower for rejection of heat to the air
 - c. Air-cooled condenser, with rejection of heat to the air
 - d. Combinations of the above
5. The condensate (liquid water) from the cooling system and/or condensate returned from outside the power plant is heated, deaerated and pressurised before entering the boiler. In plants with a fired boiler, as opposed to heat recovery steam generators (HRSG), there are a number of feedwater preheaters. Steam extracted from the steam turbine is condensed in heat exchangers, in which the feedwater on its way to the boiler is heated to a temperature that may be up to slightly above 300 °C.

Coal power plants show a very large range of efficiencies. The most advanced plants in operation today have about 45-47% net efficiency based on the lower heating value, while others have efficiencies around 30%. On a global basis the average efficiency for converting heating value of the coal into electricity is around 31-32% (Pacala and Socolow, 2004), (Schilling, 2005). The 1000 MW BoA unit of the Niederaussem power plant has probably the highest efficiency for lignite as fuel; 43.2% based on lower heating value, using a wet cooling tower (RWE, 2008). For bituminous coal, the Danish power plant Nordjyllandsværket (unit 3) has probably the highest efficiency with about 47% based on lower heating value, using once-through open loop sea water cooling (Overgaard, 2008). There is a huge potential to reduce CO₂ emissions just by increasing efficiency of coal power plants. A lot of new power plants built today have efficiencies far below what could

be achieved using state-of-the-art technology. One important point regarding efficiency is that when capturing CO₂ from a coal power plant with the goal of a certain emission g CO₂/kWh, it is of outmost importance to minimise the amount of CO₂ to be captured by designing the power plant with high efficiency.

There are a number of design choices that influences the efficiency, and the most important ones are:

- Steam pressure: Normally either sub-critical⁶ 160-170 bar, or supercritical with about 250 bar. High efficiency requires supercritical pressure, 250-350 bar
- Steam temperature, normally 530-560 °C, but numerous successful examples of plants with 580-613 °C exist. Research programs aim at 700 °C (Bugge, Kjær et al., 2006).
- Number of steam reheat: Normally one or two
- Number of feedwater preheaters: May be up to 10, and with temperatures up to 350 °C.
- High-efficiency steam turbine blading
- Drying of coal with minimal impact on plant efficiency
- Condenser pressure (which to a large extent is site specific)
- Sliding pressure operation for improved part-load performance (Vitalis, 2006)

Material technology is a key issue for improved efficiency, not only for coal power plants, but any thermal power generation technology (Viswanathan, Coleman et al., 2006). The material choice is to a large extent an economical issue. The consumption of large quantities of expensive Ni-based alloys has significant influence in this respect, and a successful development of an improved ferritic steel to be used at temperatures up to 650 °C would be very important.

The configuration of the most advanced steam cycles are highly optimised with respect to efficiency, meaning that a further increase in efficiency depends on steam pressure and temperature, which again depend on materials.

⁶ Critical pressure of water is 220.64 bar

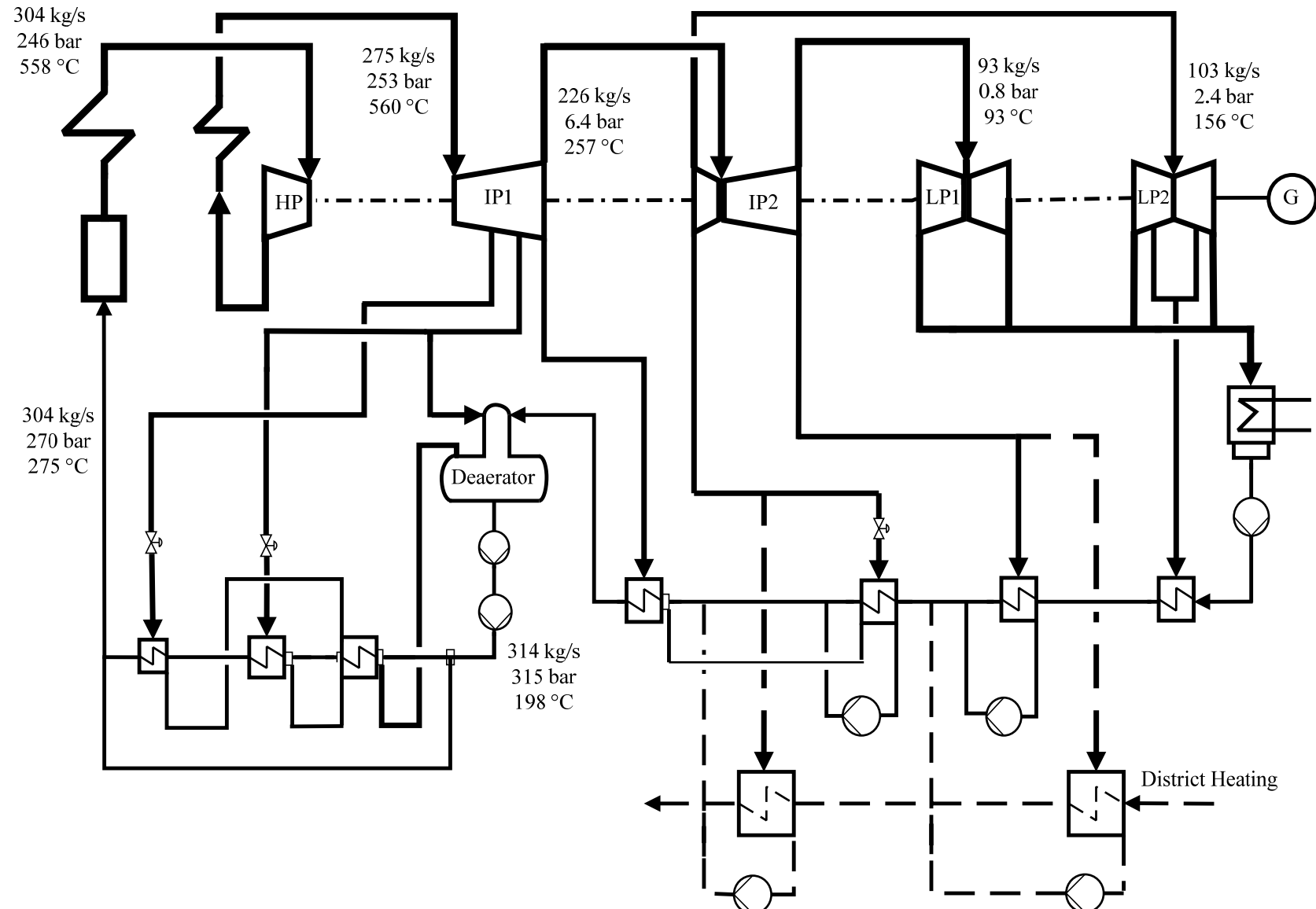


Figure 102 Example of a steam cycle flow diagram for a coal power plant. With dashed lines, a typical district heating configuration.

6.1.2 Pulverised Coal Combustion (PCC)

The most common process for coal-based power generation is Pulverised Coal Combustion (PCC) taking place at a pressure close to atmospheric. An illustration of a conventional steam cycle with coal combustion is given in Figure 104. The technology is well developed, and there are thousands of units around the world, accounting for well over 90% of coal-fired capacity. PCC can be used to fire a wide variety of coals, although it is not always appropriate for coals with high ash content.

The coal is ground to a fine powder with most of the coal particles being less than 300 µm. Depending upon the moisture content, the coal might be dried before the combustion. The pulverised coal is blown with part of the combustion air into the combustion chamber (or furnace chamber) of the boiler through a series of burner nozzles. Combustion takes place at temperatures from 1300 to 1700 °C, depending on coal type and moisture content. Particle residence time in the combustion chamber is typically 2-5 seconds, and the particles must be small enough for complete burnout to have taken place during this time. At various heights in the combustion chamber, secondary and tertiary air may also be added. The walls of the combustion chamber is made up by a steel tubes, so-called water wall, to which much of the heat released by combustion (typically 50%) is transferred by radiation (see Figure 103). Inside these tubes, pressurised water flows at a saturated state and steam is being generated.

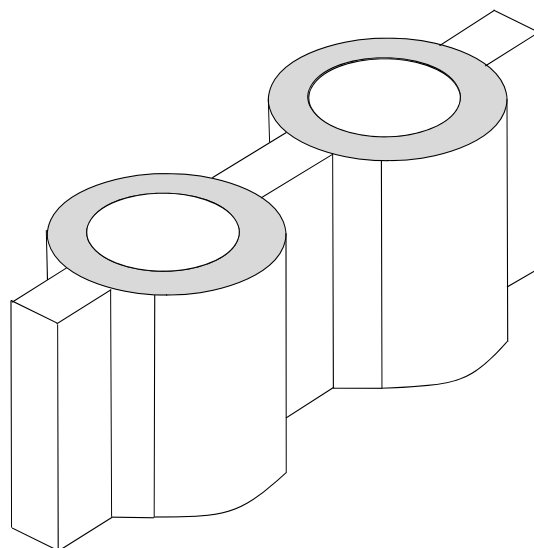


Figure 103 Section of a boiler water wall with vertical tubes welded together.??flytt denne??

Above the combustion chamber, two different boiler designs are used. One is the traditional two-pass layout where there is a combustion chamber, topped by heat transfer tube banks where heat is transferred mainly by convection from the combustion gas to water/steam flowing inside the tubes. The flue gases then turn 180°, and pass downwards through further tube banks. The other design is to use a tower boiler, where virtually all the heat transfer sections are mounted vertically above each other, over the combustion chamber.

At the exit of the boiler, the flue gas is cooled in a heat exchange with incoming combustion air. The most common type of an air preheater is the Ljungström regenerative rotating wheel (ASME, 1995). This type of heat exchanger is used in a number of plants for heat exchange between the in- and outgoing flue gas stream from a wet flue gas desulfurisation scrubber (see Chapter 6.3.2).

Most PCC boilers operate with what is called a dry bottom, meaning that there is no formation of slag. The temperatures are kept below that of ash melting. Most of the ash (60-80%) passes out with the flue gases as fine solid particles to be collected in electrostatic precipitator or fabric filters downstream the boiler (see Chapter 6.3.1). A flue gas from coal combustion has a typical particle loading of 4-5 g/m³.

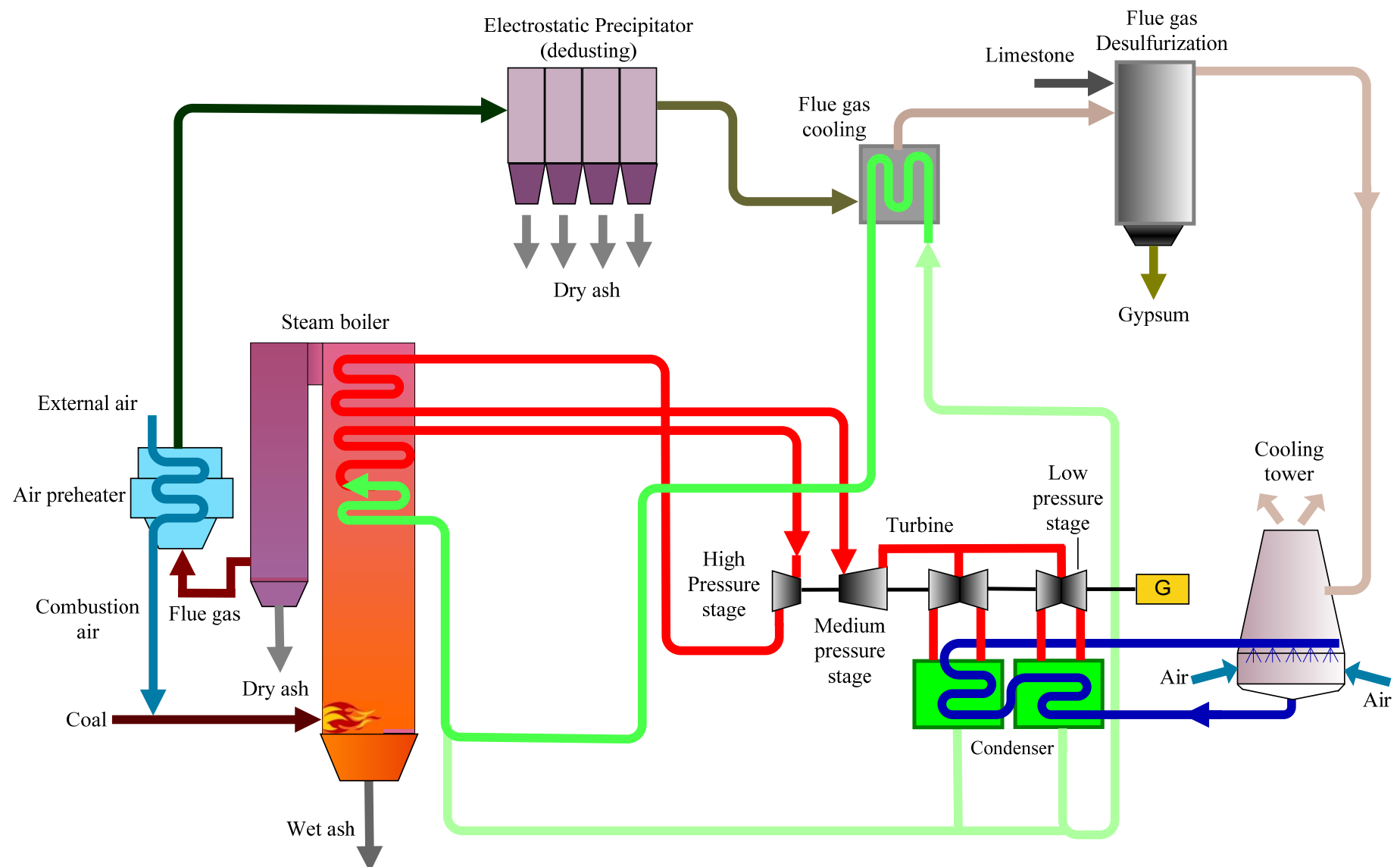


Figure 104 Coal-fired power plant with main components. The flue gas is rejected through the cooling tower.

6.1.3 Circulating Fluidised Bed Combustion (CFBC)

The key feature of the CFBC process is the recirculation of the coal particles between the furnace and the cyclone. In the following these major components will be discussed more closely. A schematic diagram of a CFBC set-up can be seen in Figure 105.

The first step in the CFBC process is the treatment and preparation of the fuel. In general, this technology operates at particle sizes of less than 25 mm. The presence of coarse particles can exhibit a negative influence on the fluidisation, resulting in combustion and heat transfer problems. Another important point is the prevention of agglomeration of solids, also known as sintering or slagging. With the merging of particles, a number of negative effects like plugging of furnace internals, adherences to the combustor walls or non-homogeneous fluidisation of the bed may take place. The prevention of corrosion needs to be carried out by removing the alkaline components. Dehydration of the fuel and the separation of non-combustible parts can also be necessary if biomass or other waste-like fuels are used.

The furnace of a CFBC unit can be divided from the bottom up into three zones. A fluidised bed zone close to the gas distributor, where the combustion takes place, a transient zone and a pneumatic transport zone. The last two ones are usually merged to the so-called freeboard zone and differ from each other by the interaction of the particles with the flow field. In the transient zone a two-directional flow of the particles takes place. In the center area the particles flow in an upward direction whereas a dense downward stream of the solid phase takes place in the near-wall region. In contrast, the pneumatic transport zone is characterised by an upward motion of the particles over the whole cross-section. The fluidisation of the fuel particles inside the riser is achieved by primary and secondary air injection. The latter one is added to the freeboard zone in order to improve the combustion efficiency by burning the unoxidised fuel particles with the additional oxygen. In general, the air flow moves at a superficial gas velocity of 3 to 10 m/s.

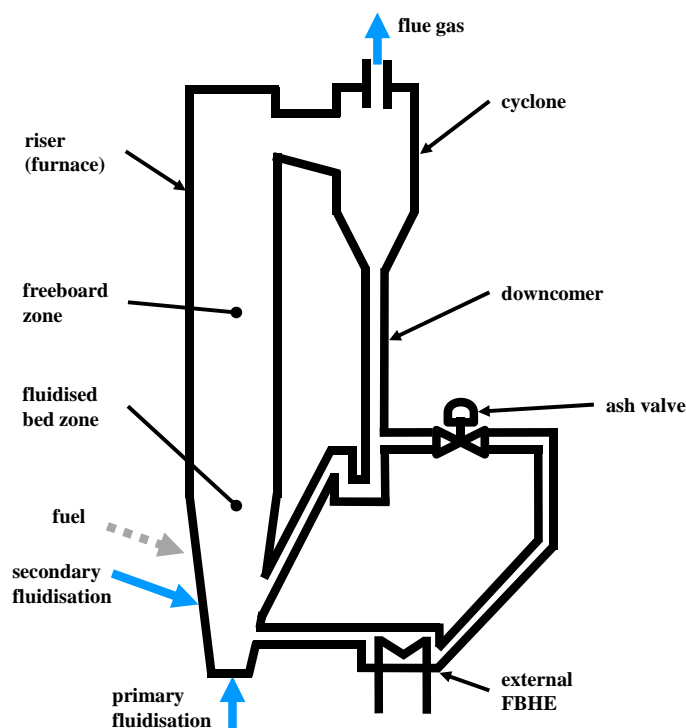


Figure 105 Key components and set-up of a CFBC process with external FBHE
(FBHE - fluidised bed heat exchanger)

Due to the intensive circulation, the concentration of the particles and the heat transfer from the solid material to the flue gas decreases gradually from top to bottom of the combustor. However, the temperature inside the furnace is distributed relatively homogenously with values between 800 and 900 °C.

In consequence of the high velocities and the small particle sizes, the concentration of solid material at the top of the combustor is also relatively high. The unburned fuel particles and other material is separated from the flue gas by a cyclone.

The solid material regained by this operation is usually fed back to the CFBC process via the downcomer. Thereby, the application of internal or external fluidised bed heat exchangers (FBHE) allow the cooling of collected particles by water or steam and in the following an anew hand-over to the furnace. The temperature of both the combustor and the FBHE unit can be adjusted by varying the solid material flow-rate. This is of particular importance in the case of fuels with low heating values as the temperature in the fluidised bed zone has to be kept at a stable level. The heat exchangers can be arranged as evaporators, re- or superheaters. The solid flow into these units is controlled by so-called ash valves. A major advantage of this configuration is the high heat transfer coefficient of the FBHE tubes. Depending on the furnace height and with it also on the actual flow pattern, the values vary between 200 W/m²K at the top and 1200 W/m²K at the bottom of the unit. Moreover, this additional correcting variable is especially useful in case of varying fuel quality as the combustion and emission performance can be controlled.

Besides for the control of the temperature, heat exchangers are used for the generation of hot water, steam or superheated steam and for the protection of furnace interiors from thermal damages. The hot flue gas leaving the cyclone is fed into superheater/reheater and economiser units to increase the steam and feed water temperature. The remaining heat of the flue gas can be used to dry the fuel or preheat of the primary and secondary air. In the fluidised bed zone two kinds of heat exchangers are located. The heat exchanger inside the particle circulation area has the purpose to control the bed temperature and to evaporate water. The one close to the primary air nozzles has only one function, to cool down the so-called bed bubble caps and thereby ensure their error free operation.

The rather large recirculation flow of solids constitutes a very much higher heat capacity compared with the gas flow through the riser. This helps to smooth any temperature gradient and short-term temperature transients in the system. Consequently, combustion conditions are relatively uniform through the riser, although the bed is somewhat denser near the bottom. There is an extensive mixing, and residence time during one pass is very short.

Steam is produced in the water wall of the riser, as well as by heat recovery of the flue gases downstream the cyclone. In some designs, heat transfer surfaces (tubes, plates) may be placed inside the riser and the downcomer.

For CFBC burning a bituminous coal, the carbon content of the bed is only around 1%, with the rest of the bed made up of ash, together with sand (if needed), and possibly lime. Overall carbon conversion efficiencies is normally over 98%.

CFBCs are designed for a particular coal to be used. CFBC is principally of value for low grade, high ash coals which are difficult to pulverise, and which may have variable combustion characteristics. It is also suitable for co-firing coal with low grade fuels, including some waste materials. The use of limestone injection into the riser is a well proven method for sulfur removal as an alternative to flue gas desulfurisation.

The low combustion temperature give much less formation of NOx compared to PCC plants. The formation of nitrous oxide (N₂O) is higher than that for PCC.

At the moment, the output power of operating fluidising bed combustion facilities ranges from 1 MWth to over 500 MWe. In general, CFBCs are used in a number of units around 250-300 MWe size. Facilities with higher output power, like the 460 MWe plant in Lagisza, Poland are mostly supercritical unit.

The thermal efficiency of CFBC units is commonly a little lower than that for an equivalent size PCC plant by 3 to 4 percentage points. In a CFBC, the heat losses from the cyclone are considerable, which results in reduced thermal efficiency. The typical use of a low grade coal with variable characteristics tends to result in lower efficiency. The addition of sorbent and subsequent removal with the ash also results in heat losses. The supercritical unit at Lagisza referred to above is expected to have a LHV-based net plant efficiency of about 43%.

There was rapid growth in the coal-fired power generation capacity using CFBCs between 1985 and 1995, but it still represents less than 2% of coal power capacity in the world. CFBC power plants represent the market for relatively small units in terms of utility requirements. They are used more extensively by industrial and commercial operators in smaller sizes, both for the production of process heat, and for on-site power supply. A few are used by independent power producers, mainly in sizes in the range of 50 to 100 MWe range.

6.1.4 Pressurised Fluidised Bed Combustion (PFBC)

PFBC – Pressurised Fluidised Bed Combustion – is a method for combustion of mainly solid fuels (may in principle be any fuel) in a bubbling (or stationary) fluidised bed under pressurised condition. The combustion air needs to be pressurised before combustion and the hot gas downstream the combustion process is expanded. The most reasonable process design with respect to efficiency is to have this type of combustion process integrated in a gas turbine cycle. The exhaust from the gas turbine has the potential for heat recovery and additional power generation, and all the plants built so far are combined gas turbine and steam turbine cycles.

The stationary fluidised bed combustor is put inside a pressure vessel, where in addition to the fluidised bed itself there are cyclones, recycle downcomer for solids separated in the cyclone, ash cooler, ash removal, coal and sorbent feed systems.

The main reasons for pressurisation is to get more compact systems, increase in heat transfer due to lower gas volume and the possibility of utilising a gas turbine. The main advantages of the PFBC technology is the ability of handling fuels in different qualities, high energy efficiency, good environmental performance and potentially moderate specific investment.

Coal is crushed to the required size of less than 5 mm and mixed with sorbent (usually limestone or dolomite) and water and fed as paste into the fluidised bed. The sorbent reacts with the sulfur dioxide (SO_2) to form calcium sulphate (CaSO_4). Coal of various qualities can be fed pneumatically as dry suspension in air via lock hoppers. Combustion takes place at a temperature of about 800-850 °C and at pressures in the range of 12-16 bar. The temperature is limited upwards by sintering and agglomeration of the ash. There are a large number of atmospheric fluidised bed combustion plants, and 850 °C is a typical combustion temperature. Boiler tubes for steam production are immersed directly in the bed of solids. Particles (ash, sorbent) in the flue gas are removed in one or more cyclones, with about 98 % efficiency. The gas is then expanded through a turbine.

The flue gas from the gas turbine has a temperature of about 400 °C and preheats feedwater going to the pressurised fluidised bed boiler. Steam is generated in the tubes immersed in the bed. The

tubes are surrounded by bed material of 850 °C and superheated steam is generated and fed to the conventional steam turbine to generate power.

Load reduction is accomplished by lowering the bed level and lowering fuel input. By lowering the bed level, less steam is produced and also the gas temperature to the gas turbine is reduced because some of the tube bundle is now above the bed level. Bed level is rapidly raised and lowered by using reinjection vessels. When a load reduction is called for, bed material is withdrawn and stored in the reinjection vessels. If load is increased, the stored bed material is reinjected back into the bed. A load change rate of 4 %/min is possible with this system. More gradual changes are accomplished by changes in coal feed and ash withdrawal rates.

After some smaller demonstration plants were built and operated, a number of PFBC plants have been built, though not in recent years. Some of these plants are still in operation.

1. Värtan, Stockholm, Sweden, power output 135 MW, start-up in 1990
2. Escatron, Endesa, Spain, 79,5 MW, 1990
3. Tidd, AEP, Ohio, USA, 73 MW, 1991
4. Wakamatsu, EPDC, Kyushu, Japan, 71 MW, 1994
5. Tomato-Atsuma, Hepco, Japan, 85 MW, 1995
6. Trebovice, Czech Republic, 70 MW, 1996
7. Karita, KyEPCO, Kyushu, Japan, 350 MW, 1999
8. Osaki, Chugoku, Japan, 250 MW, 1999
9. HKW Cottbus, KFB/SWC, Germany 71 MW, 1999

The gas turbine of a PFBC combined cycle generates about 20-23 % of the total power output and the remaining 77-80 % is generated by the steam turbine. In a natural gas-fired combined cycle, the gas and steam turbine percentages of power output are about 66/33%. The PFBC configuration is therefore unable to take full advantage of further improvements in gas turbine technology. A more severe limitation of the potential efficiency is the combustion temperature or bed temperature which cannot be increased much above 850-900 °C, depending on ash properties. The turbine inlet temperature is therefore restricted by the bed temperature. The steam condition (pressure, temperature) is decoupled from the flue gas temperature and thus the gas turbine process places no restriction on the steam temperature. It is therefore possible to take advantage of super critical steam condition in the PFBC combined cycle, though this has not been done in any plants so far. With the newer PFBC designs, an efficiency of 44-46 % (LHV) is achievable, but typical plant efficiency is about 42 % (LHV).

PFBC has less formation of NO_X compared to PCC because of the rather low and the evenly distributed temperature in the bed. The formation of nitrous oxide (N₂O) is higher than for PCC. The emission of sulfur compounds is low because of the use of a sorbent to bind the sulfur, and subsequent removal of the sulfur as part of the ash.

A number of operational problems have been reported from the relatively few PFBC plants that have been built (Jansson, 1996), (NETL, 2001), (Goto and Okutani, 2002) and (Wright, Stringer et al., 2003). The most severe problem has been deposition, corrosion and erosion in the hot section of the turbine. The gas entering the turbine during normal operation contains several hundred parts per million of very fine (less than 5 µm) solid particles. The problem has to some extent been caused by malfunctions in the cyclones. It may seem like cyclones alone cannot remove particles sufficiently, and that for example ceramic filters need to be used in combination with the cyclones. An unexpected problem with the gas turbine has been high-cycle fatigue damage (cracks) to low-pressure turbine blades caused by resonance that was created after changing the number of guide vanes ahead of the low-pressure turbine. Erosion and corrosion of the heat transfer surfaces in the fluidised bed has also been reported as a problem. In addition, there have also been some problems with the coal and sorbent pressurised feeding systems.

It does not seem like PFBC technology has reached a maturity level where it competes with PCC. In the 1990s the PFBC technology gained a lot of interest, but considerable less now.

6.1.5 Integrated Gasification Combined Cycle (IGCC)

Process design

The power block of an IGCC plant is similar to that of a natural gas fired combined cycle plant which includes a gas turbine and a steam cycle. An IGCC plant also includes the major functions necessary to produce a gaseous fuel through gasification of coal, biomass, residual oil, pet coke or others. These are feedstock preparation, gasifier, cooling and heat recovery equipment, air separation (if oxygen-blown) and gas cleanup. A simple flow diagram is shown in Figure 106.

Various types of gasifier are used. Gasifiers for coal used in IGCC are typically entrained flow slagging gasifiers which operate at around 40-70 bar and 1500 °C, well above the melting point of the ash to ensure that the molten ash (slag) has a sufficiently low viscosity to flow easily out of the gasifier. Entrained flow gasifiers use pulverised coal with typical particle diameters of 100 µm. For pressurised gasification of coal (as with PFBC), the supply of coal into the system is more complex than for PCC. Some gasifiers use bulky lock-hopper systems to inject the coal, while others have the coal fed in as water-based slurry. Sufficient oxygen (95 mole % purity) from an air separation unit (ASU) is fed to the gasifier which through partial oxidisation of the feedstock provides heat to achieve the desired operating temperature and converts the feedstock into a syngas mixture. When steam is required to ensure sufficient carbon conversion (avoid solid carbon product), this is bled from the power block's steam turbine.

The hot raw syngas exiting the gasifier needs to be cooled down for “cold” gas cleanup (including removal of slag particles and different trace elements, sulfur and if relevant CO₂ capture). A full water quench is one method of cooling the syngas, another method is to mix it with recycled syngas which has already been cooled. The latter method includes utilisation of the sensible heat in the syngas by generating steam in syngas coolers which is sent to the steam cycle for increased power generation.

The remaining gas mixture after the gas cleanup is the fuel for the gas turbine (GT). The fuel consists mainly of CO and H₂. When CO₂ is captured, the fuel consists of mainly H₂. The fuel is moisturised, preheated and diluted with nitrogen from the ASU before combustion in the gas turbine's diffusion combustor. To achieve higher plant net power output and efficiency, some of the ASU air is bled from the GT's compressor discharge. To which extent compressor discharge air bleed is used to feed the ASU can vary in the range 0-70%. A minimum 30% air compression capacity in the ASU itself ensures that it can be started independently of the gas turbines. The heat recovery steam generator (HRSG) utilises the GT exhaust heat to produce superheated steam at different pressure levels which is fed to a steam turbine.

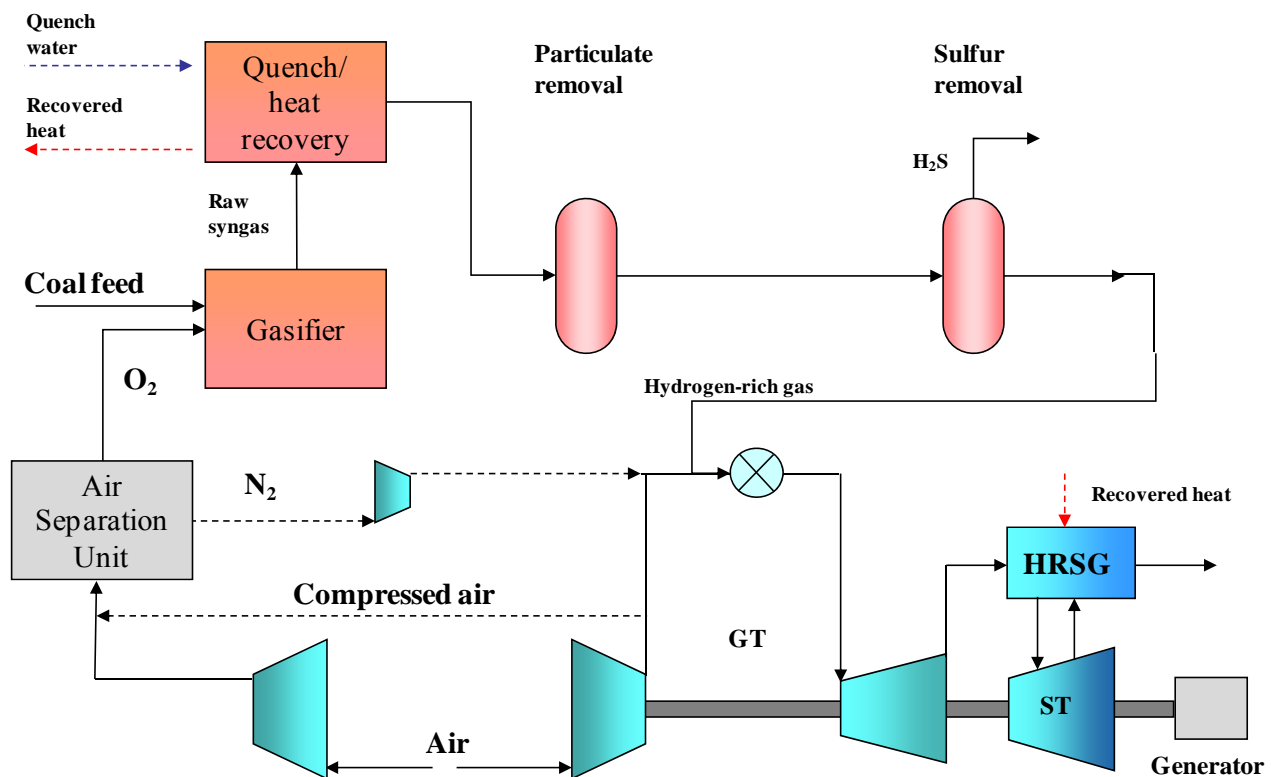


Figure 106 Integrated gasification combined cycle (IGCC) - flow diagram

As of 2007 (GTW, 2007), there are 16 IGCC plants in commercial operation using different feedstock including coal, pet coke, oil residues and biomass. Additionally, in Nakoso, Japan, a 250 MW IGCC with air-blown gasifier was started up in 2008. The total power output of these plants is more than 4000 MW. Some information about these is given in Table 6.1.

Table 6.1 Operating IGCC plants as of 2007 (GTW, 2007)

Project/location	Feedstock	Gas turbine	Gasification technology	Power MW	Start-up
Nuon, Buggenum, Netherlands	coal/biomass	Siemens SGT5-2000E (V94.2)	Shell	253	1994
Wabash River, Indiana, USA	coal	GE 7FA	ConocoPhillips E-Gas	262	1995
Tampa Electric, Florida, USA	coal/coke	GE 7F	GE	250	1996
Frontier oil, Kansas, USA	pet coke	GE 6B	GE	45	1996
SUV, Vresova Czech Republic	coal/coke	2*GE F9E	Lurgi	350	1996
Schwarze Pumpe Germany	lignite/waste	GE 6B	Sustec	40	1996
Shell refinery Pernis, Netherlands	visbreaker tar	2*GE 6B	Shell	120	1997
Elcogas, Puertollano, Spain	coal/pet coke	Siemens SGT5-4000E (V94.3)	Krupp-Uhde Prenflo	310	1998
ISAB Energy Italy	asphalt	Siemens SGT5-2000E(LC) (2*V94.2K)	GE	510	1999
Valero (Premcor) Delaware, USA	pet coke	2*GE 6FA	GE	240	2000
Sarlux/Enron Sardinia, Italy	visbreaker tar	2*GE 9E	GE	550	2000
API Energia Falconara, Italy	oil residue	Alstom KA13E2	GE	250	2001
Exxon Chemical, Singapore	ethylene tar	2*GE 6FA	GE	180	2002
Nippon Petroleum Negishi, Japan	asphalt	Mitsubishi M701F	GE	350	2004
ENI Sannazzaro Italy	oil residue	Siemens SGT5-2000E(LC) (V94.2K)	Shell	250	2006
ICCT, Yankuang, China	coal	GE 6B	OMB	72	2006
Clean Coal Power Nakoso, Japan	coal	Mitsubishi M701DA	Mitsubishi	250	2008

IGCC availability

Beginning in the mid-1990s, a number of IGCC plants were built and operated meaning a base of experience has begun to develop. These plants have confirmed the exceptionally low (SO_x , NO_x , particulate matter and, if required, mercury) and less toxic (waste water and slag) emissions from this technology. They have also confirmed the expectations of improved thermal efficiency, even if parallel advances in other coal-based technologies have not allowed this to be translated into the competitive advantage originally contemplated.

However, the reliability and availability of demonstration IGCC's has not been as high as desired by the power industry or as actually achieved by gasification plants operating in the chemical and other non-power industries. The success of IGCC in realising its potential is therefore also

depending on establishing the reasons for this reduced reliability and taking appropriate steps to improve it.

Four of the earlier IGCC units Buggenum, Polk, Puertollano and Wabash, typically show typical time-availability around 70-80%. At the same time other gasification plants show time-availability in the range 96-98% (Laege and Pontow, 2002), (Mook, 2004). Over half of the unplanned unavailability in these four IGCC plants is caused by the power island, and actually not by the fuel and combustion systems, but rather a number of mature components (Higman, DellaVilla et al., 2006). Generally in industrial applications, Air Separation Units (ASU) provide a reliability of over 99% and an overall availability of over 98%. In an IGCC the ASU contributes with slightly more to unplanned unavailability compared to other uses of ASUs. The gasification reactor itself does not contribute much to the unplanned unavailability – although the refractory lined systems do require some planned maintenance and shutdown of the IGCC plant. The syngas cooler has typically been the major source of unplanned unavailability in the gasification part of the plant.

It has been demonstrated that oil-based IGCC units in Italy reach over 90% time-availability (Jaeger, 2006). There is no fundamental reason that prevents coal-based IGCCs from reaching over 90 % time-availability in the future (Phillips, 2006).

IGCC efficiency

Several factors influence the plant efficiency:

- Coal type: Coals of high rank can be gasified more efficiently than coals of low rank. The higher moisture and ash content of low rank coals require a higher degree of oxidation (more oxygen) to achieve slagging temperatures because of the energy needed to vaporise the moisture and melt the ash.
- Gasification technology: Gasifiers with a dry feed are more efficient than gasifiers with a slurry feed because less water must be vaporised. Gasifier technologies which include syngas coolers for heat recovery of the sensible heat of the hot gas are more efficient than those with a water quench.
- Degree of ASU integration: Integration of the air separation unit with the gas turbine increases the electrical efficiency. By supplying part or all of the ASU air from the GT compressor outlet, less efficient compression in a separate compressor is reduced or avoided.
- Technology level: Gas turbine technology and turbine inlet temperature will together with the choice of steam cycle have a significant impact on electrical efficiency. It should be noted that new gas turbines are primarily made for natural gas as fuel. The ability to use syngas from a gasifier is something that typically becomes available through a modification of the original fuel supply and combustor system. This means that the most advanced gas turbine technology with respect to efficiency and low NO_x formation in the combustor is available for natural gas as fuel before it is available for syngas. The gas turbine manufacturers' philosophy differs quite a lot in this respect. Another aspect is that gas turbines with syngas as fuel operate at reduced turbine inlet temperature compared to using natural gas. This means reduced efficiency and power output.

New IGCC plants will have net plant efficiency in the range of 39-48% (LHV). The wide range is explained by the factors given above.

The higher capital costs in comparison to PCC plants and uncertainties related to availability (~80%) are the biggest challenges for IGCC. However, there are also process-related issues concerning the reliability and the little operating experience. On the technical side, the power and efficiency losses due to the reduction of the turbine inlet temperature can be considered as the major challenges.

6.2 Internal combustion engines

Internal combustion engines (ICE) exist in a large number for stationary power generation, but with a relatively speaking small power output per unit. The largest ICEs are used in large ships, like container ships and oil tankers. As of 2008, the largest internal combustion engine ever built is the Wärtsilä-Sulzer RTA96-C, a 14-cylinder, 2-stroke turbocharged diesel engine that was designed to power the Emma Maersk, the largest container ship in the world. This engine weighs 2300 tonnes, and when running at 102 RPM produces 109,000 bhp (80.1 MW) with an efficiency that in optimal operating conditions can exceed 50% (Wikipedia, 2008b). The ICEs used in power generation and in combined heat and power applications typically produce 20MW or less of power, most common is the range 1-5 MW.

CO₂ capture for ICE could be done by using hydrogen as fuel, where the hydrogen is produced in plants where CO₂ capture is integrated, or hydrogen is produced with some form of renewable energy source (Damm and Fedorov, 2006). CO₂ capture from the flue gas of ICEs can only be done in stationary plants, which means that the large fleet of ICEs used in the transportation sector rely on hydrogen as fuel.

Because of the rather small unit size of ICEs this technology is not further discussed in this book.

6.3 Flue gas cleaning technologies in power plants

In this chapter an overview of gas cleaning technologies are presented. These technologies are important for power plants in order to meet environmental performance targets, as well as to constitute significant investment and O&M costs.

6.3.1 Particle removal from flue gas

Particle removal is used for combustion solid fuels, while for natural gas there is virtually no formation of particles during combustion.

Electrostatic precipitator (ESP) is the most widely used particulate emissions control technology in coal-fired power plants. In an ESP the flue gas flow is channelled into lanes formed by the collection plates or tubes. Discharge electrodes are centred between each collection plate/tube to provide a negative charge to the surrounding particles. A pulsating DC voltage in the range of 20-100 kV is used. The collection plates/tubes are positively grounded and act as a magnet for the negatively charged dust particles. The collected dust is transported down the collection plates and electrode with the assistance of a rapper or vibrator system into the collection hoppers. An ESP can provide 99-99.9% removal efficiency⁷. Gas temperature range is 130-180 °C, and pressure drop as low as 1-2 mbar. A limitation is fly ash with high electrical resistivity resulting from burning coals with low sulfur content. It is common to condition the flue gas with elemental sulfur, ammonia and sulphur trioxide to decrease the resistivity.

A fabric filter unit consists of one or more isolated compartments containing rows of fabric bags in the form of round, flat, or shaped tubes, or pleated cartridges. Particle-laden gas passes up (usually) along the surface of the bags then radially through the fabric. Particles are retained on the upstream face of the bags, and the cleaned gas stream is vented to the atmosphere. The filter is operated cyclically, i.e. alternating between relatively long periods of filtering and short periods of cleaning.

⁷ Removal efficiency or collection efficiency is defined as the ratio of the mass of particles being removed to the mass of particles in the flue gas upstream the particle removal device

During cleaning, dust that has accumulated on the bags is removed from the fabric surface and deposited in a hopper for subsequent disposal. Fabric filters collect particles with sizes ranging from submicron to several hundred microns in diameter at efficiencies generally in excess of 99-99.9%. Gas temperatures temperature range is 120-180 °C, and pressure drop is typically in the range 10-50 mbar. Limitations are imposed by gas characteristics (temperature and corrosivity) and particle characteristics; primarily stickiness.

6.3.2 Flue gas desulfurisation (FGD)

After combustion, the sulfur of the fuel is oxidised to mainly sulfur dioxide (SO_2) and sulfur trioxide (SO_3). Flue gas desulfurisation (FGD) can be divided into the following five methods:

- 1) wet scrubbers
- 2) spray dry scrubbers
- 3) sorbent injection processes
- 4) dry scrubbers
- 5) sea water scrubbing

Wet scrubbers are the most widely used technology in the FGD market with over 80% of the installations by power plant capacity. It is followed by spray dry scrubbers and sorbent injection systems.

Wet scrubbers use calcium-, sodium- and ammonium-based sorbents in a slurry mixture with water, which is injected into the scrubber to react with the sulfur dioxide (SO_2) in the flue gas. The preferred sorbent in operating wet scrubbers is limestone followed by lime. These are favoured because of their availability and relative low cost. SO_2 is an acid gas and thus the sorbent slurries or other materials used to remove the SO_2 from the flue gases are alkaline. The reaction taking place in wet scrubbing using limestone (CaCO_3) slurry produces calcium sulfite (CaSO_3), which is oxidised to form gypsum ($\text{CaSO}_4 \cdot 2\text{H}_2\text{O}$).

For the contacting between the sorbent and the flue gas a variety of scrubber designs is used:

Spray tower: the scrubbing liquid is pumped to a high pressure and spray nozzles atomise it into the reaction chamber providing large particle contacting area between the liquid and the gas.

Plate tower: The liquid flows across a number plates where the gas is dispersed into bubbles, which provides a large liquid/gas contacting area.

Packed tower: The liquid sorbent is introduced at the top of packing through a distributor and flow downwards as a film on the packing material surface. The flue gas flow upward counter-current to the liquid.

Fluidised packed tower: This design is similar to a packed tower, except that the packing material is particles which are fluidised by the flue gas flow. The fluidisation of the packing material keeps it clean and improves the mass transfer between the flue gas and the liquid sorbent.

Wet scrubbers can achieve removal efficiencies up to 97-99%. Treatment of waste water is required in wet scrubbing systems.

Spray dry scrubbers: The sorbent usually used is lime or calcium oxide (CaO). The lime slurry, also called lime milk, is atomised by spraying it into a reactor vessel in a cloud of fine droplets. Water is evaporated by the heat of the flue gas. The residence time (typically 10 seconds) in the reactor is sufficient to allow for the sulfur dioxide (SO_2) and also other acid gases such as SO_3 and

HCl to react with the hydrated lime to form a dry mixture of calcium sulfate (CaSO_4) and calcium sulfite (CaSO_3). Waste water treatment is not required in spray dry scrubbers because the water is completely evaporated in the spray dry absorber. This process requires the use of an efficient particulate control device such as an ESP or fabric filter. The absorber construction material is usually carbon steel making the process less expensive in capital costs compared with wet scrubbers. However, the necessary use of lime in the process increases the operational costs.

Spray dry scrubbers are limited in size compared to wet scrubbers. Normally the largest plant size for the spray dry scrubbers is around 200MW. Spray dry scrubbers achieve removal efficiencies in excess of 90% and up to slightly above 95%.

Sorbent injection processes: Limestone (CaCO_3) or hydrated lime (Ca(OH)_2) is injected to react with sulfur dioxide (SO_2), either in the upper part of combustion chamber with temperatures in the range 750-1250 °C, in the economiser section of the boiler at a temperature in the range of 300-650 °C, or in the flue gas duct downstream after the air preheater where the flue gas temperature may be about 150 °C. Combinations of injection points are done in some plants.

The sulfur being captured from the flue gas ends up as either calcium sulfate (CaSO_4) and calcium sulfite (CaSO_3). This is later captured in a fabric filter or ESP together with unused sorbent and fly ash.

Dry scrubbers: Dry sorbent injection for reducing the SO_2 emission is commonly used in Circulating Fluidised Bed or Moving Bed combustion boilers. Hydrated lime (Ca(OH)_2), limestone (CaCO_3) or dolomite ($\text{CaCO}_3 \cdot \text{MgCO}_3$) are commonly used for this purpose. The sorbent is injected into the bed zone where the combustion reactions take place. The sulphur of the fuel is captured as calcium sulfate (CaSO_4), which is retained in the ash. A typical SO_2 removal efficiency is in the range of 93-97% at a Ca/S molar ratio of 1.2-1.5. This is a simple method of capturing sulphur from a fuel. However, there are two main disadvantages of this system; firstly the large quantities of sorbent required which is approximately twice that of a wet scrubber system to achieve the same SO_2 removal, and secondly the large quantities of strongly alkaline waste produced, which is generally disposed of in a landfill.

The sea water scrubbing process exploits the natural alkalinity of sea water to absorb acid gases. Sea water contains sodium (Na), magnesium bicarbonate ($\text{Mg}(\text{HCO}_3)_2$), and small quantities of calcium bicarbonate ($\text{Ca}(\text{HCO}_3)_2$). The flue gas flows through an absorption tower with a counter-current flow of seawater. During this process SO_2 is absorbed by the sea water, before passing to a water treatment plant where further sea water is added to increase the pH. Air is supplied to oxidise the absorbed SO_2 to sulphate (SO_4^{2-}) and to saturate the sea water with oxygen. The sea water is then discharged to the sea. This system is a simple and inherently reliable one with low capital and operational costs, which can remove up to 99% of SO_2 , with no disposal of waste to land. However, heavy metals and chlorides, if not removed before the SO_2 capture, are present in the water released to the sea.

6.3.3 NO_x reduction

NO_x is a term for mono-nitrogen oxides - NO and NO_2 . When NO_x reacts with volatile organic compounds, in the presence of sunlight, photochemical smog is formed. This is causing a pollution problem typically occurring in cities during warm periods. NO_x reacts to form nitric acid (HNO_3) when dissolved in atmospheric moisture. The nitric acid is a component of acid rain.

NO_x is formed in the combustion process of power plants, as well as other types of combustion processes. The three primary sources of NO_x in combustion processes are:

- thermal NO_x
- fuel NO_x
- prompt NO_x

Thermal NO_x formation, which is highly temperature dependent, is the most relevant source when combusting natural gas. **Fuel NO_x** tends to dominate during the combustion of fuels, such as coal, which have significant nitrogen content, particularly when burned in combustors designed to minimise thermal NO_x. The contribution of **prompt NO_x** is normally considered of less importance.

To minimise emissions of NO_x there are some primary measures that reduces the formation of NO_x, and there are flue gas treatment methods that can be used downstream the combustion process.

The primary measures are discussed in the following (Sloss, 1992):

Low NO_x burners: The fuel and the combustion air are mixed at each burner in order to create larger and more branched flames. Peak flame temperature is thereby reduced, and results in less NO_x formation. The larger flame structure also reduces the amount of oxygen available in the hottest part of the flame. This technology is used both in PCC and natural gas combustion plants.

Fuel staging: The technique consists of staging the combustion fuel in a number of streams, which are delivered to the combustion chamber at convenient locations. The simplest fuel staging features a sequence of fuel streams that are located along the furnace so as to set a progressive increase of the stoichiometry ratio from extremely fuel-lean (air excess ratio $\lambda >> 1$) to the nominal excess air that warrants complete combustion ($\lambda > 1$). The reactions inset by each fuel stream provide precursors and radicals that participate in the reduction of previously formed NO (Zabetta, Hupa et al., 2005).

Reburning: The combustion is divided into three zones. In the primary zone the main fuel is burned in low excess-air conditions to reduce initial NO_x formation. In the next combustion zone, the reburning zone, a secondary fuel (commonly natural gas) is injected in a reducing atmosphere ($0.7 < \lambda < 1$), where hydrocarbon radicals are formed which reacts with NO to form N₂. Hydrocarbon radicals are hydrocarbon compounds where a hydrogen atom is removed, e.g. methyl as the radical of methane. Combustion is completed in the third zone where more combustion air is added.

Flue gas recirculation: Flue gas is recirculated in order to lower the flame temperature, and thereby reduce the NO_x formation in the flame zone.

Water and steam injection: For gas turbines, a very common method for NO_x reduction is to inject water or steam into the combustion chamber. The purpose is to reduce the flame temperature. Both liquid water and steam efficiently reduces the NO_x formation. The ratio of water or steam to fuel is in range of 1.0-2.0 on mass basis. Steam injection is also commonly used for power augmentation in simple cycle gas turbines. For that purpose, more steam than for NO_x reduction is used; normally the steam to fuel ratio is in the range of 2.5-5. For simple cycle gas turbines; injection of liquid water increases power output, but reduces efficiency. Injection of steam increases both power output and efficiency. In a combined cycle plant, injection of water or steam reduces the plant efficiency.

In addition to or as an alternative to primary measures related to the combustion itself, the NO_x reduction can be done by flue gas treatment methods. The two most commonly used in commercial plants today, are in the following explained:

Selective Non-Catalytic Reduction (SNCR): A reagent, as ammonia or urea ($\text{CO}(\text{NH}_2)_2$), is injected into the flue gas in the boiler within an appropriate temperature window that is 900–1100 °C. Emissions of NO_x can typically be reduced by 30% to 50%. The NO_x and reagent react to form nitrogen and water. If the temperature of the flue gas is too low or if the distribution of the reagent is uneven or excessive, slip of ammonia may be a problem. Formation of ammonium bisulfate (NH_4HSO_4) and nitrous oxide (N_2O) may under certain conditions be a problem if sulfur trioxide (SO_3) is present in the flue gas. The SNCR reagent storage and handling systems are similar to those for SCR systems. However, because of higher stoichiometric ratios, both ammonia and urea SNCR processes require three or four times as much reagent as SCR systems to achieve similar NO_x reductions. SNCR is used commercially on coal-, oil- and gas-fired boilers. This technology is not used in gas turbines.

Selective Catalytic Reduction (SCR): In SCR systems NO and NO_2 is converted into N_2 and H_2O by injection of vaporised ammonia (NH_3) or urea being converted to ammonia, into the flue gas upstream the SCR. The reduction of NO and NO_2 takes place in the presence of a catalyst. Commercial catalysts usually have an active phase of vanadium pentoxide (V_2O_5) and certain metal (as tungsten or molybdenum) oxides as promoters on a titanium dioxide carrier. SCRs operate within the temperature range 200–450 °C, but the most typical operating temperature is about 350 °C. The main reactions are:



NO is the dominant nitrogen oxide in flue gases (approximately 90%), and therefore the first reaction is the most important. In the catalyst, sulfur dioxide, SO_2 , may partly be oxidised into sulfur trioxide, SO_3 . At low temperatures, SO_3 reacts with ammonia to form ammonium sulfates. During operation deactivation mechanisms as sintering, poisoning and pore blockage result in lower reduction rate and the catalysts have to be replaced. Ammonia slip is a potential problem, as for SNCR.

6.3.4 Mercury control

The predominant forms of mercury (Hg) in coal-fired flue gas are elemental mercury and oxidized to HgCl_2 . The fraction of oxidized mercury in the stack effluent of a particular power plant depends on the coal type, combustion efficiency, and the pollution control equipment used. Essentially all of the mercury entering the furnace with the coal is vaporized and exists in the elemental form until the flue gas is cooled below about 540 °C (Gale, Lani et al., 2008). In oxidized form mercury can be captured by the existing air pollution control system, like ESP and FGD. It appears that on average 50% of the mercury is removed in the ESP (particulate control) and 50% of the remainder is removed in the flue gas desulfurisation (FGD), resulting in a total mercury removal of 75%. If a high dust selective catalytic reduction (SCR for NO_x reduction) is present, the total removal can be up to 90% (Meij and Winkel, 2006). Injection of activated carbon particles and injection chlorine can improve the mercury capture. Carbon filter beds can also be used.

The mercury content of coal can be reduced prior to combustion by reducing the ash components, which contains trace minerals including mercury.

7 Steam cycle cooling systems

There are a number of cooling technologies that are being used in power cycles, in a number of other industrial applications as well for air-conditioning systems in buildings. The purpose of the cooling system is to reject the heat of condensation of the steam coming from the steam turbine of the power plant. For power cycles with CO₂ capture, there are additional cooling requirements. Basically, four principles are being used in power plants. These are illustrated in Figure 7.1. The choice between these depends very much on the heat sink. The main decisive characteristics of the heat sink are the temperature, how much heat can be rejected and environmental limitations. When designing a power plant with a condensing steam turbine, a goal is to use the optimal condenser pressure. The lower the condensation pressure is the higher is the steam turbine power output. On the other hand, a low condenser pressure causes larger dimensions and cost of the steam turbine and condenser.

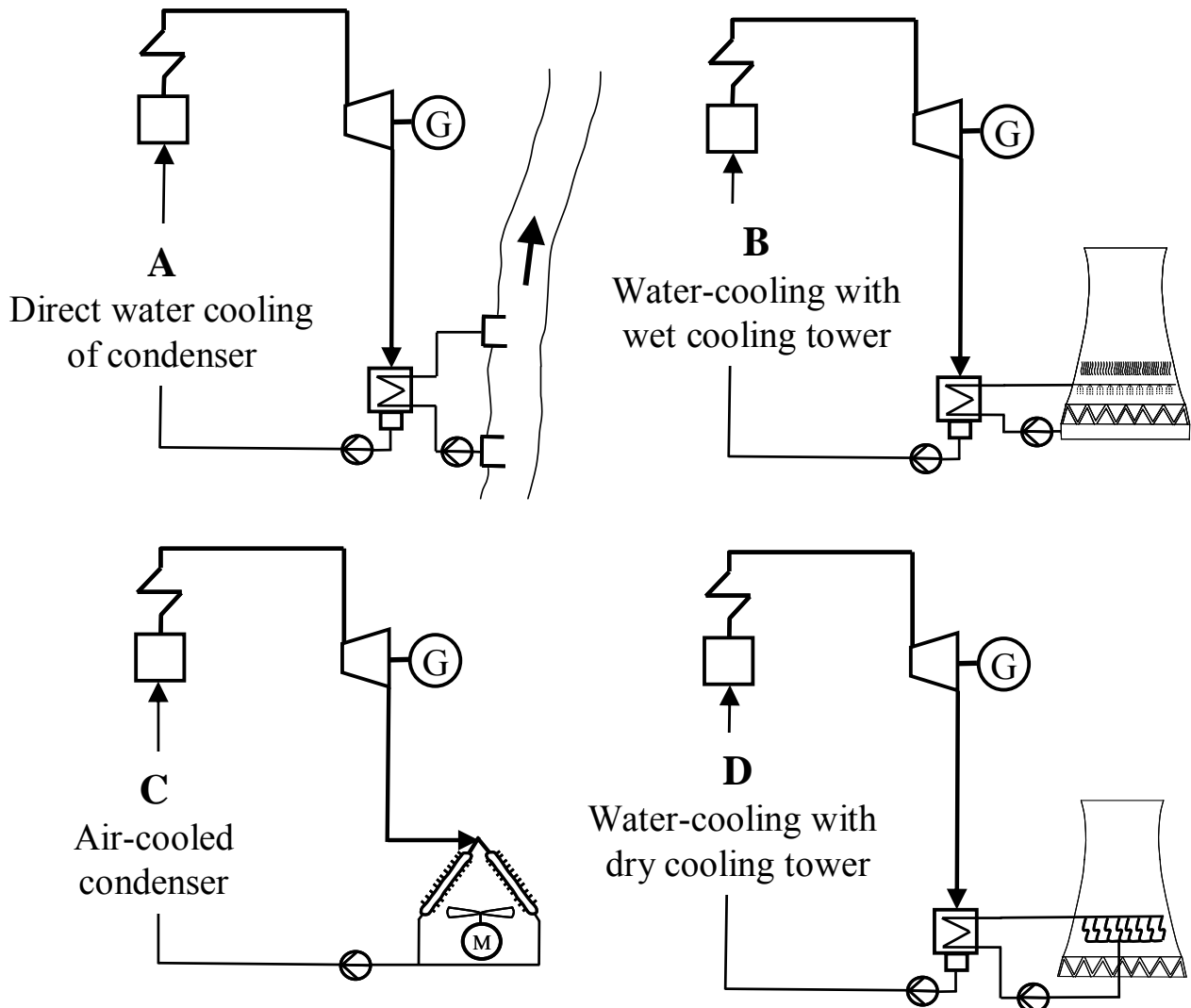


Figure 7.1 Four steam cycle cooling systems

A - Direct water cooling of the condenser:

This is normally the first choice for cooling system of a power plant. It enables the lowest possible condenser pressures. The power plant needs to be located near the ocean, a river or cooling pond. Cooling water from the ocean is typically taken up from 50-80m depth. When taking cooling water from a river, there is most often a restriction on how much heat can be rejected into the river. The typical increase of the cooling water temperature through the condenser is 10K. The condenser is a large heat exchanger with cooling water flowing inside a large number of horizontal tubes, and condensing steam on the outside of these tubes. The minimum temperature difference in the condenser is most often in the range 3-5K. This method of cooling is normally the most economical. However, there are some cases with small plants where air cooling (see below) is competitive.

B - Water cooling with wet cooling tower:

In cases where a large amount of cooling water is not available, it is common to use a wet cooling tower. In this case the steam turbine condenser is the same as described above, but the cooling water is being cooled in a separate process in a cooling tower. The temperature reduction is obtained by evaporative cooling of water droplets in an unsaturated air stream. The water droplets are cooled because the evaporation at the droplets' surface is taking place at the wet bulb temperature of the air. As long as the relative humidity of the air is less than 100%, the water droplets are cooled below the dry bulb temperature of the air. The lower limit for the cooling of the water is the wet bulb temperature of the incoming air. Most cooling tower designs are with a counter-current flow of air and water. Air is flowing into the cooling tower close to the bottom of it, and then with an upward flow. The air flow is either by natural draught or induced draught. A cooling water loop is used to bring the heat from the condenser to the cooling tower. An example of a wet natural draught cooling tower is given in Figure 7.2. Evaporation losses are about 1% by mass of the circulation rate for every 5 °C of cooling. A smaller fraction of the water is lost because of entrainment of the air, typically around 0.25% of the circulation rate. The entrainment loss depends on whether a demister is used. A blowdown of the water is needed to prevent salt and chemical treatment build-up. Make-up water has to be added continuously to a wet cooling tower.

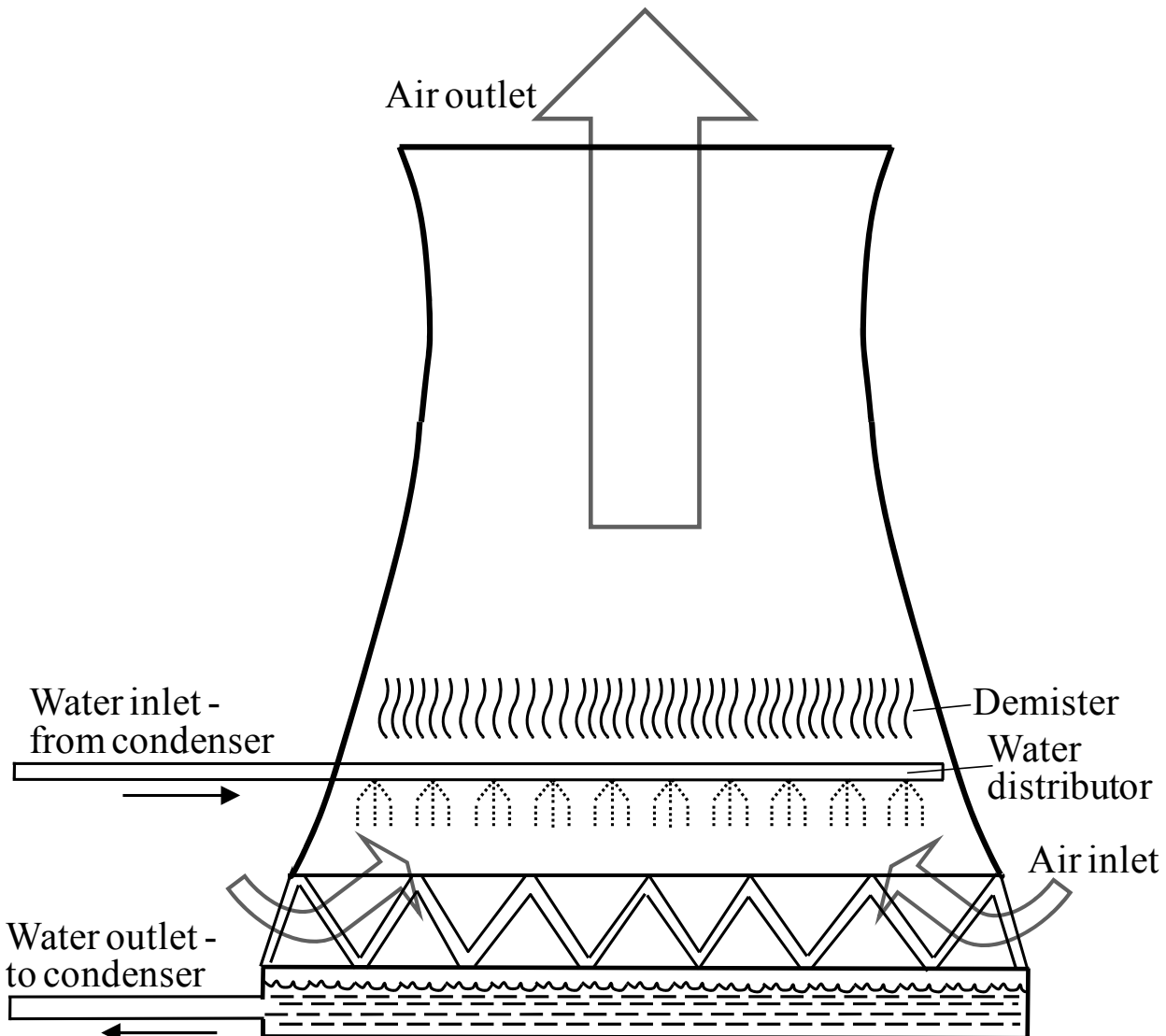


Figure 7.2 Large cooling tower. The height may be up 160m.

C - Air-cooled condenser:

In cases where cooling water is not available or is too expensive, air cooling is used. Air-coolers are typically built up by plate fin heat exchangers. On the air-side the heat transfer coefficient is much lower than on the condensing steam side. This is compensated to some extent by a large heat transfer surface on the air-side as well as forced flow of air. In a power plant with air cooling, a large number of air fans are used, which constitute significant power consumption. The temperature at which the steam is condensed is limited by the dry bulb temperature of the air.

D - Water-cooling with dry cooling tower

Air cooling can be applied in a dry cooling tower. This type of system is applied when there is no availability of water and where power is expensive. A closed loop of cooling water is circulating between the steam condenser and the cooling tower. The cooling tower may have natural draught air flow, or it may be assisted by fans at the tower air inlet.

In the following a brief guideline for the determination of steam condensing pressure is given. A TQ-diagram is shown in Figure 7.3. The cooling water temperature increase through a condenser is typically in the range 10-15K. A minimum temperature difference of 3-5K is normally used. Based on these temperature differences and the cooling water inlet temperature, the temperature at which the steam condenses can be determined. An example is given in Table 7.1. In Figure 7.4 typical intervals for steam condenser pressures are given for the cooling methods presented in Figure 7.1.

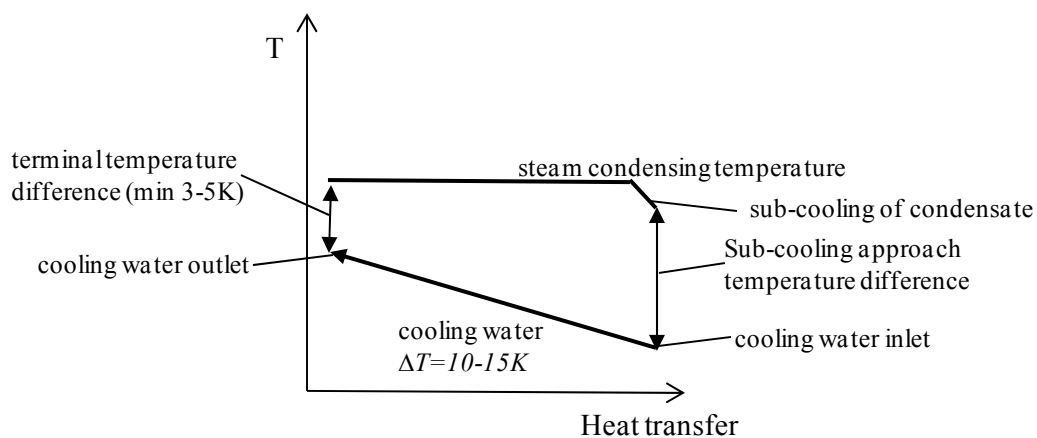


Figure 7.3 *TQ*-diagram of a water-cooled steam condenser.

Table 7.1 Determination of steam condenser pressure based on the assumption of 15 °C cooling water inlet temperature, cooling water temperature increase of 10K, and a minimum temperature difference of 4K. The condensing pressure is found as the saturation pressure for 29 °C.

Cooling water inlet temperature	15 °C
Cooling water temperature increase	10 K
Cooling water exit temperature	25 °C
Temperature difference, "approach"	4 K
Steam condensing temperature	29 °C
Steam pressure, saturation pressure for steam condensing temperature	0.04 bar

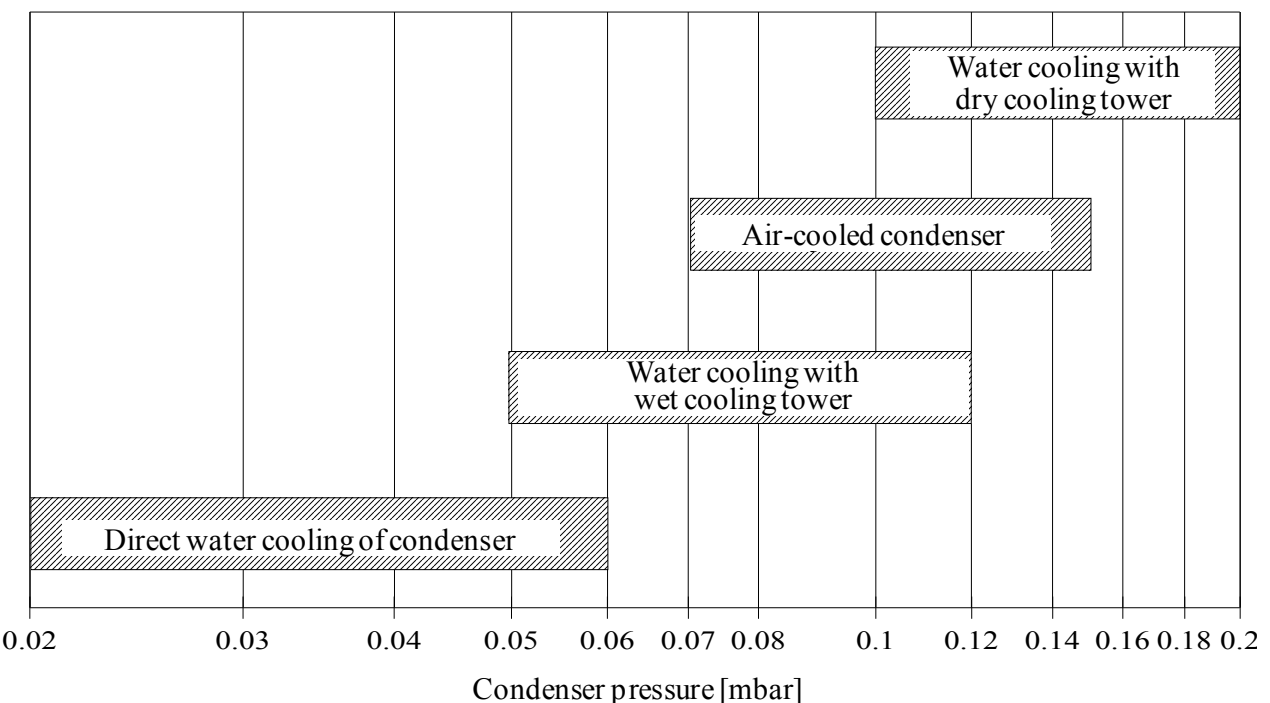


Figure 7.4 Typical intervals for steam condensing pressure for the four methods of cooling presented above.

I Figure 7.5 er det vist hvordan virkningsgrad og ytelse påvirkes av kondensatortrykk for de fire mest vanlige kjølemetoder. Direkte vannkjølt kondensator gir både høyest effekt og virkningsgrad. I og med at valg av kjølemetode for et kombinert gassturbin-/dampturbinanlegg kun innvirker på dampturbinprosessen, vil det være en proporsjonalitet mellom endring i virkningsgrad og ytelse. Det er liten forskjell mellom vannkjøling med vått kjøletårn og luftkjølt kondensator med hensyn til virkningsgrad og ytelse, mens vannkjøling med tørt kjøletårn kommer klart dårligst ut. Det er i Figure 7.5 også vist hvordan en endring i luft- og kjølevannstemperaturen fra 8 til 20 °C innvirker på et anlegg med vått kjøletårn. Virkningsgraden påvirkes nesten ikke, mens ytelsen går betydelig ned. Nedgangen i ytelse skyldes hovedsakelig at gassturbinens ytelse reduseres ved høyere lufttemperatur.

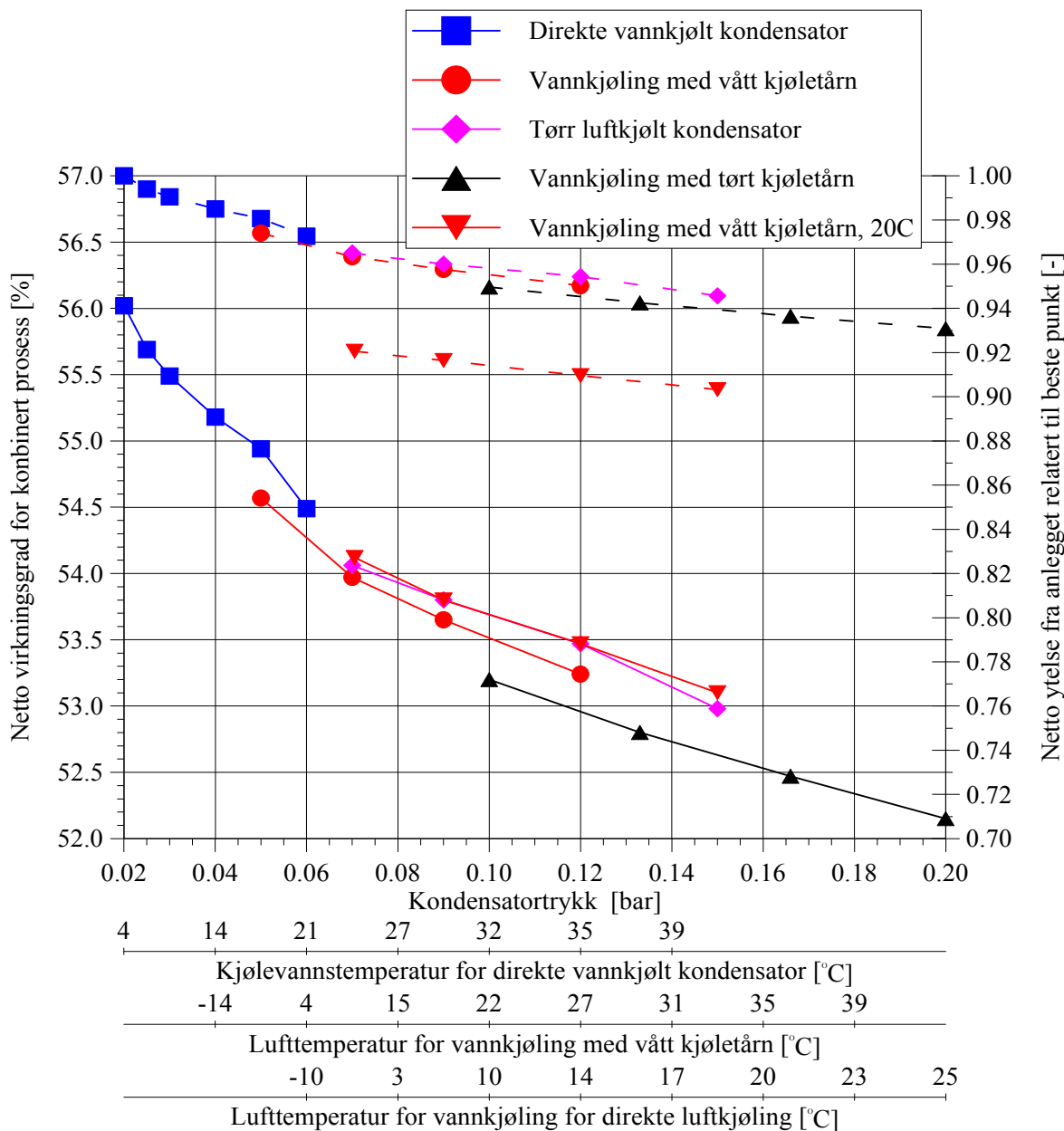


Figure 7.5 Virkningsgrad og relativ ytelse for et kombinert gassturbin-/dampturbinanlegg som funksjon av kondensatortrykk, for de forskjellige kjølemetoder. Nederste kurveskare (heltrukne linjer) er for virkningsgrad (venstre akse) og øverste kurveskare (stippled linjer) er for relativ ytelse (høyre akse). Både luft- og kjølevannstemperatur benyttet i beregningene er 8 °C. Luftfuktighet er 60% RH. Det er også vist for et anlegg med vått kjøletårn hvordan anlegget påvirkes ved å endre de nevnte temperaturer til 20 °C. Beregningene er utført med GTPROT™. Helt nederst er det gitt typiske sammenhenger mellom kjølevanns-/lufttemperatur og kondensatortrykk (Kehlhofer, 1991).

8 Efficiency calculation

8.1 Mechanical efficiency

Mechanical efficiency: $\eta_m = 99.6\%$

8.2 Generator efficiency

Generator efficiency: $\eta_g = 98.5\%$

8.3 Auxiliary power

Natural gas fired: $\eta_{aux} = 98.5\%$ of net plant output

Coal fired:

CFB Petcoke $\eta_{aux} = 92.5\%$ of plant output

PF Hard coal $\eta_{aux} = 94.5\%$ of plant output (steam-driven main boiler feed pump)

PF Lignite $\eta_{aux} = 92\%$ of plant output

8.4 Efficiency calculation

The efficiency shall be calculated according to the following formula:

$$\eta_{net,PI} = \frac{[(W_T + W_C)\eta_m \eta_g + W_{ST} \eta_m \eta_g + \sum W_{p,i}] \eta_{aux}}{\dot{m}_f LHV} \quad (66)$$

$\eta_{net,PI}$	net efficiency for Power Island	-
\dot{m}_f	fuel flow rate	kg/s
LHV	lower heating value	kJ/kg
W_T	turbine work, calculated as fluid enthalpy change	kW (>0)
W_C	compressor work, calculated as fluid enthalpy change	kW (<0)
η_m	mechanical efficiency	-
η_g	generator efficiency	-
W_{ST}	steam turbine work, calculated as fluid enthalpy change	kW (>0)
W_P	pump work, feedwater pumps, cooling water pumps, etc.	kW (<0)
η_{aux}	auxiliary power efficiency (power island only!)	-

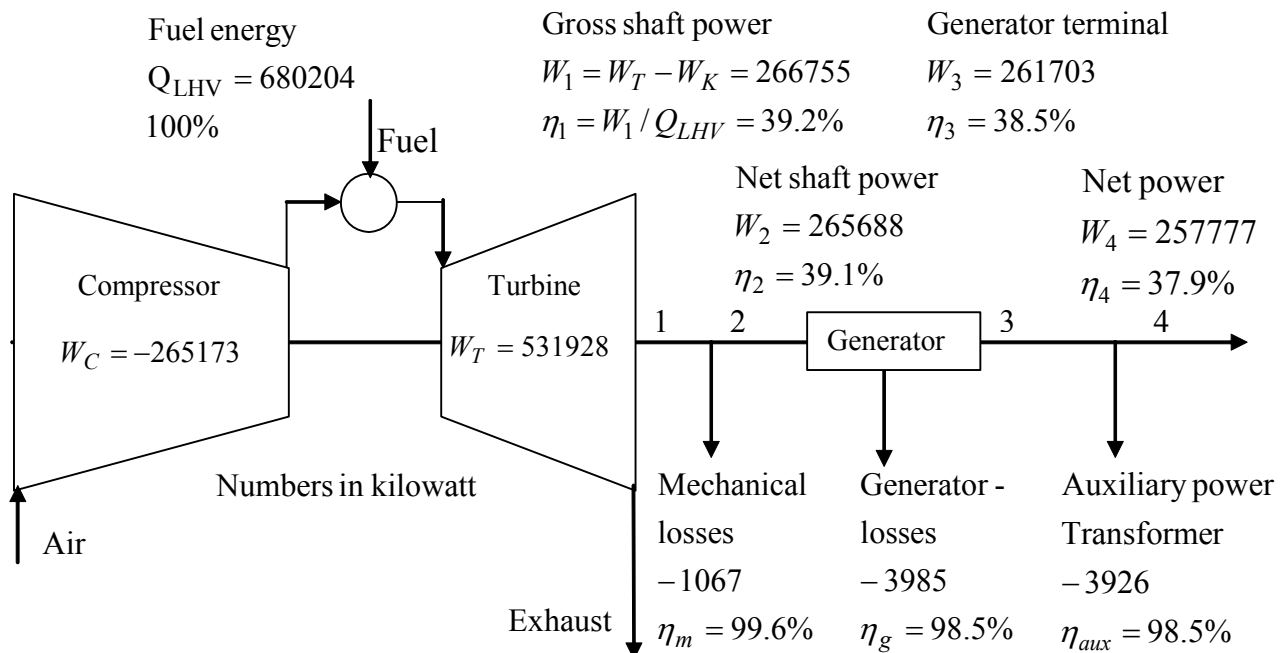


Figure 6 Example of “net plant efficiency” calculation for a gas turbine

8.5 Fans and blowers

Electrical motor and mechanical efficiency = 93%
Isentropic efficiency = 80%

9 Simulering av dampprosess

9.1 Design vs. simulering

Det er viktig å kunne skille mellom *simulering* og *design*. Med simulering forstår å kunne beregne utgangen fra en komponent når inngang og komponent-parametere er gitt. Design består i å beregne komponent-parametere når inngang og utgang er spesifisert. Ved betrakting av en bestemt komponent med inngang \underline{X} , komponent-parametere \underline{U} og utgang \underline{Y} (se Figure 7) kan en sette opp følgende:

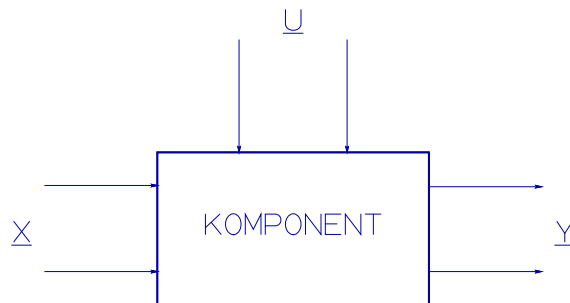


Figure 7 Innganger, utganger og parametere for en komponent

\underline{X} = inngangsvektor

\underline{Y} = utgangsvektor

\underline{U} = parametervektor

simulering : Gitt $f(\underline{X}), f(\underline{U})$ beregn $f(\underline{Y})$

design : Gitt $f(\underline{X}), f(\underline{Y})$ beregn $f(\underline{U})$

Ved spesifikasjon av \underline{X} og \underline{Y} ved design kan disse vektorene være uavhengige av hverandre, eller de kan relateres til hverandre ved for eksempel at en temperaturdifferanse angis i stedet for temperatur for en varmeveksler, eller at trykkforhold angis i stedet for trykk for en kompressor. Vektorene \underline{X} og \underline{Y} kan inneholde størrelser (for hver inngående og utgående prosesstrøm) som trykk, temperatur, indre energi, entalpi, hastighet, mengde og sammensetning av prosessmediet (for eksempel molfraksjoner). \underline{Y} kan i tillegg inneholde størrelser som varmeovergangstall, masseovergangstall og virkningsgrader. Innholdet i vektoren \underline{U} er avhengig av type komponent og ikke minst detaljeringsgrad i analysen; for en varmeveksler kan \underline{U} inneholde størrelsen varmeoverførende areal ved en enkel analyse og ved en mer detaljert analyse geometri-data som for eksempel antall rør og finner pr. rør.

De fleste prosess-simulatorer utfører *stasjonære (steady-state)* beregninger, det vil si at tilstandsvariablene endringer over tid ikke ivaretas. De fleste store selskaper med en portefølje av prosessanlegg, benytter denne type beregningsverktøy. Eksempler på programmer er PRO/II, HYSIS og ASPEN PLUS.

Ikke-stasjonære (eller dynamiske) simulatorer ivaretar tilstands-variablene endring med hensyn til tid. En stasjonær simulator kan beregne bestemte driftspunkter som vil forekomme innenfor et tidsintervall, men for å analysere prosessens oppførsel fra et driftspunkt til et annet (eller: fra et tidspunkt til et annet) må en dynamisk simulator anvendes. Stasjonær simulering er et spesialtilfelle av det dynamiske (*transiente*) forløp som en prosess alltid gjennomgår. Dynamiske simulatorer er viktige ved analyser av oppstartingsforløp og nedkjøring av en prosess. Dynamiske simulatorer er godt egnet for sikkerhetsmessige analyser ved plutselige endringer i prosessen (for eksempel et

rørbrudd). Eksempel på et slikt verktøy er gPROMS (PSE Ltd.).

En kan skille mellom to anvendelser og derigjennom også to forskjellige detaljnivåer for modelleringen:

Operatøroplæring: De fleste dynamiske simulatorer er laget for treningsformål. Modellene som benyttes er ofte veldig forenklet med tanke på fysiske prinsipper og lover, men reflekterer dog rimelig godt virkeligheten gjennom et fornuftig valg av tidskonstanter ("godt nok"-prinsippet).

Tekniske analyser av driftssituasjoner: Oppstart- og nedkjøringsforløp av prosesser simuleres. Videre så benyttes slike analyser for å se hva som skjer ved utfall av utstyr eller oppreten av feil i komponenters virkemåte. Eksempler kan være tap av kjølevann i en kjernekraftverk, rørbrudd eller oppstart av kompressorer. Gode resultater fordrer omfattende modeller, og en ser at slike beregninger på større systemer ofte utføres av spesialiserte selskaper.

Ikke-stasjonære beregninger benyttes typisk (bør i allfall) i slutten av en designfase, hvor resultatene kan føre til redesign av deler av prosessen. Slike verktøy benyttes ofte for å forklare uønskede driftsegenskaper.

Dynamisk prosess-simulering er ansett som vanskeligere enn stasjonær simulering både med hensyn til modellering av komponenter, mengde av inndata og løsningsprosedyre. I det følgende vil kun stasjonær simulering bli behandlet. De fleste av de teknikker som vil behandles i det følgende er generelle og kan også brukes i design-beregninger.

9.2 Simulering av motstrøms varmeveksler

For en generell varmeveksler, se Figure 8, en sette opp følgende tre ligninger for å beskrive varmeovergang og entalpiendringer i kald og varm strøm.

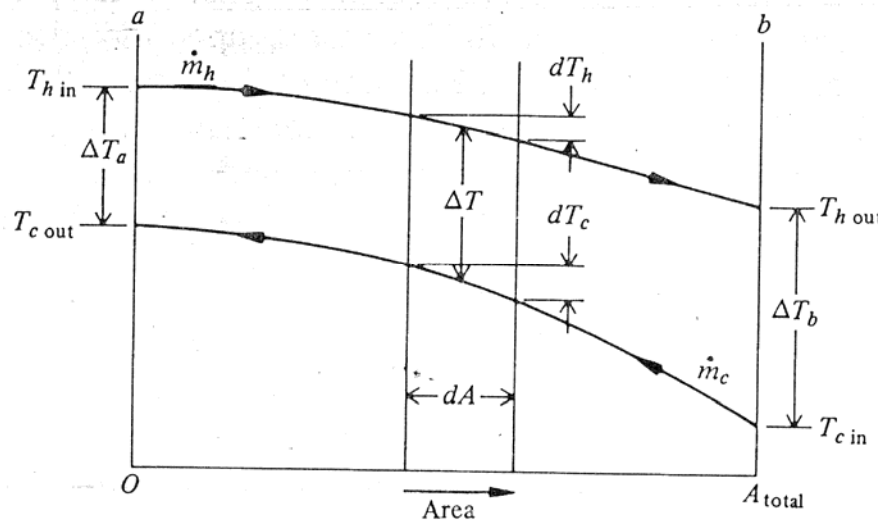


Figure 8 Temperaturprofiler i motstrøms varmeveksler

Differensiell ligningssystem:

$$\begin{aligned}
 dQ &= (T_h - T_c) U \, dA \\
 &= -\dot{m}_h C_p h \, dT_h \\
 &= -\dot{m}_c C_p c \, dT_c
 \end{aligned} \tag{67}$$

Fra varmelæren husker vi at dette ligningssystemet ble brukt til å utlede formelen for gjennomsnittelig temperaturdifferanse (LMTD). For simuleringsformål ønsker vi isteden eksplisitte uttrykk for utløpstemperaturene. Det kan vises at differensialligningssystemet leder fram til følgende uttrykk for utløpstemperaturene:

$$\begin{bmatrix} T_{c,ut} \\ T_{h,ut} \end{bmatrix} = \begin{bmatrix} \frac{1-\beta}{\gamma-\beta} & \frac{\gamma-1}{\gamma-\beta} \\ \beta \frac{\gamma-1}{\gamma-\beta} & \gamma \frac{(1-\beta)}{\gamma-\beta} \end{bmatrix} \begin{bmatrix} T_{c,inn} \\ T_{h,inn} \end{bmatrix} \quad (68)$$

hvor β og γ er definert ved

$$\beta = \frac{\dot{m}_c C p_c}{\dot{m}_h C p_h} ; \quad \gamma = e^{UA \left(\frac{1}{\dot{m}_c C p_c} - \frac{1}{\dot{m}_h C p_h} \right)} \quad (69)$$

For ulineære problemer (Cp eller U varierer) kan man dele heteflaten i flere segmenter, og anvende Eq. (68) på hvert segment. Man kan også utlede tilsvarende formler for fordamper, kondensator og medstrøms varmeveksler.

Fordamper:

$$T_{h,ut} = \gamma T_{h,inn} + (1-\gamma) T_{evap} \quad (70)$$

$$\gamma = e^{\frac{-UA}{\dot{m}_h C p_h}} \quad (71)$$

Kondensator:

$$T_{c,ut} = \gamma T_{c,inn} + (1-\gamma) T_{kond} \quad (72)$$

$$\gamma = e^{\frac{-UA}{\dot{m}_c C p_c}} \quad (73)$$

Medstrøms varmeveksler:

$$\begin{bmatrix} T_{1,ut} \\ T_{2,ut} \end{bmatrix} = \begin{bmatrix} \frac{\gamma+\beta}{1+\beta} & \frac{1-\gamma}{1+\beta} \\ \frac{\beta(1-\gamma)}{1+\beta} & \frac{1+\beta\gamma}{1+\beta} \end{bmatrix} \begin{bmatrix} T_{1,inn} \\ T_{2,inn} \end{bmatrix} \quad (74)$$

hvor β og γ er definert ved

$$\beta = \frac{\dot{m}_1 C p_1}{\dot{m}_2 C p_2} ; \quad \gamma = e^{-UA \left(\frac{1}{\dot{m}_1 C p_1} + \frac{1}{\dot{m}_2 C p_2} \right)} \quad (75)$$

9.3 Beregning av varmeovergangstall

Varmeovergangstallene kan beregnes med følgende ligning:

$$U = \frac{1}{\frac{1}{h_g} + \frac{d_y}{2\lambda} \ln \frac{d_y}{d_i} + \frac{d_y}{d_i \cdot h_d}} \quad (76)$$

Filmkoeffisientene h_g og h_d må da beregnes f.eks. ved bruk av Nusselt-korrelasjoner. Disse kan ofte være unøyaktige, så ofte velger man isteden å korrellere det totale varmeovergangstallet mot den verdien man har i designpunktet (U_0). Som vi skal se senere kan man på denne måten eliminere usikkreheten i multiplikasjonsfaktoren i Nusselt-relasjonen, og varmeovergangstallet vil stemme bedre jo nærmere designpunktet man er. Vi kan da sette:

$$\frac{U}{U_0} = \frac{\frac{1}{h_{g,0}} + \frac{d_y}{d_i h_{d,0}}}{\frac{1}{h_g} + \frac{d_y}{d_i h_d}} \quad (77)$$

I fordampere og economisere er det slik at det ytre varmeovergangstallet (h_g) er 10 til 100 ganger mindre enn varmeovergangstallet på dampsiden (h_d). I tillegg vil begge verdier alltid variere på samme måte (++,--). Derfor kan følgende tilnærmelse gjelde i disse komponentene:

$$\frac{U}{U_0} = \frac{h_g}{h_{g,0}} \quad (78)$$

Verdien på h_g kan så beregnes ved å bruke en Nusselt-korrelasjon:

$$Nu = C \text{ Re}^m \text{ Pr}^n = \frac{h_g d_y}{\lambda_g} \quad (79)$$

Her er C , m og n konstanter som hovedsaklig avhenger av geometrien.

Reynoldstallet Re kan skrives:

$$Re = \frac{\dot{m}_g d_y}{\mu_g S} \quad (80)$$

Hvor S er tverrsnittsarealet for gasstrømmen. Følgende uttrykk fås ved å relatere varmeovergangstall mellom to forskjellige driftstilstander:

$$\frac{U}{U_0} = \frac{C \left[\frac{\dot{m}_g d_y}{\mu_g S} \right]^m \text{ Pr}^n \lambda_g d_y}{C \left[\frac{\dot{m}_{g,0} d_y}{\mu_{g,0} S} \right]^m \text{ Pr}_{0,0}^n \lambda_{g,0} d_y} \quad (81)$$

De geometriske konstantene forsvinner, og de fysikalske egenskapene for røykgassen som Pr , λ og μ kan med relativt god nøyaktighet antas konstant. Dermed ender vi opp med følgende enkle relasjon for det totale varmeovergangstallet:

$$\frac{U}{U_0} = \left[\frac{\dot{m}_g}{\dot{m}_{g,0}} \right]^m \quad (82)$$

Verdien på m er 0.56 – 0.58 for forsatte (staggered) rør, og 0.59 – 0.65 for flukterende (in-line) rør.

9.4 Simulering av dampturbiner

For å finne dampmengden gjennom turbinen benyttes ofte en ligning som kalles kjeglesetningen:

$$\frac{\dot{m}}{\dot{m}_0} = \frac{P_\alpha}{P_{\alpha,0}} \sqrt{\frac{P_{\alpha,0} v_{\alpha,0}}{P_\alpha v_\alpha}} \sqrt{\frac{1 - \left[\frac{P_\omega}{P_\alpha} \right]^{\frac{n+1}{n}}}{1 - \left[\frac{P_{\omega,0}}{P_{\alpha,0}} \right]^{\frac{n+1}{n}}}} \quad (83)$$

Hvor:

\dot{m} = massestrøm

P = trykk

v = spesifikt volum

α = innløp

ω = utløp

0 = referansestilstand

n = polytropisk ekspansjonsekspont

$(n+1)/n$ har hovedsaklig størrelsesorden 2. For turbiner med høyt trykkforhold vil det siste rotutrykket være svært nærl, og det kan neglisjeres. Vi står da igjen med samme ligning som for ventil med kritisk strømning (choked nozzle):

$$\frac{\dot{m}}{\dot{m}_0} = \sqrt{\frac{p_\alpha \rho_\alpha}{p_{\alpha,0} \rho_{\alpha,0}}} ; \frac{p_\alpha}{p_{\alpha,0}} = \left[\frac{\dot{m}}{\dot{m}_0} \right]^2 \frac{\rho_{\alpha,0}}{\rho_\alpha} \quad (84)$$

Ved dellast viser det seg at volumstrømmen i damp-turbinen holder seg nogenlunde konstant. Dette betyr at hastighetsprofilene ikke forandrer seg nevneverdig og at virkningsgraden for turbinen ikke forandres noe særlig.

9.5 Simuleringseksempel

Se øving 6 i Tema TEP9

http://www.ept.ntnu.no/fag/tep9/innhold/oving_tep9.pdf

10 Typical computational assumption for steam cycles

For those who want to make heat and mass balance calculations for steam cycles, this section provides guidelines on assumptions of data. The data are for large (>300 MW), high-efficiency plants.

10.1 Coal & natural gas fired boilers

One pressure level, single reheat, 250 bar, 560 °C/560 °C.

Boiler efficiency: η_{boiler} = maximum 95% for Hard Coal Boiler

Pressure losses:

- $\Delta p_{cold} = 3\%$ for each heat exchanger
- $\Delta p_{reheat, cold, tot} = 10\%$
- $\Delta p^{“steam pipe + valve”} = 7\%$

Temperature losses:

- from superheater/reheater to turbine = 2 K

Temperature differences:

- $\Delta T_{steam/gas} = 25\text{ K}$
- $\Delta T_{gas/liquid} = 10\text{ K}$
- $\Delta T_{approach, ECO} = 5\text{ K}$

Natural circulation is assumed.

Blowdown = 0 %

Preheating of combustion air: Primary air up to 300 °C / Secondary air up to 350 °C

Excess air: 15 - 18%

10.2 HRSG

Triple pressure, single reheat, 125 bar/30 bar/4.5 bar, 560 °C/ 560 °C.

Reheat: mix superheated IP steam with cold reheat steam before reheat.

$\eta_{HRSG} = 99.7\%$ (heat losses)

Pressure losses:

- $\Delta p_{HRSG, hot} = 4\text{ kPa}$
- $\Delta p_{cold} = 3\%$ for each heat exchanger
- $\Delta p_{reheat, cold, tot} = 10\%$
- $\Delta p^{“steam pipe+valve”} =$
 - HP 7 %
 - IP 9 % (when steam flows directly to IP turbine)
 - IP 9 % for Reheat/IP-steam mixing (assuming pressure loss of 2% from HP turbine exit to HRSG, 3% in HRSG Reheater, and 5% from HRSG to IP turbine inlet)
 - LP 12 %

Temperature losses:

- from superheaters/reheater to turbine = 1 kJ/kg (approximately 0.5 K)

Temperature differences:

- $\Delta T_{steam/gas} = 25\text{ K}$
- $\Delta T_{pinch point, gas/boiling liquid} = 10\text{ K}$
- $\Delta T_{gas/liquid} = 10\text{ K}$
- $\Delta T_{approach, ECO} = 5\text{ K}$

Natural circulation.

Blowdown = 0 %

10.3 Condenser

10.3.1 Water cooling

Condenser pressure: $P_{\text{cond}} = 0.040 \text{ bar}$ ($T_{\text{sat}} = 29 \text{ }^{\circ}\text{C}$)

Cooling water pump work: about 0.5% of steam turbine power

Cooling water pressure: 2-2.5 bara

Limitations on cooling water outlet temperature: Maximum $T_{\text{cw out}} = 25 \text{ }^{\circ}\text{C}$ ($T_{\text{cw in}} = 15 \text{ }^{\circ}\text{C}$)

Cooling water temperature in Norway: assume $8 \text{ }^{\circ}\text{C}$.

Saturated condensate at condenser outlet to be assumed.

10.4 Steam turbines

Isentropic efficiency, dependency on pressure:

- $\eta_{HP} = 90\%$
- $\eta_{IP} = 92\%$
- $\eta_{LP} = 88\%$

HP steam turbine admission temperature = $560 \text{ }^{\circ}\text{C}$

The total isentropic efficiency for HPT, IPT and LPT should be the same disregarding the number of steam extraction points.

Minimum steam quality = 0.87 (kg steam/kg steam+liquid water)

Pressure losses for steam extraction:

- HP-extraction pipe + preheater, $\Delta p = 3 \text{ \%}$
- LP-extraction pipe + preheater, $\Delta p = 5 \text{ \%}$

10.5 Pumps

Total efficiency: $\eta_p = 70 \text{ \%}$.

Pump work: (*sat* = saturated liquid)

$$W_{\text{pump}} = \dot{m} \cdot v_{\text{sat}}(T_{in}) \cdot (p_{out} - p_{in}) / \eta_p \quad (85)$$

10.6 Feedwater preheating

Coal-fired steam cycle:

- 2 feedwater preheaters + 1 deaerator + 4 condensate preheaters
- Deaerator
 - Saturated liquid at outlet
 - Pressure = 12.5 bar
- final preheating temperature $265 \text{ }^{\circ}\text{C}$
- extraction pressures: 51 / 26 / 13 / 5 / 1.9 / 0.8 / 0.3 bara

Combined cycle:

- no feedwater preheating with turbine steam extraction
- feedwater preheating with exhaust gas heat to $T_{H2O}=95 \text{ }^{\circ}\text{C}$
- Deaerator
 - Saturated liquid at outlet
 - Pressure = 1.2 bar ($T_{\text{sat}} = 105 \text{ }^{\circ}\text{C}$)

Closed feedwater heater:

- $\Delta p_{\text{cold}} = 1 \text{ \%}$
- $\Delta p_{\text{hot}} = 1 \text{ \%}$
- terminal temperature difference, $T_{\text{sat. steam}} - T_{\text{condensate out}} = 3 \text{ }^{\circ}\text{C}$
- drain cooler approach, $T_{\text{condensed steam}} - T_{\text{condensate in}} = 6 \text{ }^{\circ}\text{C}$

- condensed steam sent to feedwater heater at lower pressure (finally to deaerator or condenser)

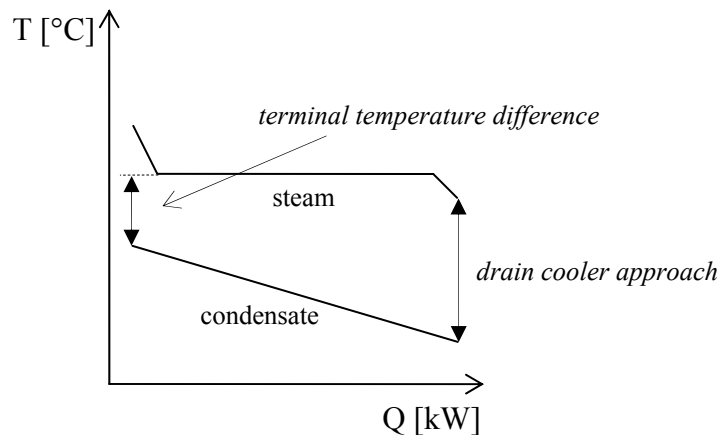


Figure 9 Temperature profile in a closed feedwater heater.

10.7 Fans and blowers

Electrical motor and mechanical efficiency = 93%

Isentropic efficiency = 80%

References

- ASME, S. (1995). "The Ljungström Air Preheater 1920." Retrieved 08.04.2008, 2008, from <http://files.asme.org/ASMEORG/Communities/History/Landmarks/5586.pdf>.
- Basu, P. (1999). "Combustion of coal in circulating fluidized-bed boilers: a review." Chemical Engineering Science **54**(22): 5547-5557.
- Bolland, O. (1991). "Comparative evaluation of advanced combined cycle alternatives." Journal of Engineering for Gas Turbines and Power **113**(2): 190-197.
- Bolland, O., M. Førde, et al. (1996). "Air bottoming cycle: Use of gas turbine waste heat for power generation." Journal of Engineering for Gas Turbines and Power **118**(2): 359-367.
- Bolland, O. and J. F. Stadaas (1995). "Comparative evaluation of combined cycles and gas turbine systems with water injection, steam injection, and recuperation." Journal of Engineering for Gas Turbines and Power **117**(1): 138-145.
- Boyce, M. P. (2002). Handbook for cogeneration and combined cycle power plants. New York, ASME Press.
- Bugge, J., S. Kjær, et al. (2006). "High-efficiency coal-fired power plants development and perspectives." Energy **31**(10-11): 1437-1445.
- Chen, L. G., J. L. Zheng, et al. (2003). "Power, power density and efficiency optimization for a closed cycle helium turbine nuclear power plant." Energy Conversion and Management **44**(15): 2393-2401.
- Damm, D. L. and A. G. Fedorov (2006). Design and analysis of zero CO₂ emission powerplants for the transportation sector. American Society of Mechanical Engineers, Heat Transfer Division, (Publication) HTD, Chicago, IL.
- Dechamps, P. J. (1998). "Advanced combined cycle alternatives with the latest gas turbines." Journal of Engineering for Gas Turbines and Power **120**(2): 350-357.
- Devotta, S. and F. A. Holland (1985). "Comparison of theoretical Rankine power cycle performance data for 24 working fluids." Journal of Heat Recovery Systems **5**(6): 503-510.
- Dostal, V., P. Hejzlar, et al. (2006). "The supercritical carbon dioxide power cycle: Comparison to other advanced power cycles." Nuclear Technology **154**(3): 283-301.
- Gale, T. K., B. W. Lani, et al. (2008). "Mechanisms governing the fate of mercury in coal-fired power systems." Fuel Processing Technology **89**(2): 139-151.
- Goto, H. and S. Okutani (2002). Operating Experiences of 71MW PFBC Demonstration Plant. Impact of Mineral Impurities in Solid Fuel Combustion: 663-674.
- GTW (2007). Where have we been and where are we headed? Gas Turbine World, Pequet Publishing Inc. **37**: 11-18.
- Guo, X.-D. and L.-S. Wang (1992). Feasibility study of the intercooled-supercharged gas turbine engine. American Society of Mechanical Engineers, International Gas Turbine Institute (Publication) IGTI, Houston, TX, USA, Publ by ASME.
- Heppenstall, T. (1998). "Advanced gas turbine cycles for power generation: a critical review." Applied Thermal Engineering **18**(9-10): 837-846.
- Higman, C., S. DellaVilla, et al. (2006). The Reliability of Integrated Gasification Combined Cycle (IGCC) Power Generation Units. Achema 2006. Frankfurt: 11.
- Hirs, G. G., M. T. P. A. Wagener, et al. (1995). Performance analysis of the dual gas turbine combined cycle. American Society of Mechanical Engineers, Advanced Energy Systems Division (Publication) AES, San Francisco, CA, USA, ASME.
- Horlock, J. H. (1995). "Combined power plants - past, present, and future." Journal of Engineering for Gas Turbines and Power **117**(4): 608-616.
- IEA-CCC. (2008). "Clean Coal Technologies." Retrieved April 13, 2008, from <http://www.iea-coal.org.uk>.
- Jaeger, H. (2006). "Refinery IGCC plants are exceeding 90% capacity factor after 3 years." Gas Turbine World **36**(1): 20-26.
- Jansson, S. A. S. A. (1996). "Coal-fired PFBC machine: Operating experience and further

- development." Paper - American Society of Mechanical Engineers: 1-5.
- Kalina, A. L. and H. M. Leibowitz (1987). APPLYING KALINA TECHNOLOGY TO A BOTTOMING CYCLE FOR UTILITY COMBINED CYCLES. American Society of Mechanical Engineers (Paper), Anaheim, CA, USA, ASME.
- Kehlhofer, R. (1999). Combined-cycle gas & steam turbine power plants. Tusla, Okla., PennWell.
- Korobitsyn, M. (2002). "Industrial applications of the air bottoming cycle." Energy Conversion and Management **43**(9-12): 1311-1322.
- Laege, J. and B. Pontow (2002). 30 Years of Successful Operation: Developments and Improvements in a Large-scale Gasification Plant. IChemE Gasification Conference, Noordwijk.
- Meij, R. and H. t. Winkel (2006). "Mercury emissions from coal-fired power stations: The current state of the art in the Netherlands." Science of The Total Environment **368**(1): 393-396.
- Miller, B. G. (2005). Coal energy systems. Amsterdam, Elsevier Academic Press.
- Mook, N. (2004). Update on Operation – Economic Improvement Opportunities. GTC Conference, Washington DC.
- NETL (2001). Tidd PFBC Demonstration Project. Morgantown and Pittsburgh, DOE National Energy Technology Laboratory: 1-36.
- Overgaard, P. (2008). "Coal-fired power plants." Retrieved April 13, 2008, from http://www.dongenergy.com/engineering/engineering_services/coalfired+power+plants/index.htm.
- Pacala, S. and R. Socolow (2004). "Stabilization Wedges: Solving the Climate Problem for the Next 50 Years with Current Technologies." Science **305**(5686): 968.
- PEI (2006). "CFB breakthrough." PEI Power Engineering International **14**(8): 31-35.
- Phillips, J. N. (2006). I & C needs of integrated gasification combined cycles. 16th Annual Joint ISA POWID/EPRI Controls and Instrumentation Conference and 49th Annual ISA Power Industry Division, POWID Symposium 2006, San Jose, CA.
- Poullikkas, A. (2005). "An overview of current and future sustainable gas turbine technologies." Renewable and Sustainable Energy Reviews **9**(5): 409-443.
- Reh, L. (1999). "Challenges of circulating fluid-bed reactors in energy and raw materials industries." Chemical Engineering Science **54**(22): 5359-5368.
- RWE. (2008). "Modern power plant engineering." Retrieved April 13, 2008, from <http://www.rwe.com/generator.aspx/konzern/fue/strom/fossil/moderne-kraftwerkstechnik/language=en/id=272318/moderne-kraftwerkstechnik.html>.
- Saleh, B., G. Koglbauer, et al. (2007). "Working fluids for low-temperature organic Rankine cycles." Energy **32**(7): 1210-1221.
- Saravanamuttoo, H. I. H., G. F. C. Rogers, et al. (2001). Gas turbine theory. Harlow, Prentice Hall.
- Schilling, H.-D. (2005). "How did the efficiency of coal-fired power stations evolve, and what can be expected in the future?" Retrieved April 13, 2008, from <http://www.sealnet.org/s/8.pdf>.
- Sloss, L. L. (1992). Nitrogen Oxides Control Technology Fact Book.
- Spector, R. B. and R. F. Patt (1997). Projection of advancements in aeroderivative gas turbine technology for the next two decades. American Society of Mechanical Engineers (Paper), Orlando, FL, USA, ASME.
- Traupel, W. (1966). Thermische Turbomaschinen. Berlin, Springer.
- Tuzson, J. (1992). "Status of steam-injected gas turbines." Journal of Engineering for Gas Turbines and Power **114**(4): 682-686.
- Vijayaraghavan, S. and D. Y. Goswami (2005). "Organic working fluids for a combined power and cooling cycle." Journal of Energy Resources Technology, Transactions of the ASME **127**(2): 125-130.
- Viswanathan, R., K. Coleman, et al. (2006). "Materials for ultra-supercritical coal-fired power plant boilers." International Journal of Pressure Vessels and Piping **83**(11-12): 778-783.
- Vitalis, B. P. (2006). "Constant and sliding-pressure options for new supercritical plants." Power **150**(1).
- Wikipedia. (2008b). "Wärtsilä-Sulzer RTA96-C." Retrieved April 16, 2008, from http://en.wikipedia.org/w/index.php?title=W%C3%A4rtsil%C3%A4-Sulzer_RTA96-C&oldid=21811111

C&oldid=198685637.

- Woodruff, E. B., H. B. Lammers, et al. (2004). Steam Plant Operation, McGraw-Hill Professional.
- Wright, I. G., J. Stringer, et al. (2003). "Materials issues in bubbling PFBC systems." Materials at High Temperatures **20**: 219-232.
- Zabetta, E. C., M. Hupa, et al. (2005). "Reducing NOx emissions using fuel staging, air staging, and selective noncatalytic reduction in synergy." Industrial and Engineering Chemistry Research **44**(13): 4552-4561.
- Zhang, X. R., H. Yamaguchi, et al. (2007). "Theoretical analysis of a thermodynamic cycle for power and heat production using supercritical carbon dioxide." Energy **32**(4): 591-599.